Pretreatment to the leaching of copper sulphides minerals in oxidizing media

Víctor Alejandro Quezada Reyes

UNIVERSITAT DE BARCELONA

2020

Pretreatment to the leaching of copper sulphides minerals in oxidizing media

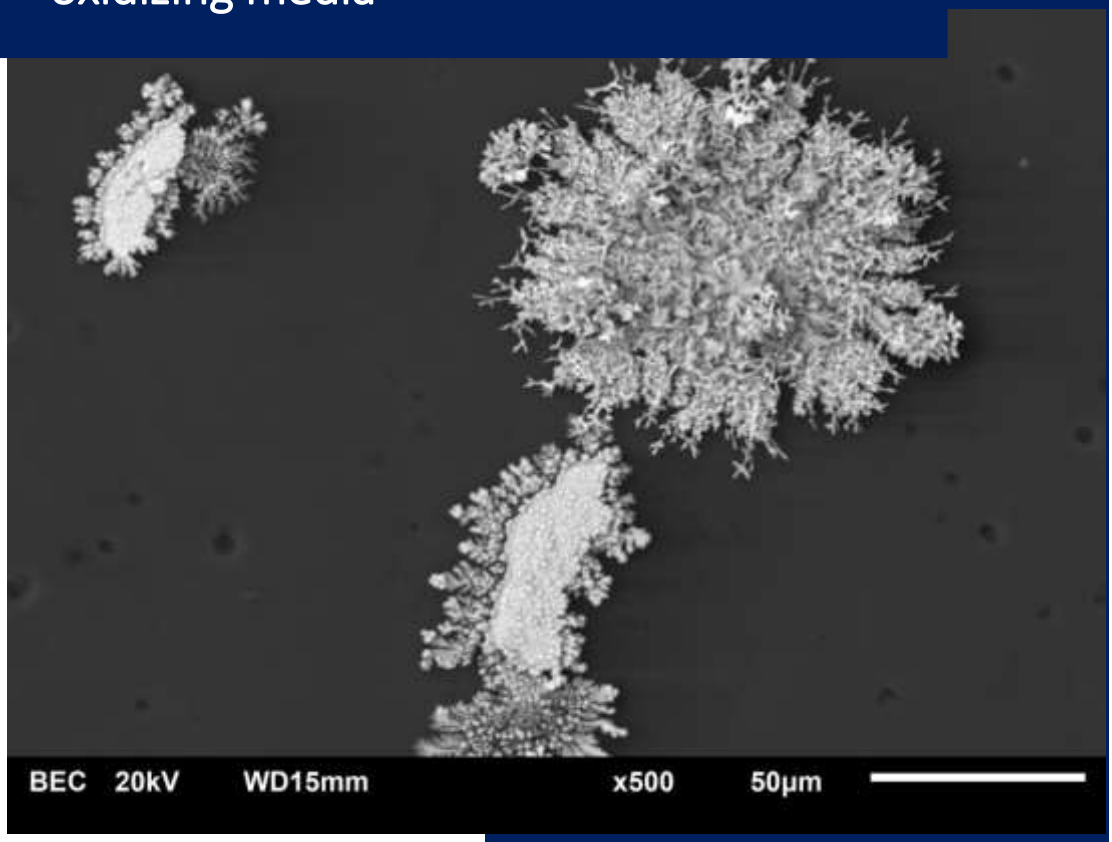

Author:

Víctor Quezada Reyes

Program name: Doctorado en Ingeniería y Ciencias aplicadas

Thesis title: Pretreatment to the leaching of copper sulphides minerals in oxidizing media

Doctoral student

Víctor Alejandro Quezada Reyes

Thesis supervisors

Dr. Antoni Roca Vallmajor, Departamento de Ciencia de los Materiales y Química Física, Universitat de Barcelona, Barcelona, Spain.

Dr. Oscar Benavente Poblete, Departamento de Ingeniería Metalúrgica y Minas, Universidad Católica del Norte, Antofagasta, Chile.

Thesis tutor

Dr. Antoni Roca Vallmajor, Departamento de Ciencia de los Materiales y Química Física, Universitat de Barcelona, Barcelona, Spain.

ACKNOWLEDGEMENTS

I sincerely thank God for the health, opportunities, abilities, family and friends that throughout my life have allowed me to preserve and enjoy.

I would also like to thank my tutors Dr. Oscar Benavente and Dr. Antoni Roca. Also, thanks to my dear Dra. Montserrat Cruells. Many thanks for believing in this idea, for the guidance and for teaching me about theory and life, especially from life. Thank you for those extensive days between reactors, SEM and knowledge. More than a thesis, a life experience.

I extend my thanks to the Department de Ciència de Materials i Química Física of the Universitat de Barcelona for assisting me and receiving so well since the first day , I especially thank to Esther Vilalta for her enormous patience and willingness every time I needed her help. I also thank the Departamento de Ingeniería Metalúrgica y Minas of the Universidad Católica del Norte for trusting and allowing me to perform this doctorate.

I cannot leave out of this page the Department of Chemical Engineering of the University of Cape Town, especially Dr. Jochen Petersen for welcoming me into his research team and giving me the opportunity to perform an internship in South Africa.

Finally, thank those people who have always been with me and believed when it was perhaps more difficult to do so. Especially to my mother, my sister, my unconditional and beautiful Evelyn Melo; Luis Beiza and Manuel Cánovas.

Moltes gràcies a tots

Dedicated to my mother, Yoice Reyes Diaz

TABLE OF CONTENTS

LIST OF FIGURES

LIST OF TABLES

ABBREVIATIONS

Cochilco: Chilean Copper Commission

PLS: Pregnant leaching solution

ICP-OES: Inductively Coupled Plasma–Optical Emission Spectrometer

SHE: Standard hydrogen electrode

AAS: Atomic Absorption Spectrometry

SEM: Scanning Electron Microscopy

XRD: X-ray diffraction

ROM: Reflection Optical Microscopy

ANOVA: Analysis of Variance

EDS: Energy-Dispersive X-ray spectroscopy

ABSTRACT

Copper production in Chile is developed by hydrometallurgical and concentration; copper concentrates are traditionally treated by the pyrometallurgical route. According to Cochilco, copper produced in 2019 by hydrometallurgical process represent a 27.3% of Chilean total copper production. However, this contribution is estimated to decrease to 11.6% by 2029, due to the depletion of copper oxides and the appearance of copper sulphides, mainly chalcopyrite, being this mineral refractory to conventional leaching conditions.

An alternative to improve leaching efficiency is pretreatment prior to leaching, especially the effect of curing time. This variable can increases the kinetics of copper extraction, especially in sulphides ores, however, there is limited research about it. Studies on pretreatment evaluate the effect on leaching efficiency but not previous leaching. Furthermore, the reactions that govern this phenomenon have not been clearly identified. Therefore, the objective of this thesis is the evaluation of the effect of acid curing on the copper extraction from sulphides minerals in oxidizing media and in presence of chloride.

A pure sample of chalcopyrite, chalcocite and a mine ore were used. Tests evaluating the effect of curing time, KNO_3, NaCl and H_2SO_4 concentration have been carried out. The chalcopyrite sample effect was evaluated by ANOVA. The product generated in the pretreatment (agglomerates) has been characterized using different characterization techniques, such as: X-Ray diffraction, Scanning Electron Microscopy and Reflection Optical Microscopy. Furthermore, the effect of pretreatment has been evaluated on the leaching efficiency at different temperatures, leaching residues have also been characterized.

In the pretreatment of the chalcopyrite sample and mine ore, under the conditions of 15 kg/t of H_2SO_4, 25 kg/t of NaCl and 15 days of curing time, the following products were identified: $CuSO_4$, $NaFe_3(SO_4)_2(OH)_6$, $Cu_2Cl(OH)$ and S^0. Regarding the chalcocite sample, under the conditions of with 30 kg/t of H_2SO_4, 40 kg/t of NaCl and 7 days of curing time, the following products were identified: $Cu_{1.75}S$, Cu(OH)Cl, Na_2SO_4 and $CuSO_4$. Finally, copper sulphides ore pretreatment improved leaching efficiency, between 4 and 6%, reaching a copper dissolution of 94% from chalcopyrite at 90 °C, strengthening the hydrometallurgy as an alternative treatment for copper sulphides ores.

RESUMEN

La producción chilena de cobre procede de la hidrometalurgia y la concentración; el concentrado de cobre es tratado tradicionalmente mediante pirometalurgia. De acuerdo a Cochilco, el cobre producido en el año 2019, vía hidrometalurgia, fue un 27.3% del cobre chileno producido. Sin embargo, se prevé que esta aporte baje a un 11.6% para el año 2029, debido al agotamiento de los óxidos de cobre y la aparición de los sulfuros, principalmente calcopirita, siendo este mineral refractario a condiciones convencionales de lixiviación.

Una opción para mejorar la eficiencia de lixiviación es el pretratamiento, especialmente el efecto del tiempo de curado. Esta variable mejora la cinética de disolución, principalmente en minerales sulfurados de cobre, sin embargo, existe escasa investigación al respecto. Estudios sobre el pretratamiento evalúan el efecto en la eficiencia de lixiviación pero no antes. Además, las reacciones que gobiernan estos fenómenos no han sido identificadas. Así, el objetivo de esta tesis es la evaluación del efecto del curado ácido en la extracción de cobre desde minerales sulfurados en condiciones oxidantes y en la presencia de cloruro.

Muestras puras de calcopirita, calcosina y un mineral industrial de mina han sido utilizadas. Se desarrollaron pruebas evaluando el efecto del tiempo de curado y la concentración de KNO_3, NaCl y H_2SO_4 y analizadas por ANOVA (calcopirita). Los productos formados en el pretratamiento (aglomerados) se caracterizaron utilizando diversas técnicas, tales como: Difracción de rayos X, Microscopio electrónico de barrido y Microscopia de luz reflejada. Además, el efecto del pretratamiento ha sido evaluado en la eficiencia de lixiviación a varias temperaturas, los residuos de lixiviación también han sido caracterizados.

En el pretratamiento, el mineral de calcopirita y de mina, bajo las condiciones utilizadas en este estudio (15 kg/t of H_2SO_4, 25 kg/t of NaCl y 15 días de tiempo de curado), los siguientes productos fueron identificados: $CuSO_4$, $NaFe_3(SO_4)_2(OH)_6$, $Cu_2Cl(OH)$ y S. Sobre la calcosina, bajo las condiciones utilizadas en este estudio, con 30 kg/t of H_2SO_4, 40 kg/t of NaCl y 7 días de tiempo de curado, los productos identificados fueron: $Cu_{1.75}S$, Cu(OH)Cl, Na_2SO_4 and $CuSO_4$. Finalmente, el pretratamiento mejora la eficiencia de lixiviación, entre 4 y 6%, alcanzando una extracción de cobre de 94% desde la calcopirita a 90 °C, fortaleciendo la hidrometalurgia como alternativa de tratamiento para minerales sulfurados de cobre.

1 Introduction and objectives

1.1 State of the art

As Chile transitions from a developing economy to a developed one, mining plays a vital role in sustaining the economy while minimizing the ecological impact on the environment, as well as promoting social growth (Ghorbani and Kuan, 2017). Therefore, copper production becomes fundamental as Chilean main export product. Copper production in Chile is developed by hydrometallurgical and concentration by flotation processes; copper concentrates obtained by flotation are traditionally treated by the pyrometallurgical route. The objective of the pyrometallurgical process is to separate the impurities contained in the copper concentrate by fusion at a temperature around 1,200 °C, to obtain high purity copper anodes. The stages involved in the pyrometallurgical process are matte smelting, batch converting to blister, fire refining and anode casting. The intermediate products obtained in each stage are matte (65% Cu), blister copper (98-99% Cu) and anodic copper (98.5-99% Cu). Finally, in the electrorefining process the anodes are dissolved and high purity copper cathodes (> 99.99% Cu) are obtained (Pradenas et al., 2015). Figure 1 shows a diagram of the conventional copper pyrometallurgical process.

Figure 1. Diagram of conventional copper pyrometallurgical process

Conventional hydrometallurgy treatment consists of 3 main stages. The first is leaching, where mineral dissolution occurs through the action of an acidic solution. The product that is obtained in the leaching stage is known as Pregnant Leaching Solution (PLS).

Then, the solvent extraction stage generate an electrolyte solution with high acid and copper concentration and low presence of impurities. This electrolyte enters to the last stage, electrowinning, where high purity copper cathodes, (>99.99% Cu) are obtained. Figure 2 shows the conventional copper hydrometallurgical process.

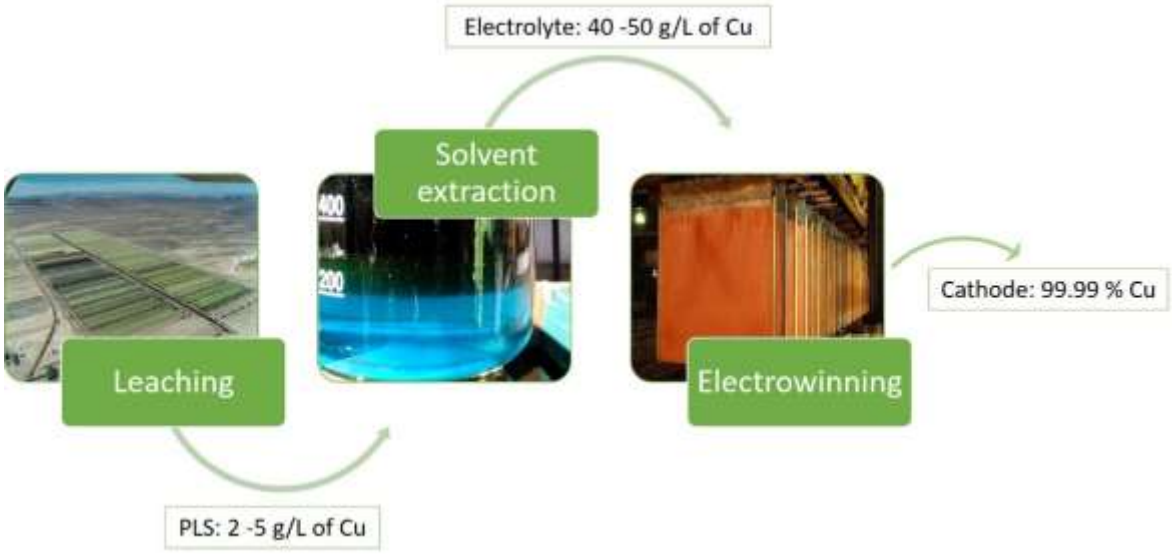

Figure 2. Diagram of conventional copper hydrometallurgical process

According to the Chilean Copper Commission (Cochilco), copper produced by hydrometallurgical process plants represent a 27.3% of Chilean total copper production (Cochilco, 2019). However, a decrease in copper production due to hydrometallurgical processes is estimated to drop to 11.6% by 2029, due to the depletion of copper oxides from the deposits. That is why mining operations are changing to flotation concentration processes due to the appearance of primary copper sulphides, mainly chalcopyrite. Chalcopyrite ($CuFeS_2$) is the most abundant copper-bearing resource, accounting for more than 70% of global copper reserves (Zhao et al., 2019). Therefore, the abundance of chalcopyrite in the deposits is a natural condition. It is estimated that of the current 31 hydrometallurgical operations in Chile, by 2030 only 19 could remain in operation. The decreasement of Chilean hydrometallurgical copper production, will generate an unused plants with a capacity close to 1.3 million (Cochilco, 2019).

One of the challenges for hydrometallurgical processes is the treatment of refractory copper minerals under conventional leaching conditions, such as black copper oxides (Benavente et al., 2019; Quezada et al., 2020) and primary sulphides minerals, mainly chalcopyrite ($CuFeS_2$) (Beiza et al., 2019; Wang, 2005). The slow dissolution kinetics of chalcopyrite is due to the formation of a product layer that inhibits the contact of the solution with the mineral (Nicol, 2017). This layer has been studied by multiple authors (Dutrizac, 1990; Lv et al., 2019; Nicol and Zhang, 2017).

To improve copper extraction and dissolution kinetics, various leaching media have been proposed, such as: chloride media (Dutrizac, 1992; Lundström et al., 2005; Viñals et al., 2003), nitrate media (Gok and Anderson, 2013; Hernández et al., 2019), bioleaching (Petersen and Dixon, 2007, 2002; Tanne and Schippers, 2019), ammonia solution (Adebayo and Sarangi, 2011; Baba et al., 2014; Moyo et al., 2019, 2018); the chloride media being one of the most studied and effective due to the reactivity of the chloride ion with sulphide ores (Velásquez Yévenes, 2009).

The presence of the chloride ion benefits the dissolution of copper sulphides minerals because can form chloro-complexes with copper. The greater anodic activity in chloride media can change the morphology of surface and the reaction products (Carneiro and Leão, 2007). However, the dissolution kinetics of chalcopyrite continues to be a challenge because in most cases, a passivation layer is formed on the surface of the chalcopyrite particles. This results in slow kinetics and poor copper recoveries due to the formation of a "diffusion barrier" between the solution and chalcopyrite grains (Wang et al., 2016). Although there is still some controversy about the exact composition of this passivation layer, elemental sulphur or polysulphides are observed consistently in the dissolution of chalcopyrite (Córdoba et al., 2008a; Hackl et al., 1995; Nicol and Zhang, 2017).

Today, research focuses more on how to improve the dissolution kinetics of primary copper sulphides, mainly chalcopyrite ($CuFeS_2$). Regarding secondary sulphides, chalcocite (Cu_2S) and covellite (CuS), are two of the most common copper minerals. Chalcocite is the most abundant copper sulphide mineral after chalcopyrite, and the easiest to dissolve in chloride media (Miki et al., 2011). This property makes it very attractive mainly for those

deposits with a low copper grade. The hydrometallurgical process is considered as a viable alternative, which has led to its implementation at an industrial level, such as the Cuprochlor Process (Herreros and Viñals, 2007) and bioleaching media (Niu et al., 2015; Rodríguez et al., 2003). Chalcocite and covellite are also formed as intermediates products during chalcopyrite leaching (Senanayake, 2009). Therefore, understand the behavior of chalcocite is also understand the dissolution of chalcopyrite.

The effect of leaching pretreatments, especially the effect of the curing time, was identified as beneficial in the dissolution of copper sulphide minerals (Cerda et al., 2017; Hernández et al., 2019; Velásquez-Yévenes and Quezada-Reyes, 2018). According to (Dhawan et al., 2013), curing time generates a homogeneous distribution of the acid in the mineral bed, increases the kinetics of copper dissolution, benefiting the inhibition of aluminum-silicate minerals. However, (Lu et al., 2017) points out that there is limited research regarding the effect of curing time on the dissolution of copper ores.

In recent years, the effect of acid curing has been studied mainly for chalcopyrite in chloride media, however for copper sulphides minerals there is no extensive research. Results obtained by Quezada (Quezada et al., 2018), indicate the benefit of the curing time for a chalcocite/covellite mineral in columns leaching. It has been demonstrated that ore agglomerated with sulphuric acid, chloride ions and extensive curing time enhances the dissolution rate of a secondary copper sulphide ore. The authors point out that it is possible to obtain a 72% of Cu extraction when the ore is agglomerated and curing for 50 days using chloride media. According to the Analysis of Variance, curing time is the variable that has the greatest contribution in copper extraction (92.37%) versus chloride concentration (7.05%), under the conditions studied. A similar trend in results have been obtained in column leaching of chalcopyrite ore with a P_{80} of 5 mm achieved a maximum dissolution of 43% of copper using chloride media at room temperature after 100 days of curing time (Velásquez-Yévenes and Quezada-Reyes, 2018).

Thus, this research focuses on the effect of acid curing on copper sulphide minerals in oxidizing media. The characterization of products after leaching has been developed in order to propose mechanisms that explain the benefit of acid curing. High purity minerals

have been used in order to avoid characterization noise, however, the application of the obtained results has also been applied to a mine ore. The objectives proposed in this thesis are:

1.2 Objectives

General objective

Evaluation of the effect of acid curing on the copper extraction from sulphides minerals in oxidizing media and in presence of chloride.

Specific objectives

Characterization of feed minerals, pretreatment products and leaching residues using chemical analysis, X-ray Diffraction (XRD), Reflection Optical Microscopy (ROM) and Scanning Electron Microscopy (SEM).

Quantification of the effect of variables such as curing time, sulphuric acid concentration, concentration of oxidizing agents and concentration of chloride ions in the pretreatment of a copper sulphide mineral using Analysis Of Variance (ANOVA)

Propose product formation mechanisms in the pretreatment of copper sulphide minerals through the action of oxidizing agents and/or chloride agents before leaching

2 Methodologies and characterization techniques

2.1 Reagents and mineral samples

The chemical reagents used in this study are shown in Table 1. All the reagents have an analytical grade (AG) and all the solutions used were prepared with distilled water.

2.1.1 Reagents

Table 1. Chemical reagents used during the present investigation

Reagents	Formula	Purity	Use
Sulphuric acid	H_2SO_4	96 %	Agglomeration and leaching solution
Sodium chloride	NaCl	AG	Agglomeration and leaching solution
Potassium nitrate	KNO_3	AG	Agglomeration solution
Oxygen gas	O_2	99.99 %	Oxidation
Nitrogen gas	N_2	99.99 %	Removal of oxygen

Sulphuric acid

A sulphuric acid (H_2SO_4), analytical grade with a purity of 96 %, a molecular weight of 98.08 g/mol and a density of 1.84 g/mL was used.

Sodium chloride

The sodium chloride (NaCl) used in the agglomeration and leaching tests was analytical grade with a molecular weight of 58.44 g/mol.

Potassium nitrate

The potassium nitrate (KNO_3) used in the agglomeration tests was analytical grade with a molecular weight of 101.10 g/mol.

Oxygen gas

Oxygen gas (O_2) was oxygen ultrapure (5.2) with a purity of 99.999%, it had less than 5 ppm of nitrogen and less than 3 ppm of water. The oxygen gas used had a molecular weight of 32.00 g/mol.

Nitrogen gas

Nitrogen gas (N_2) was nitrogen technical (5.0) with a purity of 99.999%, it was less than 5 ppm of oxygen and less than 3 ppm of water. The nitrogen gas used had a molecular weight of 28.01 g/mol.

2.1.2 Mineral samples

The minerals samples used in this study are of natural origin and collected in the Antofagasta Region, Chile. The samples have been collected from to mine sites.

Chalcopyrite

The sample was collected from "La Atómica" deposit located near the town of Mejillones, (Antofagasta Region) with a rock size between 4 and 2 centimeters and a total mass of approximately 500 grams. The collected sample has a high purity of the main species (chalcopyrite), according to visual analysis. The purity of this sample reduces noise when analyzing results. An image of the initial sample is shown in Appendix 1.

Mine ore

The mineral sample was collected from a mining company located in the Antofagasta Region, Chile. It was collected as a mineral resource from the primary area of the deposit. The sample had a size between 5 and 3 centimeters and a total mass of 35 kilograms. An image of the initial sample is shown in Appendix 2.

Chalcocite

The sample was collected from the "La Atómica" deposit located in the town of Mejillones, (Antofagasta Region) was a single piece whose dimensions were 15 x 13 centimeters with a mass of 800 grams. The collected sample has a high purity of the main species (chalcocite), according to visual analysis. The purity of this sample reduces noise when analyzing results. An images of the initial sample is shown in Appendix 3.

2.2 Experimental methodology

2.2.1 Mechanical sample preparation

All samples used in the curing and leaching tests have been primarily crushed by a jaw crusher, followed by a secondary and tertiary cone crusher, then dry milled in a ball mill and finally screened in a size fraction of -38 + 25 μm. The size reduction has been carried out in a closed crushing and grinding circuit.

2.2.2 Aglomeration and curing

Chalcopyrite sample

For the curing tests, 2 g of chalcopyrite sample were used in each test. The sample was agglomerated with the solution (H_2SO_4, NaCl or KNO_3), and covered to avoid evaporation. Different concentrations of sulphuric acid, NaCl concentration, KNO_3 and curing times have been evaluated in the chalcopyrite sample. A solid/liquid ratio of (mass sample/volume) 10/1 was used for wetting the sample, i.e, per one gram of mineral; 0.1 mL of solution was added. The agglomerated sample was allowed to cure at room temperature for 0, 5, 10 and 15 days, depending on the curing time to evaluate. All samples have been agglomerated in contamination-free environments and placed in watch glasses covered with a protective film. Once the sample was agglomerated, it was placed in a light-free space at room temperature.

Mine ore

For the curing tests using a mine ore, 2 g were used in each agglomerated sample. The sample was agglomerated with the solution (H_2SO_4 and NaCl dissolved) and covered to avoid evaporation. Different concentrations of NaCl and curing times were evaluated in the mine ore sample. The concentration of sulphuric acid (15 kg/t) was kept constant according to results obtained in tests performed on chalcopyrite sample. A solid/liquid ratio of 10/2.2 was used for wetting of the sample, i.e, per one gram of mineral; 0.22 mL of solution was added. The agglomerated sample was allowed to cure at room temperature for 0, 5, 10 and 15 days, depending on the curing time to evaluate. All samples were agglomerated in contamination-free environments and placed in watch glasses covered with a protective

film. Once the sample was agglomerated, it was placed in a light-free space at room temperature.

Chalcocite sample

Chalcocite was evaluated in tests using 2 g of sample, studying the curing time and using a base-case of sulphuric acid and NaCl, 15 kg/t and 25 kg/t, respectively. A solid/liquid ratio of 10/1.7 was used for the wetting the sample, i.e, per one gram of mineral, 0.17 mL of solution was added. The sample was agglomerated with the solution (H_2SO_4 and NaCl) and exposed to 3 different conditions:

a) Exposed to the air, the agglomerated samples were not covered and exposed to a temperature between 20 and 23 °C.

b) In a sealed container of known volume, the agglomerates samples were placed in a sealed container with a capacity of 250 mL which was sealed to prevent evaporation.

c) Without the presence of oxygen (under nitrogen atmosphere). The agglomeration and washing solution used were previously injected with nitrogen gas to remove dissolved oxygen according to conditions proposed by (Butler et al., 1994).In addition, the agglomeration of the sample under nitrogen conditions has been performed in an anaerobic glove box to remove the O_2 presence. The nitrogen used was ultra-pure 5.0 (99.99%). the agglomerates samples were placed in a sealed container with a capacity of 250 mL without the presence of oxygen.

The agglomerated sample was allowed to cure at room temperature for 1, 3, 5, 7 and 10 and days. Once the sample was agglomerated, it was placed in a light-free space at room temperature. Once the curing time that most benefits copper extraction was determined, the effect of 30 and 40 kg/t of H_2SO_4 and 40 kg/t of NaCl (saturation point of the solution) was evaluated.

2.2.3 Washing of cured samples

Once the curing time was completed, samples of chalcopyrite, chalcocite and mine ore, were washed using a dilute solution of sulphuric acid (0.5 g/L), by mechanical agitation

using an overhead stirrer at 300 min^{-1} mechanical stirrer at a solid/liquid ratio of 1/100, room temperature for 5 minutes. In those curing tests, using an O_2-free solution, the washing solution was previously injected with nitrogen to remove oxygen from the aqueous system. All liquid samples were filtered (0.2 μm) and the metal concentrations in the filtrate were determined by Inductively Coupled Plasma–Optical Emission Spectrometer (ICP-OES).

2.2.4 Anova analysis

The Taguchi method is a statistical technique initially designed for quality improvement in manufacturing processes. This method has been widely used in engineering design (Phadke, 1989; Ross, 1996). The Taguchi method consists of procedures for system design, parameter design and tolerance design to obtain a robust process that results in the best product quality (Taguchi, 1993, 1987). Taguchi's method uses an orthogonal arrangement as its core element. In this investigation, the Taguchi method was used only for tests performed with the chalcopyrite sample. The effect of NaCl and KNO_3 on curing tests were evaluated using tests designed with the Taguchi method. In both cases, a L_{16} (4_3) design was considered with three parameters and four levels for each one.

The R language (R Core Team, 2019) and the DoE.base experiment design library (Grömping, 2018) were used to analyze the results, by using an analysis of variance (ANOVA) and finding the optimal parameterization. In order to observe the different effects of uncontrollable factors (noise sources) on this process, each experiment was performed in duplicate under the same operating conditions. Performance characteristics were implemented by maximizing Equation 1 (Copur et al., 2015; Çopur et al., 2007), given by:

$$\mathrm{SN_L} = -10\ \mathrm{Log}\left[\frac{1}{\mathrm{n}}\sum_{\mathrm{i}=1}^{\mathrm{n}}\frac{1}{\mathrm{Y_i^2}}\right] \qquad \text{(Eq.1)}$$

The SN_L response is the performance characteristic that we are trying to maximize, n is the number of repetitions performed for an experimental configuration and Y_i is the performance value for the i_{th} experiment. It is possible that the experiments that correspond to the optimal operating conditions are not in the design given by the orthogonal arrangement. In those cases, the performance value for the optimal conditions can be predicted using the balanced characteristics of the orthogonal arrangement (Çopur

et al., 2007). For these purposes, an additive linear model is considered, shown in Equation 2 given by:

$$Y_i = \mu + X_i + e_i \quad (Eq.2)$$

Where μ is the general average of the performance value, X_i is the fixed effect of the combination of parameter levels used in the ith experiment and e_i is the random error of the i*th* experiment.

The order of the experiments was obtained by transferring the parameters to the columns of the orthogonal arrangement $L_{16}(4^3)$. The order of the experiments is random in order to avoid additional sources of noise that were not initially considered and that could occur during the experiments and affect negatively (Copur et al., 2015).

The F test evaluated the process parameters and determined if they had significant effects on the performance value. The F value of the process parameters is the ratio between the average of the squared deviations from the mean of the quadratic error. In general, the higher the F value, the more significant the effect on the performance value due to change in the parameter.

Basic diagnostics were applied to assess the reliability of our linear models and evaluate whether they were appropriate. The graphical analysis of the residuals shows that the shape of the data is acceptable. Therefore, the data can be considered to follow the normality assumption required for linear models. Moreover, in both cases, the data does not break the heteroscedasticity assumption of the linear model (i.e., constant variance of the residuals).

2.2.5 Leaching

Magnetic stirring leaching

The chalcopyrite mineral was leached using a magnetic stirrer, at the programmed curing time. Leaching experiments were carried out in a 200 mL leaching vessel with a four neck lid (Figure 3). The sample was immersed in a 100 mL of the leaching solution containing 0.2 M H_2SO_4 (19.6 g/L) and 50 g/L of Cl ion. The agitation was applied using an IKA C-MAG HS 7 magnetic stirrer at 200 min^{-1} and heated to the required leaching temperature: 25,

50, 70 and 90 °C (±1 °C). When solution reached the desired temperature, 2 g of sample (cured or not) was added to the leaching solution and the process was carried out with a duration of 48 hours. Samples (3 mL aliquots) were periodically withdrawn for chemical analysis at the predetermined time. The extracted samples were filtered (0.2 µm) and the metal concentrations in the filtrate were determined by Inductively Coupled Plasma–Optical Emission Spectrometer (ICP-OES). The pH and redox potential solution (vs Ag/AgCl), were regularly measured using a Crison pH meter Basic 20. All potentials were converted to values against the standard hydrogen electrode (SHE). Solid residues after each leaching experiment were analyzed by X-ray diffraction to explain the behavior of solids during leaching at different experimental conditions. SEM analysis were also performed.

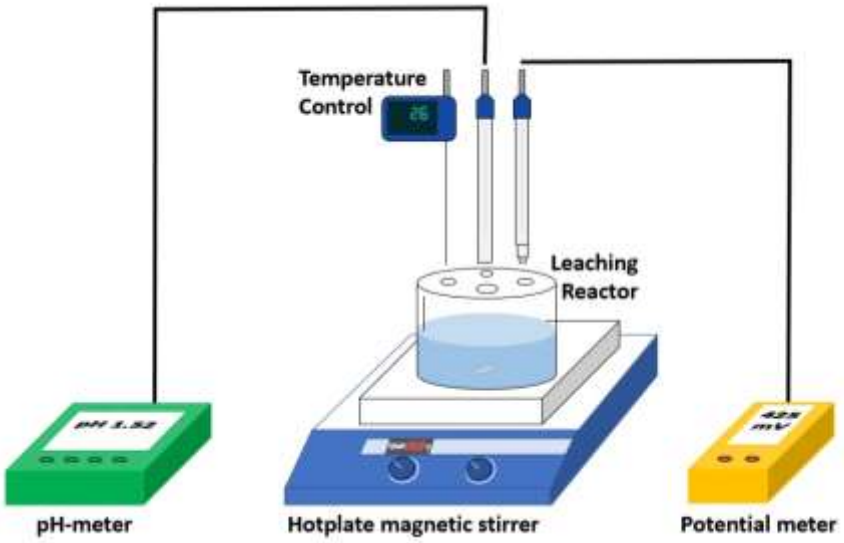

Figure 3. Scheme of magnetic stirrer leaching system

Mechanical stirring leaching

In the case of chalcocite mineral, 6 leaching tests were performed. Once the curing time was completed, leaching test were carried out at 25 and 50 °C, with and without pretreatment. Furthermore 2 leaching tests were performed (without pretreatment) with oxygen injection (1.0 L/min) and the other with nitrogen injection (1.5 L/ min). The leaching experiments were carried out in a 300 mL leaching vessel with a four neck lid. The sample was immersed in a 200 mL of the leaching solution containing 0.2 M H_2SO_4 (19.6 g/L) and 50 g/L of Cl^- ion. The agitation was applied using a RZR 1 overhead stirrer at 300 min^{-1} (Heidolph, Schwabach, Germany) and heated to the required leaching temperature: 25 and

50 (±1 °C) by a in a thermostatically controlled water bath (See Figure 4). When the solution reached the desired temperature, 2 g of sample (cured or not) was added to the leaching solution which were leached for a maximum of 12 h.

In the case of the mine ore, 8 leaching tests were performed. Once the curing time was completed, leaching test were carried out at 25, 50, 70 and 90 °C, with and without pretreatment. The leaching conditions for mine ore were the same as those used for chalcocite. For mine ore, leaching tests evaluating the effect of O_2 and nitrogen have not been performed.

For both chalcocite and mine ore leaching tests, samples (3 mL aliquots) were periodically withdrawn for chemical analysis at the predetermined time. The samples were filtered (0.2 µm) and the metal concentrations in the filtrate were determined by Inductively Coupled Plasma–Optical Emission Spectrometer (ICP-OES). The pH and redox potential solution (vs SHE, here and in all the work), were measured regularly using a pH meter device (Model 3510-JENWAY, Essex, UK) and (Basic 20-Crison Instruments S.A, Barcelona, Spain). The solid residues after the leaching experiment were analyzed by X-ray diffraction to explain the behavior of solids during leaching at different experimental conditions. SEM analysis were also performed.

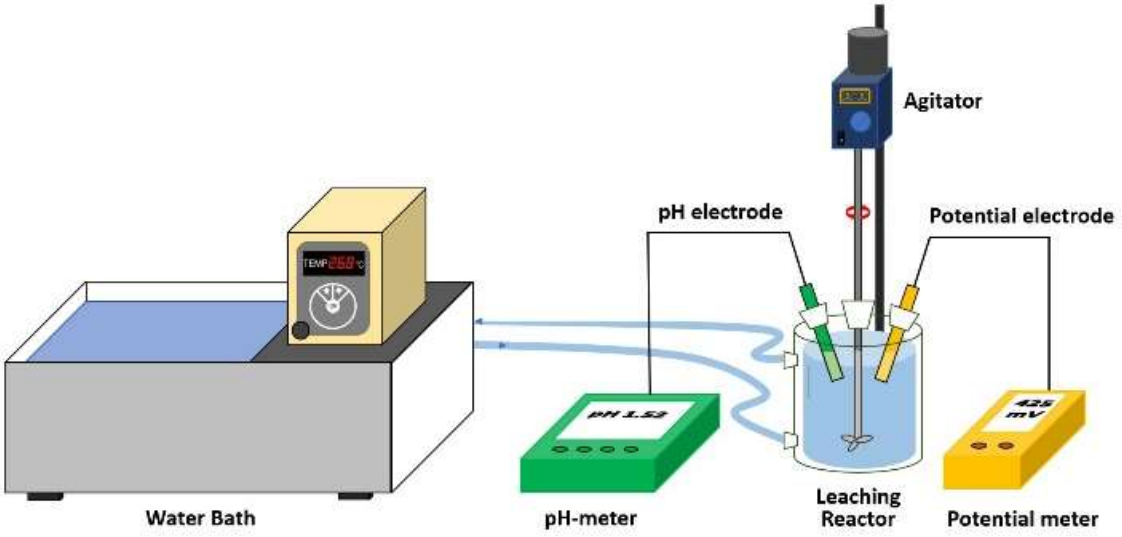

Figure 4. Scheme of mechanical stirrer system

2.3 Characterization techniques

The characterization of the samples was developed in 3 different Universities. At Universidad Católica del Norte (Chile) solid chemical characterization was performed using the Atomic Absorption Spectrometry (AAS) technique and Qemscan analysis for mineralogical characterization. At Universitat de Barcelona (Spain), mineralogical characterization was performed using X-ray diffraction, MOR and SEM. In the case of liquid samples, these were characterized at the Universitat de Barcelona and Cape Town University (South Africa) using the ICP-OES technique.

2.3.1 Chemical characterization

2.3.1.1 Inductively Coupled Plasma–Optical Emission Spectrometry

The chemical composition of the liquids samples (for samples obtained in all chalcopyrite and mine ore tests) was determined by an inductively coupled plasma–optical emission spectroscopy (ICP-OES) Perkin Elmer brand and Optima 3200 RL model (equipment used at the Universitat de Barcelona). The samples were filtered using 0.2 µm filter. For the analysis, 1 mL of the sample was pipetted into a 100 mL volumetric flask and made up with 1 % wt HNO_3. For the analysis of copper, four multi-element standards were used depending on the maximum and minimum range of the copper concentration to be analyzed.

The chemical composition of the liquids (for samples obtained in chalcocite tests) was determined by an inductively coupled plasma–optical emission spectroscopy (ICP-OES) Varian brand and 730 ES model (equipment used at the Cape Town University). The samples were filtered using 0.2 µm filter. For the analysis, 1 mL of the sample was pipetted into a 100 mL volumetric flask and made up with 2 % wt HNO_3. For the analysis of copper, six multi-element standards were used: 0.5, 1, 2, 6, 10 and 20 mg/L to perform the calibration.

2.3.1.2 Atomic Absorption Spectrometry

This technique was used to measure total copper and iron concentrations in solution after dissolution under different conditions. Furthermore, the chemical characterization of the solid samples was obtained using this technique, measuring the grade of total copper, soluble copper and total iron. The chemical characterization of solids was carried out at the Universidad Católica del Norte, using an Atomic Absorption Spectrometer, Varian brand (SpectrAA-50/55). The detection limit of the method is 0.004 % for solids analysis and 0.011 % for analysis of elements in solution (copper and iron).

2.3.1.3 Elemental analysis

The sulphur in the samples was analyzed at Scientific and Technological Center of the University of Barcelona using an elemental analyzer Thermo EA Flash 2000 (Thermo Scientific, Milan, Italy) working in standard conditions recommended by the supplier of the instrument (helium flow 140 mL/min, combustion furnace at 950 °C, chromatographic column oven at 65 °C).

2.3.2 Mineralogical characterization

2.3.2.1 X-ray diffraction

Mineralogical data were obtained by X-ray diffraction (XRD) analysis using a diffractometer (PANalytical X'Pert PRO MPD Alpha1), operating at 4° to 100° 2θ, 45 kV, 40 mA, Kα 1.54 Å, step size 0.017°, and a time per step of 150 s. X-ray diffraction analysis and crystalline phase identification were interpreted using the software X'pert HighScore Plus v.3.0e.

2.3.2.2 Stereo Microscope

Stereo microscope analysis was also used in some cases. A Reflection Stereo Zoom Microscope (Motic, SMZ-168) was used for a superficial visual analysis. The microscope had a halogen fiber optic illuminator light box (Motic, MLC-150C). All the samples were mounted in an epoxy resin and the images recorded photographically.

2.3.2.3 Reflection Optical Microscope

Optical microscope analysis was also used in some cases. A Reflection Optical Microscope (Zeiss, Axiovert 100, Milan, Italy) was used for a superficial visual analysis. All the samples were mounted in an epoxy resin and the images recorded photographically.

2.3.2.4 Scanning Electron Microscopy

Morphological characterization was performed using field emission scanning electron microscopy (SEM-JEOL J-7100F, Tokyo, Japan), operated at 20 kV under high vacuum conditions (Emitech K-950X) with an energy-dispersive X-ray spectroscopy (EDS) microanalysis system (Oxford Instruments INCA). Mineral samples were metallized with a thin layer of carbon to improve their conductivity.

2.3.2.5 Qemscan

Quantitative Evaluation of Minerals using scanning electron microscopy is used to perform the automated identification and quantification of ranges of elemental definitions that can be associated with inorganic solid phases, such as minerals, alloys, slags, etc. The analyses were made using a QEMSCAN® model E430, which is based on a ZEISS EVO 50 Scanning Electron Microscope (SEM) combined with Bruker Series 4 energy dispersive spectrometer (EDS) detectors.

3 Pretreatment and leaching of a chalcopyrite mineral

3.1 Literature Review

General properties of chalcopyrite

Chalcopyrite is the most abundant copper sulphide in the Earth's crust (70% of copper reserves in the world) (Wang, 2005). The composition of chalcopyrite is approximately: 34.6 % Cu, 30.5 % Fe and 34.9 % S. The chemical formula of the chalcopyrite can be written as $Cu^{1+}Fe^{3+}(S^{2-})_2$ (Mikhlin et al., 2004). It is a brassy yellow color with a metallic luster and a greenish black stripe. The hardness varies between 3.5 and 4.0 on the Mohs scale. The specific gravity ranges between 4.1 and 4.3 (Haldar, 2017). Chalcopyrite is derived from the Greek words “chalkos”, copper and “pyrites” strike fire and it is also known as copper pyrite (A. Baba et al., 2012). According to (Boekema et al., 2004) chalcopyrite ($CuFeS_2$) is a semiconductor with unusual magnetic and electrical properties.

The crystal structure of chalcopyrite is tetragonal. Each sulphur atom is surrounded by four atoms of iron and copper (two Fe and two Cu atoms) and each Fe or Cu atom forms a tetrahedral coordination with four S atoms (Córdoba et al., 2008a; Mikhlin et al., 2016). The crystal structure of chalcopyrite is represented in Figure 5 (De Oliveira and Duarte, 2010). Due to its crystalline structure, chalcopyrite is the most stable mineral among copper sulphides (Chatterjee et al., 2015).

Chalcopyrite, as a copper source, is found mainly in porphyry deposits and hydrothermal vein deposits (Zhao et al., 2014). In these deposits it is normally associated with pyrite (FeS_2), calcite ($CaCO_3$), bornite (Cu_5FeS_4), sphalerite (ZnS), chalcocite (Cu_2S), covellite (CuS), enargite (Cu_3AsS_4) or molybdenite (MoS_2) (Cháidez et al., 2019; Dong et al., 2013; Velásquez Yévenes, 2009). The main route of treatment of chalcopyrite ores has been the concentration by flotation and subsequent pyrometallurgical processes. Although 80–85% of the world Cu production is through pyrometallurgy (Zhong and Li, 2019). However, the hydrometallurgical treatment of chalcopyrite is very difficult. The slow kinetics of copper dissolution caused by a passivity of the mineral surface hampers commercial applications of the hydrometallurgical technologies (Martins et al., 2019; Mikhlin et al., 2004).

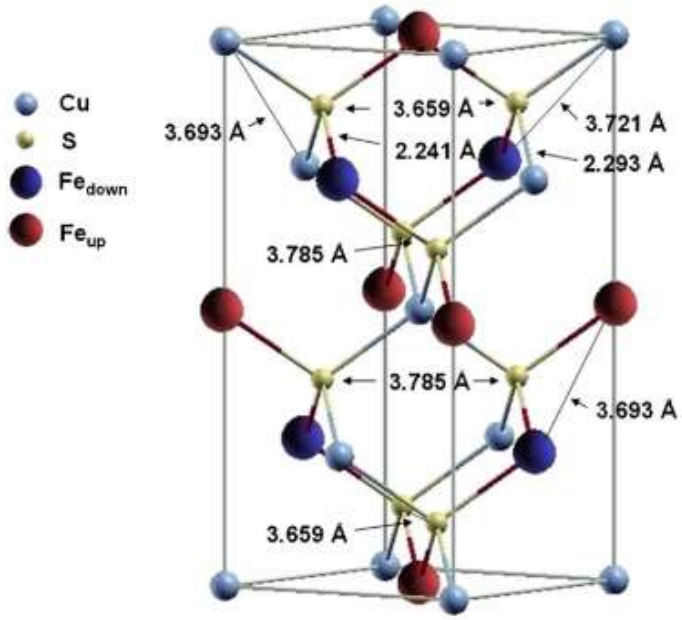

Figure 5. Unit cell of the chalcopyrite

3.1.1 Pretreatment of chalcopyrite prior leaching

A pretreatment prior to leaching consists of agglomeration and curing. These methods are crucial for the success of the leaching. The addition of a raffinate solution in the agglomeration can facilitate the adhesion of fine to coarse particles to increase the permeability of the heap. Curing leads to a homogeneous distribution of the acid in the ore bed along with a greater porosity (Jansen and Taylor, 2003). This is the best opportunity to improve the application of the leaching solution before building the heap, improving the leaching rate from low grade ores (Kodali, 2010).

According to (Dhawan et al., 2013), curing time generates a homogeneous distribution of the acid in the mineral bed, increases the kinetics of copper dissolution as well as benefiting the inhibition of aluminum-silicate minerals. However, (Lu et al., 2017) points out that there is limited research regarding the effect of curing time on the dissolution of copper ores. Most studies on pretreatment (especially curing time) have been

conducted on chalcopyrite (Cerda et al., 2017; Hernández et al., 2019; Velásquez-Yévenes and Quezada-Reyes, 2018).

The benefit of curing time has been studied by (Velásquez-Yévenes and Quezada-Reyes, 2018) evaluating the behavior of chalcopyrite from a mine ore using columns leaching. The authors evaluated 4 curing times: 30, 50, 80 and 100 days for a mineral agglomerated with 5 kg/t H_2SO_4 and using discard brine (32 g/L Cl^-) evaluating the pretreatment effect on leaching efficiency. The maximum copper dissolution (43%) was reached for a pretreatment with 100 days of curing and subsequent column leaching at room temperature with intermittent irrigation. The evaluation of temperature, as part of the pretreatment, has been investigated by (Cerda et al., 2017). The authors demonstrate that a maximum of 93 % copper extraction was obtained when the ore (mainly chalcopyrite) was treated with 90 kg Cl^-/t ore, 40 days of curing time and 50 ◦C in flask leaching. The reactions proposed by (Cerda et al., 2017) for the pretreatment, consider the effect of Cu^{2+} and Cl^- on chalcopyrite, generating covellite and CuCl as a products (Eq.3). Covellite will react in the presence of H^+ and O_2. The effect of pretreatment in covellite would not generate the Cu^{2+} necessary for the reaction on chalcopyrite (Eq.4). Therefore, Eq.4 would not generate Cu^{2+} in the system, limiting Eq.3. However, chalcocite could be a source of Cu^{2+} given the proposed reaction generated in the pretreatment (Eq.5). The presence of Cu^{2+} could also be added to the solution previously. The corresponding Gibbs energy values are negative so these reactions are thermodynamically feasible (See Table 2).

Table 2.Proposed equations for pretreatment step (adapted from (Cerda et al., 2017))

N°	Equation	ΔG 25 °C (kcal/mol)	ΔG 50 °C (kcal/mol)
(3)	$CuFeS_2 + 2Cu^{2+} + 2Cl^- \rightarrow 2CuCl + CuS + Fe^{2+} + S$	-15.6	-16.4
(4)	$2CuS + 4H^+ + O_2 + 2Cl^- \rightarrow 2CuCl^+ + 2H_2O + 2S$	-55.2	-53.2
(5)	$2Cu_2S + 4H^+ + O_2 \rightarrow 2CuS + 2Cu^{2+} + 2H_2O$	-68.1	-65.9

The study of (Hernández et al., 2019) evaluated the effect of NaCl and $NaNO_3$ on the pretreatment of a mine ore, whose main copper mineral is chalcopyrite. The authors obtain

an optimum copper extraction of 58.6% with the addition of 23.3 kg of $NaNO_3$/t, 19.8 kg of NaCl/t, after 30 days of curing time at 45 °C. In addition, they evaluate the effect of pretreatment by leaching efficiency using mini-columns. The optimum copper extraction of 63.9% was obtained in a leaching test carried out at 25 °C, with the use of 20 g/L of chloride. Furthermore, the authors propose the following pretreatment mechanism for chalcopyrite (Eq.6). According to them, the reaction is thermodynamically possible under atmospheric pressure and between 25 and 45 °C.

$$2CuFeS_2 + 10H_2SO_4 + 10NaNO_3 + 4NaCl \rightarrow 2CuCl_2 + Fe_2(SO_4)_3 + 10NO_2 + 4S + 10H_2O + 7Na_2SO_4 \quad \text{(Eq.6)}$$

3.1.2 Chalcopyrite leaching: Main parameters in chalcopyrite leaching

Chloride concentration

The presence of chloride ions in the chalcopyrite leaching has a positive effect regarding the copper dissolution kinetics (Dutrizac, 1992; Hirato et al., 1987; Rasouli et al., 2020; Rene Winand, 1991; Ruiz et al., 2015; Torres et al., 2019). According to (Carneiro and Leão, 2007) the authors report an increase in copper dissolution from 45% (without the presence of NaCl) to 91% using 1 M NaCl, in ferric sulfate solutions at 95 °C and an initial pH of 0.15. However, an increase in the concentration of NaCl (from 1 to 2 M) does not have a significant effect on the dissolution of chalcopyrite. The presence of Cl^- benefits the dissolution of copper from the chalcopyrite because of the following reasons: (i) formation of copper chloride complexes; (ii) increase in the anodic current during chalcopyrite leaching, (iii) changes on the surface form and properties of the reaction product (Carneiro and Leão, 2007).

A positive effect of the presence of chloride ions in the chalcopyrite dissolution has been reported by (Z. Y. Lu et al., 2000); they propose that at concentrations greater than 0.5 M NaCl the leaching kinetics does not increase (test performed at 0.8 M H_2SO_4, 95 °C and d_{50}= 15.1 µm) (see Figure 6).

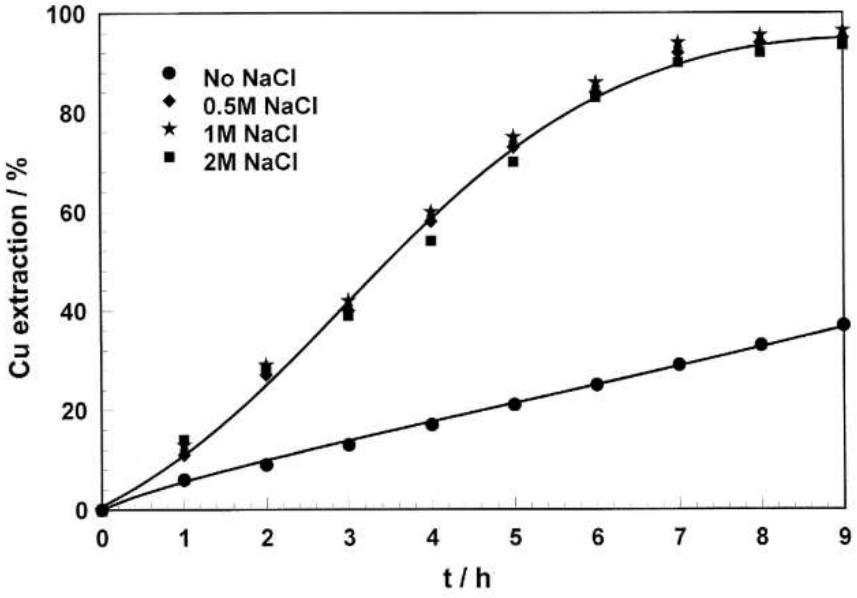

Figure 6. Effect of NaCl concentration on the leaching of the chalcopyrite concentrate. Initial conditions: 32 g solid with d_{50}= 15.1 µm, 800 mL of 0.8 M H_2SO_4 and 95 °C (Z. Y. Lu et al., 2000)

According to the study performed by (Torres et al., 2019), the predominant species in the Cu^{2+}/Cl^- system in the concentration intervals studied were $CuCl^+$ and Cu^{2+} (Torres et al., 2019). The authors propose the formation data for cupric chloride complexes (Table 3). The authors assume that chloro-cuprous species are present in a low concentration in the studied systems because of high solution potential. Cupric monochloride complex ion ($CuCl^+$) might play a role in copper extraction from copper ore. Both the cupric ion (Cu^{2+}) and the cupric chloride complex ($CuCl^+$) are able to dissolve chalcopyrite according to equations (11) and (12) in Table 4.

Table 3. Formation data for cupric chloride complexes (adapted from (Torres et al., 2019))

N°	Reaction	ΔG (kJ/mol) at 60 °C	K
(7)	$Cu^{2+} + Cl^- \rightarrow CuCl^+$	-3.150	K_1 = 3.118
(8)	$CuCl^+ + Cl^- \rightarrow CuCl_{2(aq)}$	7.153	K_2 = 0.076
(9)	$CuCl_{2(aq)} + Cl^- \rightarrow CuCl_3^-$	11.196	K_3 = 0.018
(10)	$CuCl_3^- + Cl^- \rightarrow CuCl_4^{2-}$	17.197	K_4 = 0.002

In addition to the complex formation, the presence of Cl^- can increase the anodic current during chalcopyrite leaching (Beiza et al., 2019). The electrochemical study of

(Lázaro et al., 1995) show that the poor leaching kinetics derived from an anodic passivation; one theory is that the passivation is caused by the formation of an insulating layer on the chalcopyrite surface. Cyclic voltammograms for the chalcopyrite concentrate in the presence and absence of 0.5 M sodium chloride are published by (Z.Y. Lu et al., 2000).

Table 4. Calculated Gibbs free energies for the proposed oxidation reactions (adapted from (Torres et al., 2015)

N°	Reaction	ΔG (kJ/mol) 25 °C	ΔG (kJ/mol) 60 °C
(11)	$CuFeS_2 + 3Cu^{2+} + 4Cl^- \rightarrow 4CuCl + Fe^{2+} + 2S^0$	-51.08	-61.19
(12)	$CuFeS_2 + 3CuCl^+ + Cl^- \rightarrow 4CuCl + Fe^{2+} + 2S^0$	-44.61	-51.74

According to Figure 7, chloride ions have a positive effect on the electrochemical behavior of chalcopyrite. The cyclic voltammograms for the chalcopyrite evidence the substantial effect on the electrochemical behavior when the chloride ion (0.5 M sodium chloride) is present. In particular, the anodic peak A1 is twice as great in the presence of chloride ions (Z.Y. Lu et al., 2000). Similar results were obtained by (Nicol, 2017) and attributed that the oxidation peaks obtained after passivation (between 750 and 850 mV) could be associated with the oxidation of CuS_2 or a similar polysulphide.

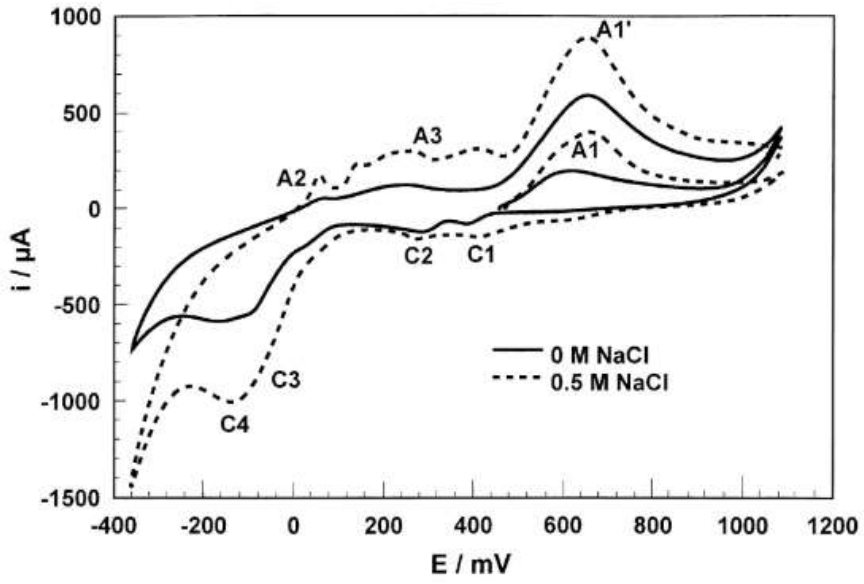

Figure 7. Voltammograms representing the NaCl effect on the oxidation/reduction of chalcopyrite. Experimental conditions: 1 M H_2SO_4 , 20 mV/s and 20 °C (Z.Y. Lu et al., 2000)

Finally, the presence of chloride also produces changes on the surface form and properties of the reaction product. The dissolution of chalcopyrite is favored because chloride modifies the morphology of the deposited sulphur, which becomes porous (Z.Y. Lu et al., 2000). According to (Majima et al., 1985), ferric chloride produced a more porous layer of elemental sulphur than with ferric sulphate. Studies performed by (Carneiro and Leão, 2007) confirmed by surface area and porosity measurements that chloride ions affect the morphology of the reaction product formed producing a porous and somewhat crystalline sulphur layer. The authors make a comparison of parameters (volume and area of microporous) of chalcopyrite concentrate and residues of ferric sulphate leaching with and without sodium chloride. The experimental conditions used by the authors: d_{50}: 5.5 µm, pH: 0.0 (initial); 50 g/L Fe^{3+}; 0.45 L/min O_2; 5.0 % solids (w/v); temperature: 95 °C, time: 4 h, NaCl: 1.0 mol/L (Carneiro and Leão, 2007). Results are included in Table 5.

Table 5. Surface parameters of chalcopyrite concentrate and residues of ferric sulphate leaching with and without NaCl (adapted from (Carneiro and Leão, 2007)

Parameter	Cpy concentrate	Residue after $Fe_2(SO_4)_3$ with NaCl	Residue after $Fe_2(SO_4)_3$ without NaCl
Surface area (m^2/g)	1.51 ± 0.23	1.41 ± 0.01	1.00 ± 0.04
Microporous vol. (cm^3/g)	(6.60 ± 0.84) $x10^{-4}$	(6.28 ± 0.05) $x10^{-4}$	(4.48 ± 0.06) $x10^{-4}$
Microporous area (m^2/g)	1.86 ± 0.23	1.78 ± 0.01	1.27 ± 0.02

Nitrate concentration

Due to its powerful oxidizing properties, nitrate media can also be used for extraction of copper from chalcopyrite (Sokić et al., 2019). The use of a $NaNO_3$ + H_2SO_4 system for the dissolution of chalcopyrite from a copper concentrate has been evaluated as an alternative. In the study carried out by (Sokić et al., 2009) they leached chalcopyrite using H_2SO_4 (1.5 M) with $NaNO_3$ at 80 °C, found that the leaching rate could be enhanced by

increasing the concentrations of $NaNO_3$. The copper extraction increased from 43 % to 75 % after 4 hours when the concentration of $NaNO_3$ was increased from 0.15 M to 0.90 M. The authors confirm that the dissolution of chalcopyrite using sulphuric acid requires an oxidizing agent because it is stable in aqueous solution up to electrochemical potential +0.337 V.

According to (Prasad and Pandey, 1998), the chalcopyrite dissolution takes place in the presence of sulphuric acid, which preferentially supplies hydrogen ions for completion of the reaction and in the presence of a small amount of nitric acid, which acted as a catalyst (Eq. 13).

$$CuFeS_2 + 5H^+ + \frac{5}{3}HNO_3 = Cu^{2+} + Fe^{3+} + 2S^0 + \frac{10}{3}H_2O + \frac{5}{3}NO \qquad \text{(Eq. 13)}$$

Nitric acid is an efficient oxidant, becoming reduced to nitric oxide (Eq.14), in which the protons are supplied by the sulphuric acid; nitric oxide can be re-oxidised to nitric acid in the presence of oxygen and water (Watling, 2013) (Eq. 15).

$$NO_3^- + 4H^+ + 3e^- = NO + 2H_2O \qquad \text{(Eq. 14)}$$

$$4NO + 3O_2 + 2H_2O += 4HNO_3 \qquad \text{(Eq. 15)}$$

According to (Hernández et al., 2015), Equation 13 can be explained alternatively by (Eq. 16). However and citing (Watling, 2013), the application of the nitrate-based leach solution presents other problems especially during subsequent solvent extraction stage.

$$CuFeS_2 + 6.667H^+ + 1.667NO_3^- = Cu^{2+} + Fe^{3+} + 2S^0 + 3.333H_2O + 1.66NO \qquad \text{(Eq. 16)}$$

Acidity

According to (Velásquez-Yévenes et al., 2010a) the authors evaluates the chalcopyrite leaching in chloride media and reports that the dissolution rate is independent of pH in the range between 0.5 and 2 (Figure 8). The authors report that at pH 2.1 it is possible to see iron precipitates in the system, but these would not affect the copper dissolution. The authors postulate according to (Dutrizac, 1981), that low acidity must be avoided due to iron hydrolysis and precipitation which can affect the leaching process.

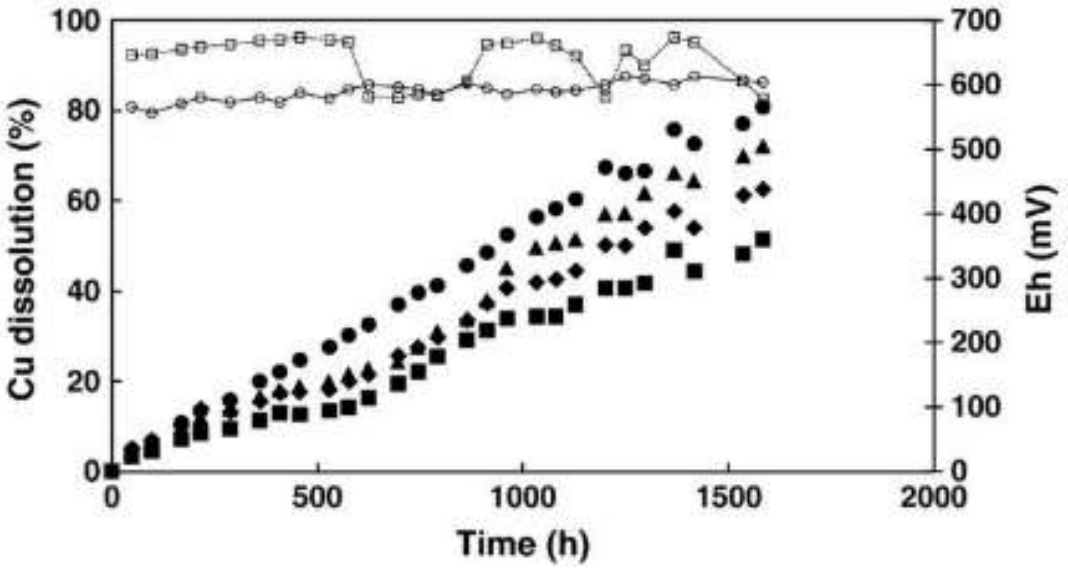

Figure 8. Effect of pH (■) 0.34, (♦) 0.7, (▲) 1.3 and (●) 2.1 on copper dissolution from chalcopyrite concentrate in 1 M chloride containing 0.2 M HCl. The solution potentials (open symbols) for the experiments at pH 0.34 and pH 2.1, are also shown (Velásquez-Yévenes et al., 2010a)

Studies performed by (Córdoba et al., 2009) report a similar trend to Velásquez et al. (2010a), but in ferric sulfate media, the chalcopyrite dissolution is favored in a pH range of 1.5 and 2, while at pH less than or equal to 1 there is a negative effect. At pH 2, the nucleation and precipitation of a passivating layer of jarosite on mineral particles was very marked. The effect of pH in the chalcopyrite dissolution has also been evaluated by (Ibáñez and Velásquez, 2013). The authors postulate that chalcopyrite leaching can be favored at a pH around 2.5 because there is no iron in solution since precipitates of this element are formed. These precipitates causing a decrease in the solution potentials where speed is acceptable. The presence of iron precipitates under the conditions studied by the authors did not affect the chalcopyrite dissolution (Ibáñez and Velásquez, 2013).

Solution potential

Several authors have carried out research seeking to establish the dependence and influence of solution potential in chalcopyrite leaching (Hiroyoshi et al., 2008, 2001; Ibáñez and Velásquez, 2013; Nicol, 2017; Warren et al., 1992). The studies conclude that this parameter is one of the most important and that its control would facilitate the chalcopyrite dissolution (Córdoba et al., 2008b; Martínez-Gómez et al., 2018; Velásquez-Yévenes et al., 2010b).

According to (Córdoba et al., 2008b) the authors determined that high potential values (over 600 mV) would generate a rapid passivation of chalcopyrite. According to these authors, the effect that the solution potential produces on the kinetics of copper extraction is more significant at high temperatures (68 °C) than at low values (35 °C). In the tests carried out at 68 °C and at the initial solution potential value of 300 and 400 mV (Ag/AgCl), copper extractions of 80 and 90% respectively were achieved, while at higher potentials the dissolutions were less than 40% (Córdoba et al., 2008b).

The study developed by (Velásquez-Yévenes et al., 2010b) studied chalcopyrite leaching in chloride solutions at 35 °C, 0.5 g/L Cu^{2+}, 0.2 M HCl and with the solution potential control by injection of nitrogen and oxygen. The authors observed that at solution potentials between 560-620 mV (SHE) chalcopyrite leached at acceptable rates. However, at solution potential values greater than these, chalcopyrite was passivated and with lower values chalcopyrite was not leached. Additionally, (Velásquez-Yévenes et al., 2010b) mention about the reversibility of the passivation. The authors observed that the dissolution rate of chalcopyrite at solution potentials of 450 mV (SHE) was very low and when the solution potential of this same experience increased to values of 550 mV (SHE), the speed was remarkably improved (Fig.9). A similar situation occurred when the solution potential decreased from 650 to 550 mV (SHE), the copper dissolution kinetics was improved at this last solution potential value.

The anodic characteristics of natural chalcopyrite electrodes in acidic chloride solutions by voltammetric test, has been studied by (Nicol et al., 2017). According to the authors, the solution potential range where the copper dissolution is increased (0.7 to 0.85 V) depends on the chloride concentration and, particularly, in the pH range between 1 and 3. Furthermore, three peaks are observed at low chloride concentrations that merge into one peak at high concentrations.

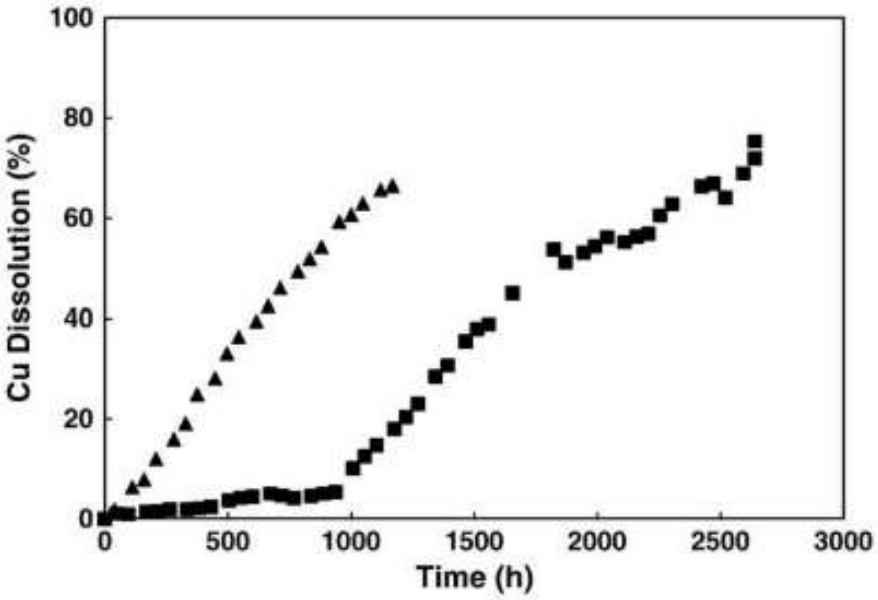

Figure 9. Copper dissolution from chalcopyrite concentrate in a solution of 0.2 M HCl and 0.5 g/L of Cu^{2+} at 35 °C and (▲) 580 mV and (■) 450 mV with potential increased to 550 mV after 936 h (Velásquez-Yévenes et al., 2010b). Passive and transpassive anodic behavior of chalcopyrite in acid solutions

Particle size

It is well known the relationship between the size of particle and copper dissolution. Particularly, regarding leaching, a smaller particle size generates a greater area of exposure of the mineral to the leaching solution (area of reaction), due to the greater release of the species of interest (Lwambiyi et al., 2009; Ruiz et al., 2014).

Tests in sulfate and chloride media evaluating the chalcopyrite dissolution were carried out by (Dutrizac, 1981). The author determined that the copper extraction increases as the mean particle size is decreased below 100 mesh (149 µm). Similar behavior was observed in the chloride system, except that the rates were correspondingly more rapid. Similar results were obtained by (Velásquez-Yévenes et al., 2010a) in leaching tests over a chalcopyrite concentrate under standard conditions at controlled solution potential. These authors demonstrate an important difference in copper extraction when comparing a size range between +25 - 38 µm versus - 25 µm. The results obtained can be observed in Figure 10.

Finally, (Dutrizac, 1981) argued that the independence of the chalcopyrite dissolution with the particle size is wrong and this is due to a problem derived of obtaining a well characterized surface area. This is ratified by (Wilson and Fisher, 1981) who concluded that In chloride media, the leaching rate is directly proportional to the surface area.

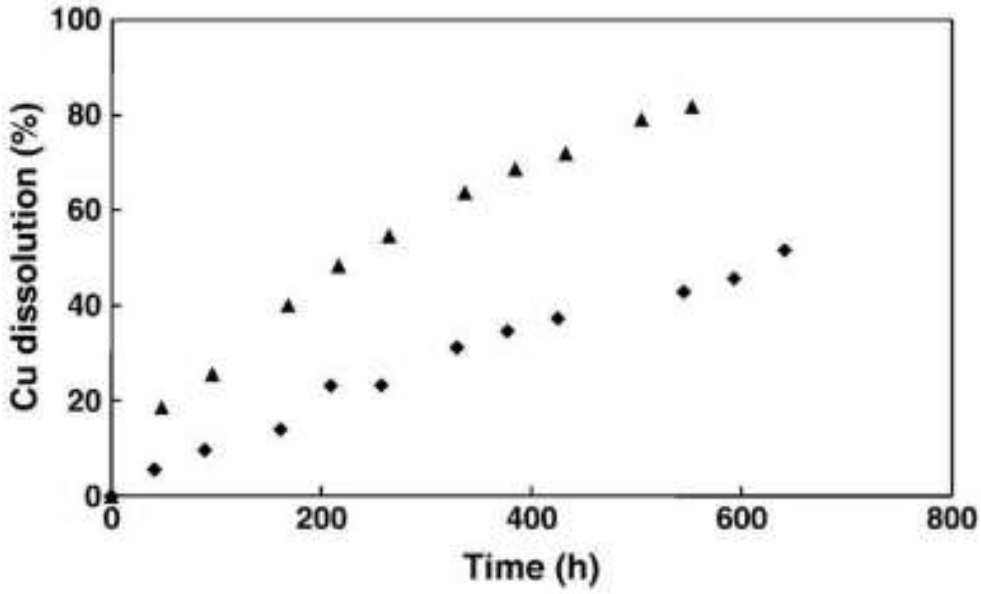

Figure 10. Leaching curves for the dissolution of (♦) +25–38 µm and (▲) −25 µm size fractions of chalcopyrite concentrate under standard conditions (Velásquez-Yévenes et al., 2010a)

Temperature

There is a general agreement of several authors that the influence of temperature on the chalcopyrite dissolution is significant; increasing the temperature improves the leaching kinetics (Ibáñez and Velásquez, 2013; Velásquez-Yévenes and Quezada-Reyes, 2018). Studies carried out by (Córdoba et al., 2008b), demonstrate the positive effect of temperature within a range 35 - 68 °C in acidic ferric sulfate leaching solutions at 400 mV (Ag/AgCl), 5 g/L of total iron and 0.5 % pulp density, obtaining an activation energy of 130.7 kJ/mol (Figure 11).

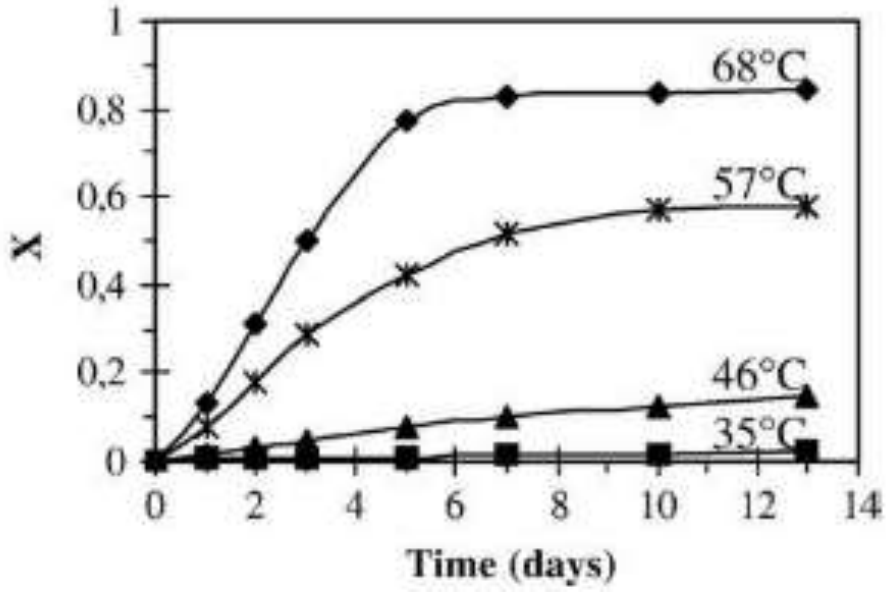

Figure 11. Influence of temperature on the chalcopyrite leaching, fraction of reacted chalcopyrite vs. Time (Córdoba et al., 2008b)

The dissolution of chalcopyrite in reactors is positively affected with the increase in temperature between 35 and 75 °C, using 50 g/L Cl^-; 0.5 g/L of Cu^{2+} and 0.2 M H_2SO_4, obtaining an activation energy value of 96.55 kJ/mol. The obtained value indicates that the dissolution rate, under the studied conditions, is controlled by the chemical reaction (Ibáñez and Velásquez, 2013). On the other hand (Majima et al., 1985) performed tests using a natural chalcopyrite sample in 0.1 M of ferric chloride, evaluating from 55 to 84 °C, reporting an activation energy of 69 kJ/mol. Variable activation energy values, below and above 85 °C, have been reported by (Z. Y. Lu et al., 2000). According to (Lawson et al., 1992) who considered oxygen solubility data (Narita et al., 1983); proposes that the activation energy during the initial stages of chalcopyrite leaching was 48 kJ/mol at low temperatures, and 20 kJ/mol at high temperatures. It can be seen that these activation energies are highly variable and depend on many experimental factors and conditions (Vyazovkin, 2016).

Excellent works from several authors compare ranges of activation energy values for chalcopyrite dissolution (Al-Harahsheh et al., 2008; Córdoba et al., 2008b; Dutrizac, 1992; Ibáñez and Velásquez, 2013; Z. Y. Lu et al., 2000; Velásquez Yévenes, 2009; Veloso et al., 2016). According to (Velásquez Yévenes, 2009), no agreement has been reached on the value of activation energy which varies between 20 and 135 kJ/mol and even higher values

have been reported. Several researchers indicates that the activation energy is dependent on the range of temperature studied and on the value of the ratio of Cu(II)/Cu(I) present in the system. Furthermore, another authors proposes that since the oxygen solubility varies with temperature, suitable corrections must be made to the measured reaction rates (Z.Y. Lu et al., 2000). A value of 42 kJ/mol was reported by (Dutrizac, 1981), as being the probable value for the leaching of reasonably pure chalcopyrite in ferric chloride solutions.

3.2 Results of pretreatment and leaching efficiency of chalcopyrite

3.2.1 Characterization of the chalcopyrite mineral

The chemical characterization of the chalcopyrite sample is shown in Table 6. A very characteristic presence of copper, iron and sulphur is observed in this type of samples, due to the weight percentage of each element in the chalcopyrite formula ($CuFeS_2$). Other minor elements were detected, such as: Na (0.220%), Ca (0.180%) and Zn (0.0800%). Additionally, after chemical characterization, the insoluble residue represented 21% of the total mass. This value suggests the presence of quartz or muscovite as insoluble phases present in the sample.

Figure 12 (X-ray diffractogram) shows that the sample contained mainly chalcopyrite and quartz, also was detected the presence of covellite, pyrite and chalcanthite. Sulphur, in addition to being associated with chalcopyrite, can be associated with other species such as chalcocite, covellite or pyrite. Table 7 shows the mineralogical composition of the sample, obtained by Qemscan analysis. The main species was chalcopyrite (73.7%), followed by quartz (16.3 %) and covellite (1.80 %). According to Qemscan analysis, quartz has a presence of 16.3% which coincides with the insoluble residue product of the chemical characterization (21%).

According to the image obtained using a reflected optical microscope, chalcopyrite was also being associated with covellite (Figure 13). The presence of chalcanthite was also evidenced by SEM analysis (Fig 14d). Figure 14c shows a particle size distribution close to 20 µm. SEM and EDS analysis showed the majority presence of chalcopyrite, quartz and copper sulphate in the initial sample. EDS analysis associated with the initial characterization of the chalcopyrite sample are presented in appendix 4. Finally, the presence of chalcanthite was measured by washing the sample in water, a 9% copper extraction was obtained.

Table 6.Chemical analysis of the chalcopyrite ore

Element	Cu	Fe	S
Mass (%)	28.5	22.8	29.7

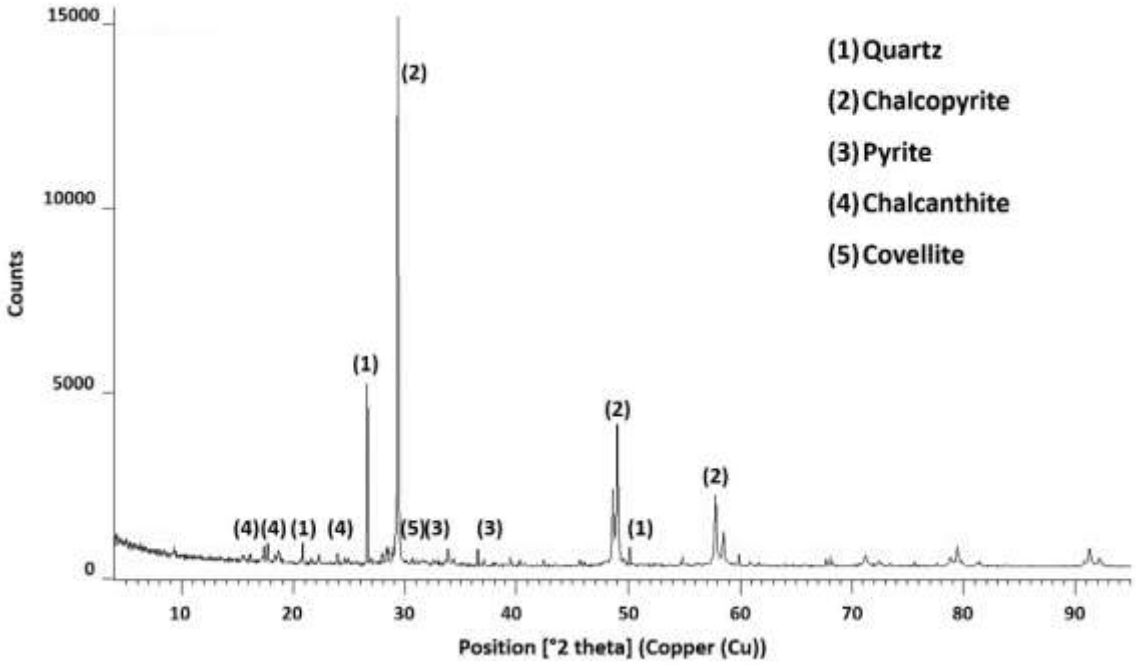

Figure 12. X-ray diffractogram of the initial sample

Table 7.Main mineralogical composition of the initial sample (mass in %) according to Qemscan analysis

Mineral	Mass, %
Chalcopyrite	73.7
Quartz	16.3
Covellite	1.80
K-Feldspar (orthoclase, anorthoclase)	1.80
Pyrite	1.30
Molybdenite	1.00
Alunite	0.900
Other gangue	2.60
Other Cu minerals	0.600

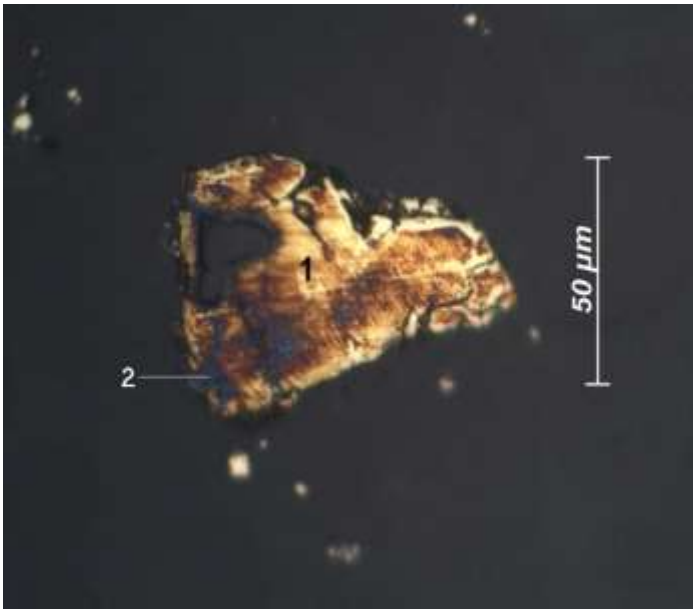

Figure 13. Reflected optical microscope image of the initial sample. 1: chalcopyrite, 2: covellite

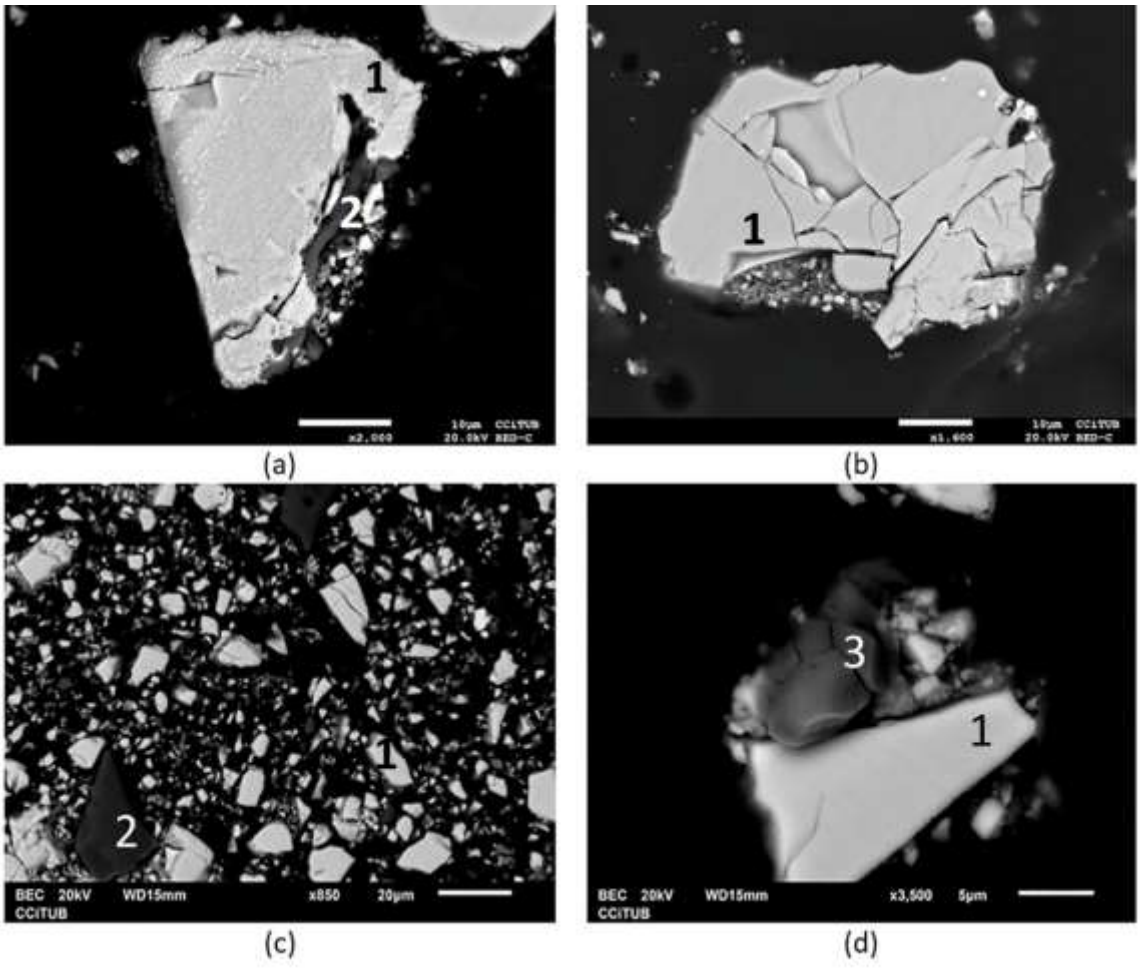

Figure 14. SEM image of the initial sample. 1: chalcopyrite, 2: quartz, 3: copper sulphate (chalcanthite)

3.2.2 Pretreatment of the chalcopyrite mineral

The effect of NaCl and KNO_3 in curing tests have been evaluated using tests designed with the Taguchi method. In both cases, a L_{16} (4^3) design has been considered with three parameters and four levels for each one, as shown in Table 8 and Table 9.

Table 8.Parameters and levels studied in the experiments with NaCl in acid media

	Parameters	Levels			
		1	2	3	4
A	Curing time (days)	0	5	10	15
B	H_2SO_4 (kg/t)	0	5	10	15
C	NaCl (kg/t)	0	5	10	15

Table 9. Parameters and levels studied in the experiments with KNO_3 in acid media

	Parameters	Levels			
		1	2	3	4
A	Curing time (days)	0	5	10	15
B	H_2SO_4 (kg/t)	0	5	10	15
C	KNO_3 (kg/t)	0	5	10	15

The effect of nitrate in the acid media

Table 10 shows the average of copper extraction (averages of duplicate tests) from the pretreatment tests using KNO_3, H_2SO_4 and different curing days. The effects on the copper extraction were minimal considering that a 9 % of copper extraction is associated to chalcanthite and it is water soluble. According to the characterization and mass balance, covellite represented 4% of total copper. Thus, a copper extraction over 13 % guarantees solubility of the chalcopyrite product from the pretreatment. Under these conditions, the non-significant effects of the variables are evident. according to (Hernández et al., 2019) reported favorable effects of using $NaNO_3$ and NaCl in the pretreatment of a copper sulphide mineral. The authors confirmed the study of (Shiers et al., 2016), who concluded that a mixture with high NaCl concentrations and $NaNO_3$ in an acid media was more effective. However, the present study did not evaluate the synergy of the two reagents, and there was no significant effect of KNO_3 as an additive in the pretreatment of a chalcopyrite mineral.

Table 10.Copper extraction (average) in the pretreatment of a chalcopyrite mineral using H_2SO_4, KNO_3 and curing time

Curing time (days)	H_2SO_4 kg/t	KNO_3 kg/t	% Cu extraction (average)
0	0	0	10.27
0	5	5	10.55
0	10	10	10.74
0	15	15	10.86
5	0	5	10.15
5	5	0	10.75
5	10	15	11.40
5	15	10	11.64
10	0	10	11.05
10	5	15	11.64
10	10	0	12.12
10	15	5	12.69
15	0	15	11.11
15	5	10	12.17
15	10	5	12.13
15	15	0	12.44

Table 11 shows the results of the ANOVA analysis based on the data in Table 10. According to this ANOVA analysis, parameter A (curing time) made the most significant contribution to the variation in the Cu extraction (54.66%) with a significant p-value, parameter B (sulphuric acid) had a moderate contribution (35.75%), with a significant p-value and finally, parameter C (KNO_3) had an extremely low contribution (0.61%), with a non-significant p-value. As can be seen, the contributions of A and B are statistically significant according to the p-values (99% confidence level).

Table 11.Results of the ANOVA analysis of the parameters for the Cu extraction, with varying concentrations of H_2SO_4 and KNO_3 and curing time (df = degrees of freedom, SSE = sum of squared errors, MSE = mean squared errors)

	Parameters	df	SSE	MSE	F value	Contribution %	P value
A	Curing time (days)	3	10.7	3.566	44.68	54.66	$1.578*10^{-9}$
B	H_2SO_4 (kg/t)	3	6.997	2.332	29.23	35.75	$7.391*10^{-8}$
C	KNO_3 (kg/t)	3	0.1192	0.0397	0.50	0.61	0.6876
	Error	22	1.756	0.0798			
	Total	31	19.57				

To obtain the optimum performance, Equation 1 is maximized according to the yield value given by Cu dissolution. The degrees of influence or effect of the parameters are shown in Figure 15. Figure 15A shows that the optimum value is obtained with level 4, which is 15 curing days. Copper extraction improve with more curing days (Cerda et al., 2017; Hernández et al., 2019; Velásquez-Yévenes and Quezada-Reyes, 2018). Note that level 1, which is 0 days, has a much poor performance than the other levels evaluated, and there is little difference between levels 3 to 4, which indicates a law of diminishing returns at this point, that is, longer curing times do not significantly increase Cu extraction. Figure 15B shows that the optimum is obtained with level 4, which is 15 kg/t of H_2SO_4, representing an almost linear performance increase for this parameter. Figure 15C shows that the optimum is obtained with level 3, with 10 kg/t of KNO_3. Numerical variations are very low compared to the other factors.

The analysis of the results shows that the optimal configuration is (4, 4, 3), i.e. , curing days (A): Level 4 or 15 days, H_2SO_4 concentration (B): Level 4 or 15 kg/t, and KNO_3 concentration (C): Level 3 or 10 kg/t. The optimal configuration is not found in the experimental results. Therefore, it is possible that the true optimum is outside the established limits. However, the extractive power of these variables is minor, representing not more than 3% of Cu extraction (without considering the dissolution of chalcanthite, which represents 9% of Cu dissolution). According to the linear model, the optimal Cu extraction with this configuration is 12.55%. This test obtained an average Cu extraction of 12.93%. Among the configurations in the orthogonal arrangement, (4, 4, 1) obtained the best performance, with a predicted Cu extraction of 12.55% (the same as the theoretical optimum, given that factor C has practically no influence), followed by (3, 4, 2) with 12.45%. Considering that the influence of factor C is not significant according to ANOVA, it makes sense that levels 1 or 2 can be used. Table 12 shows the experimental and predicted values.

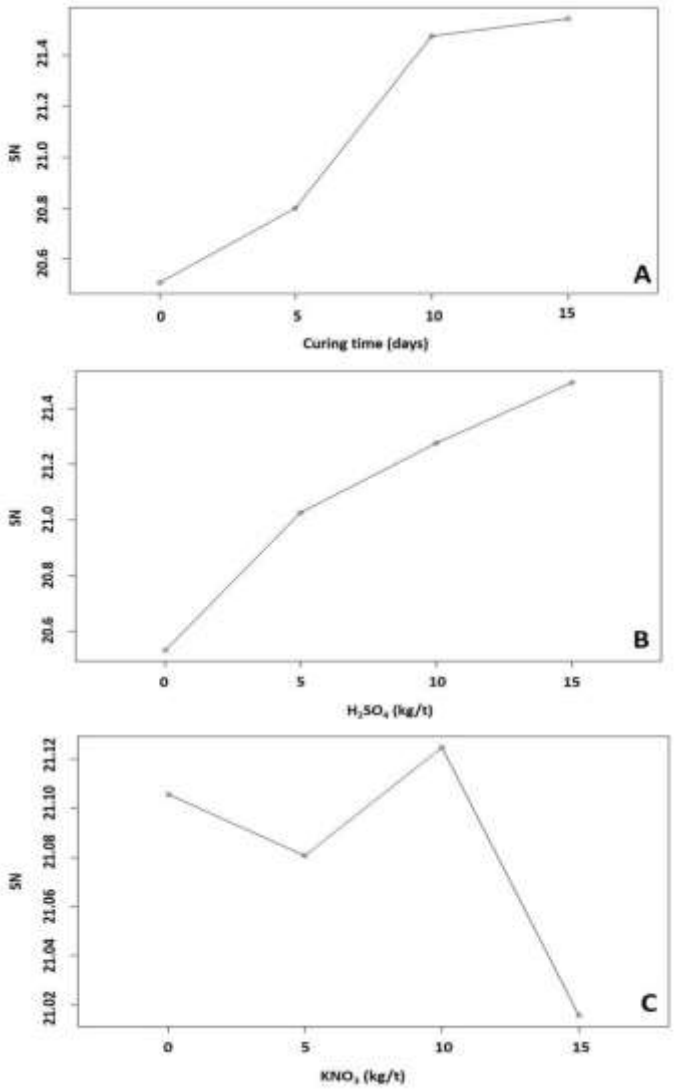

Figure 15. Effect of the parameters curing days (A), concentration of sulphuric acid (B) and concentration of KNO_3 (C) on the SN_L optimization criterion for Cu extraction prior to leaching

Table 12. Experimental results and the values predicted by the linear model given by Equation 2, with varying curing time, concentrations of H_2SO_4 and KNO_3

A	B	C	% Cu extraction (average)	Predicted % Cu
1	1	1	10.27	9.930
1	2	2	10.55	10.55
1	3	3	10.74	10.89
1	4	4	10.86	11.05
2	1	2	10.15	10.29
2	2	1	10.75	10.94
2	3	4	11.40	11.12
2	4	3	11.64	11.57
3	1	3	11.05	11.21
3	2	4	11.64	11.69
3	3	1	12.12	12.16
3	4	2	12.69	12.45
4	1	4	11.11	11.14
4	2	3	12.17	11.92
4	3	2	12.13	12.22
4	4	1	12.44	12.55

The effect of chloride in the acid media

Table 13 shows the resulting Cu extraction (average of duplicates) with the variables NaCl, H_2SO_4 and curing time. With 0 curing days, the copper extraction was between 10 and 10.82%, which is expected, considering that the sample had 9% copper associated with chalcanthite, i.e. between 1 and 2% copper had been dissolved with pretreatment. The highest copper extraction was obtained with 10 and 15 curing days. In addition, the synergy between NaCl and H_2SO_4 increased copper extraction. Some tests yielded Cu extraction of about 13%, which indicates the reactivity of the chalcopyrite under these conditions. The benefit of using NaCl in the pretreatment has been evidenced by previous research (Cerda et al., 2017; Hernández et al., 2019). However, the effect of pretreatment had only been evaluated in terms of leaching efficiency, but not prior, as in this thesis.

According to Table 13 and Table 14, parameter A (curing time) accounted for the major part of variation in the Cu extraction (56.36%), with a significant p-value. Parameter B (H_2SO_4 concentration) made an extremely low contribution (1.78%), with a non-significant p-value. Finally, parameter C (NaCl concentration) represented a moderate contribution

(23.09%), with a significant p-value. Most of these contributions are statistically significant according to the p-values obtained (significant A and C at a 99% confidence level) (Table 14).

Table 13. Copper extraction (average) in the pretreatment of a chalcopyrite mineral varying curing time, concentration of H_2SO_4 and NaCl

Curing time (days)	H_2SO_4 kg/t	NaCl kg/t	% Cu extraction (average)
0	0	0	10.27
0	5	5	10.54
0	10	10	10.63
0	15	15	10.82
5	0	5	10.08
5	5	0	10.18
5	10	15	14.71
5	15	10	14.29
10	0	10	14.56
10	5	15	16.08
10	10	0	11.87
10	15	5	16.91
15	0	15	15.95
15	5	10	15.92
15	10	5	15.91
15	15	0	12.58

Table 14.Results of the ANOVA analysis of the parameters for the Cu extraction with varying concentrations of H_2SO_4, NaCl and curing times (df = degrees of freedom, SSE = sum of squared errors, MSE = mean squared errors)

	Parameters	df	SSE	MSE	F value	Contribution %	P value
A	Curing time (days)	3	112.4	37.47	22.017	56.36	$8.047*10^{-9}$
B	H_2SO_4 (kg/t)	3	3.544	1.181	0.6942	1.780	0.5654
C	NaCl (kg/t)	3	46.04	15.35	9.018	23.09	$4.3817*10^{-4}$
	Error	22	37.44	1.702			
	Total	31	199.4				

Figure 16 shows the degrees of influence or effect of the parameters. In Figure 16A, it can be seen that the optimum is obtained at level 4 (15 days), the copper extraction improves with more curing time. Note that level 1, which is 0 days, has a much poor performance than the other evaluated levels, and that there is little difference between

levels 3 to 4, which indicates a law of diminishing returns at this point. Figure 16B shows that the optimum is obtained at level 4, which is 15 kg/t of H_2SO_4, representing a linear performance increase for this parameter. However, the ANOVA indicates that the influence of factor B is not significant. Figure 16C also shows that the optimum of NaCl is 15 kg/t. As in the other cases, level 1 with 0 kg/t has a much lower yield.

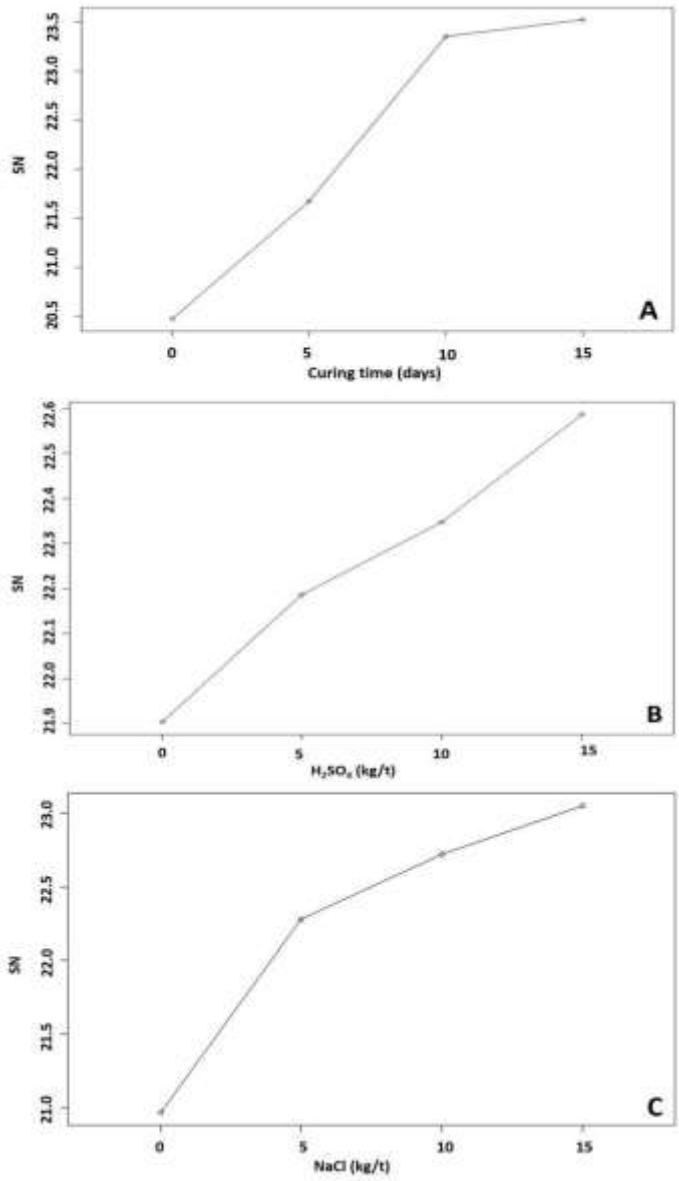

Figure 16. Effects of the parameters curing days (A), concentration of H_2SO_4 (B) and concentration of NaCl (C) on the SN_L optimization criterion for the Cu extraction prior to leaching

The best configuration is (4, 4, 4): Curing days (A): Level 4 or 15 days; H_2SO_4 concentration (B): Level 4 or 15 kg/t, and NaCl concentration (C): Level 4 or 15 kg/t. Since

the optimal levels are not found in the experimental configuration, there is a possibility that the true optimum is outside the established limits. The configuration (4, 4, 4) is not found in the orthogonal array, so it was not possible to obtain an empirical result for this configuration. However, according to the linear model, the optimal copper extraction with this configuration is 16.72%. The combination (4, 4, 4) and obtained an average Cu extraction of 19.56% was tested. In order to demonstrate the behavior of the mineral outside the studied ranges, tests were performed increasing the NaCl concentration until to 25 kg/t, this being the saturation point of the solution. The use of 25 kg/t of NaCl, under the conditions evaluated in this study is the maximum allowable according to its solubility in water.

Finally, with a combination of 15 curing days, 15 kg/t of H_2SO_4 acid and 25 kg/t of NaCl, a copper extraction of 22.66% was obtained. Among the configurations in the orthogonal arrangement, (3, 2, 4) had the best performance, with a predicted extraction rate of 16.01%, followed by (4, 1, 4) with 15.79%. Table 15 shows the details of the experimental and predicted Cu extractions.

Table 15. Experimental results and the values predicted by the linear model in Equation 2, with varying concentrations of H_2SO_4, NaCl and curing times

A	B	C	% Cu extraction (average)	Predicted % Cu
1	1	1	10.27	8.100
1	2	2	10.54	10.69
1	3	3	10.63	11.28
1	4	4	10.82	12.19
2	1	2	10.09	11.98
2	2	1	10.18	10.31
2	3	4	14.71	13.57
2	4	3	14.29	13.40
3	1	3	14.56	15.01
3	2	4	16.08	16.01
3	3	1	11.88	12.95
3	4	2	16.91	15.45
4	1	4	15.96	15.79
4	2	3	15.92	15.71
4	3	2	15.91	15.32
4	4	1	12.59	13.56

3.2.3 Characterization of pretreatments products

The best result obtained with the pretreatment of chalcopyrite, that is: 25 kg/t NaCl, 15 kg/t H_2SO_4 and 15 days of curing time. The solids obtained has been characterized to propose a mechanism associated with the pretreatment of chalcopyrite. The pretreatment product (agglomerated solids) was prepared and polished without any contact with water, preventing the dissolution of soluble phases. The briquettes formed and surface photographs are observed in Figure 17, obtained with a stereographic microscope.

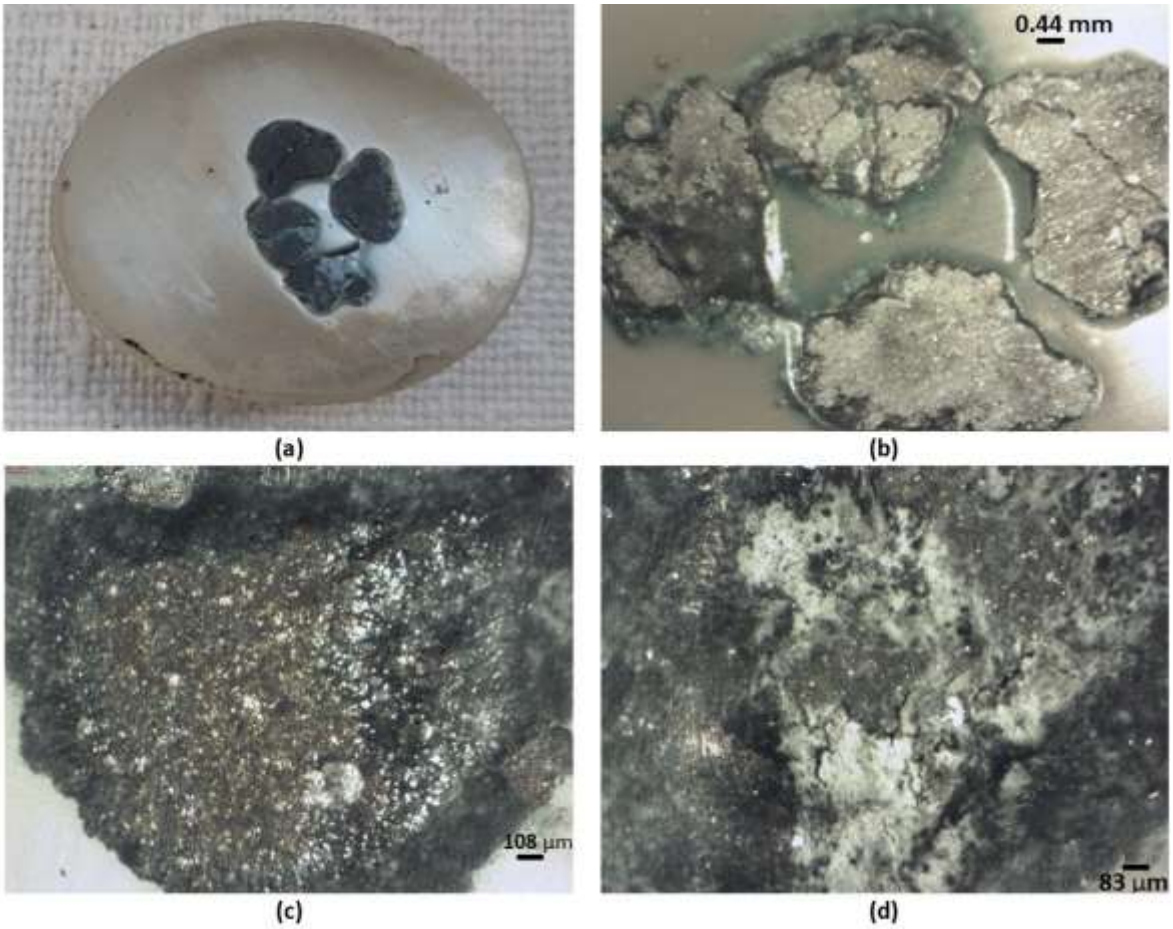

Figure 17. Images of agglomerates obtained observed in a stereographic microscope

Figure 18 shows the images performed by optical microscopy carried out over the sample with pretreatment (Figure 17a). A chalcopyrite particle eventually associated with covellite, can be seen in Figure 18a. Several cracks are observed on the particle. These cracks are not observed, or at least not so evident in the initial sample (Figure 13). Figure

18b shows something very similar to 18a, associated with the formation of cracks and even products formed on it. Eventually, there could be chemical crushing base on the shape of the particle. Figure 18c shows an area with eventual formation of copper sulfate or chloride-copper complex (green with white area). According to the copper extraction achieved, using 15 kg/t of H_2SO_4, 25 kg/t NaCl and 15 days of curing was 22.66%, evidencing the formation of new soluble phases. Therefore, Figure 18c shows the formation of a new soluble phase, such as CuCl, according to (Cerda et al., 2017) or $CuCl_2$ complex formation is also possible, according to (Hernández et al., 2019). These proposed (Eq.3 and Eq.6) have a negative Gibbs energy values, so these reactions are thermodynamically feasible.

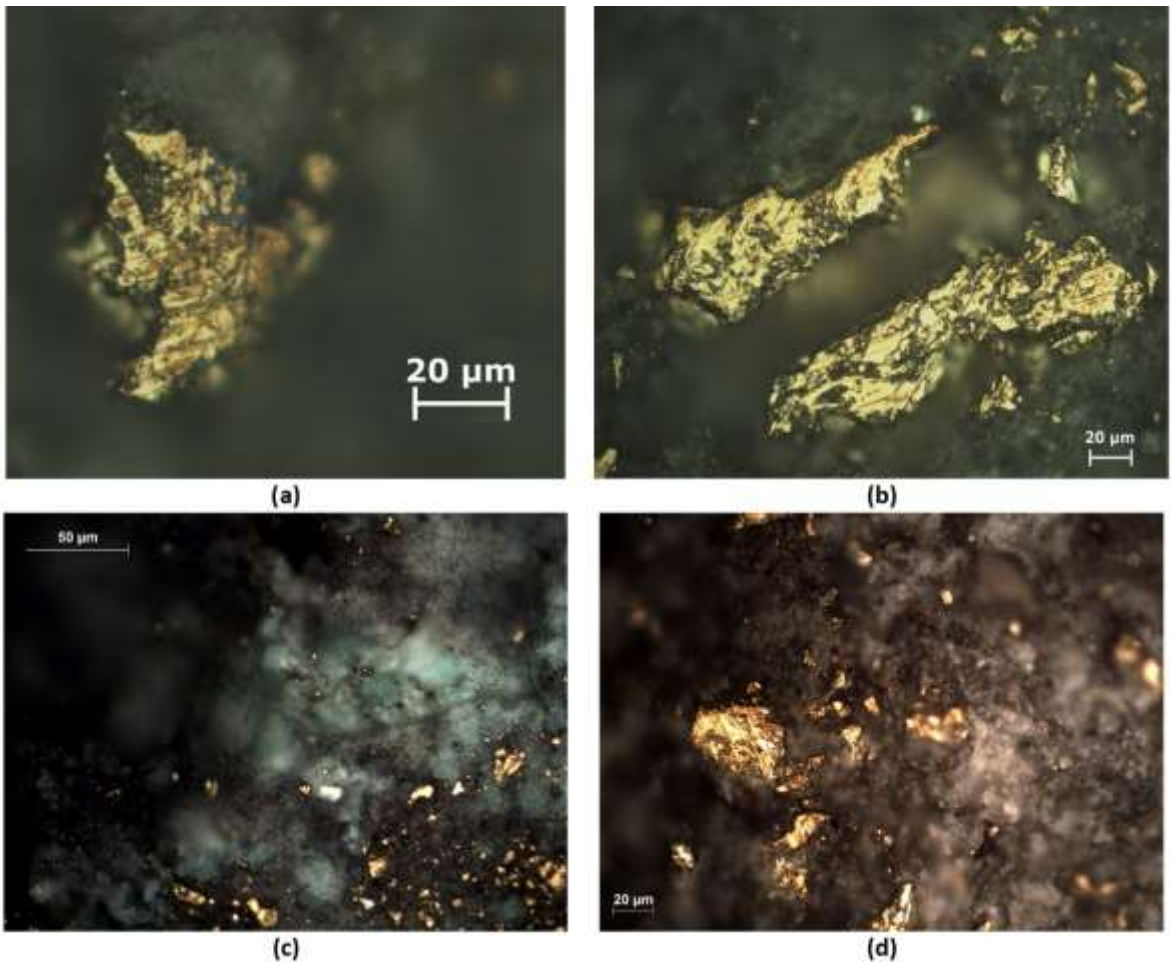

Figure 18. Reflected optical microscope images of the pretreatment products

X-ray diffraction analysis has also been performed on the pre-treatment products. Figure 19 indicates the presence of quartz and chalcopyrite. Quartz maintains its presence due to the fact that it is not reactive in acidic solutions (Bai et al., 2018). The presence of

chalcopyrite continues to be abundant. It is evident that not all $CuFeS_2$ reacted during the pretreatment, which coincides with results shown in Figure 18. Additionally, the presence of natrojarosite is evidenced ($NaFe_3(SO_4)_2(OH)_6$), product formed from the association between Na (derived from NaCl) and Fe (derived, eventually, from chalcopyrite). Both quartz, chalcopyrite, and natrojarosite are the species reported to be most abundant in the pretreatment product. Other products like ($CuSO_4$), Cu_2ClOH and S^0 have been identified. The presence of an iron sulfate has been reported as probable (Hernández et al., 2019) (according to Eq.6). Likewise, the presence of elemental sulphur has been proposed by (Cerda et al., 2017; Hernández et al., 2019). These authors proposed the formation of a complex CuCl or $CuCl_2$, which differs from what was identified in this investigation.

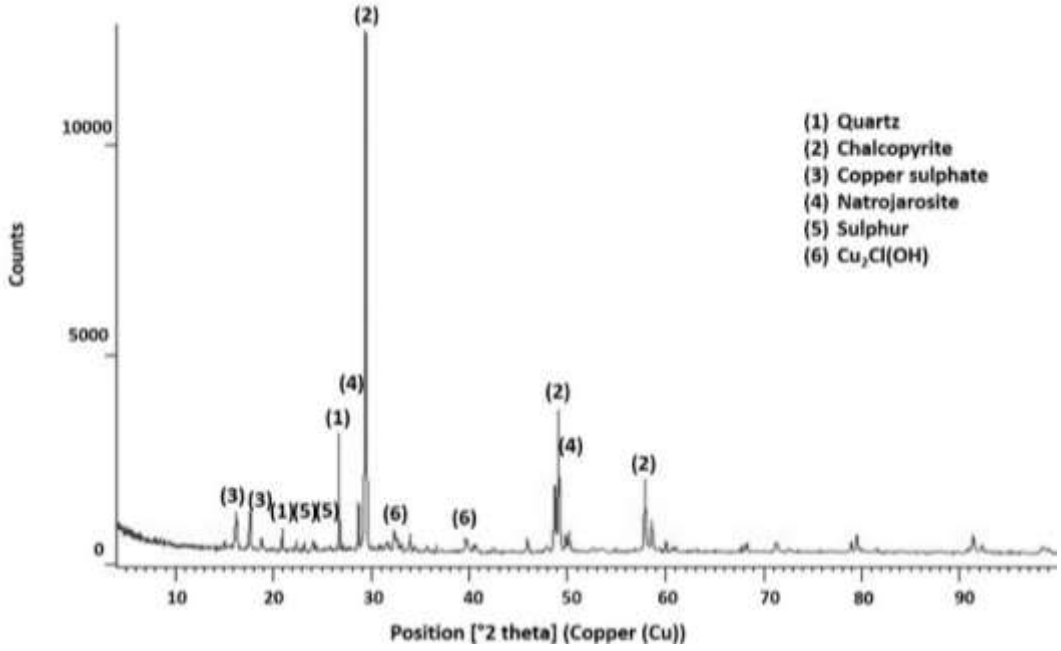

Figure 19. Species identified using X-ray diffraction analysis, products of the pretreatment of a chalcopyrite mineral with 15 kg/t H_2SO_4, 25 kg/t NaCl and 15 days of curing time at room temperature

The presence of: $CuSO_4$, $NaFe_3(SO_4)_2(OH)_6$, S^0 and $Cu_2Cl(OH)$ can be confirmed comparing the X-ray diffractogram of the original chalcopyrite with respect to the X-ray diffractrogram of the pretreatment products. Using the software X'pert HighScore Plus v.3.0e, it is possible to show the main angle or angles with the peak of presence characteristic of each species. The angle (in 2 theta) of 16.16° is characteristic of $CuSO_4$. Although, in the initial sample there is the presence of $CuSO_4$ (as chalcantite), the peak at

16.16° denotes a greater presence of this species (or at least, a very similar species in the structure) (Figure 20). By using 15 kg/t H_2SO_4, 25 kg/t NaCl and 15 days of curing at room temperature, 22.6% Cu dissolution was obtained. Considering that 9% of the copper extraction is associated with chalcantite, there is more than 10% of copper that dissolves as a result of the generation of a new soluble species.

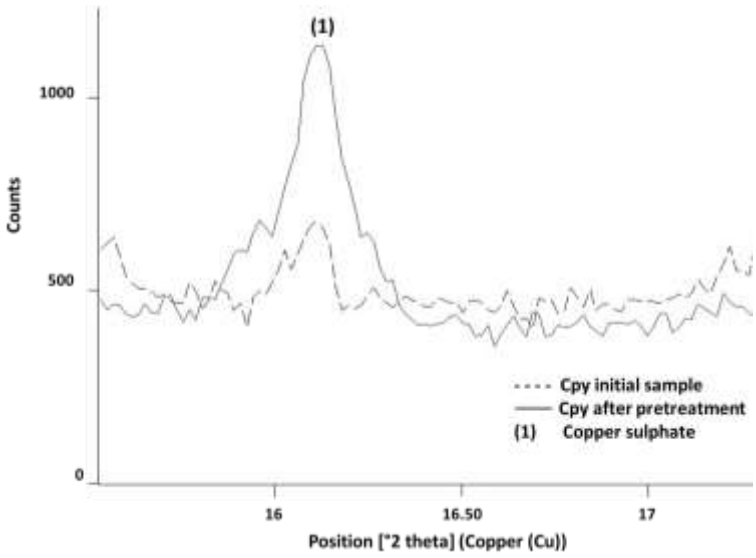

Figure 20. Identification of $CuSO_4$, using X-ray diffraction analysis, in the products of the pretreatment of a chalcopyrite with 15 kg/t H_2SO_4, 25 kg/t NaCl and 15 days of curing at room temperature

In Figure 21, the characteristic angles of the natrojarosite can be observed, such as 28.65° (21a) and 49.79° (21b), with point 28.65° being the angle associated with an intensity of 95%. According to (Gnanavel et al., 2015) In the system Na–Fe–SO_4–OH, only 4 phases are reported: the natrojarosite $NaFe_3(SO_4)_2(OH)_6$, the jarosite $Na_{0.84}Fe_{2.86}(SO_4)_2(OH)_6$ and 2 hydrated phases, the sideronatrite $Na_2FeOH(SO_4)_2.3H_2O$ and metasideronatrite $Na_2FeOH(SO_4)_2{\cdot}H_2O$. These phases are minerals but could be prepared by precipitation or under hydrothermal conditions. Therefore, the formation of an iron hydroxysulfate, such as natrojarosite, is possible.

The presence of S is also reported and compared with the initial chalcopyrite sample. In Figure 22a the presence of S^0 is evidenced by the main angle of 23.07°, which represents an intensity of 100% in the case of S^0. According to (Zhong and Li, 2019), when no strong oxidative conditions were available to produce SO_4^{2-}, the predominant S products upon

$CuFeS_2$ leaching was S^0. Therefore, it can be inferred that in the pretreatment, the formation of S^0 is possible, since the oxygen present is supplied by the solution and limited because the samples were covered.

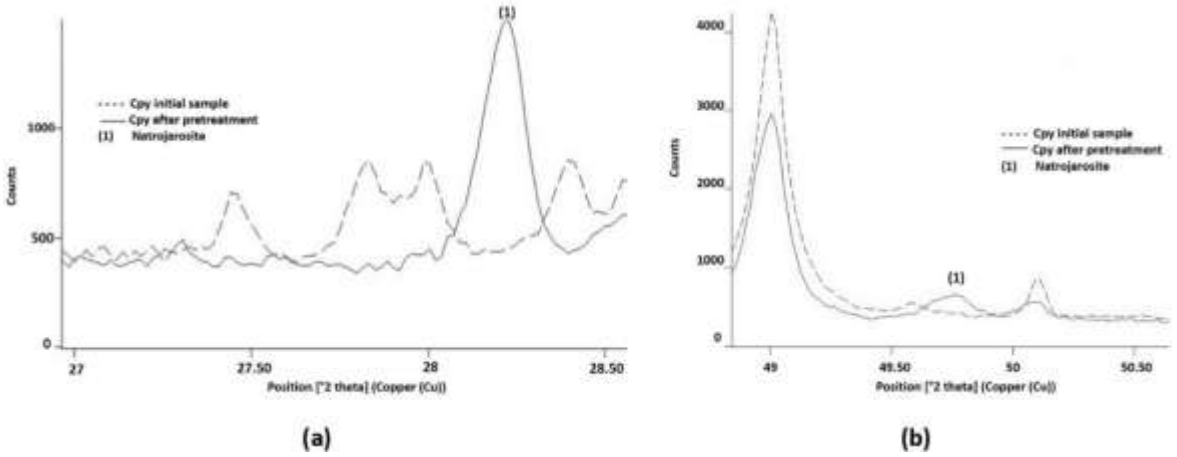

Figure 21. $NaFe_3(SO_4)_2(OH)_6$ identified, using X-ray diffraction, product of the pretreatment of a chalcopyrite mineral with 15 kg/t H_2SO_4, 25 kg/t NaCl and 15 days of curing at room temperature

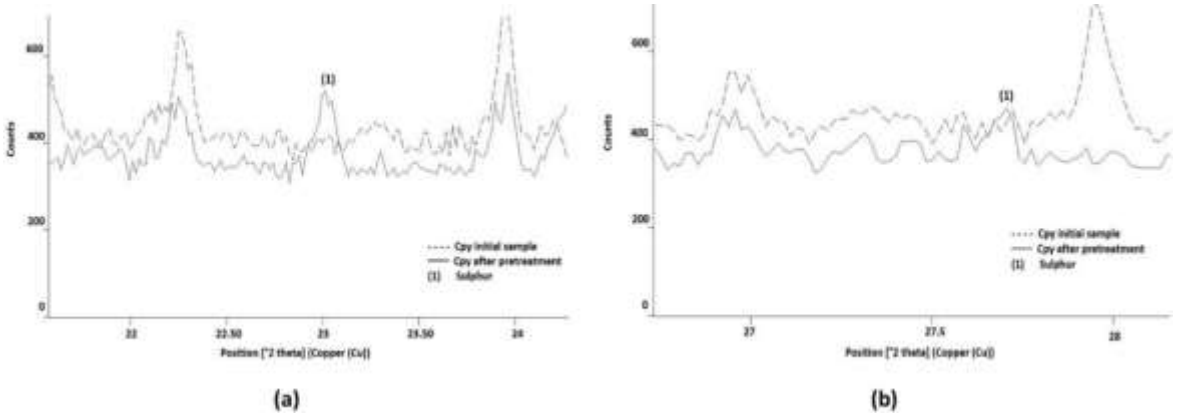

Figure 22. Elemental sulphur identified, using X-ray diffraction, product of the pretreatment of a chalcopyrite mineral with 15 kg/t H_2SO_4, 25 kg/t NaCl and 15 days of curing at room temperature

Finally, the compound $Cu_2Cl(OH)$ has also been identified by X-ray diffraction. Although the presence of this compound is demonstrated in Figure 23, the presence of other similar compounds such as Cu_2ClO_3 or $Cu_2Cl(OH)_3$ should not be ruled out. Under the studied conditions, the compound $Cu_2Cl(OH)$ has had a better fit and recognition by the software used. The main peak is associated with the position 16.23°, which coincides (overlaps) with the peak of $CuSO_4$. However, other major peaks such as 39.81° and 32.42° have been identified and are shown in Figure 23a and 23b, respectively.

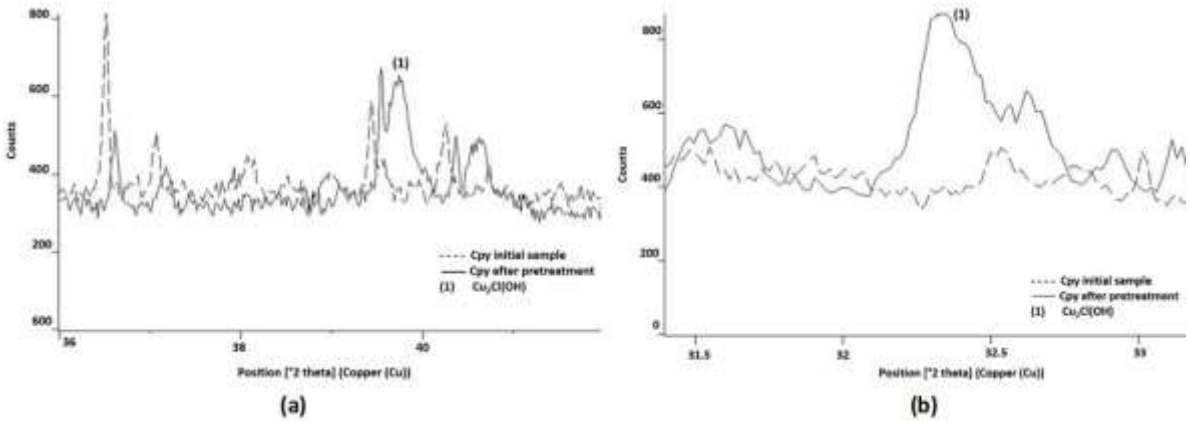

Figure 23. $Cu_2Cl(OH)$ identified, using X-ray diffraction, product of the pretreatment of a chalcopyrite mineral with 15 kg/t H_2SO_4, 25 kg/t NaCl and 15 days of curing at room temperature

SEM analysis on the sample with pretreatment) was also performed. Figure 24 shows two microphotographs of unreacted or partially attacked chalcopyrite particles. In Figure 24a' and 24b' includes the EDS analysis of zone 1 of Figure 24a and 24b. Through semi-quantitative reporting of elements, copper and iron depletion in chalcopyrite has been identified. In Figure 24a, a semi-quantitative presence of 30.50% (Cu), 27.98% (Fe) and 36.67% (S) and for Figure 24b; 19.77% (Cu), 20.63% (Fe) and 47.10% (S). This denotes a lower atomic ratio in the chemical formula of chalcopyrite, due to the dissolution of copper and iron. Furthermore, the presence of cracks on the surface and surrounding the particles is evidenced. Similar situation has been reported by (Elsherief, 2002), when in tests developed with the chalcopyrite massive electrode was cathodically leached at 20 °C in 100 g/L H_2SO_4 solutions at -900 mV, the surface shows crack and fissures during electrolysis. The authors propose that this texture is produced by the change in molar volume as chalcopyrite transforms to chalcocite and a copper deficient sulphide CuS.

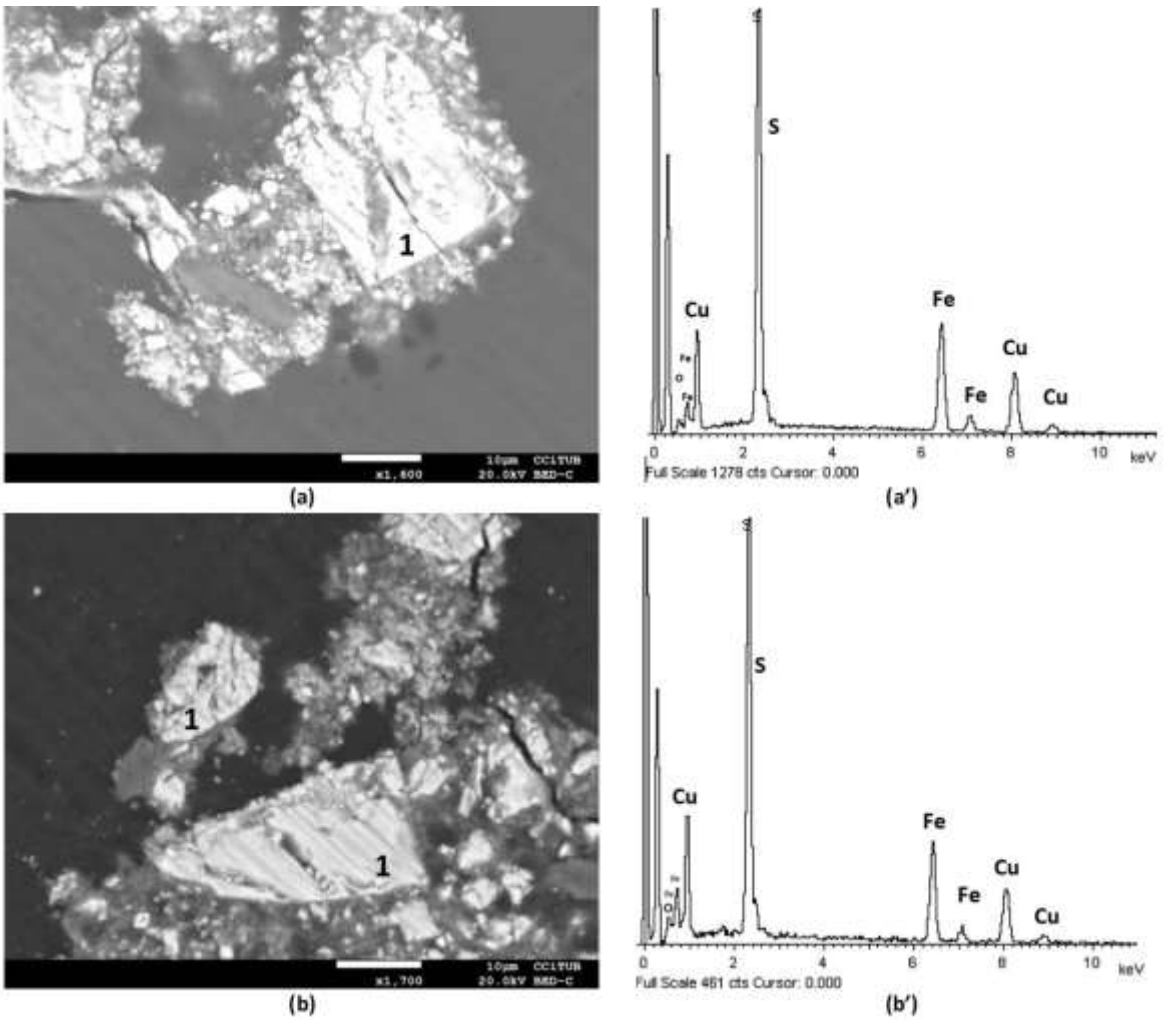

Figure 24. SEM images and EDS analysis of chalcopyrite in (1) after curing treatment with 15 kg/t H_2SO_4, 25 kg/t NaCl and 15 days of curing time at room temperature

The presence of chalcopyrite (1), copper sulfate (2) and natrojarosite (3) is reported in Figure 25a. Figure 25b shows an enlargement of the area where the natrojarosite was found. The EDS analysis associated with copper sulfate is reported in Figure 25c. Si and Al are identified, which would be associated with a silicate such as albite ($NaAlSi_3O_8$), the sodium being overlapped by copper as it is in a low presence. Based on the semiquantitative analysis, there is enough copper (24.45%), sulphur (14.30%) and oxygen (34.86%) in an atomic and weigth proportion that conforms the $CuSO_4$ formula. Figure 25d shows the EDS analysis associated with the detected natrojarosite (3). Semiquantitative analysis reports that the presence of Na (4.35%), Fe (29.70%), S (22.20%) and O (28.0%) conforms to the natrojarosite formula, although it is deficient in iron, resulting in a $NaFe_{2.3}(SO_4)_2(OH)_6$ formula, as can be observed in other natural and synthetic jarosites.

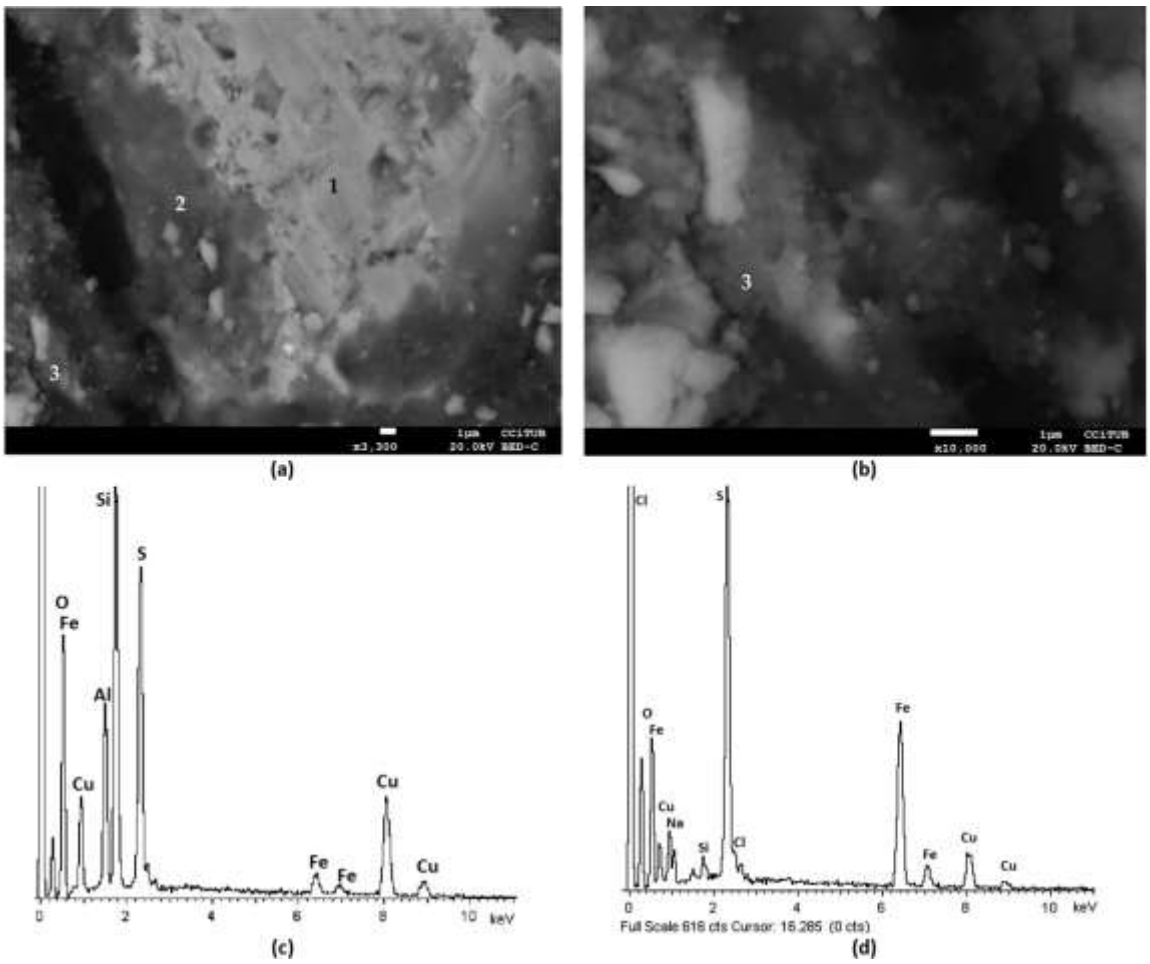

Figure 25. SEM images and EDS analysis of chalcopyrite (1), and reaction products such as: $CuSO_4$ (2) (EDS in c) and $NaFe_3(SO_4)_2(OH)$ (3) (EDS in d) product of the pretreatment of a chalcopyrite mineral with 15 kg/t H_2SO_4, 25 kg/t NaCl and 15 days of curing time at room temperature

Finally, Figure 26a identifies a compound associated with $Cu_2Cl(OH)$. Figure 26a' presents the EDS analysis associated with 26a. The presence of copper (47.56%), chloride (14.97%) and oxygen (20.75%) is sufficient for the formation of the proposed compound, although due to the non-reporting of H by the EDS analysis, the formation of Cu_2ClO should not be discarded.

Therefore, and considering all the characterization techniques applied on the pretreatment products, the following reaction that occurs under the conditions used in this study is proposed. The concentration of 15 kg/t of H_2SO_4, 25 kg/t of NaCl and 15 days of curing to a sample of natural chalcopyrite and room temperature, is governed by Eq. 17

$$3CuFeS_2 + 3H_2SO_4 + NaCl + 3O_2 = CuSO_4 + NaFe_3(SO_4)_2(OH)_6 + 6S + Cu_2Cl(OH) \qquad \text{(Eq. 17)}$$

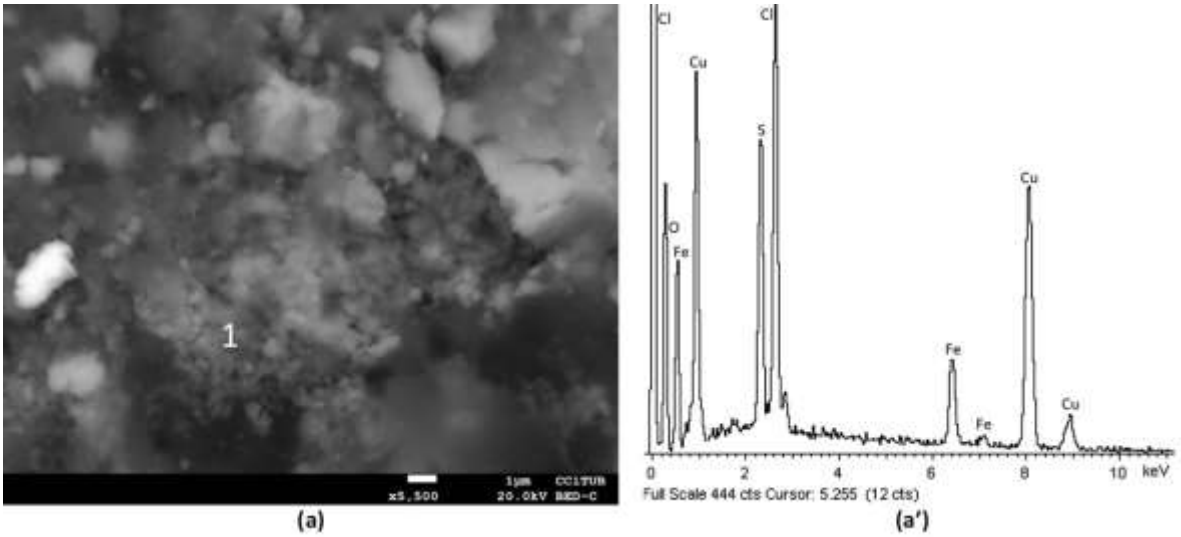

Figure 26. SEM images and EDS analysis of zone 1. The EDS confirms the formation of $Cu_2Cl(OH)$ (1) in the products of the pretreatment of a chalcopyrite mineral with 15 kg/t H_2SO_4, 25 kg/t NaCl and 15 days of curing at room temperature

3.2.4 Leaching with and without pretreatment

In order to compare the effect of the curing time, a pretreated (agglomerated and cured with 15 kg/t of H_2SO_4 25 kg/t of NaCl for a period of 15 days) and without pretreated chalcopyrite samples were leached at 25, 50, 70 and 90°C. The detail of copper and iron dissolution can be reviewed in appendix 5-8.

Leaching tests without pretreatment

Figure 27 shows the results of the leaching tests without pretreatment. A tendency is observed that benefits the copper extraction while the temperature is increased. At temperatures higher than 25°C (ambient), the passivating layer formed is less protective and more porous, which allows the dissolution of the chalcopyrite (Velásquez-Yévenes et al., 2010b). Tests without pretreatment have an almost identical behavior until the first 2 hours of leaching, reaching about 16% copper extraction, taking into account that approximately 9% copper is soluble at the initial time (copper sulfate dissolution). After 4 hours, copper extraction curves change, affected by the temperature. Test at 90 °C (♦90) and test at 70 °C (■70) achieved 90% and 87% copper extraction, respectively. Test performed at 50 °C (▲50) achieves 71% and test at 25 °C (●25) a 30%.

Test performed at 25°C achieved a stability of the copper extraction curve at 24 hours of leaching (by passivation), while the test at 50 °C achieved the passivation at 36 hours. On the other hand, the test performed at 70 °C does not evidence, clearly, passivation. Test developed at 90 °C is the test that achieved the highest copper dissolution, although there is no significant difference compared to the test at 70 °C. Similar trend in its results shows (Z. Y. Lu et al., 2000) in chalcopyrite leaching test between 85 and 95 °C. For test performed at 25°C, there is a limited dissolution of copper, that is in agreement with the fact that the dissolution of chalcopyrite requires elevated temperatures between 35 and 95°C (Lundström et al., 2005; Velásquez-Yévenes et al., 2010b).

According to chalcanthite present in the system, it is possible to obtain a fast fraction of dissolved copper. A 9% of Cu extraction is associated with chalcantite presence; this represents 0.5 g/L of Cu^{2+} at the beginning of the leaching. Although tests evaluating the effect of cupric ion are not developed in this research, authors such as (Guy and Broadbent, 1983; Veloso et al., 2016) demonstrate the benefit of Cu^{2+} at the beginning of chalcopyrite dissolution. According to (Velásquez-Yévenes et al., 2010a) the presence of a small amount of cupric ion is important in order to achieve an acceptable chalcopyrite leaching rate, but concentrations above about 0.1 g/L do not increase the rate of dissolution according to the conditions used by the authors.

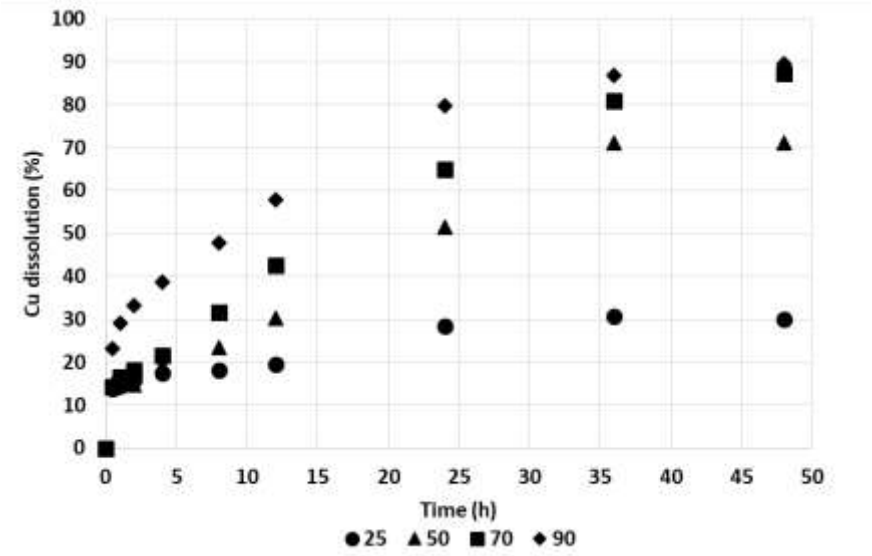

Figure 27. Dissolution of copper from chalcopyrite in 0.2 M H_2SO_4, 50 g/L of Cl^- ion from NaCl in deionized water at 25 °C (●25); 50 °C (▲50); 70 °C (■70) and 90 °C (♦90) without pretreatment

Leaching tests with pretreatment

The results obtained during leaching tests performed with pretreatment, are shown in Figure 28. It is observed that the test at 90 °C reached a copper extraction of 94 %, at 70°C of 92%, at 50°C of 77%, and the test performed at 25°C of 29% of copper extraction. There is a similar behavior with tests without pretreatment; by increasing the temperature increased the copper extraction. However, tests performed at 70°C and 50°C, reached almost 5% more than the tests developed without curing and test performed at 90 °C achieved an almost complete copper dissolution. For test at 25°C, a passivation curve can be seen after 24 hours of leaching; however, it has a kinetic behavior identical to the 50 °C test during the first 4 hours of leaching, mainly benefited by the soluble phases produced in the pretreatment.

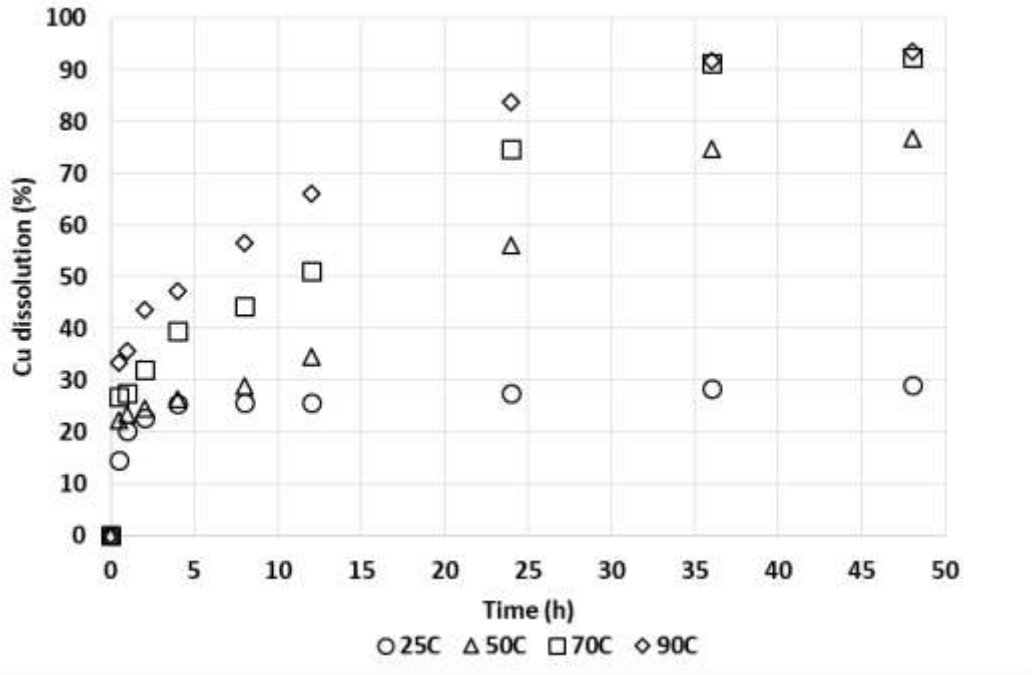

Figure 28. Dissolution of copper from chalcopyrite in 0.2 M H_2SO_4, 50 g/L of Cl^- ion from NaCl in deionized water at 25 °C (○25); 50 °C (△50); 70 °C (□70) and 90 °C (◊90) with pretreatment

Figure 29 shows the comparison between tests with and without pretreatment. It is observed that, the curing time benefits the kinetics of copper extraction, on average 6% more than the uncured test (cases of 50 and 70°C). The curing time benefits the copper extraction over time, favored by the oxidation of the mineralogical species present (Jansen and Taylor, 2003). For curing tests, the stability of the copper extraction curve is reached

before the tests without curing. This is due the sulphatation generated as pretreatment, forming copper sulphate, mainly.

Tests with acid curing accelerate the dissolution kinetics in the first 4 hours of treatment. Results from this section agree with those proposed by (Velásquez-Yévenes and Quezada-Reyes, 2018) where the curing time increases copper extraction about 5% in column leaching tests using a chalcopyrite mineral. The same copper extraction is achieved much earlier at 90 °C than at 70 °C, or at 70 °C than at 50 °C. Increasing the temperature not only increases copper extraction, but reaction time is significantly reduced.

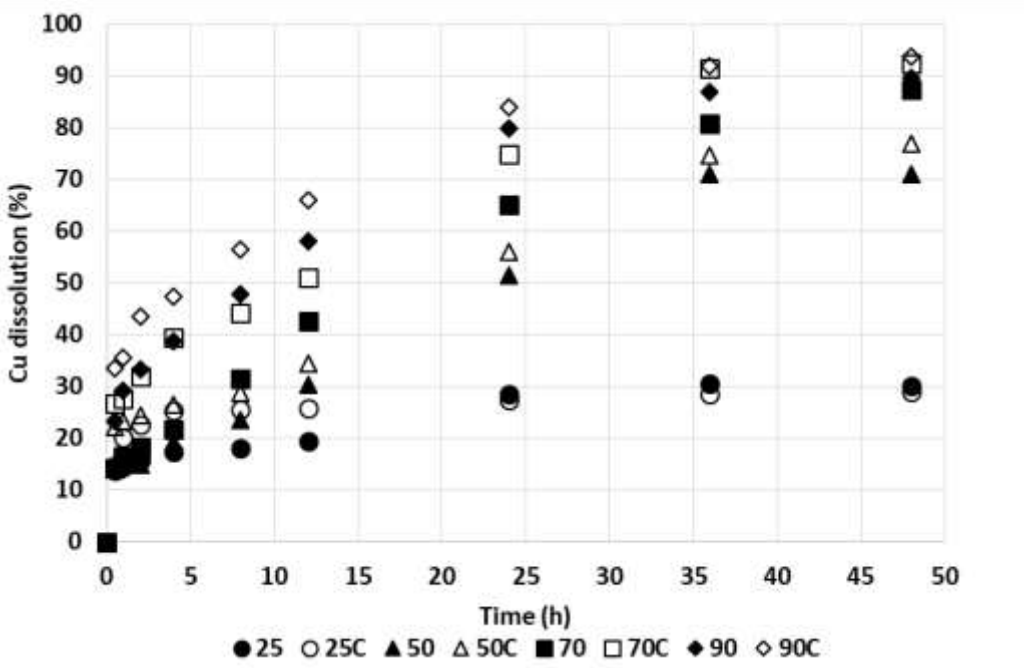

Figure 29. Dissolution of copper from chalcopyrite in 0.2 M H_2SO_4, 50 g/L of Cl from NaCl in deionized water. Without pretreatment at 25 °C (●25); 50 °C (▲50); 70 °C (■70) and 90 °C (♦) with pretreatment and 25 °C (○25); 50 °C (△50); 70 °C (□70) and 90 °C (◊90) with pretreatment

Tables 16 and 17 presents the summary of leaching test at 24 and 48 hour, respectively. The initial pH and Eh are from the leaching solution (before adding the mineral) and the final value corresponds to the last sample (48 hours). Regarding the pH, it is observed that there is no variation in leaching tests at 25 °C, denoting a very low consumption of acid in this regard. At temperatures above 25 °C, an increase in pH is evident, denoting a greater reactivity of the mineral with the solution, generating consumption of the present acid. According to (Velásquez-Yévenes et al., 2010a) leaching

of chalcopyrite in chloride media is independent of pH in a range between 0.5 and 2. In this investigation, the effect of pH seems not to be limiting for the dissolution of chalcopyrite. The behavior of Eh shows a maximum of 723 mV for the test with pretreatment at 50 °C. In all tests, the solution potential increases approximately 100 mV, mainly due to the rapid generation of Cu^{2+} associated with chalcanthite and copper sulfate produced by pretreatment. Finally, as the leaching time progresses (24 hours versus 48 hours) the difference in copper extraction decreases, between tests with and without pretreatment. The greatest difference in copper extraction is achieved in tests at 70 °C and 24 hours of leaching (almost 10 points difference in copper extraction).

Table 16.Summary of leaching test results at 24 hour

	Pretreatment			Leaching parameters			Leaching results		
Test	Curing time (days)	H_2SO_4 (kg/t)	NaCl (kg/t)	Temp. (°C)	H_2SO_4 (M)	NaCl (g/L)	% Cu extraction	pH range	Eh range (mV) SHE
1	0	0	0	25	0.2	50	28.5	0.56 - 0.58	598-639
2	15	15	25	25	0.2	50	27.5	0.51 - 0.51	607-671
3	0	0	0	50	0.2	50	51.5	0.63 - 1.05	606-664
4	15	15	25	50	0.2	50	56.0	0.60 - 0.89	607-723
5	0	0	0	70	0.2	50	65.0	0.55 - 1.04	609-708
6	15	15	25	70	0.2	50	74.8	0.51 - 0.97	605-695
7	0	0	0	90	0.2	50	79.8	0.48 -1.11	581-704
8	15	15	25	90	0.2	50	83.9	0.48 - 1.18	594-695

Table 17.Summary of leaching test results at 48 hour

	Pretreatment			Leaching parameters			Leaching results		
Test	Curing time (days)	H_2SO_4 (kg/t)	NaCl (kg/t)	Temp. (°C)	H_2SO_4 (M)	NaCl (g/L)	% Cu extraction	pH range	Eh range (mV) SHE
1	0	0	0	25	0.2	50	30.1	0.56 - 0.66	598-648
2	15	15	25	25	0.2	50	29.1	0.51 - 0.55	607-672
3	0	0	0	50	0.2	50	71.1	0.63 - 1.25	606-657
4	15	15	25	50	0.2	50	77.2	0.60 - 1.09	607-723
5	0	0	0	70	0.2	50	87.3	0.55 - 1.55	609-698
6	15	15	25	70	0.2	50	92.4	0.51 - 1.33	605-716
7	0	0	0	90	0.2	50	89.6	0.48 - 1.59	581-711
8	15	15	25	90	0.2	50	93.6	0.48 - 1.70	594-702

3.2.5 Characterization of leaching residues

The characterization of leaching residues has been carried out in all tests, using XRD and SEM. Table 18 presents a summary of the main species identified in the corresponding diffractogram. The information obtained from the diffractogram of the residue associated with the test with lower (at 25 °C without pretreatment), and higher copper extraction (at 90 °C with pretreatment) are shown in Figure 30 and 31, respectively.

X-ray diffraction over the residues, obtained at 25 °C, show the majority presence of chalcopyrite and quartz in both residues. The presence of CuS_2 polysulfide, declared as a potential responsible for the inhibition of chalcopyrite leaching in these experimental conditions (Nicol and Zhang, 2017; Nicol, 2017), was observed but in lesser presence. Likewise, X-ray diffraction reports the presence of natrojarosite in minor amounts; jarosites are also declared responsible for the inhibition of chalcopyrite leaching (Córdoba et al., 2009). Finally, the presence of elemental sulphur was also observed.

Regarding the tests carried out at 50 °C, the same trend was detected, although with a greater increase in elemental sulphur, for tests with and without pretreatment. In tests at 70 °C, the majority presence of elemental sulphur and quartz was observed, and a minor presence of chalcopyrite and natrojarosite was also detected. Regarding the presence of CuS_2, it was observed but in minority form. The main angle of CuS_2 is overlapped with that of sulphur (31.4). The other angles of the species are detected. Although the presence of CuS_2 is unclear, it should not be ruled out. Clearly, the increase in the presence of S^0 is due to the product released by the leached chalcopyrite, benefited by temperature and pretreatment. Leaching tests at 50 and 70 °C also show the presence of covellite, which may be the product of the chalcopyrite dissolution. In tests at 90 °C, the presence of abundant elemental sulphur and quartz are identified. The presence of unreacted chalcopyrite and natrojarosite is also evident. In the case of CuS_2, its presence cannot be demonstrated, since its angles are not clearly identified.

In tests performed by (Dutrizac, 1983) the author shows that the formation of jarosite ($MFe_3(SO_4)(OH)_6$ where M = Na, K, Rb, or NH_4), the temperature is a key factor for

the formation of jarosite. Increasing temperatures significantly increase the extent of iron precipitation especially in the range 70 to 110 °C. According to (Z. Y. Lu et al., 2000) the formation of natrojarosite can occur at a pH close to 0.9 in tests performed at 95 °C. Furthermore, in chloride media the natrojarosite can be formed according to Eq.18. A problem associated with the precipitation of natrojarosite is that decreasing the acid concentration also slightly decreases the rate of copper extraction, due to chalcopyrite passivation (Córdoba et al., 2009; Martins et al., 2019; Nava and González, 2006).

$$3Fe^{3+} + 2SO_4^{2-} + 6H_2O + Na^+ = NaFe_3(SO_4)_2(OH)_6 + 6H^+ \qquad \text{Eq. 18}$$

Table 18.Summary of species identified using X-ray diffraction analysis. Tests developed with pretreatment are identified with a (C)

Test	Most abundant species	Minority species
25 °C (C)	$CuFeS_2$, SiO_2, S and FeS_2	CuS, $NaFe_3(SO_4)_2(OH)_6$ and CuS_2
25 °C	$CuFeS_2$, SiO_2, S and FeS_2	CuS, $NaFe_3(SO_4)_2(OH)_6$ and CuS_2
50 °C (C)	$CuFeS_2$, SiO_2, S, CuS and FeS_2	$NaFe_3(SO_4)_2(OH)_6$ and CuS_2
50 °C	$CuFeS_2$, SiO_2, S, CuS and FeS_2	$NaFe_3(SO_4)_2(OH)_6$ and CuS_2
70 °C (C)	SiO_2, S and FeS_2	$CuFeS_2$, CuS, $NaFe_3(SO_4)_2(OH)_6$ and CuS_2
70 °C	SiO_2, S and FeS_2	$CuFeS_2$, CuS, $NaFe_3(SO_4)_2(OH)_6$ and CuS_2
90 °C (C)	SiO_2 and S	$CuFeS_2$, FeS_2, CuS and $NaFe_3(SO_4)_2(OH)_6$
90 °C	SiO_2 and S	$CuFeS_2$, FeS_2, CuS and $NaFe_3(SO_4)_2(OH)_6$

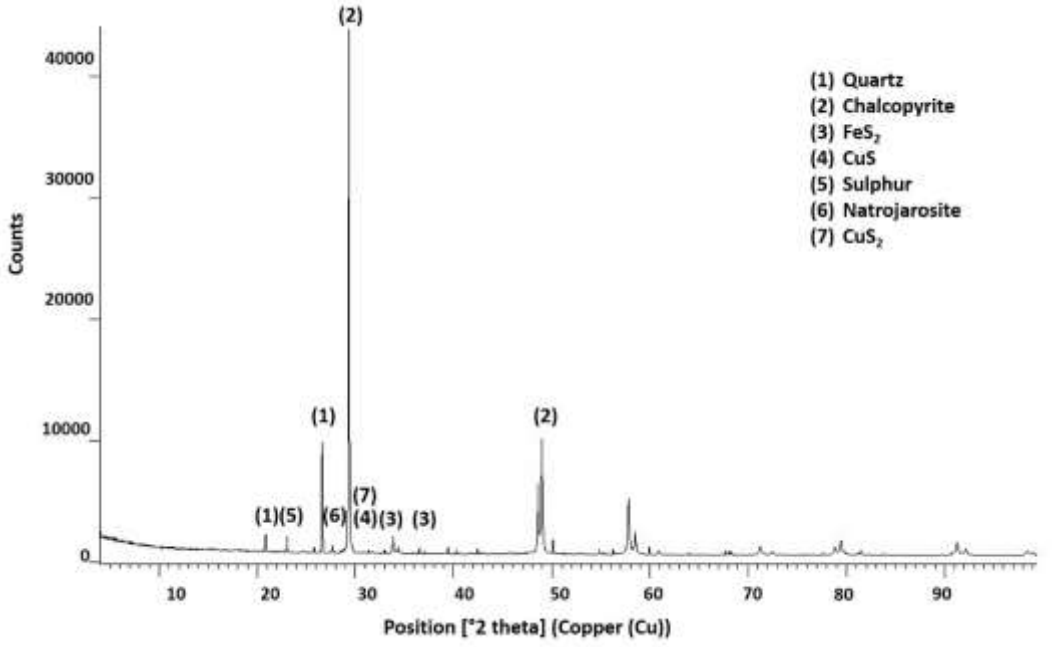

Figure 30. Species identified in the chalcopyrite leaching residue, using X-ray diffraction analysis at 25 °C and without pretreatment

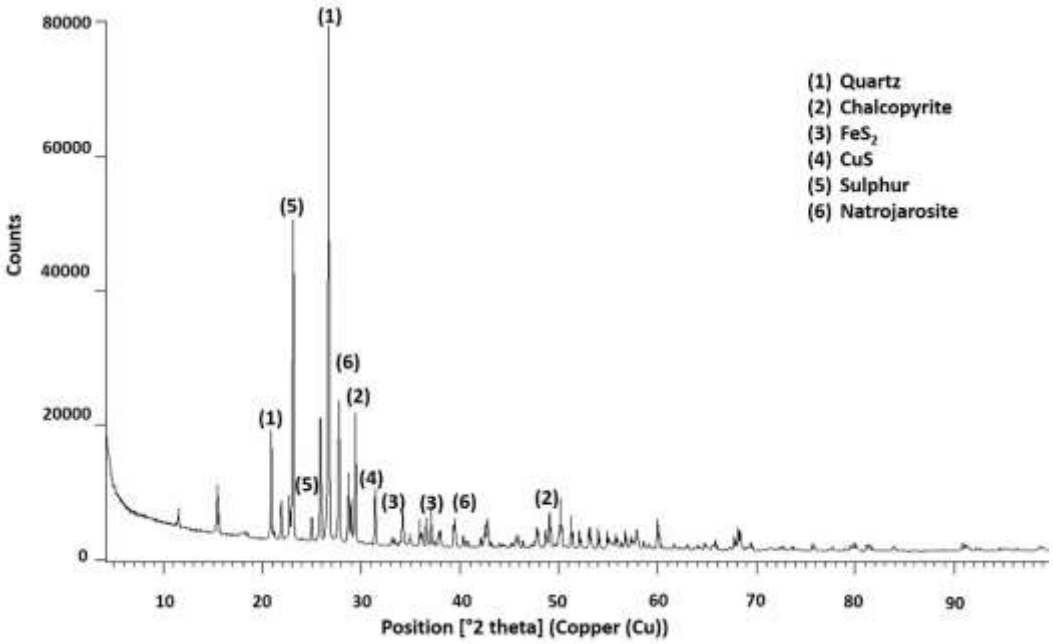

Figure 31. Species identified in chalcopyrite leaching residue, using X-ray diffraction analysis at 90 °C and with pretreatment of 15 kg/t H_2SO_4, 25 kg/t NaCl and 15 days of curing

A SEM image of the leach residue at 70 °C with pretreatment is shown in Figure 32. Unreacted chalcopyrite particles are observed with product formation on the surface of the particles (identified with 1). Figure 33 shows a sequence of SEM images and mapping analysis for four chalcopyrite particles remaining in leaching residue from leaching at 70 °C with pretreatment (Figure 32). The elements analyzed were copper, iron and sulphur. Figure 33b shows the presence of copper around the chalcopyrite particles, and in 33d the elemental sulphur. We can associate both presences (copper and sulphur) around the chalcopyrite with CuS_2 or some similar polysulfide. The passivation process associated with polysulphides (CuS_2) is explained in term of selective dissolution of iron as in a conventional process to create a thick (with time) layer of copper polysulfide(s). Additionally, in all the tests performed at 70 °C, the solution potential was measured in a range between 600-700 mV (SHE). This potential range was declared as appropriate for the formation of CuS_2 or some other polysulfide (Nicol and Zhang, 2017).

Although the presence of elemental sulphur is abundant in Figure 33, authors such as (Córdoba et al., 2009) in chalcopyrite leaching tests at 68 °C, propose that the elemental sulphur formed during chalcopyrite dissolution is porous and does not contribute to the passivation of the chalcopyrite surface. The authors propose that species like jarosite seem to be responsible for the passivation of chalcopyrite. According to (Majima et al., 1985) the elemental sulphur layer formed on the chalcopyrite surface after leaching in a ferric chloride solution is porous and not a barrier to further leaching, in tests performed at 90 °C using $FeCl_3$ and HCl.

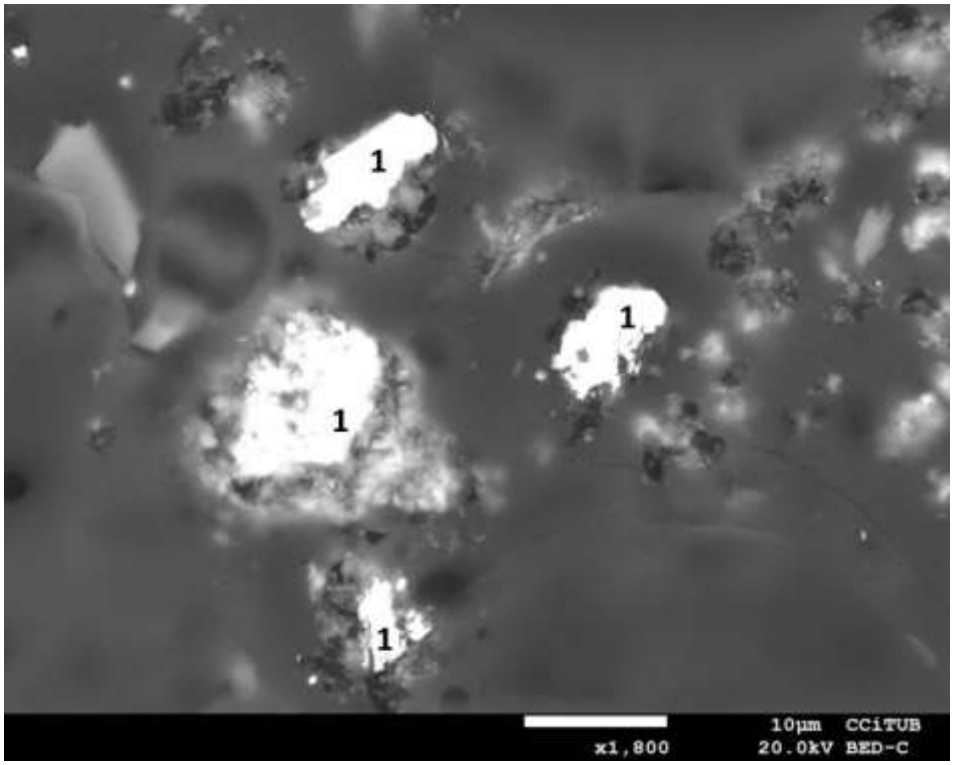

Figure 32. SEM image of leaching residue from test at 70 °C with pretreatment. $CuFeS_2$ identify with (1)

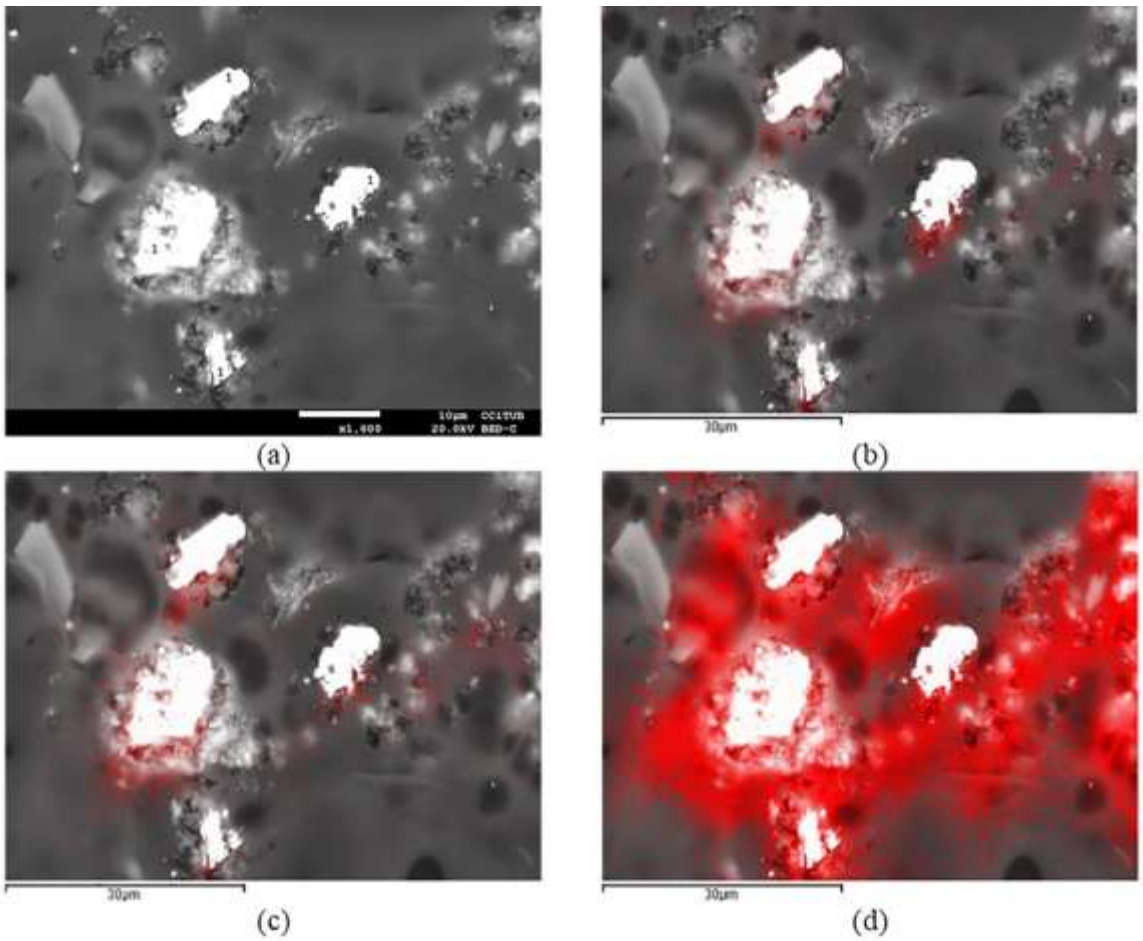

Figure 33. SEM mapping analysis generated in leaching residue performed at 70 °C with pretreatment. In (a) chalcopyrite particles (1). Different elements are showed in red colour by the superposition of (a) over (b) copper, (c) iron and (d) Sulphur

3.3 Results of pretreatment and leaching efficiency of the mine ore

3.3.1 Characterization of the mine ore

The chemical characterization of the mine ore sample is observed in Table 19. A sample with a copper grade of 0.790% is observed; 2.52% iron and 2.49% sulphur. Furthermore, 9.70% aluminum is detected, which can be mainly associated with silicate species. Additionally, after chemical characterization, the insoluble residue represented 80% of the total mass. This value suggests the presence of quartz or muscovite as insoluble phases present in the sample. Finally, the presence of soluble phases was measured by washing the sample in water, a 1.30% copper extraction was obtained.

Figure 34 (X-ray diffractogram) shows that the sample contained mainly muscovite and quartz. Minor presence of species such as chalcopyrite, pyrite and orthoclase were detected. Other copper species have not been detected due to its low presence. Table 20 shows the mineralogical composition of the sample, obtained by Qemscan analysis. The main species was muscovite (54.18%), followed by quartz (29.67 %) and pyrite (1.80 %). Chalcopyrite is the most abundant copper mineral (1.99%), representing 84% of the total copper in the sample. The second largest contributor of copper is chalcocite (0.150%), representing 10% of the total copper in the sample. Finally, covellite (0.06%) is identified, representing 5.3% of the total copper in the sample.

The high presence of Muscovite ($KAl_2(AlSi_3O_{10})(OH)_2$) coincides with the high presence of aluminum in the sample (9.70%). Furthermore, muscovite and quartz represent 84% of the total sample, which coincides with the insoluble residue of the chemical characterization (80%).

Table 19. Chemical analysis of the mine ore

Element	Cu	Fe	S	Al
Mass (%)	0.79	2.52	2.49	9.70

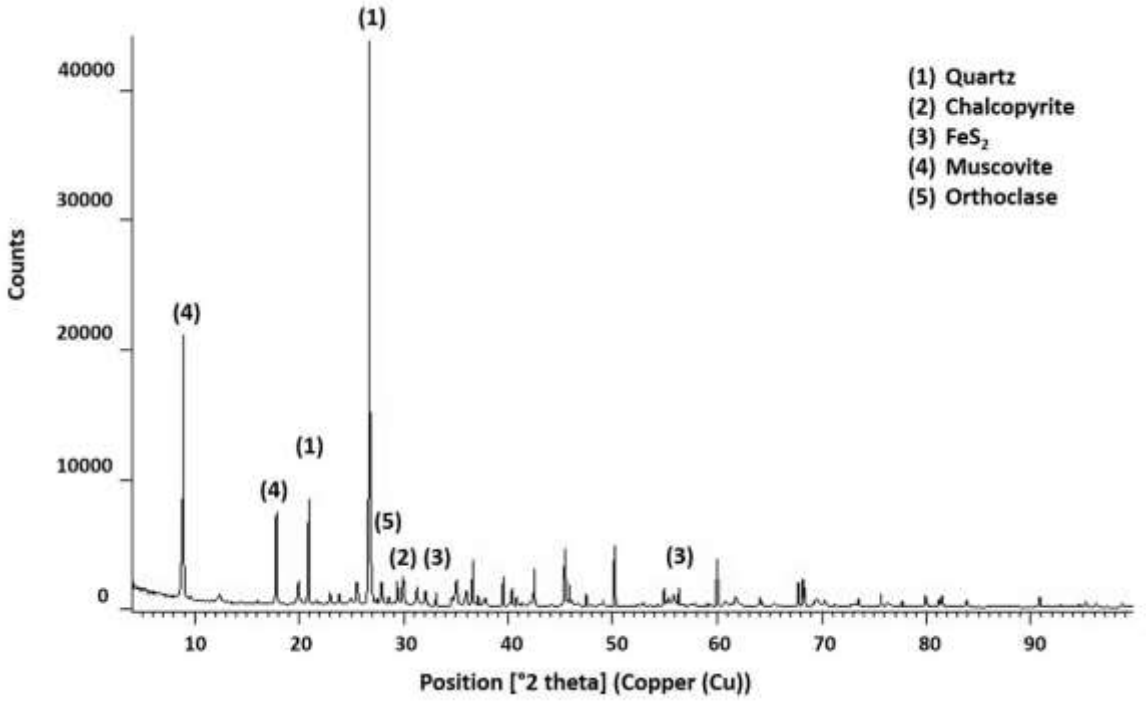

Figure 34 . X-ray diffraction pattern of the initial sample of the mine ore

Table 20. Main mineralogical composition of the initial sample (mass in %) of the mine ore according to the Qemscan analysis

Mineral	Mass, %
Muscovite	54.2
Quartz	29.7
Pyrite	3.73
Orthoclase	3.08
Kaolinite	2.51
Chalcopyrite	1.99
Smectite	1.32
Alunite	1.18
Chalcocite	0.150
Covellite	0.060

According to the image obtained using a reflected optical microscope, chalcopyrite and pyrite have been recognized according to the characteristic brightness of each species (Figure 35). SEM analysis showed the majority presence of muscovite and quartz in the initial sample. Figure 36a shows an analyzed area of the sample and Figure 37b shows the enlargement of the lower left area of Figure 36a. Finally, chalcopyrite, pyrite and muscovite

are identified in Figure 36a. The EDS analysis associated to each species is represented in Figure 37.

In general, the sample has a majority of gangue associated with muscovite and quartz (approximately 85%). The copper species are in minority presence, which coincides with the nature of the sample. According to (Bai et al., 2018) species such as quartz and biotite are not reactive against the presence of sulphuric acid. Muscovite has also been declared of low reactivity in acidic medium (Deshenthree Chetty, 2018). In the same way, pyrite is an inert sulphide, strong oxidants have to be employed for its efficient dissolution, no such conditions exist in the proposed treatment (Antonijević et al., 1997).

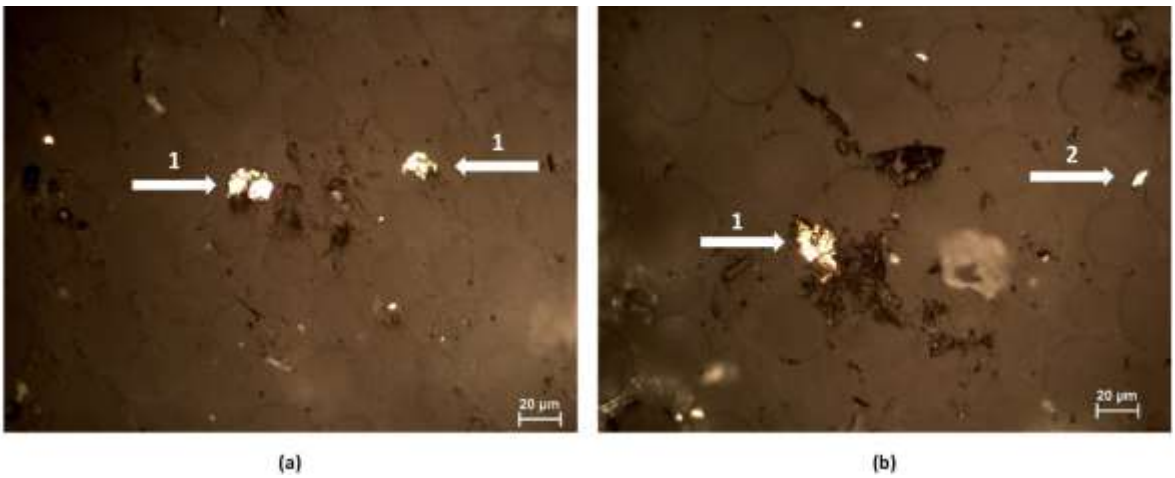

Figure 35. Reflected optical microscope image of the initial sample. 1: chalcopyrite, 2: pyrite

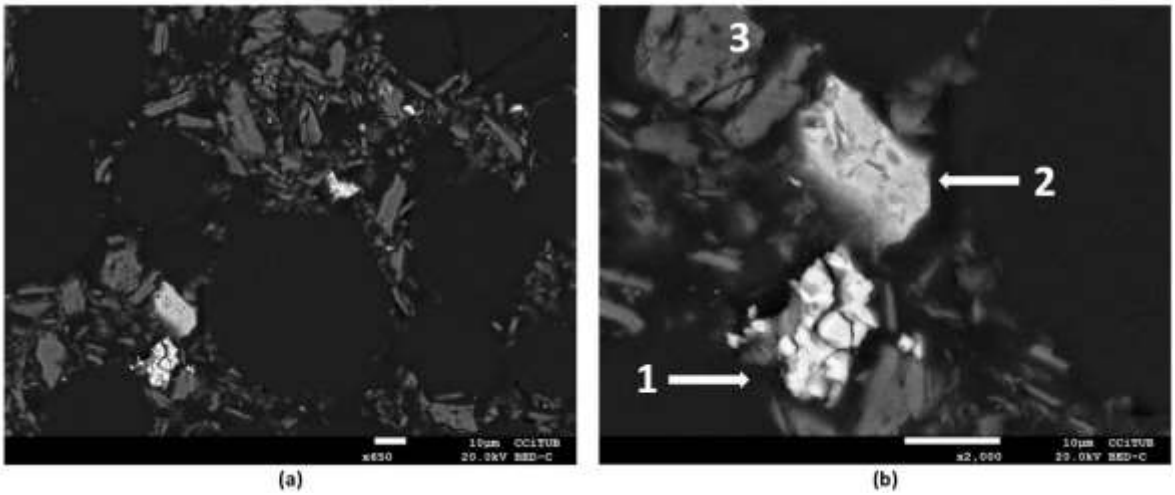

Figure 36. SEM image of the initial sample. 1: chalcopyrite, 2: pyrite, 3: muscovite

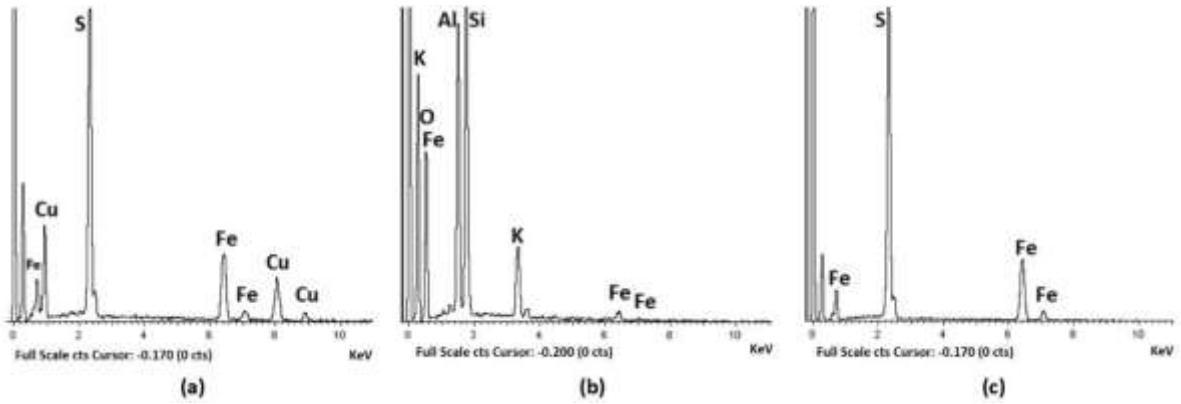

Figure 37. EDS analysis associated with Figure 36. In (a) chalcopyrite spectrum is represented, (b) muscovite and (c) pyrite

3.3.2 Pretreatment of the mine ore

The evaluation of the mine ore pretreatment is carried out considering the results obtained in chalcopyrite ore as a reference (section 3.2.2). Thus, the effect of the days of curing is first evaluated using 15 kg/t H_2SO_4 and 25 kg/t NaCl. Figure 38 shows that the curing days benefit the copper extraction. The best result is obtained after 15 days of curing, reaching a copper extraction of 27.4%. Copper extraction at 0 days of curing reaches 4.0%. A test using only water, without pretreatment or reagents, dissolves 1.50% copper. This shows that minerals such as chalcocite may be reacting and not necessarily chalcopyrite. It is important to remember that chalcopyrite contributes 84% of the total copper in the system. Therefore, a copper extraction over 16% only guarantees chalcopyrite reaction, this occurs over 5 days of curing time.

Considering 15 days as the cure time and 15 kg/t H_2SO_4, the NaCl concentration between 0 and 25 kg/t was evaluated. Figure 39 shows that between 15 and 25 kg/t there is a very small difference with respect to copper extraction (0.5% difference). The benefit of NaCl in the pretreatment coincides with (Hernández et al., 2019; Velásquez-Yévenes and Quezada-Reyes, 2018) and it is consistent with the reaction proposed in Eq.17. Finally, and in order to guarantee the greatest reactivity in the system, 15 kg/t of H_2SO_4, 25 kg/t of NaCl and 15 days of curing are used for the leaching tests and characterization of products in pre-treatment.

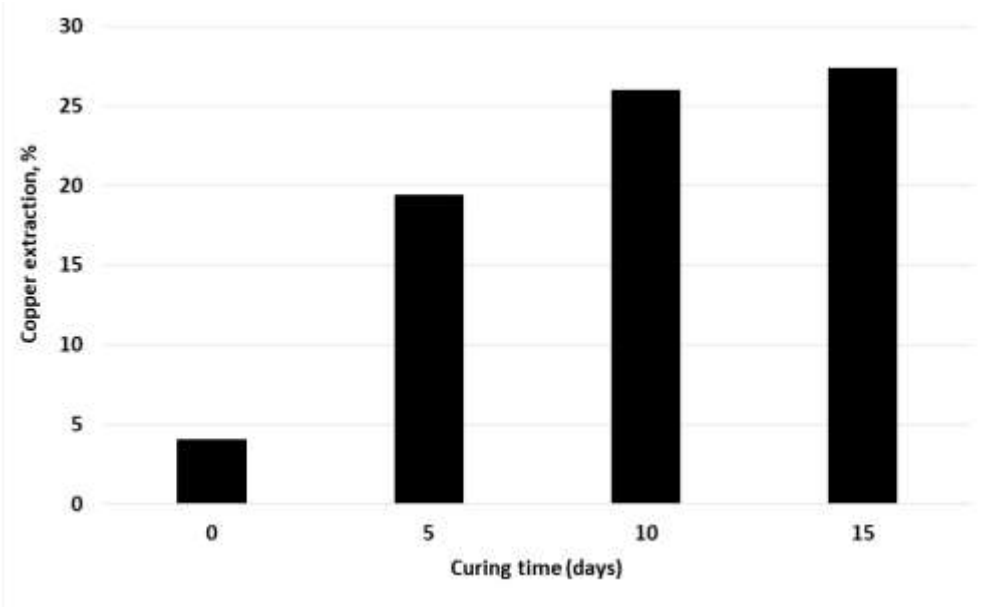

Figure 38. Effect of curing time on copper extraction from the mine ore using 15 kg/t H_2SO_4 and 25 kg/t NaCl

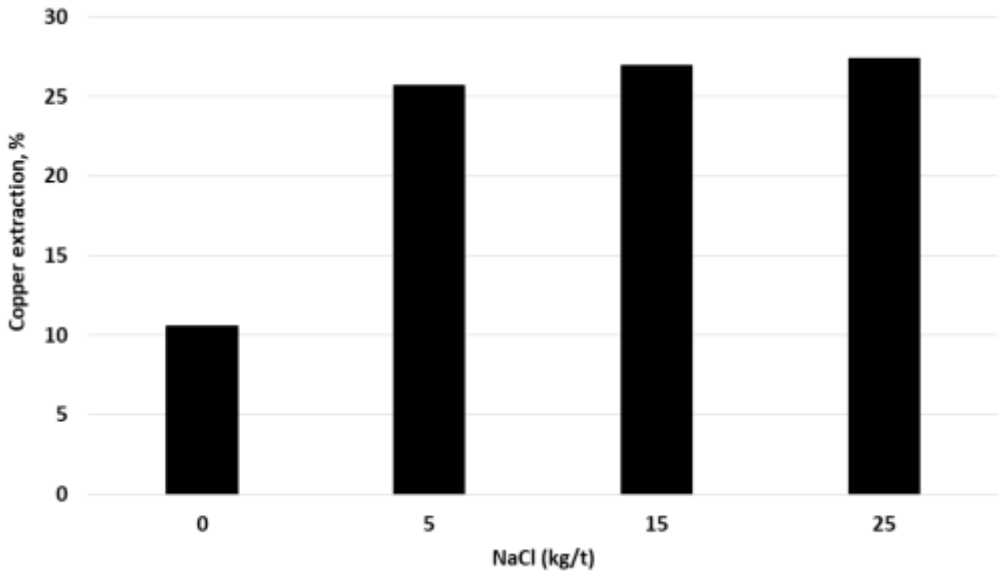

Figure 39. Effect of NaCl concentration on copper extraction from the mine ore using 15 kg/t H_2SO_4 and 15 days of curing

3.3.3 Characterization of pretreatments products

Figure 40 shows the characterization performed by optical microscopy carried out over a sample with pretreatment using 15 kg/t H_2SO_4, 25 kg/t NaCl and 15 days as curing time. It is possible to see a chalcopyrite particle with green edges, showing the formation of new products. These products can be associated with copper sulphate or chloride-copper complexes, as evidenced in section 3.2.2. In Figure 40b a similar behavior is evidenced although with a greater intensity in the formation of reaction products around the particle.

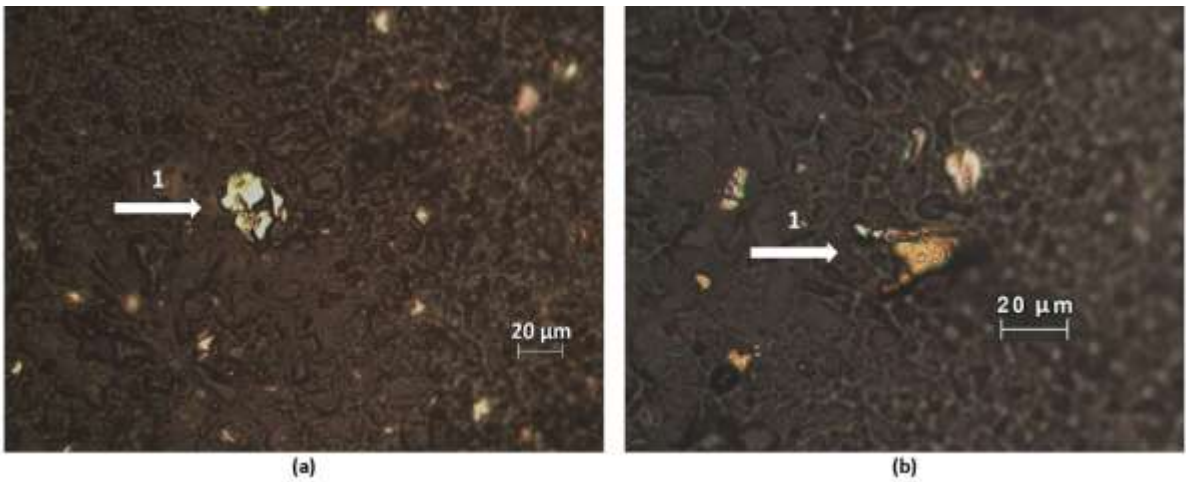

Figure 40. Reflected optical microscope image of the pretreatment product using 15 kg/t H_2SO_4, 25 kg/t NaCl and 15 days of curing time for the mine ore, 1: chalcopyrite particle

According to X-ray diffraction analysis, the identified species are shown in Figure 41. Species such as quartz and muscovite are still the most abundant, according to the initial sample. Other species such as pyrite and orthoclase are still present although a minority presence is always suggested. Chalcopyrite is still present and other species resulting from the pre-treatment, such as copper sulfate, iron sulfate or elemental sulphur, have not been identified. However, the presence of these species should not be ruled out. These species may be present but at a content below the detection limit of the diffraction technique. Finally, sodium chloride (NaCl) has been identified as a product of this pretreatment. This is due to the high presence of NaCl used in the formation of the solution that agglomerates the sample. It is possible to associate the presence of NaCl at angles 31.69 and 45.43, being the main angles of this species. According to (Zhang et al., 2013) the presence of this salt is stable and possible under ambient conditions.

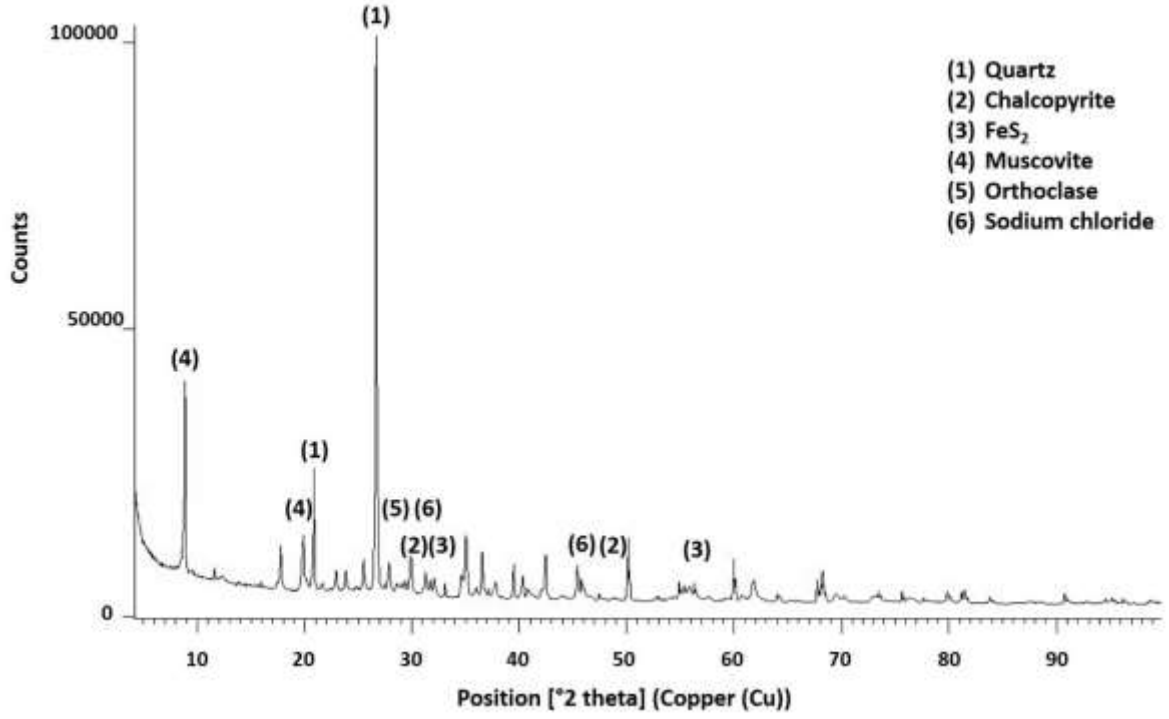

Figure 41. Species identified, using X-ray diffraction analysis, product of the pretreatment of the mine ore with 15 kg/t H_2SO_4, 25 kg/t NaCl and 15 days of curing at room temperature

The initial sample is compared to the sample with pretreatment, by comparing the diffractograms associated with each sample. Following the reaction proposed in Eq.17, according to the products formed in the pretreatment of a chalcopyrite mineral, the eventual (and minority) formation of $CuSO_4$, $NaFe_3(SO_4)_2(OH)_6$ and elemental sulphur is evaluated.

Figure 42 shows the identification of NaCl as a product in the pretreatment. This presence is associated with the most important angle of NaCl (31.69) in Figure 42a, followed by the angle 56.45 in Figure 42b. This presence is normal, considering the high concentration of NaCl added, although this salt was dissolved in the agglomeration solution. According to eq.17, the chalcopyrite pretreatment, considering the conditions used in this study, the formation of natrojarosite is proposed. If we compare the initial diffractogram versus the pretreatment diffractogram and observe the main angles of the natrojarosite, slight hints of presence are observed, but none of which guarantees absolute presence. Figure 43 shows the variation in the presence of natrojarosite before and after pretreatment. For there to be a greater presence, it is also required that the iron react,

which is associated with chalcopyrite and pyrite mainly. If chalcopyrite reacts, iron will be available. It is important to remember that the presence of chalcopyrite in this mineral is 1.99%. Therefore, the confirmation of the presence of natrojarosite is very difficult.

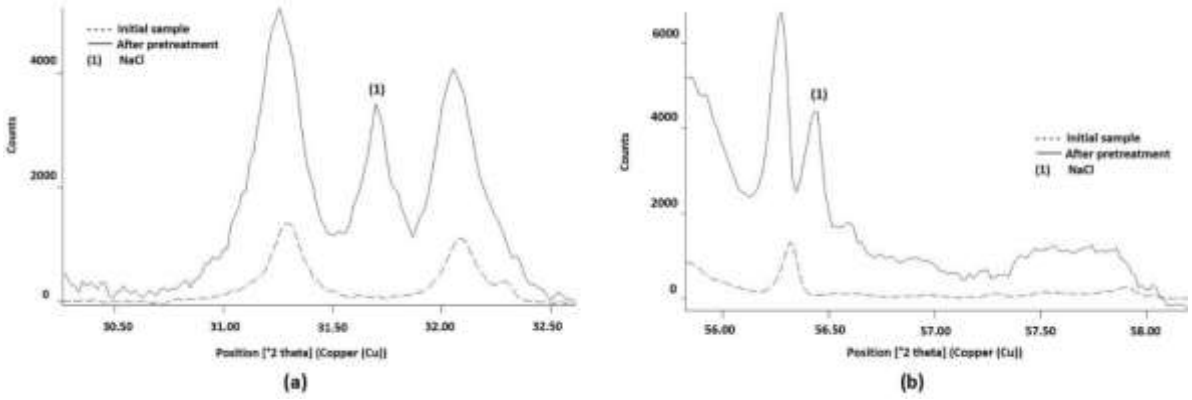

Figure 42. NaCl identification, using X-ray diffraction analysis, product of the pretreatment of the mine ore with 15 kg/t H_2SO_4, 25 kg/t NaCl and 15 days of curing time at room temperature

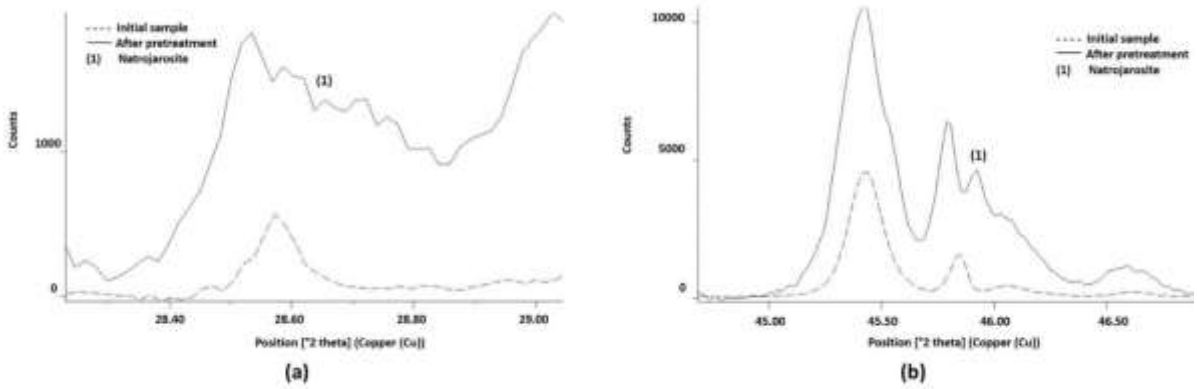

Figure 43. $NaFe_3(SO_4)_2(OH)_6$ identification, using X-ray diffraction analysis, product of the pretreatment of the mine ore with 15 kg/t H_2SO_4, 25 kg/t NaCl and 15 days of curing time at room temperature

Regarding the $CuSO_4$, it is difficult to confirm its presence due to the low presence of chalcopyrite that exists in the original sample. Figure 44 shows one of its secondary peaks but not the main angles. However, the intensity associated with this angle is very low. Finally, the eventual presence of elemental sulphur is shown in Figure 45 associated with secondary but not main angles. In the case of $Cu_2Cl(OH)$, no main or secondary angle is observed. So its presence, at least through X-ray diffraction analysis, cannot be confirmed.

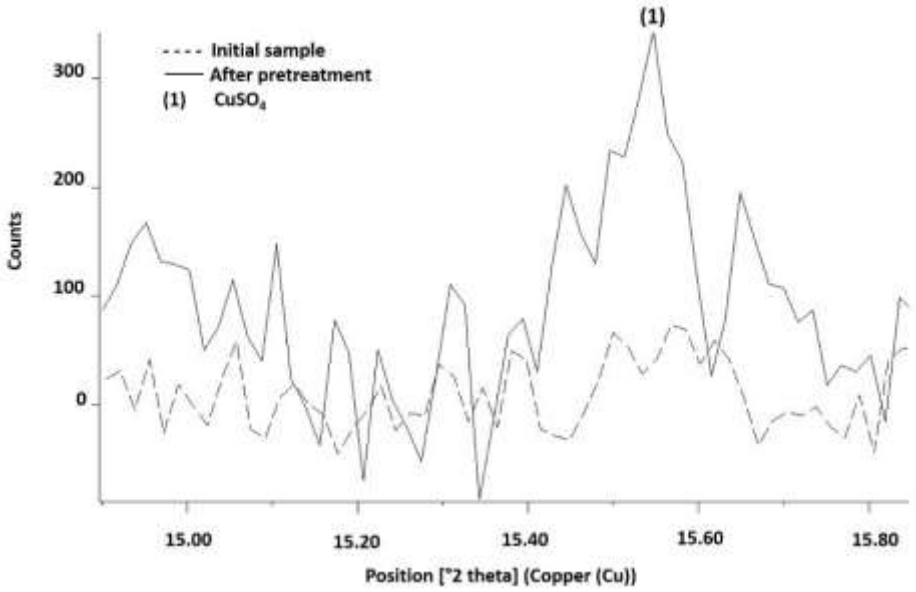

Figure 44. $CuSO_4$ identified, using X-ray diffraction analysis, product of the pretreatment of a mine ore with 15 kg/t H_2SO_4, 25 kg/t NaCl and 15 days of curing time at room temperature

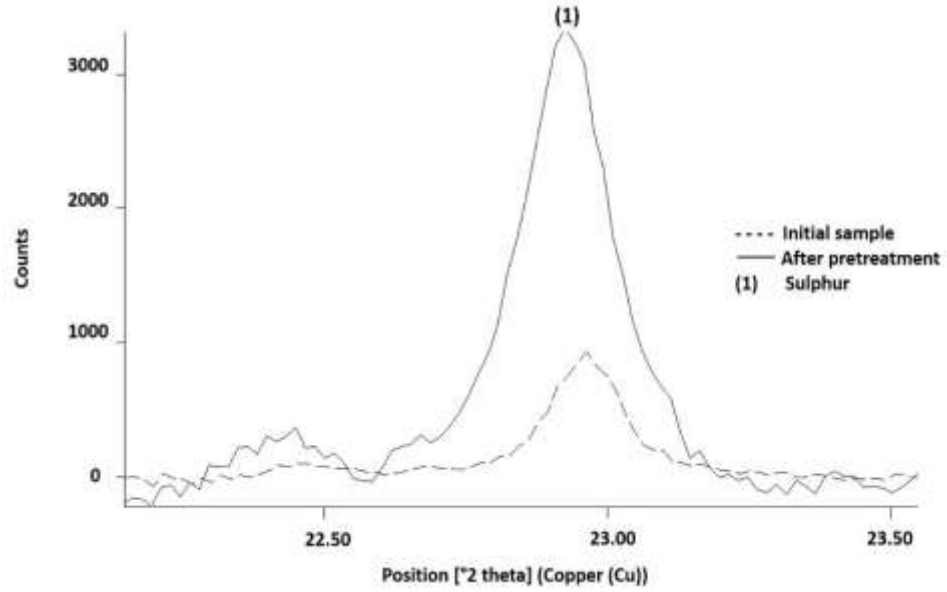

Figure 45. Elemental sulphur identified, using X-ray diffraction analysis, product of the pretreatment of the mine ore with 15 kg/t H_2SO_4, 25 kg/t NaCl and 15 days of curing at room temperature

SEM analysis was used to identify species formed in the pretreatment of the sample. As in X-ray diffraction analysis, due to the low presence of chalcopyrite, the search for species using SEM has been limited. The species quartz, muscovite and pyrite are easy to detect. Furthermore, unreacted chalcopyrite has been identified and is shown in Figure 46. It is possible to appreciate a chalcopyrite without pretreatment effects and very stable in

chemical composition 46a'. The presence of NaCl has also been detected and confirmed, mainly in a cubic form and well defined in Figure 47. The chemical composition of NaCl is evidenced in Figure 47a', whose Si contribution is negligible and does not alter the final composition. Finally, Figure 48 shows the presence of elemental sulphur and Figure 48 'the associated chemical composition.

According to the identified species, both in X-ray diffraction and SEM analysis, the importance of characterization to a pure species is evident, which reduces noise in interpretation and gives better conditions for postulating mechanisms. As postulated in Eq.17, the pre-treatment of chalcopyrite in chlorinated media prior to leaching, proposes products such as $CuSO_4$, $NaFe_3(SO_4)_2(OH)_6$, elemental sulphur and $Cu_2Cl(OH)$, also considering studies developed by (Cerda et al., 2017; Hernández et al., 2019). Therefore, according to the conditions used in this chapter, we can suggest the possibility of identifying $CuSO_4$, $NaFe_3(SO_4)_2(OH)_6$ and elemental sulphur. Species like $Cu_2Cl(OH)$ or similar have not been identified, due to the low presence of chalcopyrite in the sample (1.99%). Performing this type of tests with a pure mineral becomes highly recommended.

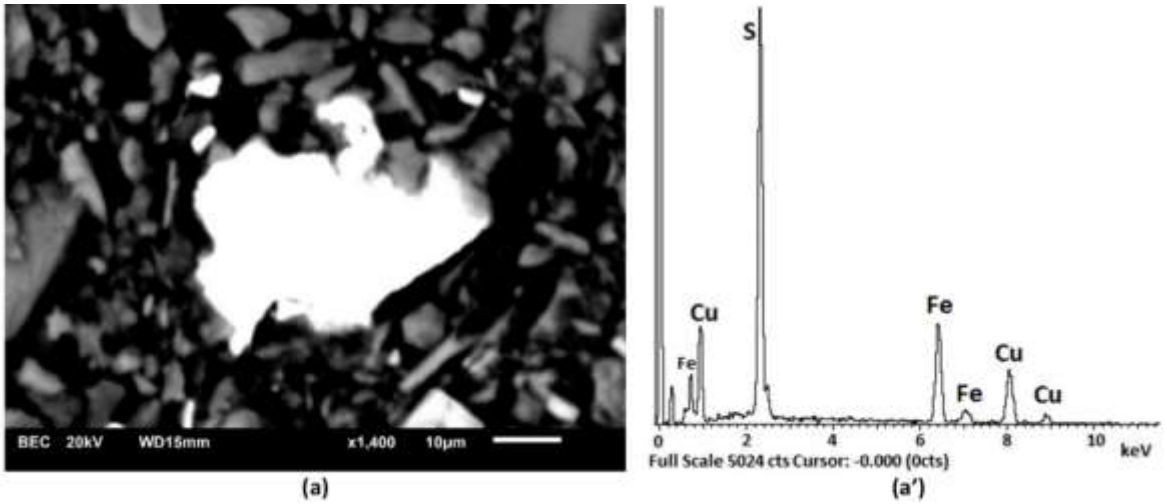

Figure 46. Chalcopyrite particle in products of the pretreatment of the mine ore with 15 kg/t H_2SO_4, 25 kg/t NaCl and 15 days of curing time at room temperature

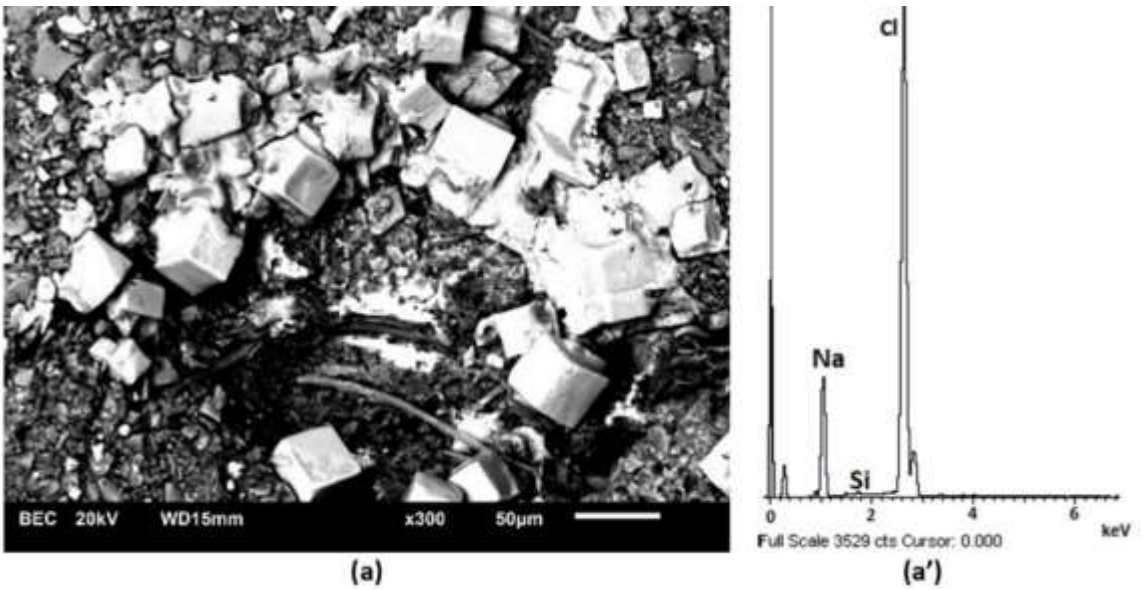

Figure 47. NaCl product of the pretreatment of a chalcopyrite mineral with 15 kg/t H_2SO_4, 25 kg/t NaCl and 15 days of curing time at room temperature

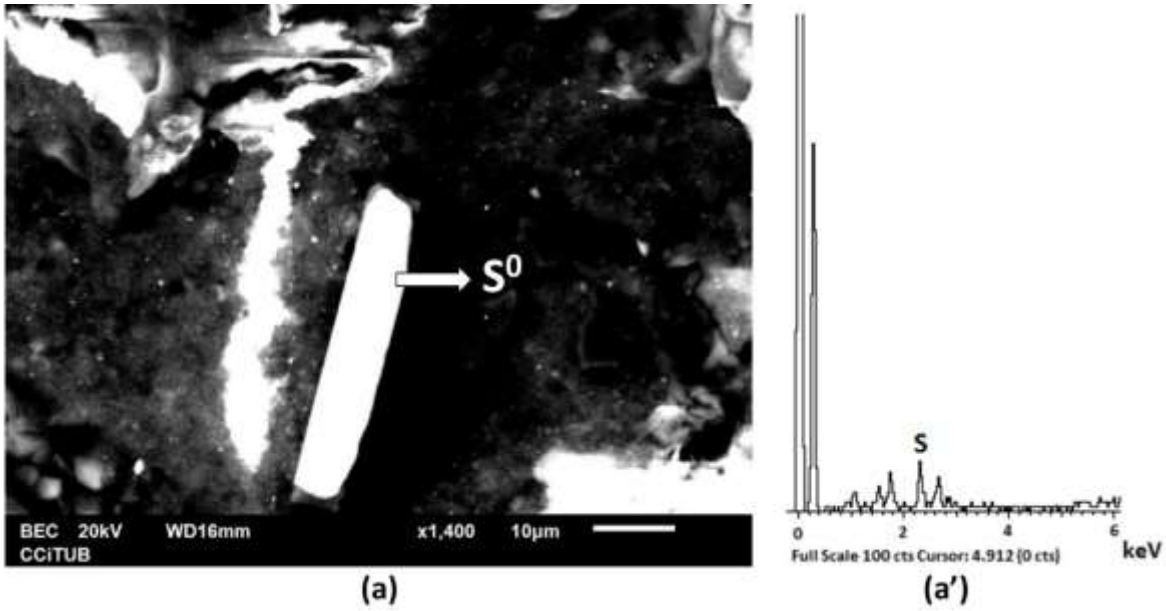

Figure 48. Elemental sulphur in product of the pretreatment of a chalcopyrite mineral with 15 kg/t H_2SO_4, 25 kg/t NaCl and 15 days of curing time at room temperature

3.3.4 Leaching with and without pretreatment

The effect of pretreatment on copper leaching efficiency on mine ore is evaluated by leaching tests. Eight leaching tests were performed at 25, 50, 70 and 90 °C, with and without pretreatment. The detail of copper and iron dissolution can be reviewed in appendix 9-12.

Leaching tests without pretreatment

Figure 49 shows the results of the leaching tests without pretreatment. It is observed that as the temperature increases, the leaching efficiency increases. The test carried out at 25 ° C shows a very classic behavior of a mineral whose main contribution is chalcopyrite (Watling et al., 2014), reaching 16.7% copper extraction and a clear passivation. Considering that chalcopyrite represents 84% of total copper, it can be inferred that the extracted copper would be associated with other more soluble phases such as chalcocite (10% of total copper), and covellite (5% of total copper). According to (Dutrizac, 1981) It is always important to consider these contributions, although small, this presences can undermine the extraction of copper, especially at low temperatures. By increasing the temperature to 50 °C a copper dissolution of 44.3% was reached. When increasing to 70 °C, the final copper extraction was 64.4%, showing no clear passivation after 48 hours of leaching. Finally, the test carried out at 90 °C reached a copper extraction of 88.6%.

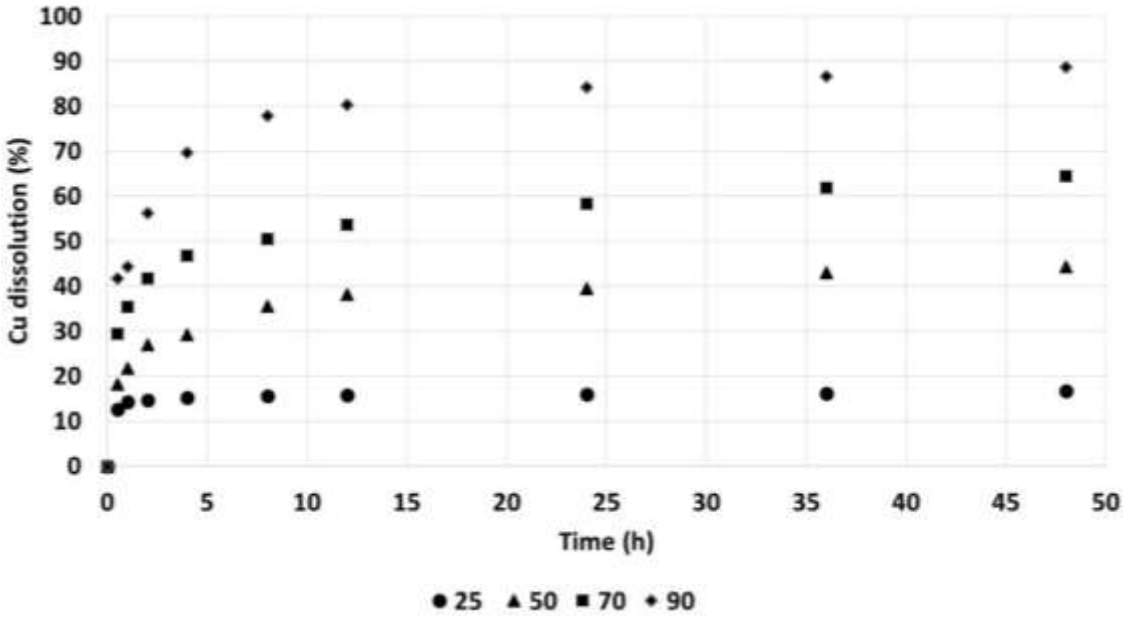

Figure 49. Copper dissolution from the mine ore in 0.2 M H_2SO_4, 50 g/L of Cl^- ion from NaCl in deionized water at 25 °C (●25); 50 °C (▲50); 70 °C (■70) and 90 °C (♦90) without pretreatment

Leaching tests with pretreatment

For the leaching tests performed with pretreatment, the results are shown in Figure 50. A trend very similar with tests without pretreatment is observed although with a higher percentage of copper dissolution. The test carried out at 25 °C (with pretreatment) reached a copper extraction of 25.9%. This value is almost 10 points more, compared to the test without pretreatment. It is observed in Figure 50 that the passivation of the mineral is evident at 25 °C and the copper extraction is similar to the percentage of copper obtained in the curing test (27.4%). When the leaching temperature was 50 °C the copper extraction reached 48.9% extraction, then at 70 °C, 70.2% of copper dissolution was reached. Finally, at 90 °C, a 93% of copper extraction was achieved. There is a greater extraction of copper in all tests with pretreatment, resulting in an average of 5% more extraction, except at 25 °C whose difference is almost 10% more.

Figure 51 shows the comparison of the tests with and without pretreatment. For tests with pretreatment, the stability of the copper extraction was reached before the tests without pretreatment. This is because the sulfation that is generated, which becomes a soluble copper product. It is observed that all tests with pretreatment achieved higher copper extraction. In addition, pretreatment tests show greater reactivity in the first two hours of the process. However, as time and temperature increase, the difference in copper extraction decreases. Furthermore, with pretreatment at 90 °C, a copper extraction of 90% was achieved in 24 hours, while without pretreatment it took 48 hours.

According to (Hernández et al., 2019) curing time also solubilizes iron, contributing with ferric ions necessary to dissolve sulphides. This would occur in all those tests, since dissolving more than 20% of copper guarantees iron dissolution as well. This occurs in all tests leached with pretreatment and within the first hour of leaching. Furthermore, a chloride-acid media promotes the formation of copper chloride-complexes, due to the rapid incorporation of Cu^{2+} into the system by sample pretreatment (Osvaldo Herreros et al., 2005).

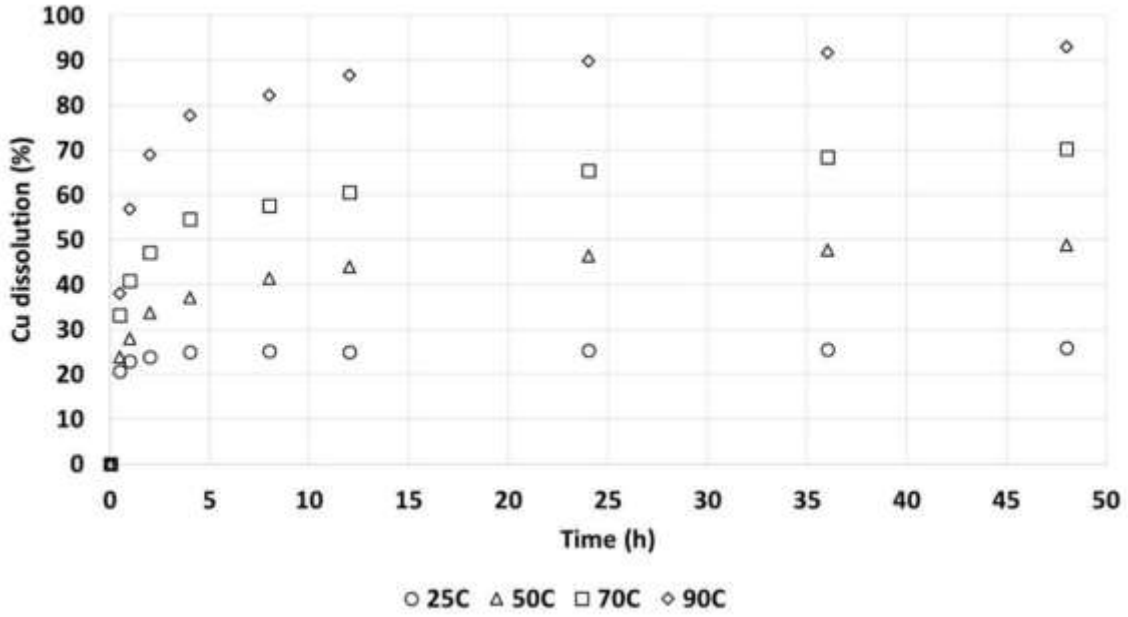

Figure 50. Copper extraction from the mine ore in 0.2 M H_2SO_4, 50 g/L of Cl^- ion from NaCl in deionized water at 25 °C (●25); 50 °C (▲50); 70 °C (■70) and 90 °C (♦90) with pretreatment

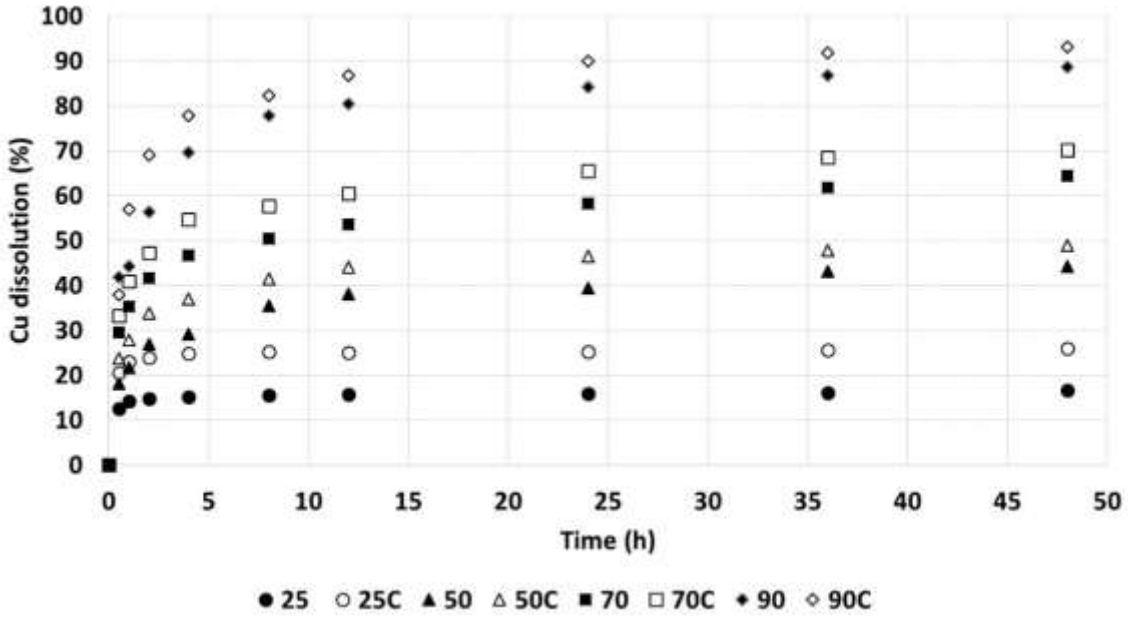

Figure 51. Copper extraction from the mine ore in 0.2 M H_2SO_4, 50 g/L of Cl from NaCl. Without pretreatment at 25 °C (●25); 50 °C (▲50); 70 °C (■70) and 90 °C (♦90) with pretreatment at 25°C (○25C); 50°C (△50C); 70°C (□70C) and 90 °C (◊90C)

Tables 21 and 22 presents the summary of results of leaching tests at 24 and 48 hour, respectively. The initial value of pH and solution potential is the value of the leaching solution (before adding the mineral) and the final value corresponds to the last sample (48

hours). Regarding the pH, it is observed that there is no variation in leaching tests at 25 °C, denoting a null consumption of acid. At temperatures above 25 °C, an increase in pH is observed. The increase in pH is more evident in tests with pretreatment, demonstrating the dissolution of soluble phases formed during the curing process.

As complementary information, Appendix 9-12 show the iron extraction achieved. Iron dissolution was greater in those tests with pretreatment, due to the very solubility of chalcopyrite. However, according to the pH values shown in Tables 21 and 22, the conditions for an eventual precipitation of iron are not evident, except in tests at 90 °C at the end with a pH above 0.9 and some jarosite may precipitate. (Z. Y. Lu et al., 2000). Finally, regarding the measured pH, it would not be a limitation in the copper dissolution, according to the indicated values (Velásquez-Yévenes et al., 2010a).

The behavior of solution potentials shows a maximum of 689 mV (SHE) for test with pretreatment at 50 °C reached at 24 hours of leaching. On average, the solution potential varied between 580 and 650 mV (SHE). In pretreatment tests the solution potential is higher, mainly due to the rapid generation of Cu^{2+} associated with the copper sulfate produced by pretreatment. Furthermore, if the $CuCl^{+}$ complex is the main active species in the leaching will benefits oxidizing conditions (Osvaldo Herreros et al., 2005). However, no significant differences were observed at the end of the tests.

Table 21.Summary of leaching test results at 24 hour

	Pretreatment			Leaching parameters			Leaching results		
Test	Curing time (days)	H_2SO_4 (kg/t)	NaCl (kg/t)	Temp. (°C)	H_2SO_4 (M)	NaCl (g/L)	% Cu extraction	pH range	Eh range (mV) SHE
1	0	0	0	25	0.2	50	15.9	0.48 - 0.50	567-633
2	15	15	25	25	0.2	50	25.3	0.49 - 0.53	590-640
3	0	0	0	50	0.2	50	39.4	0.48 - 0.60	599-645
4	15	15	25	50	0.2	50	46.5	0.48 - 0.62	602-689
5	0	0	0	70	0.2	50	58.3	0.49 - 0.72	603-650
6	15	15	25	70	0.2	50	65.5	0.48 - 0.86	601-653
7	0	0	0	90	0.2	50	84.2	0.48 - 0.92	596-650
8	15	15	25	90	0.2	50	89.9	0.49 - 0.89	592-633

Table 22. Summary of leaching test results at 48 hour

	Pretreatment			Leaching parameters			Leaching results		
Test	Curing time (days)	H_2SO_4 (kg/t)	NaCl (kg/t)	Temp. (°C)	H_2SO_4 (M)	NaCl (g/L)	% Cu extraction	pH range	Eh range (mV) SHE
1	0	0	0	25	0.2	50	16.7	0.48 - 0.52	567-642
2	15	15	25	25	0.2	50	25.9	0.49 - 0.58	590-642
3	0	0	0	50	0.2	50	44.3	0.48 - 0.57	599-647
4	15	15	25	50	0.2	50	48.9	0.48 - 0.62	602-664
5	0	0	0	70	0.2	50	64.4	0.49 - 0.74	603-661
6	15	15	25	70	0.2	50	70.2	0.48 - 0.86	601-663
7	0	0	0	90	0.2	50	88.6	0.48 - 0.97	596-640
8	15	15	25	90	0.2	50	93.0	0.49 - 0.94	592-648

3.3.5 Characterization of leaching residues

The characterization of leaching residues has been performed in all leaching tests, using X-ray analysis and SEM. Table 23 presents a summary of the main species identified by X-ray diffraction analysis. The diffractogram of the residue associated with the lower (at 25 °C without pretreatment) and higher copper extraction (at 90 °C with pretreatment) are shown in Figure 52 and 53, respectively.

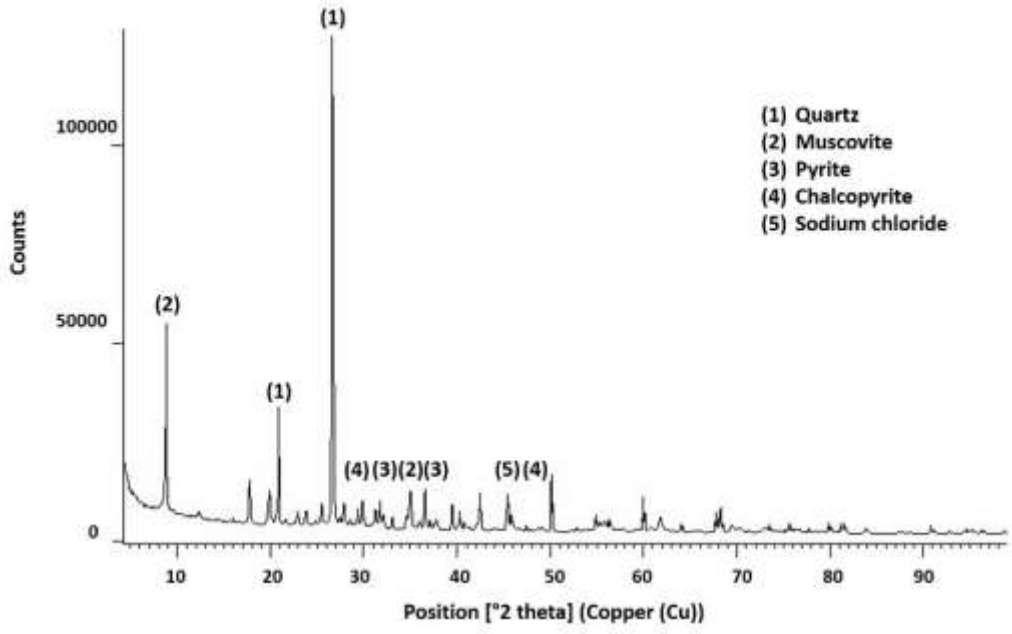

Figure 52. Species identified in the mine ore leaching residue, using X-ray diffraction analysis at 25 °C and without pretreatment

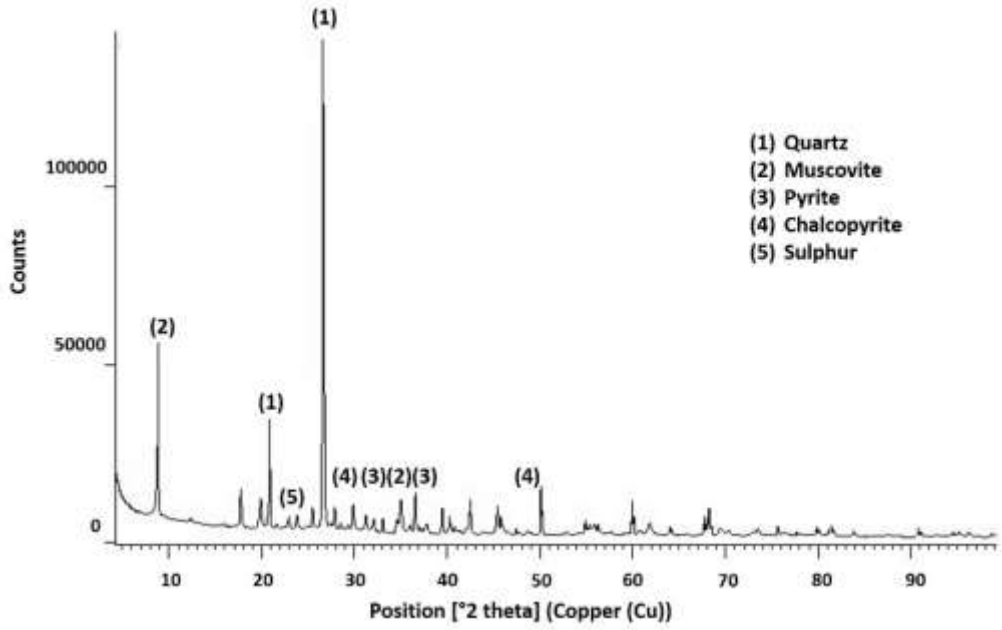

Figure 53. Species identified in the mine ore leaching residue, using X-ray diffraction analysis at 90 °C and with pretreatment of 15 kg/t H_2SO_4, 25 kg/t NaCl and 15 days of curing time

It is observed in Table 23 that there is no variation in the most abundant species in the leaching residues. Species such as quartz and muscovite are considered of low solubility in an acid media (Deshenthree Chetty, 2018). For the tests at 25 °C, the presence of unreacted chalcopyrite, is evidenced. In tests carried out at 50 °C, the presence of Cu_2S has been confirmed. This chalcocite can be mineral undissolved from the initial sample or product of the leaching of chalcopyrite. Since the presence of chalcocite is not evident at 25 °C, it is likely to be the product of chalcopyrite leaching (Arce and González, 2002). Regarding the tests carried out at 70 °C, the presence of chalcocite is no longer evident. The presence of elemental sulphur in the system is observed for the first time due to the dissolution of copper from chalcopyrite (70.2% in test with pretreatment). This does not rule out that at 25 and 50 °C the presence of elemental sulphur cannot exist, the presence would be so low that it is difficult to demonstrate. The presence of elemental sulphur is normal in leaching residues, mainly due to the chalcopyrite dissolution, even for processes such as bioleaching (Peng et al., 2019; Zhang et al., 2019).

Leaching tests at 90 °C report a composition identical to the tests at 70 °C. The presence of other species that are responsible for the passivation of chalcopyrite have not been identified, such as natrojarosite or copper polysulfides. Furthermore, in systems with the presence of $PbSO_4$, a lack of sulphuric acid could result in the precipitation of iron as plumbojarosite, and could therefore create difficulties in the recovery of valuable metals (Cháidez et al., 2019). According to the behavior of the pH in all the tests, the formation of natrojarosite is unlikely. However, according to (Z. Y. Lu et al., 2000) it is possible to find this species at pH 0.9, the above would only be possible in tests at 90 °C.

Table 23. Summary of species identified using X-ray diffraction analysis. Tests developed with pretreatment are identified with (C)

Test	Most abundant species	Minority species
25 °C (C)	SiO_2, $KAl_2(AlSi_3O_{10})(OH)_2$ and FeS_2	$CuFeS_2$
25 °C	SiO_2, $KAl_2(AlSi_3O_{10})(OH)_2$ and FeS_2	$CuFeS_2$
50 °C (C)	SiO_2, $KAl_2(AlSi_3O_{10})(OH)_2$ and FeS_2	$CuFeS_2$ and Cu_2S
50 °C	SiO_2, $KAl_2(AlSi_3O_{10})(OH)_2$ and FeS_2	$CuFeS_2$ and Cu_2S
70 °C (C)	SiO_2, $KAl_2(AlSi_3O_{10})(OH)_2$ and FeS_2	$CuFeS_2$ and S
70 °C	SiO_2, $KAl_2(AlSi_3O_{10})(OH)_2$ and FeS_2	$CuFeS_2$ and S
90 °C (C)	SiO_2, $KAl_2(AlSi_3O_{10})(OH)_2$ and FeS_2	$CuFeS_2$ and S
90 °C	SiO_2, $KAl_2(AlSi_3O_{10})(OH)_2$ and FeS_2	$CuFeS_2$ and S

Characterization by SEM demonstrates the presence of unreacted chalcopyrite in all tests. Obviously, in tests at 70 °C and 90 °C the presence becomes difficult. In Figure 54 unreacted chalcopyrite is observed in test at 25 °C without pretreatment.

The species with greatest abundance are quartz, muscovite, and pyrite. This can be identified in all leaching residues, as shown in Figure 55. In this Figure, the presence of quartz and pyrite is observed, the EDS analysis of this species are observed in Figures 55a and 55b, respectively. Finally, products associated with the passivation of chalcopyrite were not accurately identified due to the scarcity of chalcopyrite in the sample.

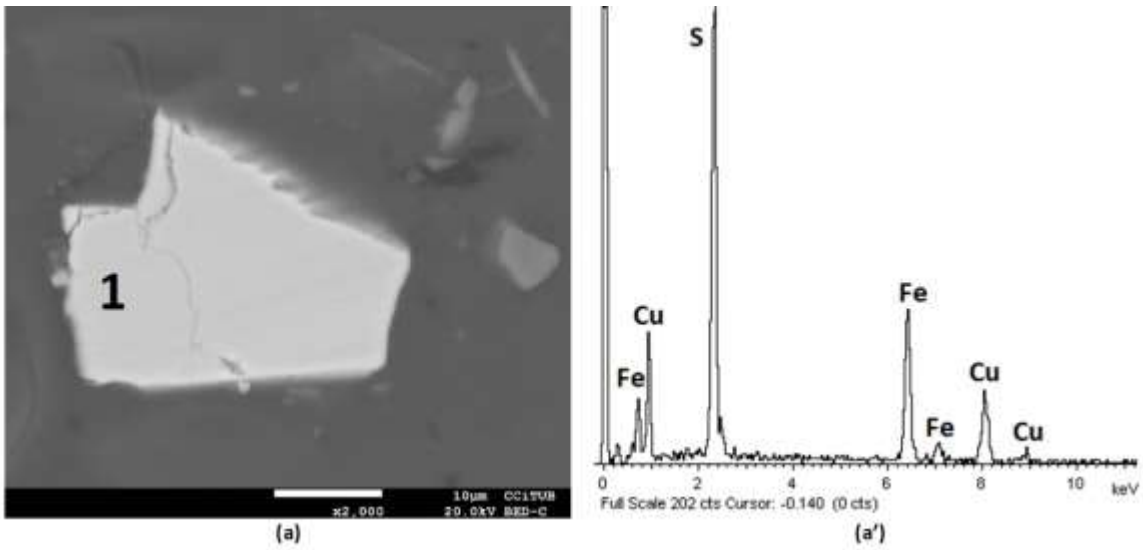

Figure 54. SEM image shows leaching residue obtained at 25 °C without pretreatment. Particle 1 identified as unreacted chalcopyrite

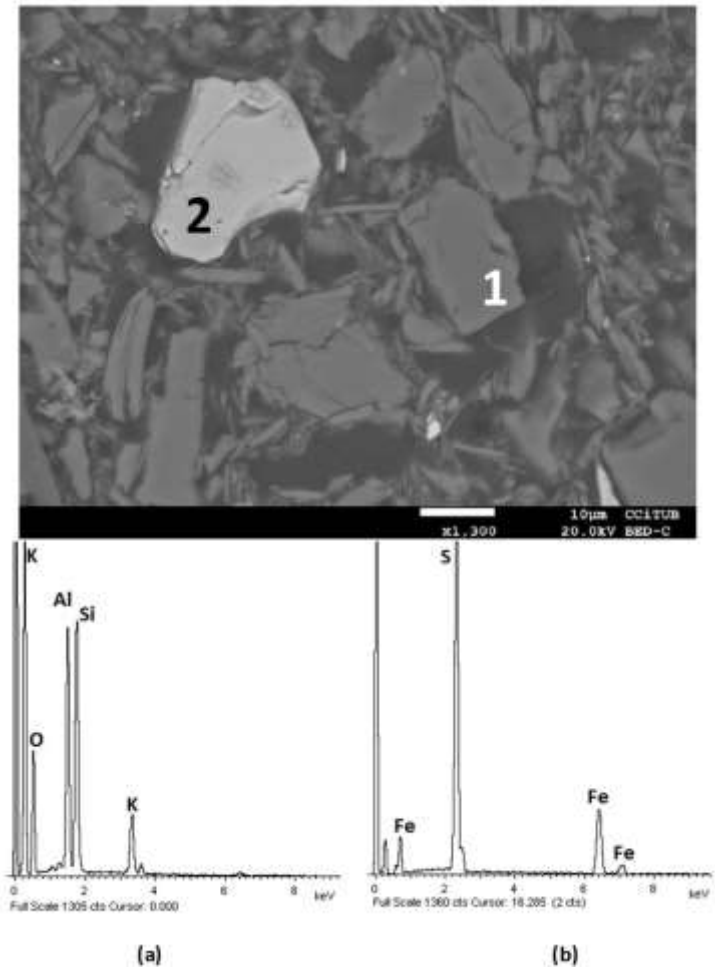

Figure 55. SEM image shows the leaching residue obtained at 90 °C with pretreatment. Particle 1 identified as quartz (a) and particle 2 as pyrite (b)

4 Pretreatment and leaching of a chalcocite mineral

4.1 Literature Review

General properties of chalcocite

Chalcocite (Cu_2S) is the most abundant copper sulphide after chalcopyrite, and the most amenable to hydrometallurgical treatment (Miki et al., 2011; Wu et al., 2013). According to (Tanda et al., 2018) chalcocite is a dark grey secondary copper sulphide mineral, commonly found in the supergene enriched environment beneath the oxidized zone of porphyry copper deposits. The stoichiometry composition of chalcocite is approximately: 79.9% Cu and 20.1% S. The crystalline structure of chalcocite is complex, and there may be differences according to its structure (Posfai and Buseck, 1994). In high chalcocite structure, sulphur atoms are arranged in hexagonal close-packing order (Fang et al., 2018). The structures of low chalcocite and djurleite are derived from the high chalcocite structure and both are monoclinic (Evans, 1979). The structure of djurleite it is in general similar to low chalcocite and are physically difficult to distinguish and probably equally common (Evans, 1981).

Today, hydrometallurgy is an alternative for the treatment of low grade copper sulphide ores, as chalcocite. Through electrochemical tests, it has been possible to determine the close relationship between chalcopyrite and chalcocite, because chalcocite or intermediate species can be found in the chalcopyrite dissolution, such as $Cu_{1.92}S$, $Cu_{1.6}S$, $Cu_{1.4}S$ and CuS (Córdoba et al., 2008b; Zeng et al., 2013). The dissolution of chalcocite is fast compared to the dissolution of chalcopyrite. However, like chalcopyrite, the dissolution of chalcocite is reduced by the formation of a product layer that inhibits dissolution. Additionally, it is well known that chalcocite dissolves in two stages (Cheng and Lawson, 1991a). The classical dissolution mechanism is shown in Equations 18 and 19. According to equation 18, in the first dissolution stage, a quick dissolution of chalcocite is achieved (between 40 and 50%). In the second stage, equation 19, the covellite product from first stage has a slow dissolution due to the formation of a product layer that inhibits the dissolution of the mineral (Cheng and Lawson, 1991a).

$$Cu_2S + 2H^+ + \frac{1}{2}O_2 = Cu^{2+} + CuS + H_2O \quad \text{(Eq.18)}$$

$$CuS + 2H^+ + \frac{1}{2}O_2 = Cu^{2+} + S + H_2O \quad \text{(Eq.19)}$$

Various leaching media have been proposed for the chalcocite dissolution, such as: bioleaching (Petersen and Dixon, 2007, 2003; Xingyu et al., 2010), ammoniacal media (Hepel and Hepel, 1977; Karimov et al., 2018) , chloride media (Cheng and Lawson, 1991a; Miki et al., 2011; Quezada et al., 2018), among others. Of these, the most studied and used on an industrial scale are chloride and a bioleaching media (Herreros and Viñals, 2007; Niu et al., 2015). In the case of the chloride media, the dissolution of chalcocite also takes place in two stages; the first stage is controlled by the diffusion of oxygen through the liquid boundary layer around the particle, and the second stage follow the traditional shrinking core model in which a shrinking core of unreacted CuS is surrounded by an elemental sulphur layer (Cheng and Lawson, 1991a). According to (Miki et al., 2011), the dissolution of this unreacted covellite can only be dissolved at potentials of about 550 mV (SHE) and above.

4.1.1 Pretreatment of chalcocite prior leaching

As mentioned above, the pretreatment prior leaching consists in agglomeration and curing. Regarding the pretreatment of chalcocite, there is limited information oriented to curing time. However, the industrial implementation of the CuproChlor process can be considered as part of the information. The CuproChlor process has been used for the dissolution of mixed copper oxide and sulphide minerals, as well as chalcocite, covellite and bornite. The process adds calcium chloride salt ($CaCl_2$) and sulphuric acid in the aglomeration step. With cuproChlor process benefits the heap permeability and generates a chloride media that benefits the dissolution of minerals such as chalcocite (Ghorbani et al., 2016). It is important to highlight that the metallurgical results obtained in column leaching tests using the CuproChlor process, was published by (Aroca et al., 2012). The authors indicate that the process allows to obtain excellent results for the treatment of copper sulphides such as chalcocite, covellite and bornite. According to (Aroca et al., 2012), it is possible to dissolve about 93% of copper in leaching times that do not exceed 120 to 140 days, against periods of almost a year that require bacterial leaching.

The effect of a pretreatment has been used by (Herreros and Viñals, 2007), treating a copper sulphide mineral supplied by a mining industry whose main copper contributor are the species djurleite-digenite ($Cu_{2-x}S$). The pretreatment consisted of adding concentrated sulphuric acid to a determined mass of ore. This mixture (agglomerate) was allowed for 8 days (curing time) at room temperature (~20 °C). The leaching of sulphide copper ores of the djurleite and digenite type was effective through agglomerative pretreatment. However, the authors not considered make a comparison with leaching tests without pretreatment. In tests performed by (Quezada et al., 2018) the reported a study on the effect of addition of chloride ion using seawater and discard brine (from desalination plants) in the agglomeration stage of a secondary copper sulphide ore. The effect of curing time on the same ore was also reported. A maximum of 72% of copper extraction was obtained using discard brine, 30 kg/t and 50 days of curing time. Tests were developed in leaching columns and using a mine ore where secondary copper sulphides prevail. The curing time, prior to the leaching stage, benefits the reactivity of the mineral with the solution, favoring the dissolution of species such as chalcocite (Dhawan et al., 2013).

According to section 3.1.1, the research developed by (Cerda et al., 2017) proposes that chalcocite, in pretreatment, will generate CuS as a product (Eq.5). Furthermore, the authors propose that the CuS generated could also react in the pretreatment releasing Cu^{2+} to the system (Eq.4). The reactions can be seen in Table 2 of section 3.1.1, both reactions being thermodynamically possible. The mechanism proposed by these authors follows the trend of the mechanism of dissolution of chalcocite in chloride media proposed by (Cheng and Lawson, 1991a) exposed in Eq.18 and 19; and also similar to the proposal about chalcocite dissolution by Fe^{3+} assistance (Wu et al., 2013).

4.1.2 Chalcocite leaching: Main parameters

Chloride concentration

The presence of chloride ion benefits the dissolution of copper from chalcocite (Herreros et al., 1999). According to (Cheng and Lawson, 1991a), the presence of chloride accelerates the first dissolution stage of chalcocite (i.e. Cu_2S -> CuS) and making the second stage reaction possible (i.e. CuS -> S). According to the study carried out by (Cheng and

Lawson, 1991a) a presence between 18 and 70 g/L of chloride would be sufficient for the dissolution of species such as chalcocite, with no significant differences over 18 g/L of Cl^- (see Figure 56). This too is believed to be due to the reduction in oxygen solubility.

According to (Cheng and Lawson, 1991a), the Cu^{2+} generated in the first reaction (Eq.18), in the presence of Cl^-, will form the $CuCl^+$ complex. The authors state that, unless the reaction pulp is oxygen deficient, cuprous ions, whether complexed or not, are not stable; they oxidize to the Cu^{2+} state. It is important to consider that the leaching tests performed by the authors were between 65-94 °C. However, according to (Senanayake, 2007), the presence of $CuCl^+$ is predominant at low chloride concentrations (<0.5 mol/L, approximately 18 g/L of Cl^-), while the $CuCl_2^-$ complex (associated to Cu^+) will be the predominant specie at concentrations <0.8 mol/L (over 28 g/L of Cl^-) at 25 °C. Other complexes such as $CuCl_2^0$ will be stable at high temperatures (102 °C). The reduction potential of the Cu^{2+}/Cu^+ couple has a value of $E_{Cu2+/Cu+}$= 0.45 V. Furthermore, (Senanayake, 2009) exposes that the formation of Cu^+ and elemental suphur in oxygenated chloride solutions is a result of the reaction between Cu^+ and hydrogen sulphide. According to (O. Herreros et al., 2005), the importance of knowing these formations is because some complexes, such as $CuCl^+$ and $CuCl_2^-$, also have the ability to dissolve species such as chalcocite and covellite.

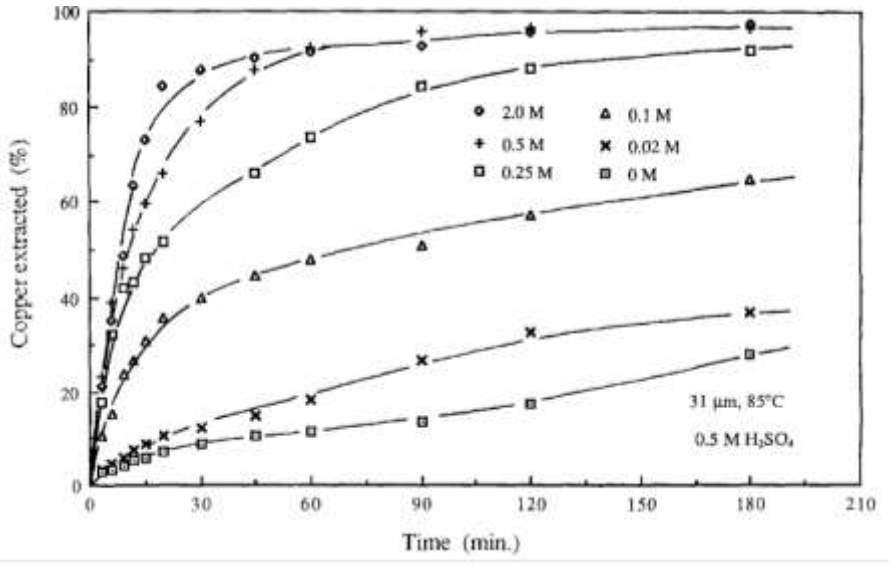

Figure 56. The effect of chloride ion concentration on copper extraction during chalcocite leaching (Cheng and Lawson, 1991a)

The presence of chloride also prevents the formation of a stable layer of elemental sulphur on the product of the first reaction (CuS) (Vračar et al., 2000). Chloride promotes the formation of crystalline sulphur rather than a crypto-crystalline or amorphous product. The effect of chloride ions on solid surface morphology was evaluated by (Hashemzadeh and Liu, 2020). The authors evaluated the leaching residue from chloride media. Leaching residues seemed to be covered by a thin amorphous layer and spherical nodules. The porosity of the surfaces, of leaching residues, increased while increasing chloride concentration. However, the same authors indicated that not only elemental sulphur is responsible for passivation; polysulphides (CuS_n) are also responsible for the slow dissolution in the second stage.

Particle size

The influence of particle size on the dissolution of a chalcocite and covellite mineral has been studied by (Grizo et al., 1982). The authors performed leaching tests in the presence of ferric sulphate. The authors determined that a particle size -63 µm optimizes the dissolution of the mineral. Reducing particle size not only benefits copper extraction but also reduces leaching times. Similar trend shows (Herreros and Viñals, 2007) in tests carried out with a mineral composed of djurleite and digenite. The authors obtained over 90% copper dissolution using a particle size of 120 µm; however they not obtained a greater difference when comparing results with a particle size of 250 µm (See Figure 57).

According to (Cheng and Lawson, 1991a), in chalcocite leaching tests, the authors evaluated 3 particle sizes (12, 36 and 58 µm). Although at 12 µm the highest copper extraction was obtained, all the evaluated particle sizes reached 90% copper dissolution after 2 hours of leaching at 85 °C, 0.5 M H_2SO_4 and 0.5 M of NaCl. The authors indicate that, at the smaller the particle size, the thicker the boundary layer surrounding the particle, and therefore the smaller the specific apparent rate constant for reactions under diffusion control. The effect of initial particle size on chalcocite leaching was investigated by (Hashemzadeh et al., 2019), evaluating various particle size fractions. The authors demonstrated the effect according to the 2 dissolution stages proposed for chalcocite. A

larger particle size will cause a decrease in the first dissolution reaction but only a slight decrease in the second stage. The results obtained by the authors are shown in Figure 58.

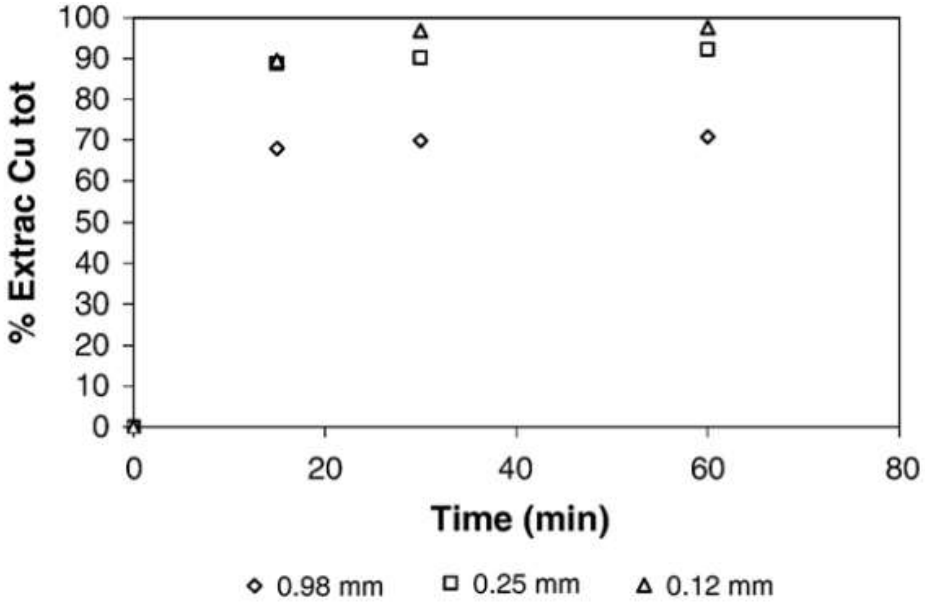

Figure 57. Copper extraction vs time as a function of particle size (20 °C, 400 rpm, 10% solids, 3 g/L Cl^-, 8 g/L H_2SO_4) (Herreros and Viñals, 2007)

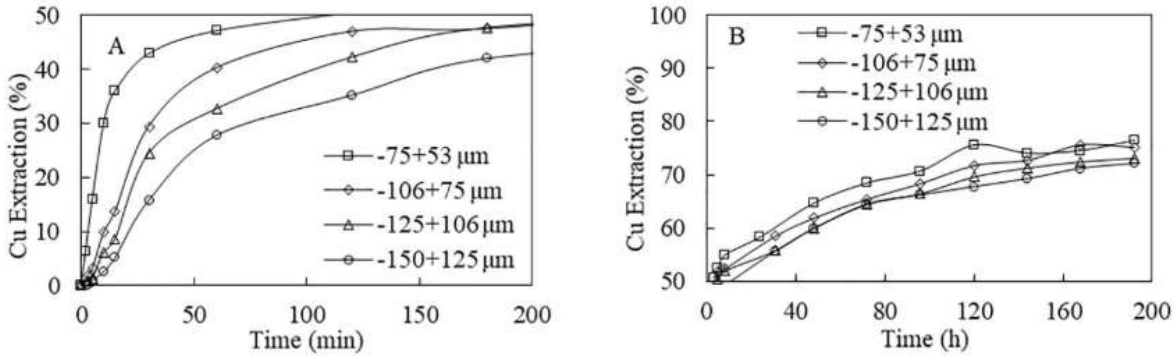

Figure 58. Copper extraction from chalcocite versus leaching time at varied initial particle sizes under the following conditions: Cu^{2+}: 0.016 M, Cl^- 1.56 M, 25 °C, pH 1.5. A: the first stage; B: the second stage (Hashemzadeh et al., 2019)

Acidity

The effect of the acid concentration was evaluated by (Cheng and Lawson, 1991a). The authors showed that the dissolution reaction of chalcocite increased when increasing the acidity from 0.02 to 0.5 M of H_2SO_4 (approximately from 1.96 to 49 g/L H_2SO_4). However, above 0.5 M (up to 2 M H_2SO_4) the effect is not significant (See Figure 59). The authors stated that the increase is by no means linear at high acidities (up to 2 M H_2SO_4), the

reduced oxygen solubility in the early stage of reaction actually resulted in a reduction in the copper dissolution rate. The study carried out by (Miki et al., 2011) also evaluates the effect of acidity in the medium but using HCl and leaching covellite. This study is useful from the point of view of the second dissolution reaction of chalcocite. The authors exposed that at high concentrations of HCl accelerated the anodic dissolution of covellite because of the formation of a $CuCl_2^-$ complex ion. The authors demonstrated that the dissolution of copper from covellite is independent between 0.1 and 0.5 M HCl (Figure 60). However, it is important to consider that the dissolution was carried out at 600 mV using cupric ions, iron ions and at 35 °C.

Tests carried out by (Vračar et al., 2000) show a behavior similar to that of (Miki et al., 2011); however, (Vračar et al., 2000) postulate that the dissolution rate would increase from 0.2 to 0.75 M of HCl, but over 0.5 M of HCl its influence on the degree of leaching is small. The tests carried out by (Vračar et al., 2000), unlike those of Miki et al, were carried out with a chalcocite-type mineral, so the acid consumption would increase when considering 2 dissolution stages.

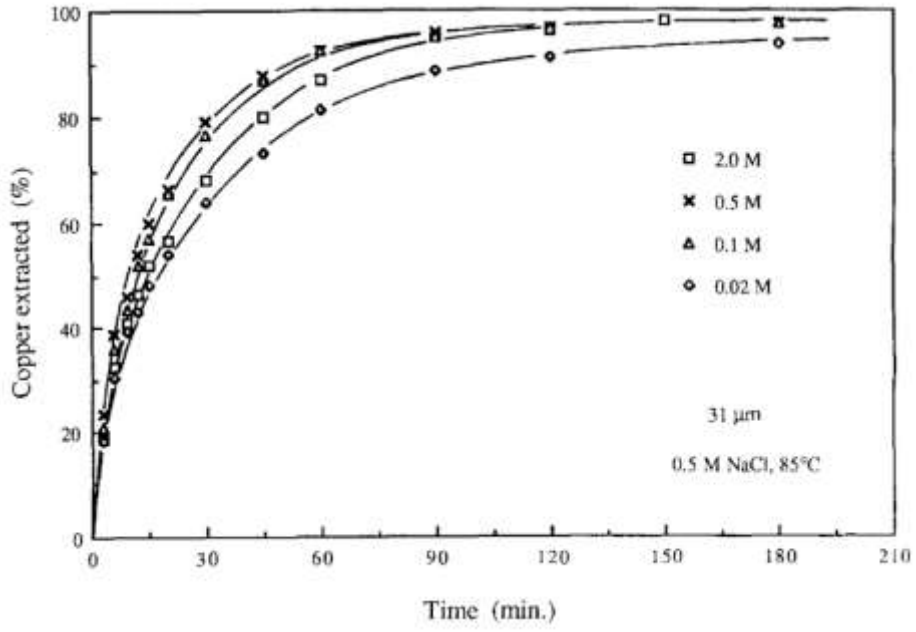

Figure 59. The effect of sulphuric acid concentration on copper extraction during chalcocite leaching (Cheng and Lawson, 1991a).

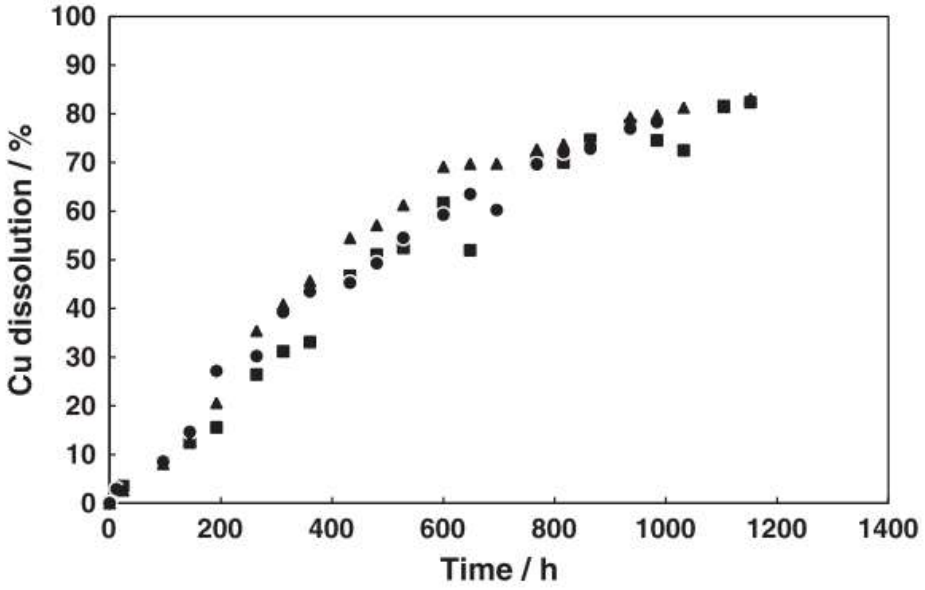

Figure 60. The effect of hydrochloric acid concentration on the dissolution of copper from synthetic covellite in dilute HCl solutions with 0.2 g/L Cu^{2+} and 2 g/L of iron at 35 °C and 600 mV. (■) 0.1 M HCl, (●) 0.2 M HCl, and (▲) 0.5 M HCl (Miki et al., 2011)

Solution potential

The effect of the solution potential has been evaluated by (Miki et al., 2011) performed leaching test with synthetic chalcocite at various potentials; 500, 550 and 600 mV (SHE). At a potential of 500 mV, about 50% of the copper dissolves but then increased at a slower rate when the potential was increased to 550 mV after 400 h of leaching. Therefore, 500 mV is a potential too low for the oxidation of the secondary covellite (second stage). An increase to 550 mV would allow the oxidation of the covellite formed. In addition, they postulate that secondary covellite (formed by the dissolution of Cu_2S) is more amenable to leaching than primary covellite.

According to (Niu et al., 2015) the rate of the second stage of chalcocite dissolution is not dependent on the solution potential in a range between 650-800 mV (SHE). The authors carried out chalcocite leaching tests in small leach columns (6 cm in diameter and 30 cm in length), trying to keep the conditions as uniform as possible and taking into account on heap bioleaching practices, according to (Ruan et al., 2013). The results obtained by (Niu et al., 2015) are shown in Figure 62.

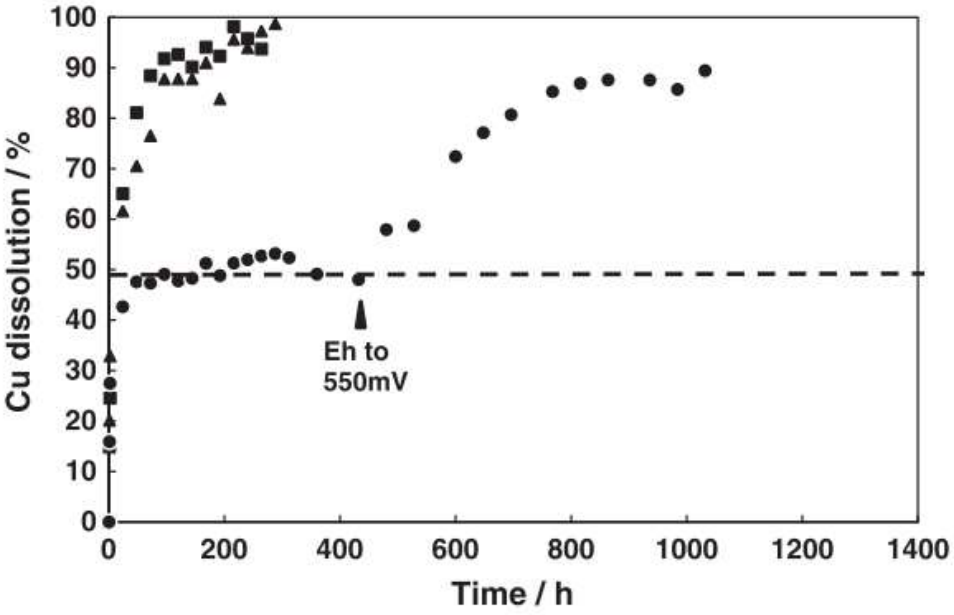

Figure 61. Copper dissolution from synthetic Cu_2S in 0.2 M HCl with 0.2 g/L Cu^{2+} and 2 g/L of iron at 35 °C. (▲) 550 mV, (■) 600 mV, and (●) 500 mV with potential increased to 550 mV after 400 h (Miki et al., 2011)

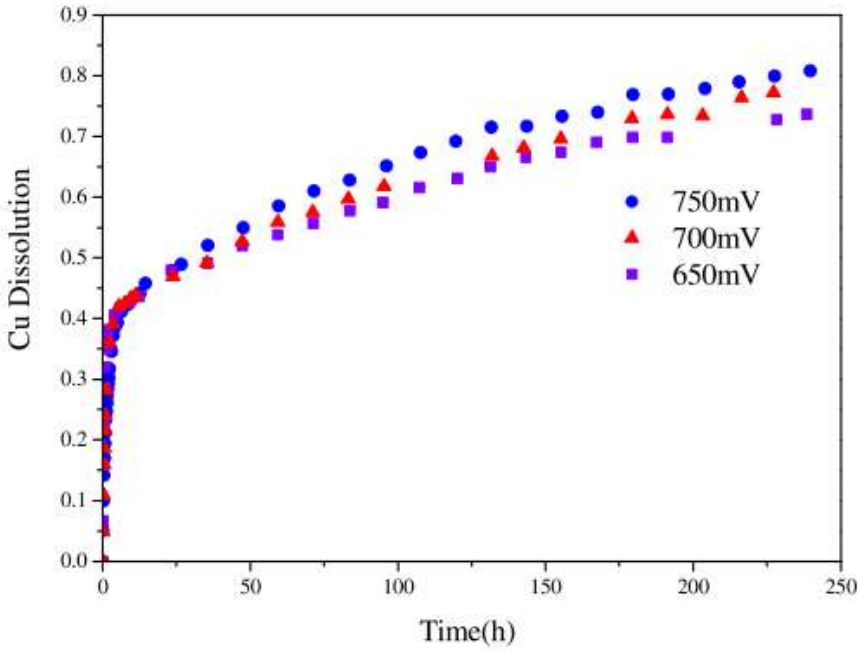

Figure 62. Effect of Eh on chalcocite dissolution. Conditions: size fraction: −54 + 30 µm; temperature, 30 °C; Fe^{3+} concentration, 10 g/L; pH, 1.05 ± 0.05 (Niu et al., 2015)

The study carried out by (Niu et al., 2015), since it is possible to compare with (Miki et al., 2011) who performed leaching tests of a synthetic covellite in 0.2 M HCl with 0.2 g/L Cu^{2+}, 2 g/L of iron at 35 °C. (Miki et al., 2011) concluded that there would be no major

difference in the copper extraction from covellite between using 600 and 650 mV but noticeably slower at 550 mV. This coincides with (Nicol and Basson, 2017) , who shows there was an important increase in the reactivity of covellite over 600 mV, being better in a chloride media up to 5 M NaCl; however, the effect is not so considerable between 1 and 5 M NaCl.

Temperature

Because chalcocite presented two dissolution stages, there were then 2 different behaviors that can be determined. It's possible to identify two inflection points in the dissolution of chalcocite. The first point identified approximately 45% of dissolved copper, in the conversion of Cu_2S into the blue-remaining CuS ($Cu_{1.0\text{-}1.2}S$). The second inflection point at approximately at 70% of copper dissolution, corresponded to the noticeable decline in leaching rate (Niu et al., 2015).

According to (Cheng and Lawson, 1991a), who performed tests of chalcocite dissolution in a chloride media, determined an activation energy of 33.5 kJ/mol in the first leaching stage, which is indicative of diffusion control. The second stage reached an activation energy of 69 kJ/mol, typical value for a reaction under surface chemical control. The value of the activation energy of the second stage is very similar to the reported by (Miki et al., 2011) on the dissolution of covellite in chloride media (72 kJ/mol). To determine this value, (Miki et al., 2011) evaluated the effect of temperature at 25, 35 and 45 °C (Figure 63). The authors even comment that this activation energy value was similar to that obtained for chalcopyrite dissolution under similar conditions (73 kJ/mol) obtained by (Velásquez-Yévenes et al., 2010a). According to (Petersen and Dixon, 2003), the activation energy values can vary from 4 to 25 kJ/mol for the first dissolution stage, while for the second stages energies from 55 to as high as 105 kJ/t were reported.

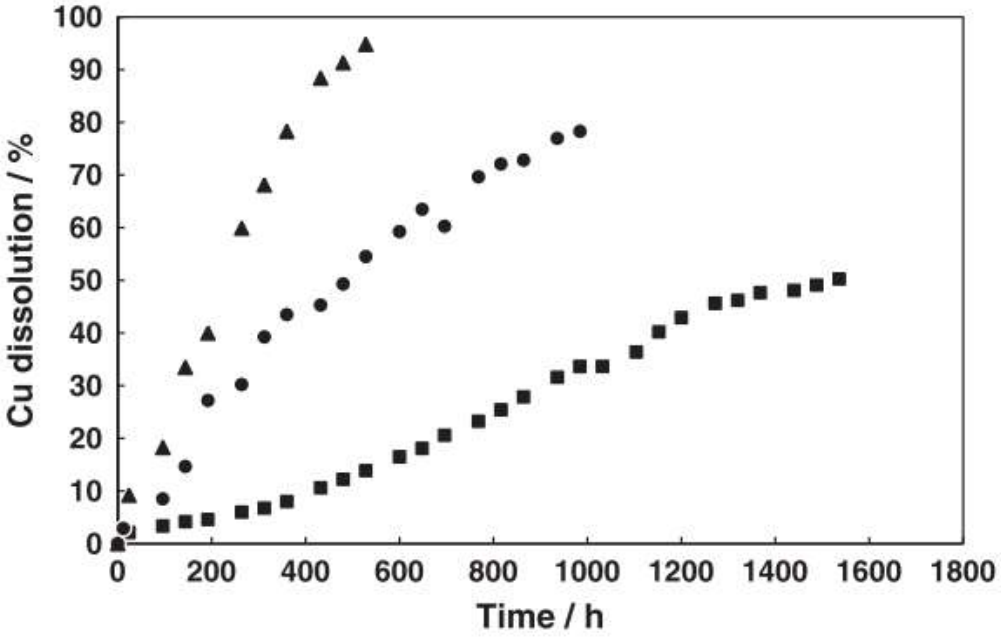

Figure 63. The effect of temperature on the dissolution of copper from synthetic covellite in 0.2 M HCl with 0.2 g/L Cu^{2+} and 2 g/L iron at 600 mV (■) 25 °C, (●) 35 °C, and (▲) 45 °C (Miki et al., 2011)

4.2 Results of the pretreatment and leaching efficiency of chalcocite

4.2.1 Characterization of chalcocite mineral

The chemical characterization of the chalcocite sample is presented in Table 24. A very characteristic presence of copper and sulphur is observed in this type of samples, due to the weight percentage of each species in the chalcocite formula (Cu_2S). The presence of copper, sulphur and iron almost entirely make up the chemical composition of the sample, demonstrating the high purity of the sample used in this study. Additionally, after chemical characterization, the insoluble residue represented 5.7% of the total mass. This value suggests the presence of quartz or muscovite as insoluble phases present in the sample. Finally, the presence of soluble phases was measured by washing the sample in water, a 0.02% copper extraction was obtained.

Table 24.Chemical analysis of the chalcocite ore

Element	Cu	S	Fe
Mass (%)	75.0	23.5	1.33

Figure 64 (X-ray diffractogram) shows that the sample contained mainly chalcocite, together with small amounts of quartz and pyrite. Table 25 shows the main mineralogical composition of the sample used, obtained by Qemscan analysis. According to this analysis, the main mineral species were chalcocite (93.7 %), followed by pyrite (2.16 %) and quartz (1.25 %). Other copper contributing minerals such as brocanthite, covellite, chalcopyrite and bornite have been identified in low concentration. According to Qemscan analysis, chalcocite contributes 98.3% of the copper in the sample, followed by brocanthite with 0.7% and 1.0% between covellite, chalcopyrite and bornite.

SEM analysis showed the majority presence of chalcocite, then quartz and pyrite (Figure 65). Finally, it is possible to appreciate that the chalcocite is released and almost not associated with any species in its structure (Figure 66). EDS analysis associated with the initial characterization of the chalcocite sample are presented in appendix 13.

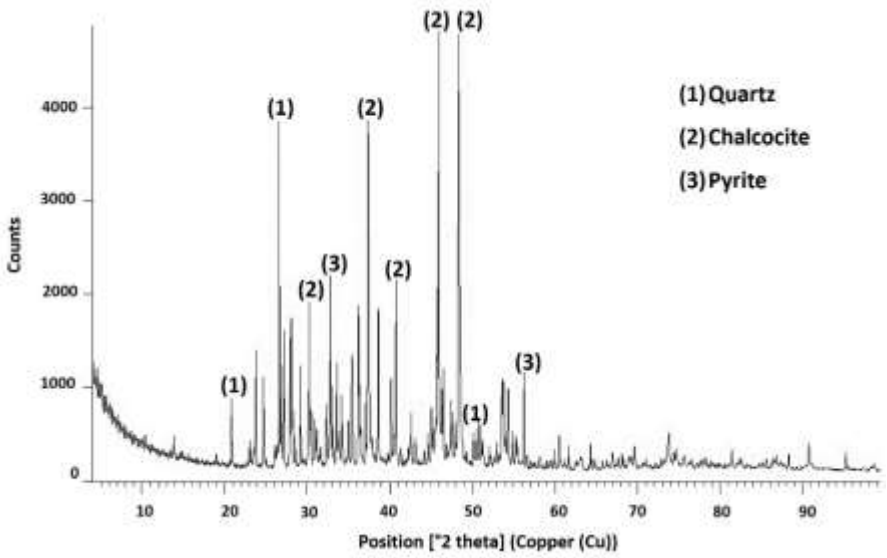

Figure 64. X-ray diffraction pattern of the initial sample of chalcocite

Table 25. Main mineralogical composition of the initial sample (mass in %) according to Qemscan analysis

Mineral	Mass, %
Chalcocite	93.7
Pyrite	2.16
Quartz	1.25
Brocanthite	1.10
Covellite	0.49
Bornite	0.49
Chalcopyrite	0.36

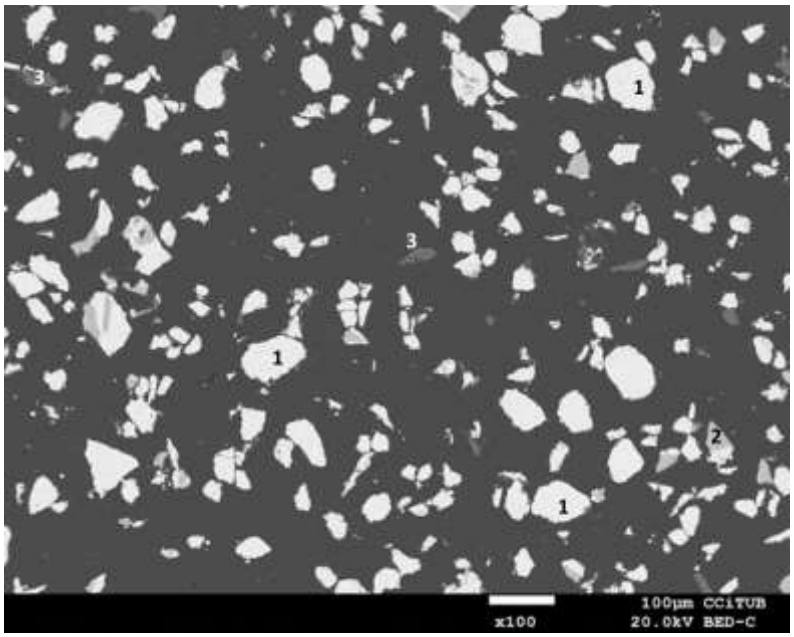

Figure 65. SEM image of initial sample. 1: chalcocite; 2: pyrite; 3: quartz

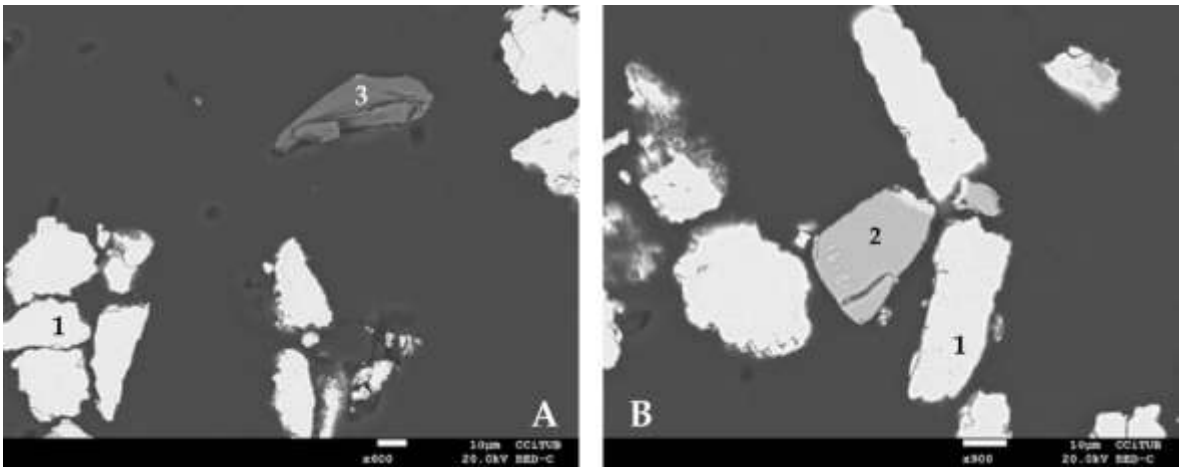

Figure 66. SEM image of initial sample. 1: chalcocite; 2: pyrite; 3: quartz

4.2.2 Pretreatment of chalcocite mineral

The results of the tests performed evaluating the curing time using 15 kg/t of H_2SO_4 and 25 kg/t of NaCl are shown in Figure 67. It can be seen that the copper extraction increased as the curing time increased for the air-tested and sealed in a container. No significant evidence is seen in copper extraction after 5 days of curing, reaching a copper extraction of 4.68%. Regarding the tests in a nitrogen media, a null effect of the curing time is evident in the copper extraction. The test at 7 days of curing in nitrogen media reached the highest copper extraction, 2.57%. With the injection of nitrogen in the system, the oxygen in the solution (used in the pretreatment, in addition to the oxygen present in the environment) was removed, and consequently limits the chalcocite reaction (Butler et al., 1994; Cheng and Lawson, 1991a).

According to the results shown in Figure 67, it was decided to consider 7 days of curing as the time to be used in the following tests. In Figure 68, the effect of the sulphuric acid concentration in the pretreatment is evaluated, considering 25 kg/t of NaCl and 7 days of curing. It can be seen in Figure 68 that at 40 kg/t of H_2SO_4 the maximum copper extraction was reached, 5.73%. When using 30 kg/t H_2SO_4, 5.40% copper extraction was achieved, being a little significant difference compared to using 40 kg/t H_2SO_4. Finally, it was decided to use 30 kg/t of H_2SO_4.

According to (Senanayake, 2007), on the surface of chalcocite, multiple reactions occur, mainly following the mechanism of chalcocite dissolution proposed by (Cheng and Lawson, 1991a). According to the authors, it benefits the reactivity of the chalcocite surface. Therefore, the presence of chloride was evaluated up to 40 kg/t of NaCl (saturation limit of the solution) and considering 30 kg/t H_2SO_4 and 7 days as curing time. Finally, a copper extraction of 6.10% was obtained using 40 kg/t NaCl, 30 kg/t H_2SO_4 and 7 days of curing time, increasing the extraction with respect to the same conditions but using 25 kg/t NaCl (5.73% copper extraction). Therefore, the conditions used and that maximize the copper dissolution in the pretreatment are: 40 kg/NaCl, 30 kg/t H_2SO_4 and 7 days of curing time. These conditions were used for the characterization of the agglomerates (section 4.2.3) and to evaluate the effect of leaching efficiency (section 4.2.4).

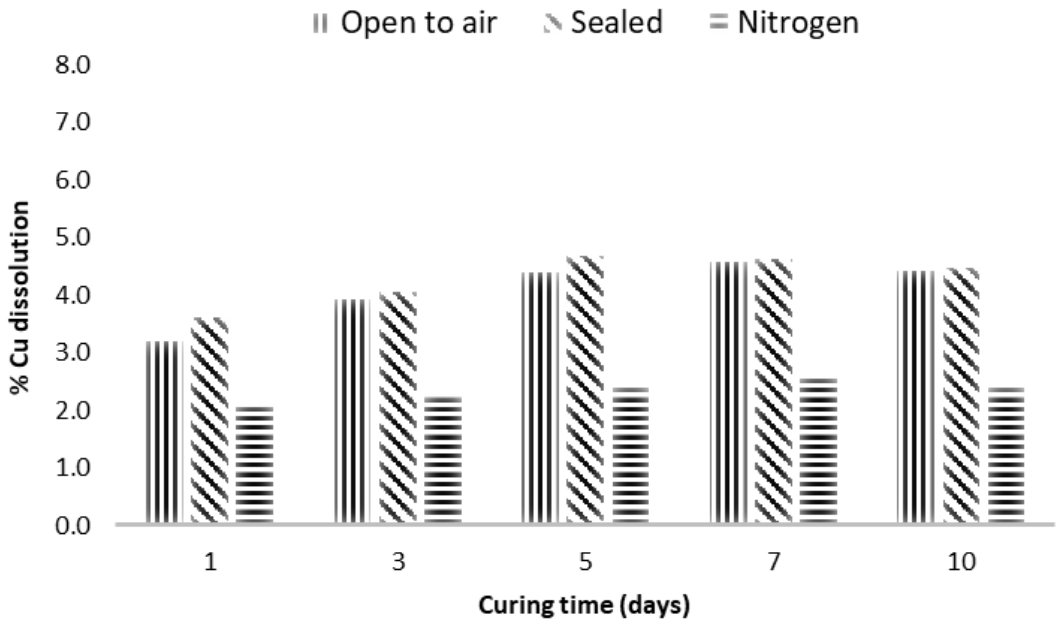

Figure 67. Copper extraction from chalcocite at different curing time using 15 kg/t H_2SO_4 and 25 kg/t NaCl at room temperature

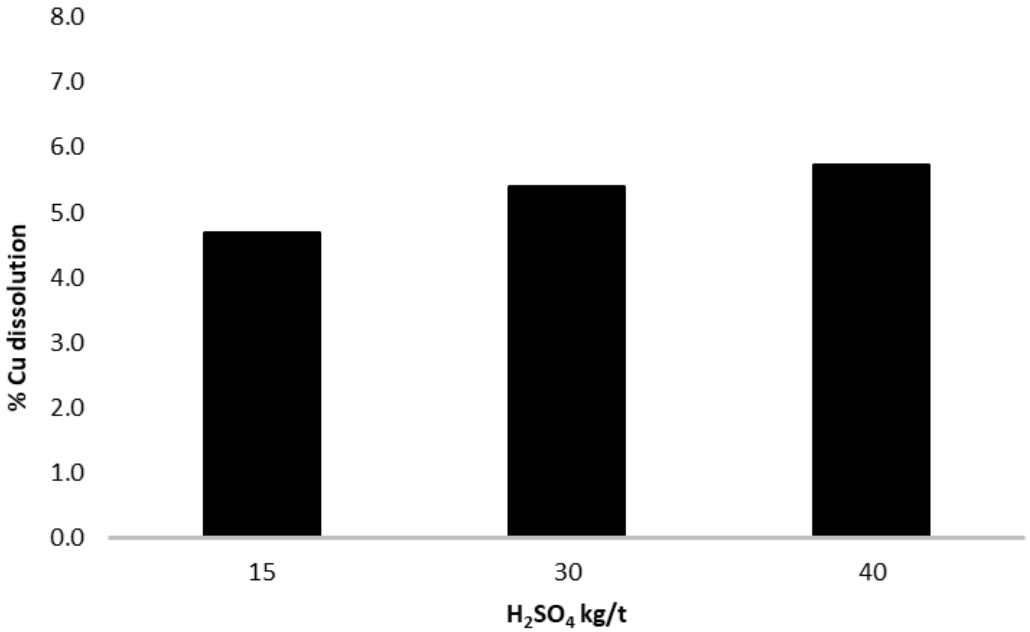

Figure 68. Copper extraction from chalcocite at different concentrations of sulphuric acid using 25 kg/t NaCl and 7 days as curing time

4.2.3 Characterization of pretreatments products

The combination obtained that maximizes the dissolution of copper from the chalcocite was: 40 kg/t NaCl, 30 kg/t H_2SO_4 and 7 days of curing time. This sample was characterized to propose the mechanism associated with the pretreatment of chalcocite. The generated glomers were prepared and polished avoiding contact with water, taking care not to dissolve the formed soluble phases.

In Figure 69 it is possible to appreciate the products identified in the pretreatment according to X-ray diffraction analysis. Species such as pyrite and quartz are still present, although in a minority level. The presence of chalcocite (Cu_2S) is no longer evident, generating a copper-depleted chalcocite ($Cu_{1.75}S$). This new phase is called anilite and has been proposed as a non-stoichiometric compound in the first leaching stage of chalcocite (Hashemzadeh et al., 2019). According to X-ray diffraction analysis, all the main peaks associated with $Cu_{1.75}S$ have been identified. The formation of other products such as $CuSO_4$ and Cu(OH)Cl have also been identified. The presence of $CuSO_4$ is related to the copper that dissolves after pretreatment (6.10% in section 4.2.2). The presence of Cu(OH)Cl coincides

with (Senanayake, 2007) who proposes a series of intermediate surface reaction on chalcocite, being Cu(OH)Cl one of the possible compounds formed. Finally, the presence of Na_2SO_4 has also been identified, mainly justified by the addition of NaCl in the system and the presence of SO_4^{2-}considered an important ion donor (generated by the sulphuric acid dissociation) (Johansson et al., 1980).

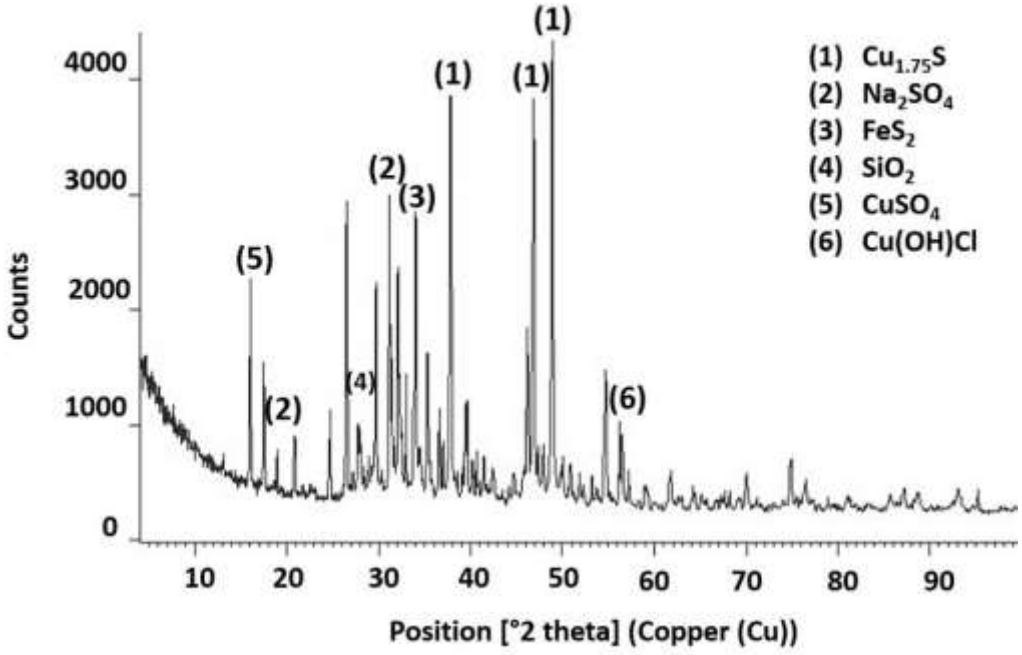

Figure 69. Species identified, using X-ray diffraction analysis, product of the pretreatment of a chalcocite mineral with 30 kg/t H_2SO_4, 40 kg/t NaCl and 7 days of curing time at room temperature

The presence of: $Cu_{1.75}S$, Na_2SO_4, $CuSO_4$ and Cu(OH)Cl can be confirmed comparing the initial diffractogram with respect to the diffractogram of the products obtained. Using the software X'pert HighScore Plus v.3.0e it is possible to show the main angle or angles with the characteristic peaks of each species.

Figure 70 shows the comparison of the initial state of the sample (dashed line) and the sample with pretreatment (continuous line). It can be seen that in all the main Cu_2S peaks (1) (32.8, 37.4, 45.9 and 48.3°) are no longer found and have been replaced by the new species $Cu_{1.75}S$ (2) (Figure 70a, b, c and d). This new species ($Cu_{1.75}S$) is associated with the depletion (oxidation) that occurs in chalcocite in the pretreatment. The $Cu_{1.75}S$ fraction is copper that does not react, remaining as a limiting stage without completing the first dissolution stage. This incomplete stage coincides with the 6.10% copper extraction that is

achieved in the pretreatment prior to leaching. Furthermore, no evidence of covellite presence has been detected in any of its most important peaks (Figure 71, absence of covellite in the main peak between 31.8 and 31.9 position).

According to (Fang et al., 2018), when copper extraction reached 10%, chalcocite would disappear and transform to digenite ($Cu_{1.80}S$), while all the intermediates were transformed to covellite when copper extraction achieved 50%. Thus, with the pretreatment, only the first stage of chalcocite dissolution (Djurleite, $Cu_{1.94}S$) would be overcome according to the conditions studied. The copper will be in the unreacted $Cu_{1.75}S$ phase and in products such as $CuSO_4$ and Cu(OH)Cl.

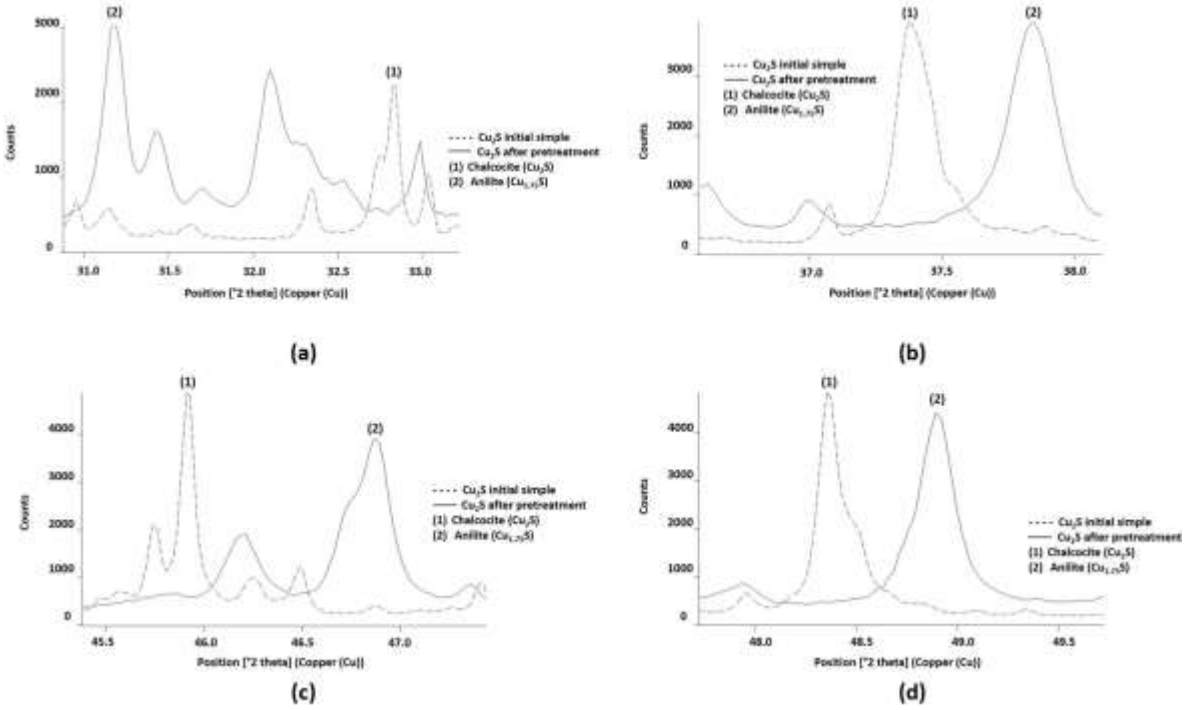

Figure 70. $Cu_{1.75}S$ identified, using X-ray diffraction analysis, products from the pretreatment of the chalcocite mineral with 30 kg/t H_2SO_4, 40 kg/t NaCl and 7 days of curing time at room temperature

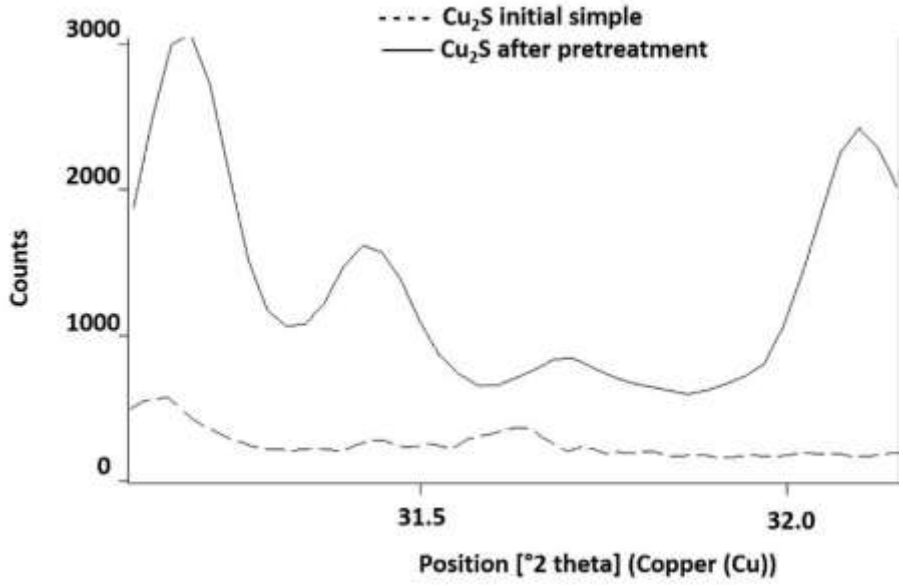

Figure 71. Absence of covellite in the main peak between 31.8° and 31.9° position, determined by X-ray diffraction analysis

Additionally, the formation of Na_2SO_4 was also been confirmed. Figure 72 shows the main peaks of the species. The formation of Na_2SO_4 was due to the dissociation of NaCl and the product generated by the dissociation of H_2SO_4. For the formation of Na_2SO_4, the presence of $SO_4^{2-}$and 2 Na ions are required to balance the oxidation. According to (Margarella et al., 2016), the presence of SO_4^{2-}in aqueous media is possible as a result of the dissociation of H_2SO_4.

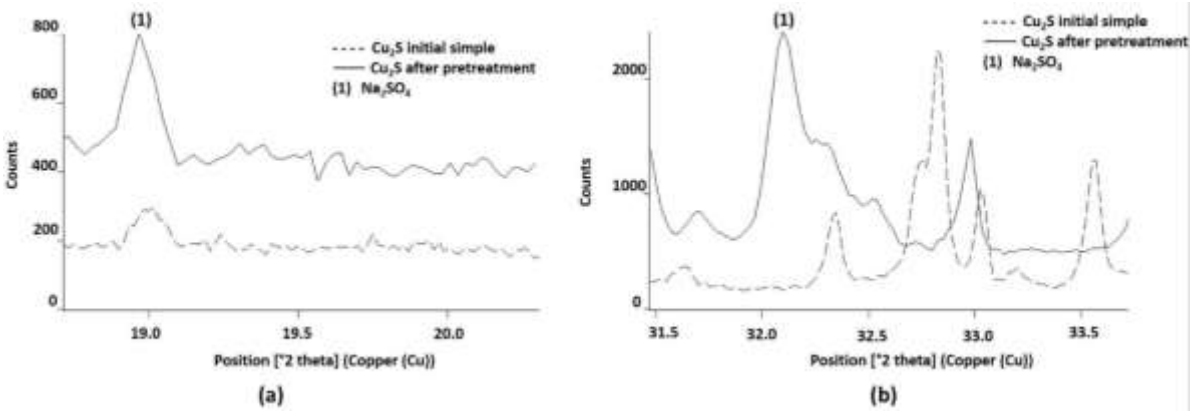

Figure 72. Na_2SO_4 identified, using X-ray diffraction analysis, products from the pretreatment of the chalcocite mineral with 30 kg/t H_2SO_4, 40 kg/t NaCl and 7 days of curing time at room temperature

The presence of $CuSO_4$ was confirmed by X-ray diffraction analysis and one of the main peaks can be seen, which appears with the pretreatment in 16.16° (Figure 73).

Furthermore, the presence of Cu(OH)Cl was also been confirmed although with less intensity than $CuSO_4$ (Figure 74) . The confirmation of $CuSO_4$ and Cu(OH)Cl coincides with that proposed by (Senanayake, 2007). According to (Senanayake, 2007), in an acid and chloride media, reactions occur on the surface of chalcocite, considering H_3O^+ (product of the first dissociation of sulphuric acid) and Cl^-. Thus, the mechanism proposed by (Senanayake, 2007), consider the formation of $Cu_2S{\blacksquare}H_3O^+{\blacksquare}Cl^-{\blacksquare}O_{2(ads)}$ according to the equations 20 and 21.

$$Cu_2S + H_3O^+ = Cu_2S \blacksquare H_3O^+_{ads} \quad \text{(Eq.20)}$$

$$Cu_2S \blacksquare H_3O^+_{ads} + Cl^- + O_2 = Cu_2S \blacksquare H_3O^+ \blacksquare Cl^- \blacksquare O_{2\,(ads)} \quad \text{(Eq.21)}$$

Equations 20 and 21 show the sequential adsorption of Cu_2S, H_3O^+, Cl^- and O_2 on the surface of chalcocite. The generated complex produces Cu(OH)Cl, CuS and H_2O_2 (Eq.22), proposing the first stage of dissolution of chalcocite. Finally, the Cu(OH)Cl complex is proposed as an intermediate copper species, while reacting with HSO_4^-, generating $CuSO_4$ (Eq. 23).

$$Cu_2S \blacksquare H_3O^+ \blacksquare Cl^- \blacksquare O_{2\,(ads)} = CuS + Cu(OH)Cl^0_{\left(\frac{ads}{aq}\right)} + H_2O_2 \quad \text{(Eq.22)}$$

$$Cu(OH)Cl^0_{\left(\frac{ads}{aq}\right)} + HSO_4^- = Cu(SO_4)^0 + Cl^- + H_2O \quad \text{(Eq.23)}$$

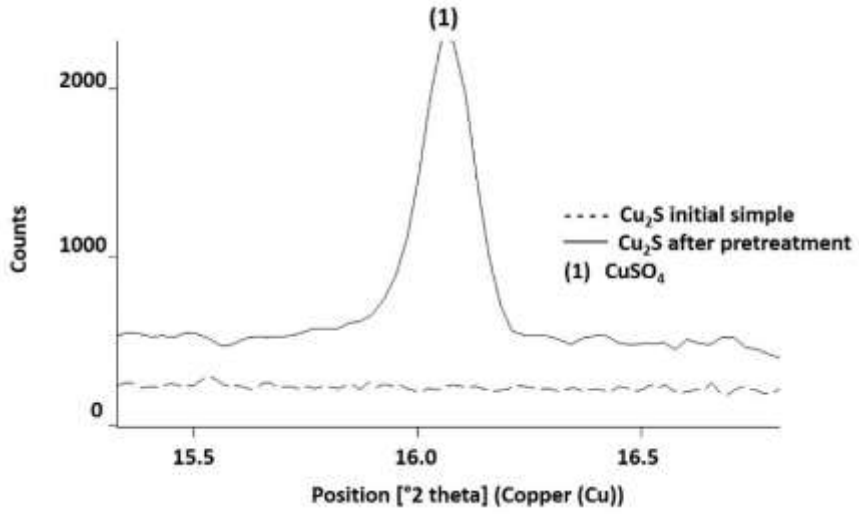

Figure 73. $CuSO_4$ identified, using X-ray diffraction analysis, products from the pretreatment of the chalcocite mineral with 30 kg/t H_2SO_4, 40 kg/t NaCl and 7 days of curing time at room temperature

SEM analysis was also been performed on the sample with pretreatment. An overview of the sample is shown in Figure 75. The majority presence of chalcocite (which reacts) and some minority species that is mainly associated with quartz is observed. Possible products can be seen on the surface of the particles. A close-up of the sample with pretreatment is shown in Figure 76; it is possible to observe the presence of a copper-depleted chalcocite (1) ($Cu_{2-x}S$) with products on its surface (2). The reaction product on $Cu_{2-x}S$ is associated with Cu(OH)Cl, which is confirmed by the percentage of presence associated with copper, chloride and oxygen (minor sulphur) generated, by semi-quantitative analysis. In the case of $Cu_{2-x}S$ a presence of copper (74.56%) and sulphur (24.04%) were evidenced, while for Cu(OH)Cl, a copper (58.53%), chloride (18.74%) and oxygen (19.75%) presence were determined. EDS analysis to chalcocite ($Cu_{2-x}S$) and Cu(OH)Cl are shown in Figure 77a and 77b, respectively.

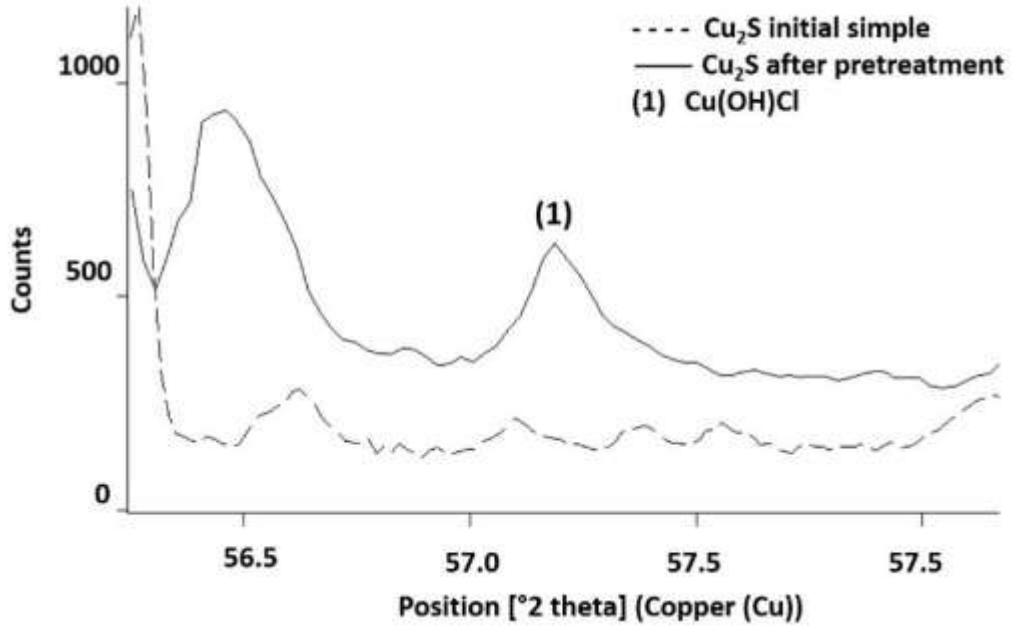

Figure 74. Cu(OH)Cl identified, using X-ray diffraction analysis, products from the pretreatment of the chalcocite mineral with 30 kg/t H_2SO_4, 40 kg/t NaCl and 7 days of curing time at room temperature

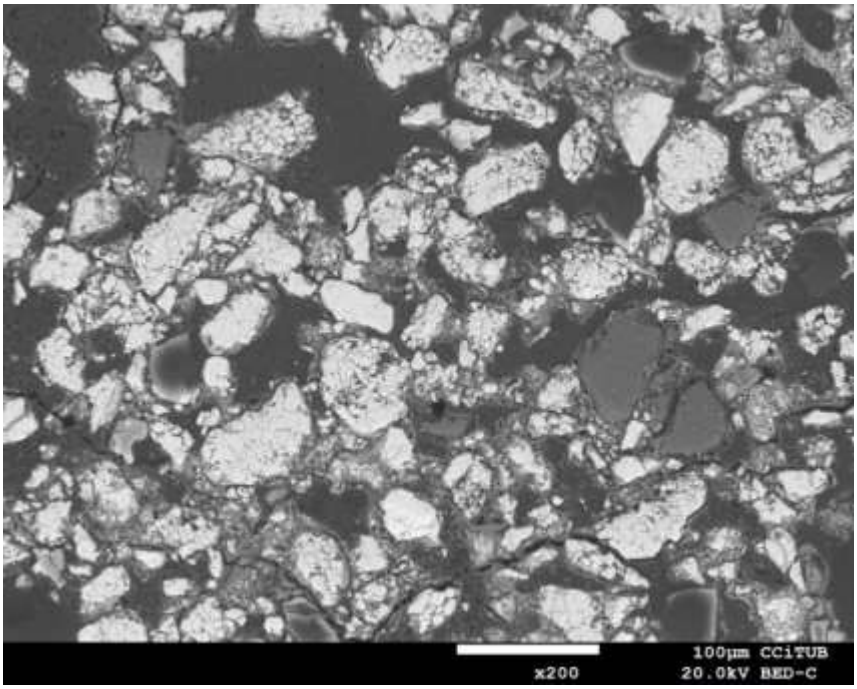

Figure 75. Cu_2S sample with pretreatment using 30 kg/t H_2SO_4, 40 kg/t NaCl and 7 days of curing time

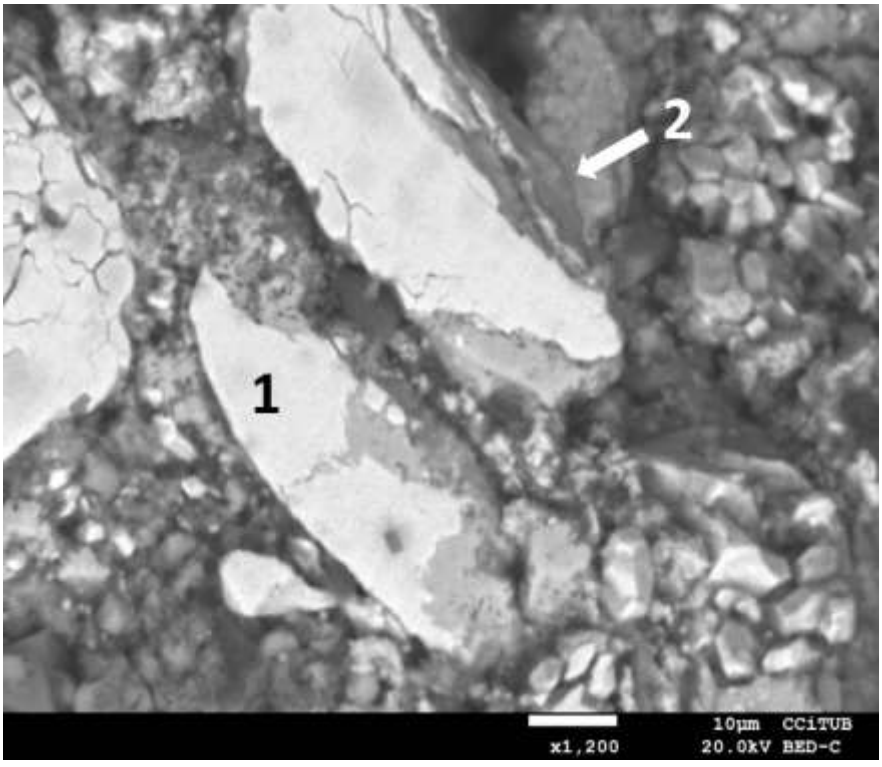

Figure 76. $Cu_{2-x}S$ (1) and Cu(OH)Cl (2) generated as a product of the pretreatment of chalcocite using 30 kg/t H_2SO_4, 40 kg/t NaCl and 7 days of curing time

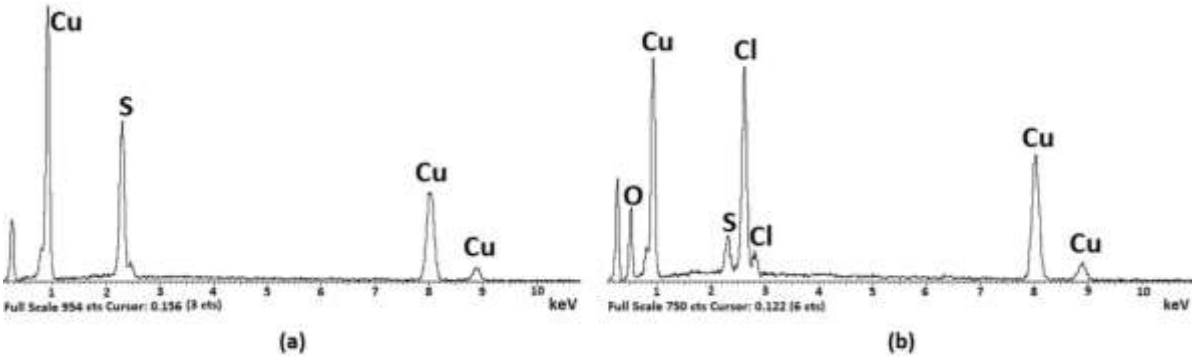

Figure 77. EDS analysis associated with Cu_{2-xS} (a) and Cu(OH)Cl (b) detected in Figure 76.

Figure 78 shows a copper-depleted chalcocite, of the form $Cu_{2-x}S$ (1) with reaction products on its surface, associated with $CuSO_4$ (2). The identification of $CuSO_4$ is verified by the percentage of presence associated with copper, sulphur and oxygen determined by EDS analysis (Figure 79). The confirmation of the presence of Cu(OH)Cl and $CuSO_4$ indicates the reactivity on the surface of the chalcocite proposed by (Senanayake, 2007). However, according to the conditions studied in this thesis, the transformation of chalcocite to covellite would be incomplete.

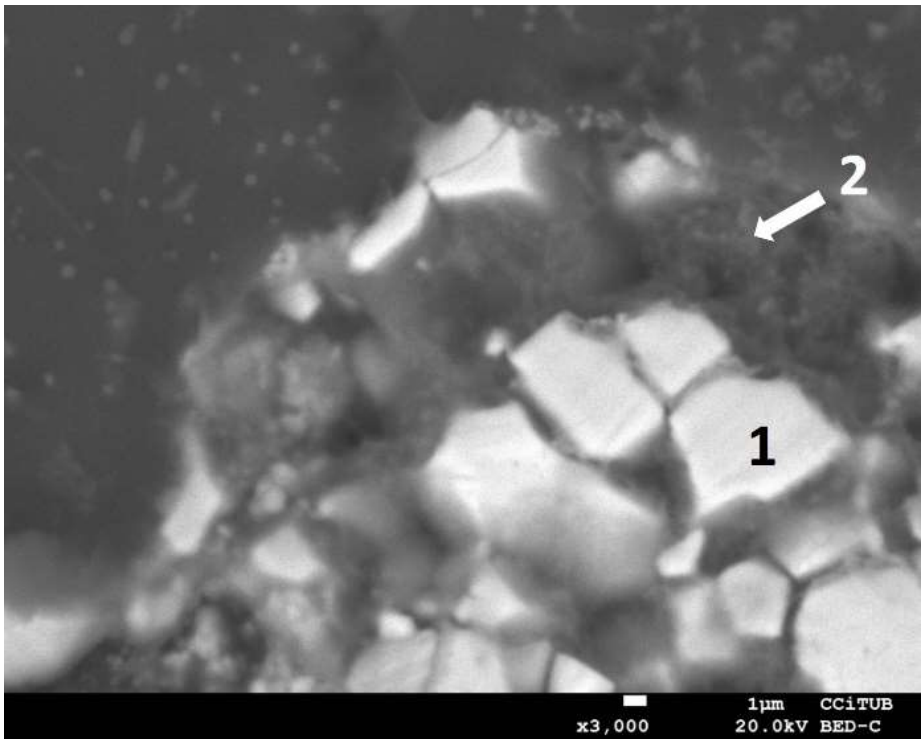

Figure 78. $Cu_{2-x}S$ (1) and $CuSO_4$ (2) generated as a product of the pretreatment of chalcocite using 30 kg/t H_2SO_4, 40 kg/t NaCl and 7 days of curing time

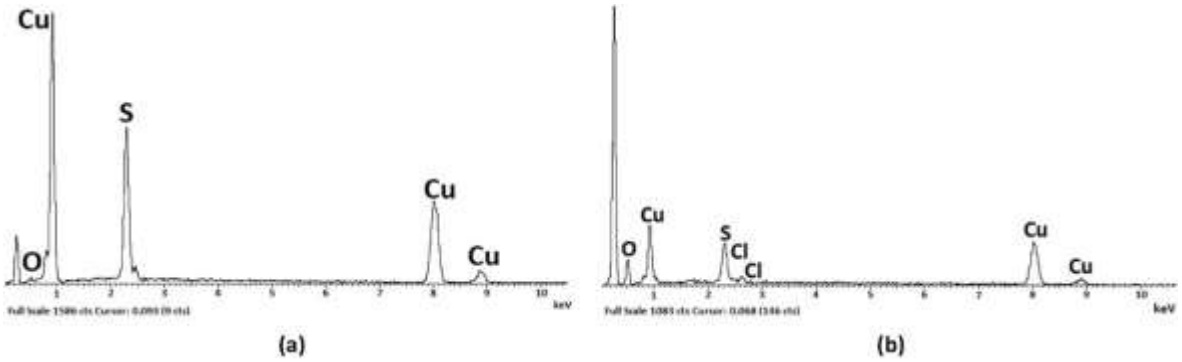

Figure 79. EDS analysis associated with $Cu_{2-x}S$ (a) and $CuSO_4$ (b) detected in Figure 78.

Furthermore, SEM and mapping analysis on the surface of the chalcocite ($Cu_{2-x}S$) have determined that the greatest presence of transformation products will occur on the surface of the chalcocite. Figure 80a shows the sample with pretreatment and whose surface has reacted generating products associated with chloride, mainly (Cu(OH)Cl); this is confirmed in the analysis according to the presence (superposition) of elements shown in Figure 80b. The detail of the superposition of copper, sulphur, oxygen and chloride is observed in Figure 81.

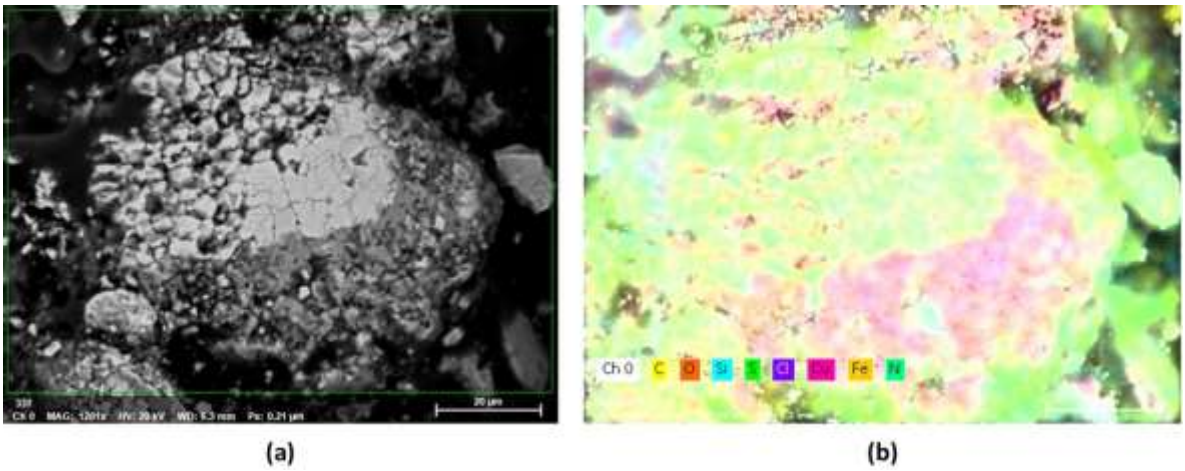

Figure 80. SEM analysis of sample with pretreatment (a), and mapping analysis associated with the presence of various elements (b)

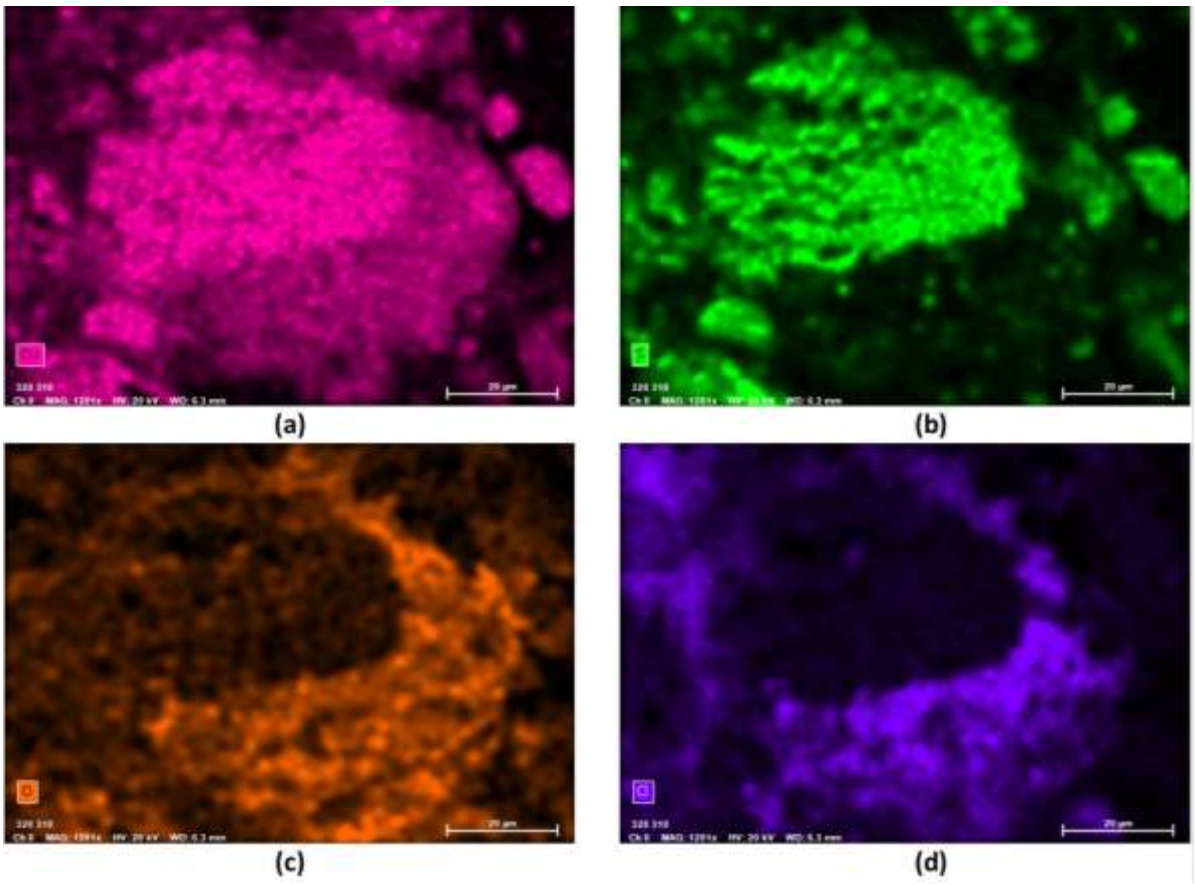

Figure 81. Presence of elements associated with Figure 80: Copper (a), sulphur (b), oxygen (c) and chloride (d)

Therefore, and considering all the characterization of the pretreatment products, the following reactions mechanism that occurs in the pretreatment of chalcocite are proposed. The concentration of 30 kg/t of H_2SO_4, 40 kg/t of NaCl and 7 days of curing time to a sample of natural chalcocite and room temperature, should governed by Eq. 24, which is the product of reactions 25 and 26.

$$4Cu_2S + 0.75H_2SO_4 + 0.5O_2 + 0.5NaCl = 4Cu_{1.75}S + 0.5Cu(OH)Cl + 0.25Na_2SO_4 + 0.5CuSO_4 + 0.5H_2O \quad \text{(Eq.24)}$$

$$2Cu_2S + 0.5H_2SO_4 + 0.25O_2 = 2Cu_{1.75}S + 0.5CuSO_4 + 0.5H_2O \quad \text{(Eq.25)}$$

$$2Cu_2S + 0.25H_2SO_4 + 0.25O_2 + 0.5NaCl = 2Cu_{1.75}S + 0.5Cu(OH)Cl + 0.25Na_2SO_4 \quad \text{(Eq.26)}$$

4.2.4 Leaching with and without pretreatment

The effect of pretreatment on copper leaching efficiency on chalcocite mineral is evaluated by leaching tests. Two leaching tests were performed at 25 and 50 °C, with and without pretreatment. Additionally, oxygen and nitrogen injection leaching tests have been performed without pretreatment and at room temperature. The detail of copper dissolution can be reviewed in appendix 14-16.

Leaching test without pretreatment

The copper dissolution from chalcocite without pretreatment can be observed in Figure 82. In this figure the results obtained in four (4) leaching tests are shown, all without pretreatment, performed at 25 and 50 °C in atmospheric condition and other two with the injection of oxygen or nitrogen at 25 °C. In the test performed at 25 °C (atmospheric condition), the classic behavior of chalcocite dissolution was observed, reaching a maximum copper extraction of 49.5% at 12 hours of leaching. It is possible to observe a dissolution slowdown after 8 hours of leaching. This behavior coincides with results obtained by (Cheng and Lawson, 1991a) who suggested that the second stage of dissolution can be described in terms of a model in which a shrinking ore of unreacted covellite is surrounded by a layer of elemental sulphur. Increasing the temperature to 50 °C (atmospheric condition) the behavior is similar, although the maximum copper extraction after 12 hours of leaching was 66.9%.

The test performed with pure oxygen injection (constant flow of 1.0 L/min) is shown as the best test in Figure 82. With oxygen injection a copper dissolution of 68.6% was achieved, unlike the test performed with nitrogen injection (constant flow of 1.5 L/min) that obtained the lowest copper extraction (21.2%) establishing the key role of the oxygen for the chalcocite dissolution (Cheng and Lawson, 1991a). Finally, the test carried out at 50 °C reached a maximum copper extraction of 66.9%.

In the second dissolution stage, passivation is mainly caused by the presence of elemental sulphur (Miki et al., 2011) or polysulphides (CuS_2) (Nicol and Basson, 2017). However, the solution potential has also been identified as a variable that limits the

covellite dissolution. Test performed at 50 °C has a slower dissolution than the test with oxygen injection (25 °C). According to (Cheng and Lawson, 1991a), the first dissolution reaction is limited by the diffusion of oxygen through the liquid boundary layer around the particles.

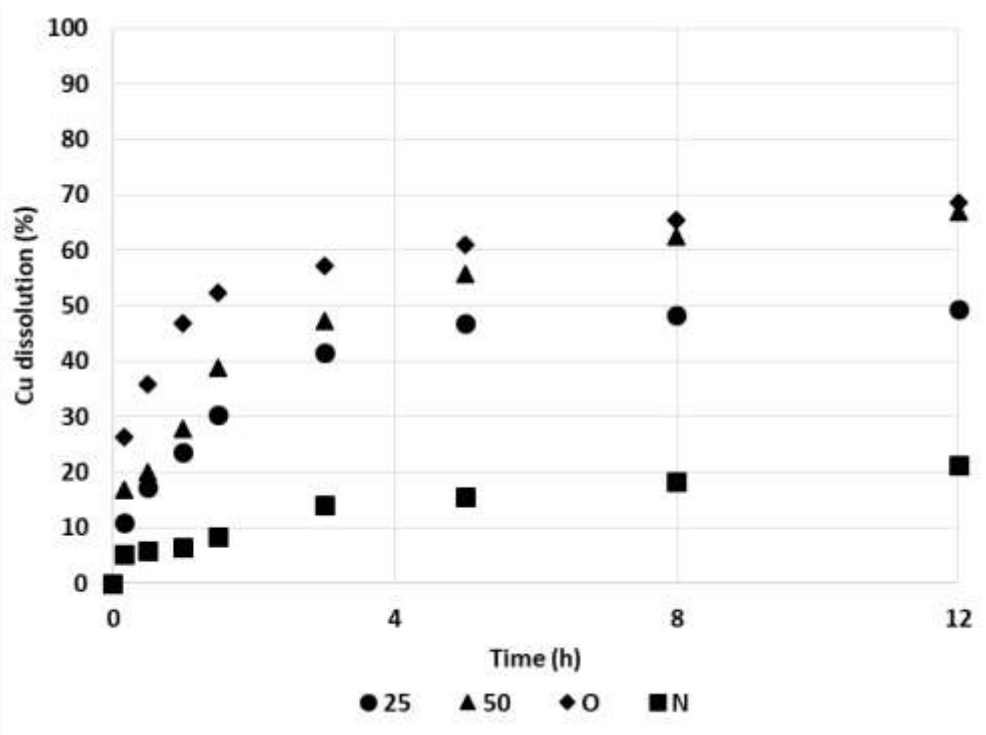

Figure 82. Copper dissolution from chalcocite in 0.2 M H_2SO_4, 50 g/L of Cl^- ion from NaCl in deionized water at 25 °C (●25); 50 °C (▲50) without pretreatment; oxygen injection (♦O) and nitrogen injection (■N) at 25 °C without pretreatment

Figure 83 shows that the solution potential begins (for all the tests) close to 590 mV (SHE) and decrease sharply at the beginning of the leaching, to a range between 380 and 420 mV. However, with oxygen injection the solution potential drops to 500 mV but increases quickly to a constant value of 640 mV. According to (Miki et al., 2011), reactions that involve dissolved oxygen contribute to the re-oxidation of copper (I) to copper (II), being an active oxidant. As (Miki et al., 2011) suggests, the rate of covellite dissolution is similar at potentials of 600 and 650 mV, however dissolution is notably lower at a lower potential of 550 mV. The above coincides with the behavior of all the tests carried out, except the test with oxygen injection.

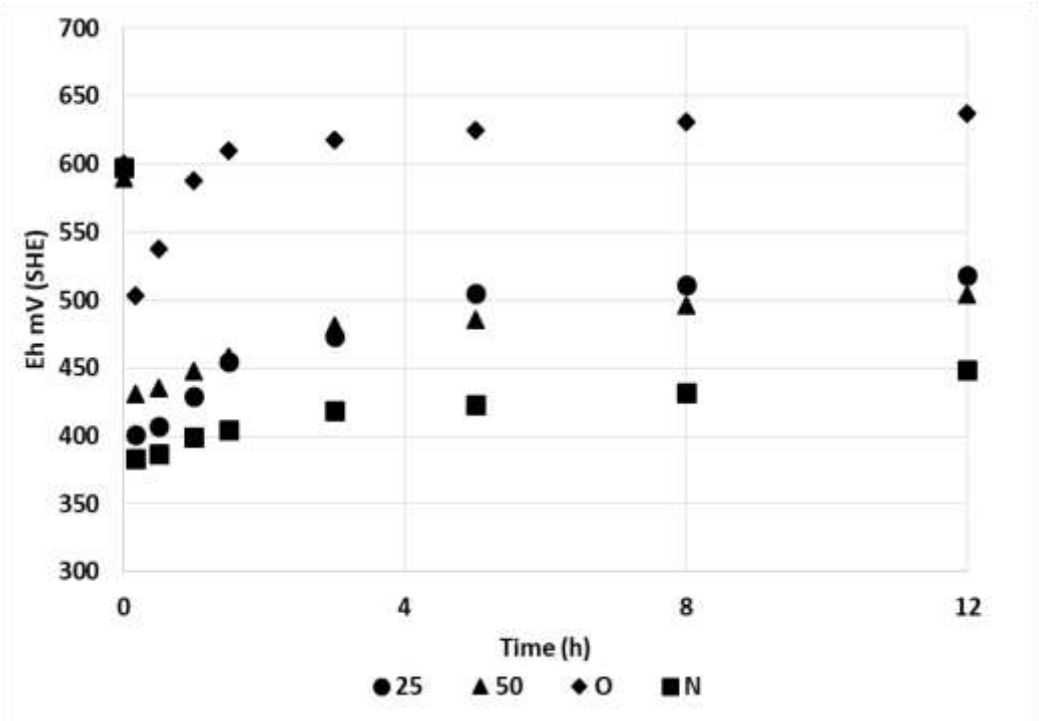

Figure 83. Behavior of solution potential on the chalcocite dissolution in 0.2 M H_2SO_4, 50 g/L of Cl^- ion from NaCl in deionized water at 25 °C (●25); 50 °C (▲50) without pretreatment; oxygen injection (♦O) and nitrogen injection (■N) at 25 °C without pretreatment

Leaching test with pretreatment

The effect of pretreatment on leaching efficiency can be observed in Figure 84. Additionally, Figure 85 shows the total number of tests carried out (6) with and without pretreatment. Figure 84 shows that the effect of pretreatment generates a small increase in copper extraction in the test carried out at 25 °C, reaching a copper extraction of 51.8% at the end of the process. A difference of 2.3% more copper than the test without pretreatment was observed. At 50 °C with pretreatment, a copper extraction of 71.5% was achieved, rising 4.6% compared to the test without pretreatment. The effect of the pretreatment, in tests at 50 °C, would allow a 33% reduction in the leaching time, achieving the same copper extraction as the test without pretreatment.

According to the results obtained, the pretreatment could not previously reverse the passivation of the second stage of chalcocite dissolution. This is based on the characterization performed on the pretreated sample and on the effect on the leaching efficiency. Thus, under the conditions studied in this work, it does not coincide with the proposal made by (Cerda et al., 2017) (Eq.5), since the dissolution of the chalcocite would

not reach a complete transformation to covellite. This would be possible only if about 50% of the copper is extracted at the beginning of the leaching (formation of a majority soluble phase as $CuSO_4$).

Finally, Tables 26 and 27 presents the summary of results of leaching tests at 5 and 12 hour, respectively. The initial value of pH and solution potential is the value of the leaching solution (before adding the mineral) and the final value corresponds to the last sample (12 hours). Regarding the pH, there is a greater variation (acid consumption) in tests with pretreatment and with oxygen injection. It is evident that the concentration of sulphuric acid is sufficient to satisfy the chalcocite dissolution, not limiting the process.

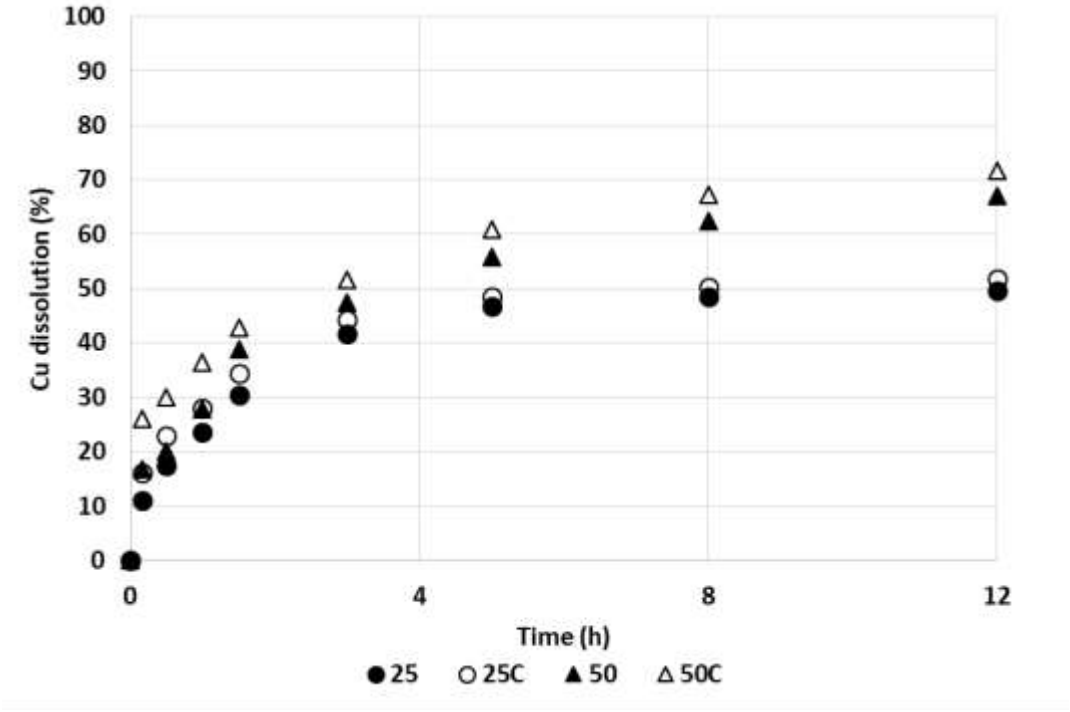

Figure 84. Copper dissolution from chalcocite in 0.2 M H_2SO_4, 50 g/L of Cl^- ion from NaCl in deionized water at 25 °C (●25); 50 °C (▲50) without pretreatment and 25 °C (○25) and 50 °C (△50) with pretreatment

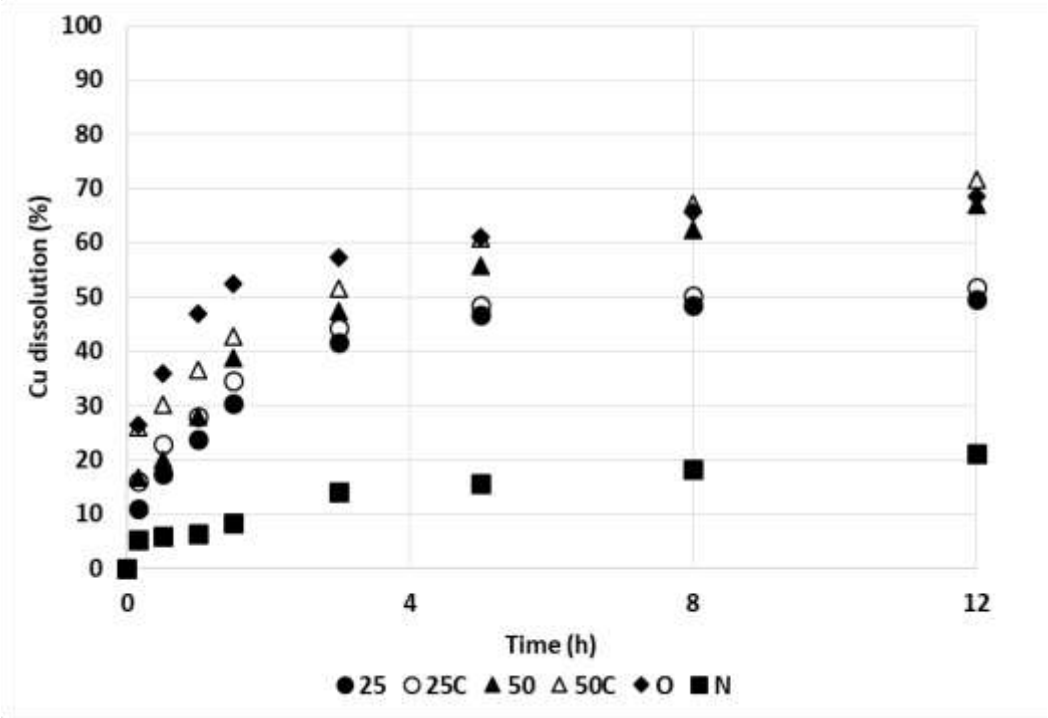

Figure 85. Copper dissolution from chalcocite in 0.2 M H_2SO_4, 50 g/L of Cl^- ion from NaCl in deionized water at 25 °C (●25); 50 °C (▲50) without pretreatment; oxygen injection (♦O) and nitrogen injection (■N) at 25 °C without pretreatment and 25 °C (○25) and 50 °C (△50) with pretreatment

Table 26. Summary of leaching test results at 5 hour

	Pretreatment			Leaching parameters				Leaching results		
Test	Curing time (days)	H_2SO_4 (kg/t)	NaCl (kg/t)	Temp. (°C)	H_2SO_4 (M)	NaCl (g/L)	Gas Injection	% Cu extraction	pH range	Eh range (mV) SHE
1	0	0	0	25	0.2	50	No	46.8	0.49 - 0.57	597-505
2	15	15	25	25	0.2	50	No	48.5	0.51 - 0.57	591-475
3	0	0	0	50	0.2	50	No	55.8	0.51 - 0.58	590-486
4	15	15	25	50	0.2	50	No	60.9	0.51 - 0.64	594-478
5	0	0	0	25	0.2	50	O_2	61.1	0.51 - 0.69	597-625
6	0	0	0	25	0.2	50	N_2	15.6	0.48 - 0.49	598-423

Table 27. Summary of leaching test results at 12 hour

	Pretreatment			Leaching parameters				Leaching results		
Test	Curing time (days)	H_2SO_4 (kg/t)	NaCl (kg/t)	Temp. (°C)	H_2SO_4 (M)	NaCl (g/L)	Gas Injection	% Cu extraction	pH range	Eh range (mV) SHE
1	0	0	0	25	0.2	50	No	49.5	0.49 - 0.68	597-518
2	15	15	25	25	0.2	50	No	51.8	0.51 - 0.63	591-523
3	0	0	0	50	0.2	50	No	66.9	0.51 - 0.61	590-504
4	15	15	25	50	0.2	50	No	71.5	0.51 - 0.68	594-496
5	0	0	0	25	0.2	50	O_2	68.6	0.51 - 0.74	597-637
6	0	0	0	25	0.2	50	N_2	21.2	0.48 - 0.52	598-449

4.2.5 Characterization of leaching residues

The characterization of the leaching residues was carried out by X-ray diffraction and SEM analysis. By X-ray diffraction, it was possible to confirm the depletion of copper in the chalcocite according to the leaching and/or pretreatment conditions.

Figure 86 shows the diffractogram associated with the leaching residue at 25 °C with pretreatment, confirming the presence of covellite, pyrite and quartz. The covellite identified was associated with the complete dissolution of chalcocite in the first dissolution stage (Cheng and Lawson, 1991a, 1991b; Xingyu et al., 2010) while quartz and pyrite show no reaction. Figure 87 shows the diffractogram of the test residue at 50 °C with pretreatment. Species such as covellite, pyrite and quartz were confirmed, although the presence of covellite decreased in intensity. In addition, the presence of elemental sulphur has also been confirmed, although in a minority amount. The presence of elemental sulphur was associated with the product generated by the second dissolution stage of the chalcocite (Cheng and Lawson, 1991b; Niu et al., 2015). According to (Miki et al., 2011), the presence of sulphur should not necessarily be associated with the passivation of covellite.

The confirmation of covellite, pyrite, quartz and elemental sulphur (in minority amount) was also confirmed in the leaching residue carried out with the injection of oxygen (Figure 88). Finally, in the case of the residue with nitrogen injection, the presence of pyrite, quartz and copper-depleted chalcocite, in the form of djurleite ($Cu_{1.94}S$) and digenite ($Cu_{1.80}S$) was confirmed (Figure 89). The presence of these intermediate species coincided with the limited dissolution of copper achieved in the leaching test, mainly limited by the low solution potential and the absence of oxygen. The CuS_2 species, associated as responsible for the passivation of covellite, has not been identified by X-ray diffraction analysis according to the conditions used in this study.

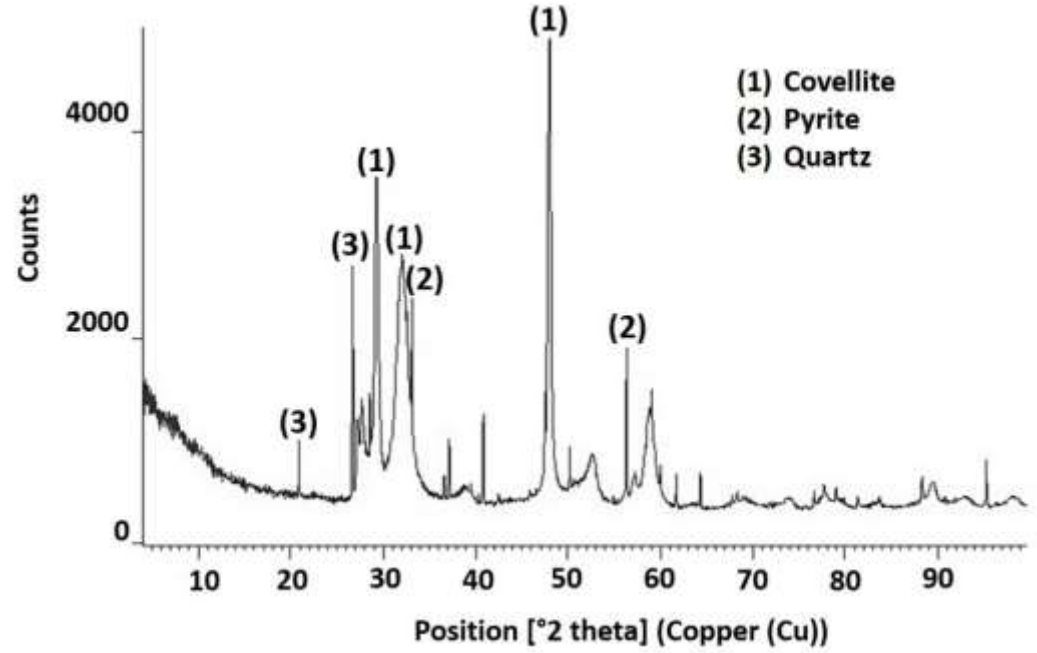

Figure 86. Species identified in chalcocite leaching residue, using X-ray diffraction analysis at 25 °C and with pretreatment of 30 kg/t H_2SO_4, 40 kg/t NaCl and 7 days of curing time

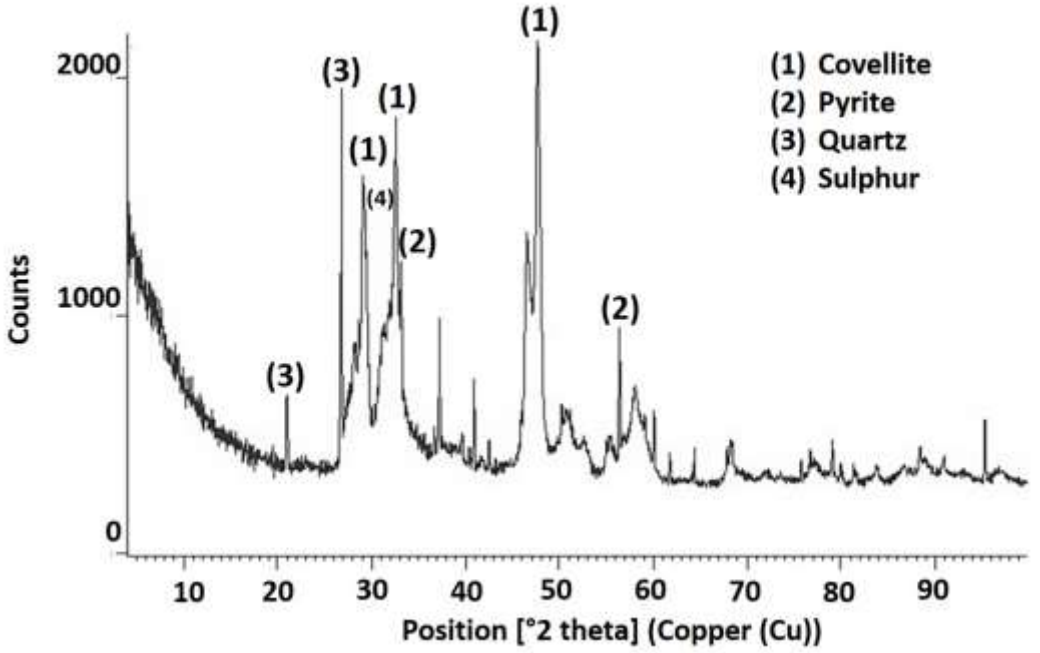

Figure 87. Species identified in chalcocite leaching residue, using X-ray diffraction analysis at 50 °C and with pretreatment of 30 kg/t H_2SO_4, 40 kg/t NaCl and 7 days of curing time

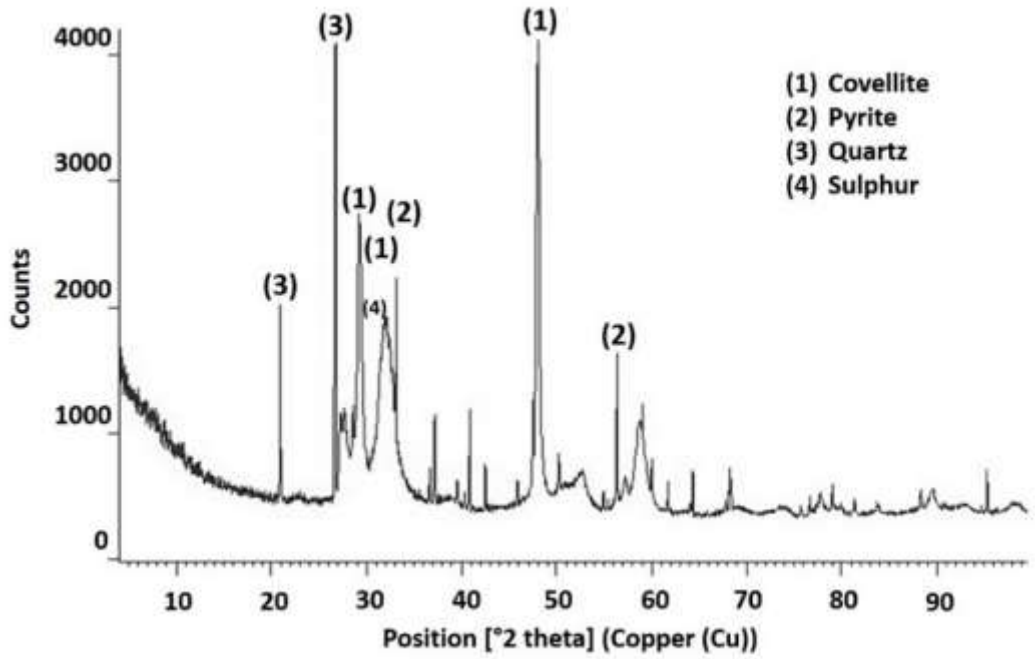

Figure 88. Species identified in chalcocite leaching residue at 25 °C with oxygen injection and without pretreatment, using X-ray diffraction analysis

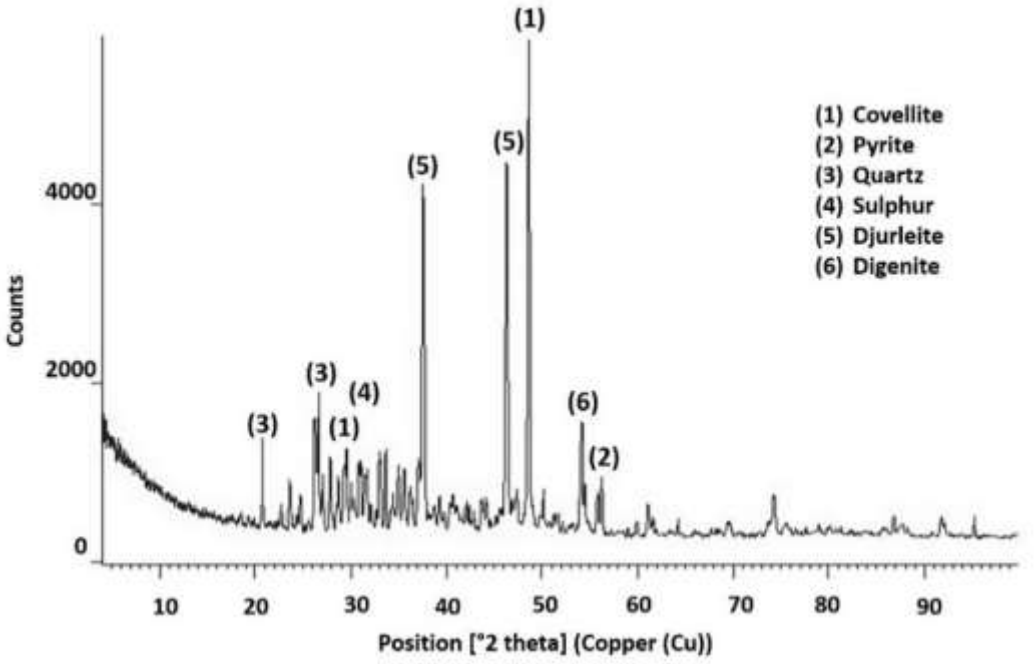

Figure 89. Species identified in chalcocite leaching residue at 25 °C with nitrogen injection and without pretreatment, using X-ray diffraction analysis

SEM analysis was also performed on the leaching residues from the test carried out at 50 °C with pretreatment, confirming the presence of covellite, pyrite and quartz, mainly. Figure 90 shows the presence of unreacted covellite associated with pyrite (such as the characterization of the initial sample). Figure 90b and 90c show the EDS analysis associated with covellite and pyrite, respectively. Elemental sulphur or CuS_2 presence was not identified. Furthermore, it is possible to observe cracks appearing on the surfaces of the solid particles. This observation was also reported by (Niu et al., 2015); these authors suggested that, after the first dissolution stage was completed (49% copper extraction), the chalcocite particles can disintegrate into smaller particles, which continue to dissolve in a second dissolution stage. This can occur even at low Cu extraction (10%).

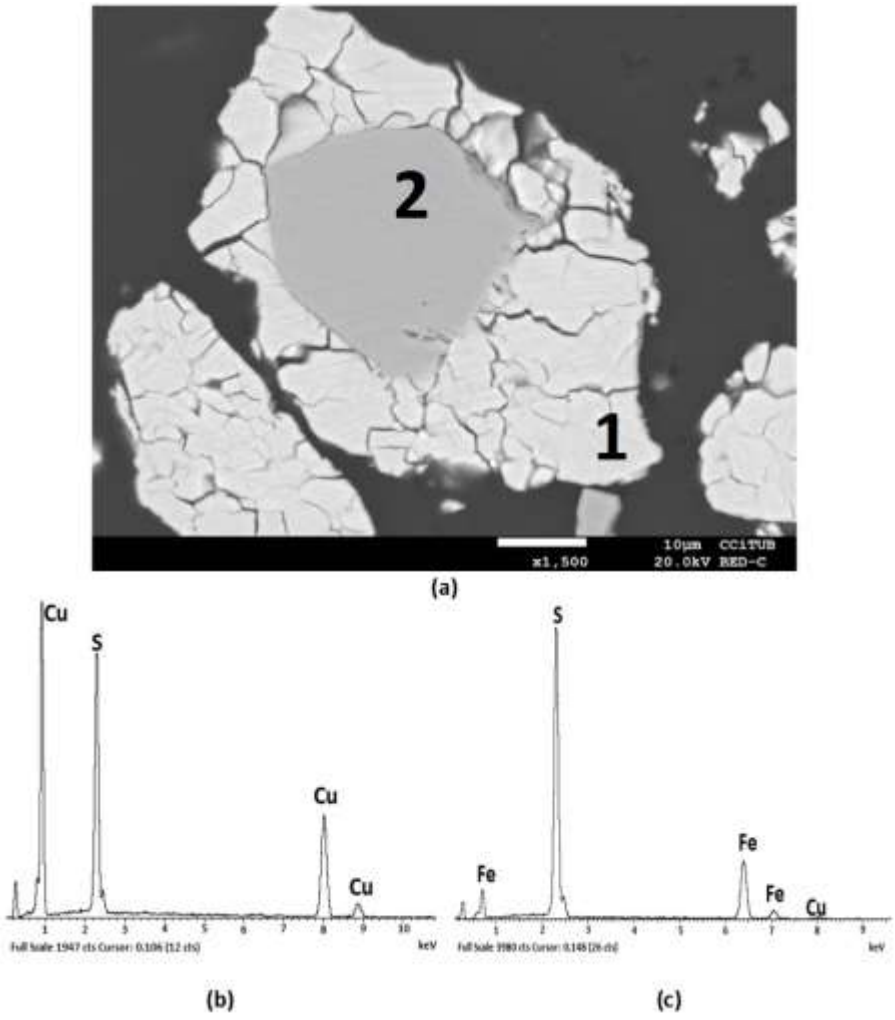

Figure 90. SEM image shows leaching chalcocite residue obtained at 50 °C with pretreatment. Particle 1 identified as unreacted covellite and particle 2 as pyrite. In (b) and (c) the EDS analysis associated to covellite and pyrite, respectively

Figure 91 shows a SEM analysis performed on the leaching residue with nitrogen injection at 25 °C, without pretreatment. The presence of an intermediate $Cu_{2-x}S$ phase associated with the incomplete transformation of chalcocite was confirmed. In addition, the morphology of the particle also coincides, showing cracks on the surfaces of the solid particles, even when the extraction of copper was low (21.2%). This result confirms that the oxidation of chalcocite to covellite is possible, but under 500 mV, is too low for the subsequent oxidation of the secondary covellite which can be at least partially dissolved by an increase to 550 mV (Miki et al., 2011). Finally, in Figure 92 the SEM analysis performed on the test leaching residue performed with the oxygen injection is observed and in 92c the EDS analysis on unreacted covellite. No species such as elemental sulphur or CuS_2 are identified, responsible for the passivation of covellite.

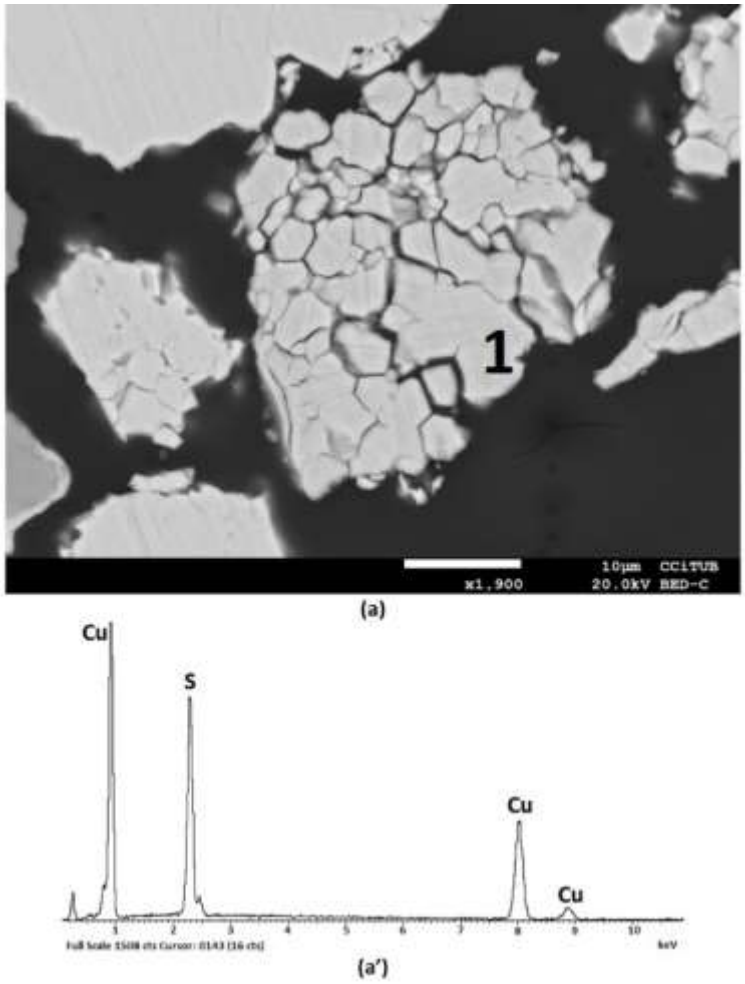

Figure 91. SEM image of leaching chalcocite residue obtained at 20 °C with oxygen injection. Particle 1 identified as unreacted covellite and (a') EDS analysis associated with covellite (1)

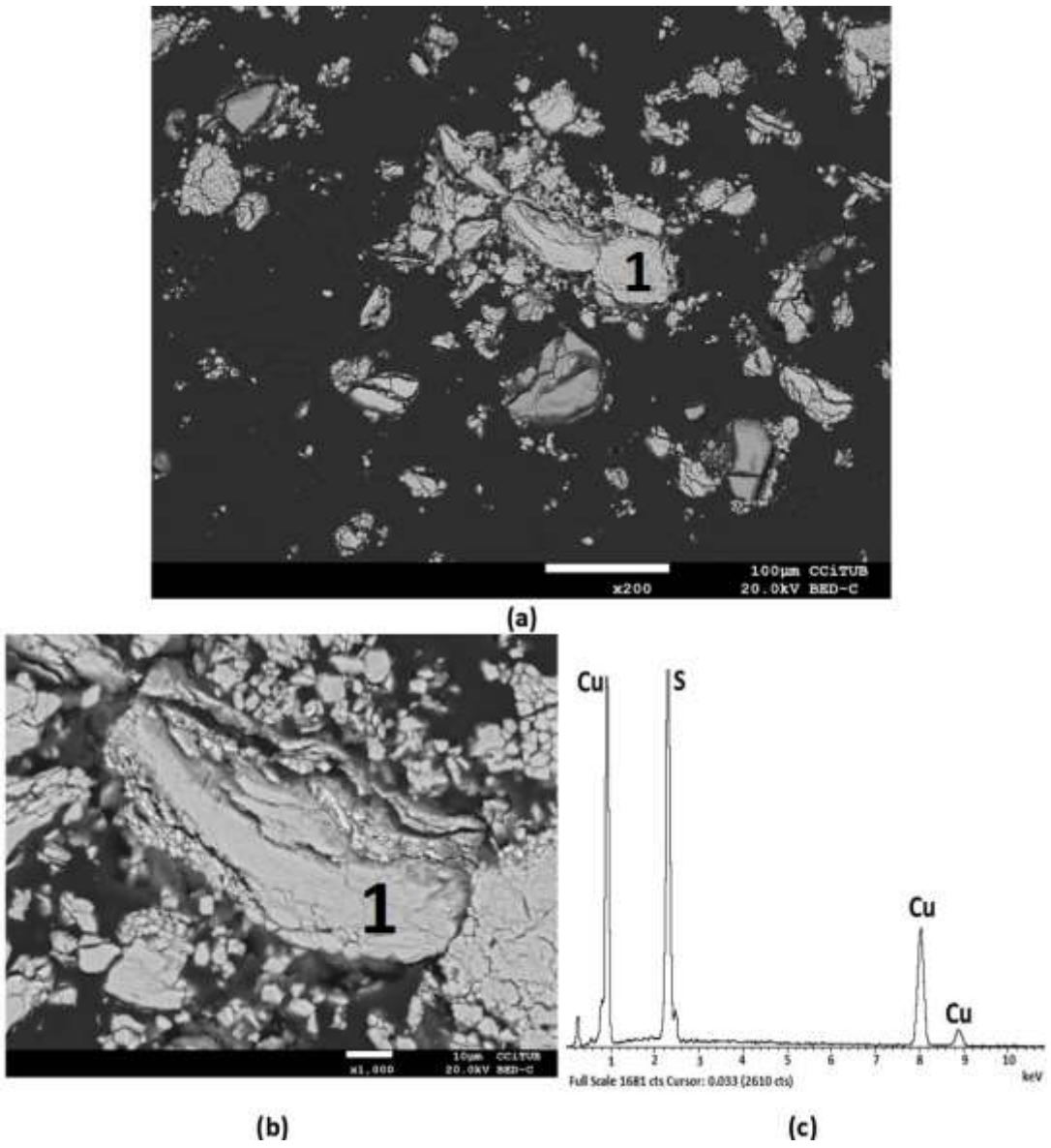

Figure 92. SEM image shows leaching chalcocite residue obtained at 20 °C with nitrogen injection. Particle 1 identified as unreacted covellite and (c) EDS analysis associated with covellite (1)

Chalcopyrite mineral

The chemical composition of the chalcopyrite sample is 28.5% Cu, 22.8%Fe and 29.7%S. The mineralogical composition indicates the presence of 74% chalcopyrite, 16% quartz, 1.80% covellite, 1.80% K-feldspar, 1.30% pyrite, and other species in minor amount.

The pretreatment of chalcopyrite sample with potassium nitrate-sulphuric acid media (15 kg/t H_2SO_4, 10 kg/t KNO_3 and 15 days of curing time) resulted in a copper extraction of 12.93%. The ANOVA analysis indicated that this combination of variables was the most influential combination. The results were consistent with the Cu extraction predicted by the model (12.55%). This pretreatment was not effective, taking into account that the soluble copper sulphate was 9%, and consequently only 3% of the chalcopyrite was sulfated with the pretreatment.

The pretreatment of chalcopyrite sample with sodium chloride-sulphuric acid media system (15 kg/t H_2SO_4, 15 kg/t NaCl and 15 days of curing time) resulted in a copper extraction of 19.56% prior to leaching. The ANOVA indicated that this combination of variables was the most influential evaluated in this study. However, the Cu extraction differed from that predicted by the model (16.72%), which may have been due to the synergy between H_2SO_4 and NaCl.

Curing time is the most influential variable in the pretreatment of a chalcopyrite mineral under the conditions evaluated in this study. According to the ANOVA analysis, its influence was 56.36% in a chloride media and 54.66% in nitrate media, both with significant p-values.

The pretreatment of chalcopyrite sample with sodium chloride-sulphuric acid media system (15 kg/t H_2SO_4, 25 kg/t NaCl and 15 days of curing) achieved a copper extraction of 22.66 % prior to leaching. In this study, NaCl benefits copper dissolution more than KNO_3 in the pretreatment of a chalcopyrite mineral.

$$3CuFeS_2 + 3H_2SO_4 + NaCl + 3O_2 = CuSO_4 + NaFe_3(SO_4)_2(OH)_6 + 6S + Cu_2Cl(OH)$$

The curing time benefits the kinetics of copper leaching from pretreated chalcopyrite. Furthermore, in synergy with the temperature (50 and 90°C) it is capable of generating 6% more of copper extraction compared to samples without curing time. A 94% of copper was extracted at 90 °C in a sample with pretreatment of 15 kg/t of H_2SO_4, 25 kg/t of NaCl and 15 days of curing time, versus 90% reached at 90 °C without pretreatment.

For comparative purposes, and during leaching at 70 °C, a copper extraction of 75% in 24 hours with pretreatment and in 32 h without pretreatment, were obtained. During leaching at 90 °C, a copper extraction of 84% in 24 hours with pretreatment and in 32 hours without pretreatment were obtained. Thus, the curing treatment significantly reduces the leaching time.

Test performed at 25°C leads to obtain a copper extraction close to 30% with and without the curing pretreatment. This fact confirms the passivation of the chalcopyrite surface at this temperature, by the formation of a compact layer of sulphur, with probably formation of jarosite and copper polysulfides.

Elemental sulphur formed at 70 °C appears to have a more porous and less rigid surface than that reported in leaching products at 25°C. A more porous film of sulphur, bordering the surface of the chalcopyrite, allows the contact of the leaching solution with the mineral.

Abundant elemental sulphur and natrojarosite, have been identified in all the leaching products, which have been proposed as responsible for the passivation of chalcopyrite. The presence of CuS_2 was observed in the tests carried out at 25 and 50 °C.

Mine ore

The chemical composition of the mine ore sample is 0.790% Cu, 2.52%Fe and 2.49%S and 9.70% Al. The mineralogical composition indicates the presence of 54.2% muscovite, 29.7% quartz, 3.73% pyrite, 3.08% orthoclase, 2.51% kaolinite, 1.99% chalcopyrite, and other elements in minor amounts.

The pretreatment of the mine ore by using 15 kg/t H_2SO_4, 25 kg/t NaCl and 15 days of curing leads to obtain 27% of copper extraction prior to the leaching step. This is mainly produced

by the generation of copper sulfate identified when comparing the diffractograms of the initial sample with that generated in the pretreatment.

The curing time benefits the kinetics of copper dissolution from chalcopyrite in a mine ore. In addition, in synergy with the temperature (50 and 90°C) it was possible to generate a difference of 5% in the extraction of copper compared to a mineral without pretreatment. A 93.1% copper extraction was obtained at 90 °C and with a pretreatment using 15 kg/t H_2SO_4, 25 kg/t NaCl and 15 days of curing time.

Leaching test carried out on the mine ore, performed at 25 °C, generates the greatest difference in copper extraction. Extraction values of 16.7% and 25.9% were obtained without and with pretreatment, respectively. Chalcopyrite passivation was quickly achieved, evidenced by the behavior of the copper extraction curve over time (around hour 4 of leaching).

For comparative purposes, and during leaching at 70 °C, a copper extraction of 65% in 24 hours with pretreatment and in 48 hours without pretreatment, were obtained. During leaching at 90 °C, a copper extraction of 90% in 24 hours with pretreatment and in 48 hours without pretreatment were obtained. Thus, the curing treatment significantly reduces the leaching time.

By X-ray diffraction analysis and SEM characterization it was not possible to accurately identify the passivation products associated with chalcopyrite leaching from mine ore. According to the pH values obtained, the conditions for the formation of products such as natrojarosite would be unlikely. The presence of elemental sulphur was identified, but not copper polysulfides, although its presence should not be ruled out.

Chalcocite mineral

The chemical composition of the chalcocite sample is 75.0% Cu, 23.5% S and 1.33% Fe. The mineralogical composition indicates the presence of 93.7% chalcocite, 2.16% pyrite, 1.25% quartz, 1.10% brocantite, 0.49% covellite, and other species in minor amount.

In the pretreatment of chalcocite sample, the curing time benefits the kinetics of copper dissolution from chalcocite mineral. With a pretreatment at room temperature using 30

kg/t H_2SO_4, 40 kg/t NaCl and 7 days of curing, 6.10% copper was obtained prior to leaching. Furthermore, under oxygen-free conditions (removal using nitrogen), a copper extraction of 2.57% was achieved.

Through the characterization by SEM and X-ray diffraction analysis of the sample with pretreatment, using 30 kg/t H_2SO_4, 40 kg/t NaCl and 7 days of curing time, the formation of products such as: Anilite ($Cu_{1.75}S$), copper sulphate ($CuSO_4$), copper oxychloride Cu(OH)Cl and sodium sulphate Na_2SO_4, was observed.

In the pretreatment of chalcocite, under the conditions used in this study (kg/t of H_2SO_4, 40 kg/t of NaCl and 7 days of curing time), the following reactions are proposed.

$$4Cu_2S + 0.75H_2SO_4 + 0.5O_2 + 0.5NaCl = 4Cu_{1.75}S + 0.5Cu(OH)Cl + 0.25Na_2SO_4 + 0.5CuSO_4 + 0.5H_2O$$

$$2Cu_2S + 0.5H_2SO_4 + 0.25O_2 = 2Cu_{1.75}S + 0.5CuSO_4 + 0.5H_2O$$

$$2Cu_2S + 0.25H_2SO_4 + 0.25O_2 + 0.5NaCl = 2Cu_{1.75}S + 0.5Cu(OH)Cl + 0.25Na_2SO_4$$

The leaching of the chalcocite mineral generated a copper extraction of 51.8% in the test carried out at 25 °C with a pretreatment using 30 kg/t H_2SO_4, 40 kg/t NaCl and 7 days of curing time. A difference of 2.3% more copper than the test without pretreatment at 25 °C was observed. At 50 °C with pretreatment, a copper extraction of 71.5% was achieved, rising 4.6% compared to the test without pretreatment. In the test performed with oxygen injection a copper dissolution of 68.6% was achieved, unlike the test performed with nitrogen injection, the lowest copper extraction (21.2%) was obtained.

For comparative purposes, and during leaching at 50 °C, a copper extraction of 60% in 5 hours with pretreatment and in 8 hours without pretreatment, were obtained. During leaching at the same temperature, a copper extraction of 65% in 8 hour with pretreatment and in 12 hour without pretreatment were obtained. Thus, the curing treatment significantly reduces the leaching time.

By x-ray diffraction analysis and SEM it is possible to confirm the presence of an intermediate $Cu_{2-x}S$ phase associated with the incomplete transformation of chalcocite, including the presence of covellite in tests on 50% of copper dissolution (first stage of

complete dissolution of chalcocite). Finally, the presence of elemental sulphur has been confirmed in leaching residues in tests using oxygen injection and 50 °C with a pretreatment of 30 kg/t H_2SO_4, 40 kg/t NaCl and 7 days of curing.

A. Baba, A., I. Ayinla, K., A. Adekola, F., K. Ghosh, M., S. Ayanda, O., B. Bale, R., R. Sheik, A., R. Pradhan, S., 2012. A Review on Novel Techniques for Chalcopyrite Ore Processing. Int. J. Min. Eng. Miner. Process. 1, 1–16. https://doi.org/10.5923/j.mining.20120101.01

Adebayo, A.O., Sarangi, K., 2011. Separation of copper from chalcopyrite - Ammoniacal leach liquor containing copper, zinc, and magnesium by supported liquid membrane. Chem. Biochem. Eng. Q. 25, 309–316.

Al-Harahsheh, M., Kingman, S., Al-Harahsheh, A., 2008. Ferric chloride leaching of chalcopyrite: Synergetic effect of $CuCl_2$. Hydrometallurgy 91, 89–97. https://doi.org/10.1016/j.hydromet.2007.11.011

Antonijević, M.M., Dimitrijević, M., Janković, Z., 1997. Leaching of pyrite with hydrogen peroxide in sulphuric acid. Hydrometallurgy 46, 71–83. https://doi.org/10.1016/s0304-386x(96)00096-5

Arce, E.M., González, I., 2002. A comparative study of electrochemical behavior of chalcopyrite, chalcocite and bornite in sulfuric acid solution. Int. J. Miner. Process. 67, 17–28. https://doi.org/10.1016/S0301-7516(02)00003-0

Aroca, F., Backit, A., Jacob, J., 2012. CuproChlor®, a hydrometallurgical technology for mineral sulphides leaching, in: 4^{Th} International Seminar on Process Hydrometallurgy. Santiago de Chile, pp. 98–110.

Baba, A.A., Ghosh, M.K., Pradhan, S.R., Rao, D.S., Baral, A., Adekola, F.A., 2014. Characterization and kinetic study on ammonia leaching of complex copper ore. Trans. Nonferrous Met. Soc. China (English Ed. 24, 1587–1595. https://doi.org/10.1016/S1003-6326(14)63229-5

Bai, X., Wen, S., Liu, J., Lin, Y., 2018. Response surface methodology for optimization of copper leaching from refractory flotation tailings. Minerals 8. https://doi.org/10.3390/min8040165

Beiza, L., Quezada, V., Melo, E., Valenzuela, G., 2019. Electrochemical Behaviour of Chalcopyrite in Chloride Solutions. Metals (Basel). 9, 1–12. https://doi.org/10.3390/met9010067

Benavente, O., Hernández, M.C., Melo, E., Núñez, D., Quezada, V., Zepeda, Y., 2019. Copper Dissolution from Black Copper Ore under Oxidizing and Reducing Conditions. Metals (Basel). 9, 1–12. https://doi.org/https://doi.org/10.3390/met9070799

Boekema, C., Krupski, A.M., Varasteh, M., Parvin, K., Van Til, F., Van Der Woude, F., Sawatzky, G.A., 2004. Cu and Fe valence states in $CuFeS_2$. J. Magn. Magn. Mater. 272–276, 559–561. https://doi.org/10.1016/j.jmmm.2003.11.206

Butler, I., Schoonen, M.A.A., Rickard, D., 1994. Removal of Dissolved Oxygen from Water : A Comparison of Four Common Techniques 9140. https://doi.org/10.1016/0039-9140(94)80110-X

Carneiro, M.F.C., Leão, V.A., 2007. The role of sodium chloride on surface properties of chalcopyrite leached with ferric sulphate. Hydrometallurgy 87, 73–82. https://doi.org/10.1016/j.hydromet.2007.01.005

Cerda, C., Taboada, M., Jamett, N., Ghorbani, Y., Hernández, P., 2017. Effect of Pretreatment on Leaching Primary Copper Sulfide in Acid-Chloride Media. Minerals 8, 1. https://doi.org/10.3390/min8010001

Cháidez, J., Parga, J., Valenzuela, J., Carrillo, R., Almaguer, I., 2019. Leaching chalcopyrite concentrate with oxygen and sulfuric acid using a low-pressure reactor. Metals (Basel). 9. https://doi.org/10.3390/met9020189

Chatterjee, R., Chaudhuri, S., Kuila, S.K., Ghosh, D., 2015. Structural, microstructural, and thermal characterizations of a chalcopyrite concentrate from the Singhbhum shear zone, India. Int. J. Miner. Metall. Mater. 22, 225–232. https://doi.org/10.1007/s12613-015-1065-3

Cheng, C.Y., Lawson, F., 1991a. The kinetics of leaching chalcocite in acidic oxygenated sulphate-chloride solutions. Hydrometallurgy 27, 249–268. https://doi.org/10.1016/0304-386X(91)90053-O

Cheng, C.Y., Lawson, F., 1991b. The kinetics of leaching covellite in acidic oxygenated sulphate-chloride solutions 27.

Cochilco, 2019. Proyección de la producción de cobre en Chile 2019 – 2030. Santiago de Chile.

Copur, M., Kizilca, M., Kocakerim, M.M., 2015. Determination of the Optimum Conditions for Copper Leaching from Chalcopyrite Concentrate Ore Using Taguchi Method. GCEC 202, 927–935. https://doi.org/10.1080/00986445.2014.891506

Çopur, M., Pekdemir, T., Çolak, S., Künkül, A., 2007. Industrial symbiosis: High purity recovery of metals from Waelz sintering waste by aqueous SO_2 solution. J. Hazard. Mater. 149, 303–309. https://doi.org/10.1016/j.jhazmat.2007.03.079

Córdoba, E.M., Muñoz, J.A., Blázquez, M.L., González, F., Ballester, A., 2009. Passivation of chalcopyrite during its chemical leaching with ferric ion at 68 °C. Miner. Eng. 22, 229–235. https://doi.org/10.1016/j.mineng.2008.07.004

Córdoba, E.M., Muñoz, J.A., Blázquez, M.L., González, F., Ballester, A., 2008a. Leaching of chalcopyrite with ferric ion. Part I: General aspects. Hydrometallurgy 93, 81–87. https://doi.org/10.1016/j.hydromet.2008.04.015

Córdoba, E.M., Muñoz, J.A., Blázquez, M.L., González, F., Ballester, A., 2008b. Leaching of chalcopyrite with ferric ion. Part II: Effect of redox potential. Hydrometallurgy 93, 88–96. https://doi.org/10.1016/j.hydromet.2008.04.016

De Oliveira, C., Duarte, H.A., 2010. Disulphide and metal sulphide formation on the reconstructed (0 0 1) surface of chalcopyrite: A DFT study. Appl. Surf. Sci. 257, 1319–1324. https://doi.org/10.1016/j.apsusc.2010.08.059

Deshenthree Chetty, 2018. Acid-Gangue Interactions in Heap Leach Operations : A Review of the Role of Mineralogy for Predicting. Metals (Basel). 8, 11. https://doi.org/10.3390/min8020047

Dhawan, N., Safarzadeh, M.S., Miller, J.D., Moats, M.S., Rajamani, R.K., 2013. Crushed ore agglomeration and its control for heap leach operations. Miner. Eng. 41, 53–70. https://doi.org/10.1016/j.mineng.2012.08.013

Dong, Y.B., Lin, H., Fu, K. Bin, Xu, X.F., Zhou, S.S., 2013. Bioleaching of two different types of chalcopyrite by Acidithiobacillus ferrooxidans. Int. J. Miner. Metall. Mater. 20, 119–124. https://doi.org/10.1007/s12613-013-0702-y

Dutrizac, J.E., 1992. The leaching of sulphide minerals in chloride media. Hydrometallurgy 29, 1–45. https://doi.org/https://doi.org/10.1016/0304-386X(92)90004-J

Dutrizac, J.E., 1990. Elemental sulphur formation during the ferric chloride leaching of chalcopyrite. Hydrometallurgy 23, 153–176. https://doi.org/10.1016/0304-386X(90)90002-J

Dutrizac, J.E., 1983. Factors affecting alkali jarosite precipitation. Metall. Trans. B 14, 531–539. https://doi.org/10.1007/BF02653939

Dutrizac, J.E., 1981. The dissolution of chalcopyrite in ferric sulfate and ferric chloride media. Metall. Trans. B 12, 371–378. https://doi.org/10.1007/BF02654471

Elsherief, A.E., 2002. The influence of cathodic reduction, Fe^{2+} and Cu^{2+} ions on the electrochemical dissolution of chalcopyrite in acidic solution. Miner. Eng. 15, 215–223. https://doi.org/10.1016/S0892-6875(01)00208-4

Evans, H.T., 1981. Copper coordination in low chalcocite and djurleite and other copper-rich sulfides. Am. Mineral. 66, 807–818.

Evans, H.T., 1979. The crystal structures of low chalcocite and djurleite. Zeitschrift fur Krist. - New Cryst. Struct. 150, 299–320. https://doi.org/10.1524/zkri.1979.150.1-4.299

Fang, C., Yu, S., Wang, X., Zhao, H., Qin, W., Qiu, G., Wang, J., 2018. Synchrotron radiation XRD investigation of the fine phase transformation during synthetic chalcocite acidic ferric sulfate leaching. Minerals 8. https://doi.org/10.3390/min8100461

Ghorbani, Y., Franzidis, J.P., Petersen, J., 2016. Heap leaching technology - Current State, innovations, and future directions: A review. Miner. Process. Extr. Metall. Rev. 37, 73–119. https://doi.org/10.1080/08827508.2015.1115990

Ghorbani, Y., Kuan, S.H., 2017. A review of sustainable development in the Chilean mining sector : past , present and future. Int. J. Mining, Reclam. Environ. 0930, 1–28. https://doi.org/10.1080/17480930.2015.1128799

Gnanavel, M., Lebedev, O.I., Bazin, P., Raveau, B., Pralong, V., 2015. Reversible transformation from amorphouse $Na_3Fe_3(SO_4)_2(OH)_6$ to crystallized $NaFe_3(SO_4)_2(OH)_6$ Jarosite-type hydroxysulfate. Solid State Ionics 278, 38–42. https://doi.org/10.1016/j.ssi.2015.05.013

Gok, O., Anderson, C.G., 2013. Dissolution of low-grade chalcopyrite concentrate in acidified nitrite electrolyte. Hydrometallurgy 134–135, 40–46. https://doi.org/10.1016/j.hydromet.2013.01.021

Grizo, A., Pacović, N., Poposka, F., Koneska, Ž., 1982. Leaching of a low-grade chalcocite-covellite ore containing iron in sulphuric acid: The influence of pH and particle size on the kinetics of copper leaching. Hydrometallurgy 8, 5–16. https://doi.org/10.1016/0304-386X(82)90026-3

Grömping, U., 2018. R package DoE.base for factorial experiments. J. Stat. Softw. 85. https://doi.org/10.18637/jss.v085.i05

Guy, S., Broadbent, C.P., 1983. Formation of copper(I) sulphate during cupric chloride leaching on a complex Cu/Zn/Pb ore. Hydrometallurgy 11, 277–288. https://doi.org/10.1016/0304-386X(83)90048-8

Hackl, R.P., Dreisinger, D.B., Peters, E., King, J.A., 1995. Passivation of chalcopyrite during oxidative leaching in sulfate media. Hydrometallurgy 39, 25–48. https://doi.org/10.1016/0304-386X(95)00023-A

Haldar, S.K., 2017. Platinum-Nickel-Chromium Deposits, in: Introduction. Elsevier, pp. 1–35. https://doi.org/10.1016/b978-0-12-802041-8.00001-8

Hashemzadeh, M., Dixon, D.G., Liu, W., 2019. Modelling the kinetics of chalcocite leaching in acidified cupric chloride media under fully controlled pH and potential. Hydrometallurgy 189, 105114. https://doi.org/10.1016/j.hydromet.2019.105114

Hashemzadeh, M., Liu, W., 2020. The response of sulfur chemical state to different leaching conditions in chloride leaching of chalcocite. Hydrometallurgy 192, 105245. https://doi.org/10.1016/j.hydromet.2020.105245

Hepel, M., Hepel, T., 1977. The anodic dissolution of chalcocite in an ammoniacal environment. J. Electroanal. Chem. 81, 161–170. https://doi.org/10.1016/S0022-0728(77)80368-9

Hernández, P.C., Dupont, J., Herreros, O.O., Jimenez, Y.P., Torres, C.M., 2019. Accelerating copper leaching from sulfide ores in acid-nitrate-chloride media using agglomeration and curing as pretreatment. Minerals 9, 1–13. https://doi.org/10.3390/MIN9040250

Hernández, P.C., Taboada, M.E., Herreros, O.O., Torres, C.M., Ghorbani, Y., 2015. Chalcopyrite dissolution using seawater-based acidic media in the presence of oxidants. Hydrometallurgy 157, 325–332. https://doi.org/10.1016/j.hydromet.2015.09.007

Herreros, O., Bernal, N., Quiroz, R., Fuentes, G., Viñals, J., 2005. Lixiviación de concentrados de cobre utilizando NaCl y el cobre soluble aportado por el propio concentrado. Rev. Metal. 41, 384–392.

Herreros, Osvaldo, Quiroz, R., Restovic, A., Viñals, J., 2005. Dissolution kinetics of metallic copper with $CuSO_4$-NaCl-HCl. Hydrometallurgy 77, 183–190. https://doi.org/10.1016/j.hydromet.2004.11.010

Herreros, O., Quiroz, R., Viñals, J., 1999. Dissolution kinetics of copper, white metal and natural chalcocite in Cl_2/Cl^- media. Hydrometallurgy 51, 345–357. https://doi.org/10.1016/S0304-386X(98)00085-1

Herreros, O., Viñals, J., 2007. Leaching of sulfide copper ore in a NaCl-H_2SO_4-O_2 media with acid pre-treatment. Hydrometallurgy 89, 260–268. https://doi.org/10.1016/j.hydromet.2007.07.011

Hirato, T., Majima, H., Awakura, Y., 1987. The leaching of chalcopyrite with cupric chloride. Metall. Trans. B 18, 31–39. https://doi.org/10.1007/BF02658429

Hiroyoshi, N., Kitagawa, H., Tsunekawa, M., 2008. Effect of solution composition on the optimum redox potential for chalcopyrite leaching in sulfuric acid solutions. Hydrometallurgy 91, 144–149. https://doi.org/10.1016/j.hydromet.2007.12.005

Hiroyoshi, N., Miki, H., Hirajima, T., Tsunekawa, M., 2001. Enhancement of chalcopyrite leaching by ferrous ions in acidic ferric sulfate solutions. Hydrometallurgy 60, 185–197. https://doi.org/10.1016/S0304-386X(00)00155-9

Ibáñez, T., Velásquez, L., 2013. Lixiviación de la calcopirita en medios clorurados. Rev. Metal. 49, 131–144. https://doi.org/10.3989/revmetalm.1217

Jansen, M., Taylor, A., 2003. Overview of gangue mineralogy issues in oxide copper heap leaching, in: ALTA Conference, May 19-. 24. Perth, Australia, p. 32.

Johansson, O., Persson, I., Wedborg, M., 1980. Calorimetric study of the thermodynamics of formation of $MgSO_4$ and $NaSO_4^-$ ion pairs at the ionic strength of seawater. Mar. Chem. 8, 191–198.

Karimov, K.A., Rogozhnikov, D.A., Naboichenko, S.S., Karimova, L.M., Zakhar'yan, S. V., 2018. Autoclave Ammonia Leaching of Silver from Low-Grade Copper Concentrates. Metallurgist 62, 783–789. https://doi.org/10.1007/s11015-018-0720-0

Lawson, F., Chu-Yong, C., Ying Lee, S., 1992. Leaching of Copper Sulphides and Copper Mattes in Oxygenated Chloride/Sulphate Leachants. Miner. Process. Extr. Metall. Rev. 8, 183–203. https://doi.org/10.1080/08827509208952686

Lázaro, I., Martínez-Medina, N., Rodríguez, I., Arce, E., González, I., 1995. The use of carbon paste electrodes with non-conducting binder for the study of minerals: Chalcopyrite. Hydrometallurgy 38, 277–287. https://doi.org/10.1016/0304-386X(94)00070-J

Lu, J., Dreisinger, D., West-Sells, P., 2017. Acid curing and agglomeration for heap leaching. Hydrometallurgy 167, 30–35. https://doi.org/10.1016/j.hydromet.2016.10.019

Lu, Z.Y., Jeffrey, M.., Lawson, F., 2000. An electrochemical study of the effect of chloride ions on the dissolution of chalcopyrite in acidic solutions. Hydrometallurgy 56, 145–155. https://doi.org/10.1016/S0304-386X(00)00068-2

Lu, Z. Y., Jeffrey, M.I., Lawson, F., 2000. Effect of chloride ions on the dissolution of chalcopyrite in acidic solutions. Hydrometallurgy 56, 189–202. https://doi.org/10.1016/S0304-386X(00)00075-X

Lundström, M., Aromaa, J., Forsén, O., Hyvärinen, O., Barker, M.H., 2005. Leaching of chalcopyrite in cupric chloride solution. Hydrometallurgy 77, 89–95. https://doi.org/10.1016/j.hydromet.2004.10.013

Lv, C., Wu, H., Lin, W., Illerup, J.B., Karcz, A.P., Ye, S., Damø, A.J., 2019. Characterization of elemental sulfur in chalcopyrite leach residues using simultaneous thermal analysis. Hydrometallurgy 188, 22–30. https://doi.org/10.1016/j.hydromet.2019.05.020

Lwambiyi, M., Maweja, K., Kongolo, K., Lwambiyi, N.M., Diyambi, M., 2009. Investigation into the heap leaching of copper ore from the Disele deposit. Hydrometallurgy 98, 177–180. https://doi.org/10.1016/j.hydromet.2009.04.016

Majima, H., Awakura, Y., Hirato, T., Tanakat, T., 1985. The leaching of chalcopyrite in ferric chloride and ferric sulfate solutions. Can. Metall. Q. 24, 283–291. https://doi.org/10.1179/cmq.1985.24.4.283

Margarella, A., Perrine, K., Lewis, T., Faubel, M., Winter, B., Hemminger, J., 2016. Dissociation of Sulfuric Acid in Aqueous Solution: Determination of the Photoelectron Spectral Fingerprints of H2SO4, HSO4−, and SO4 2− in Water. J. Phys. Chem. 117, 8131–8137. https://doi.org/10.1038/ncomms12555

Martínez-Gómez, V.J., Fuentes-Aceituno, J.C., Pérez-Garibay, R., Lee, J. chun, 2018. A study of the electro-assisted reductive leaching of a chalcopyrite concentrate in HCl solutions. Part I: Kinetic behavior and nature of the chalcopyrite reduction. Hydrometallurgy 181, 195–205. https://doi.org/10.1016/j.hydromet.2018.09.012

Martins, F.L., Patto, G.B., Leão, V.A., 2019. Chalcopyrite bioleaching in the presence of high chloride concentrations. J. Chem. Technol. Biotechnol. 94, 2333–2344. https://doi.org/10.1002/jctb.6028

Mikhlin, Y., Romanchenko, A., Tomashevich, Y., Shurupov, V., 2016. Near-surface Regions of Electrochemically Polarized Chalcopyrite (CuFeS2) as Studied Using XPS and XANES. Phys. Procedia 84, 390–396. https://doi.org/10.1016/j.phpro.2016.11.067

Mikhlin, Y.L., Tomashevich, Y. V., Asanov, I.P., Okotrub, A. V., Varnek, V.A., Vyalikh, D. V., 2004. Spectroscopic and electrochemical characterization of the surface layers of chalcopyrite ($CuFeS_2$) reacted in acidic solutions. Appl. Surf. Sci. 225, 395–409. https://doi.org/10.1016/j.apsusc.2003.10.030

Miki, H., Nicol, M., Velásquez-yévenes, L., 2011. The kinetics of dissolution of synthetic covellite , chalcocite and digenite in dilute chloride solutions at ambient temperatures. Hydrometallurgy 105, 321–327. https://doi.org/10.1016/j.hydromet.2010.11.004

Moyo, T., Petersen, J., Nicol, M.J., 2019. The electrochemistry and kinetics of the oxidative dissolution of chalcopyrite in ammoniacal solutions. Part II – Cathodic reactions. Hydrometallurgy 184, 67–74. https://doi.org/10.1016/j.hydromet.2018.12.020

Moyo, T., Petersen, J., Nicol, M.J., 2018. The electrochemistry and kinetics of the oxidative dissolution of chalcopyrite in ammoniacal solutions: Part I – Anodic Reactions. Hydrometallurgy 182, 97–103. https://doi.org/10.1016/j.hydromet.2018.10.018

Narita, E., Lawson, F., Han, K.N., 1983. Solubility of oxygen in aqueous electrolyte solutions. Hydrometallurgy 10, 21–37.

Nava, D., González, I., 2006. Electrochemical characterization of chemical species formed during the electrochemical treatment of chalcopyrite in sulfuric acid. Electrochim. Acta 51, 5295–5303. https://doi.org/10.1016/j.electacta.2006.02.005

Nicol, M., Basson, P., 2017. The anodic behaviour of covellite in chloride solutions. Hydrometallurgy 172, 60–68. https://doi.org/10.1016/j.hydromet.2017.06.018

Nicol, M., Miki, H., Zhang, S., 2017. The anodic behaviour of chalcopyrite in chloride solutions: Voltammetry. Hydrometallurgy 171, 198–205. https://doi.org/10.1016/j.hydromet.2017.05.016

Nicol, M., Zhang, S., 2017. Hydrometallurgy The anodic behaviour of chalcopyrite in chloride solutions : Potentiostatic measurements. Hydrometallurgy 167, 72–80. https://doi.org/10.1016/j.hydromet.2016.10.008

Nicol, M.J., 2017. Hydrometallurgy The anodic behaviour of chalcopyrite in chloride solutions : Overall features and comparison with sulfate solutions. Hydrometallurgy 169, 321–329. https://doi.org/10.1016/j.hydromet.2017.02.009

Niu, X., Ruan, R., Tan, Q., Jia, Y., Sun, H., 2015. Study on the second stage of chalcocite leaching in column with redox potential control and its implications. Hydrometallurgy 155, 141–152. https://doi.org/10.1016/j.hydromet.2015.04.022

Peng, T., Chen, L., Wang, J., Miao, J., Shen, L., Yu, R., Gu, G., Qiu, G., Zeng, W., 2019. Dissolution and passivation of chalcopyrite during bioleaching by acidithiobacillus ferrivorans at low temperature. Minerals 9, 4–13. https://doi.org/10.3390/min9060332

Petersen, J., Dixon, D., 2007. Principles, mechanisms and dynamics of chalcocite heap bioleaching. Microb. Process. Met. Sulfides 193–218. https://doi.org/10.1128/AEM.69.4.2230

Petersen, J., Dixon, D.G., 2003. The dynamics of chalcocite heap bioleaching. Proc. TMS Fall Extr. Process. Conf. 1, 351–364.

Petersen, J., Dixon, D.G., 2002. Thermophilic heap leaching of a chalcopyrite concentrate. Miner. Eng. 15, 777–785. https://doi.org/10.1016/S0892-6875(02)00092-4

Phadke, M.S., 1989. Quality Engineering Using Robust Design-Prentice Hall (1989).pdf. Upper Saddle River, NJ.

Posfai, M., Buseck, P.R., 1994. Djurleite, digenite, and chalcocite: intergrowths and transformations. Am. Mineral. 79, 308–315.

Pradenas, L., Zuñiga, J., Parada, V., 2015. Codelco, Chile programs its Copper-Smelting operations. Interfaces (Providence). 36, 296–301. https://doi.org/10.1287/inte.l060.0207

Prasad, S., Pandey, B.D., 1998. Alternative processes for treatment of chalcopyrite - A review. Miner. Eng. 11, 763–781. https://doi.org/10.1016/s0892-6875(98)00061-2

Quezada, V., Benavente, O., Beltrán, C., Díaz, D., Melo, E., García, A., 2020. Dissolution of Black Copper Oxides from A Leaching Residue. Metals (Basel). 10, 6–17. https://doi.org/10.3390/met10081012

Quezada, V., Velásquez, L., Roca, A., Benavente, O., Melo, E., Keith, B., 2018. Effect of curing time on the dissolution of a secondary copper sulphide ore using alternative water resources. IOP Conf. Ser. Mater. Sci. Eng. 427. https://doi.org/10.1088/1757-899X/427/1/012030

R Core Team, 2019. R: A Language and Environment for Statistical Computing. R Foundation for statistical computer. Vienna, Austria 0.

Rasouli, S., Mojtahedi, B., Yoozbashizadeh, H., 2020. Oxidative Leaching of Chalcopyrite by Cupric Ion in Chloride Media. Trans. Indian Inst. Met. 73, 989–997. https://doi.org/10.1007/s12666-020-01885-0

Rene Winand, 1991. Chloride Hydrometallurgy*. Hydrometallurgy 27, 285–316.

Rodríguez, Y., Ballester, A., Blázquez, M.L., González, F., Muñoz, J.A., 2003. New information on the chalcopyrite bioleaching mechanism at low and high temperature. Hydrometallurgy 71, 47–56. https://doi.org/10.1016/S0304-386X(03)00173-7

Ross, P.J., 1996. Loss Function, Orthogonal Experiments, Parameter and Tolerance Design, in: Taguchi Techniques for Quality Engineering. pp. 1–73. https://doi.org/ISBN-13: 978-0070539587 ISBN-10: 0070539588

Ruan, R., Zou, G., Zhong, S., Wu, Z., Chan, B., Wang, D., 2013. Why Zijinshan copper bioheapleaching plant works efficiently at low microbial activity-Study on leaching kinetics of copper sulfides and its implications. Miner. Eng. 48, 36–43. https://doi.org/10.1016/j.mineng.2013.01.002

Ruiz, M.C., Grandon, L., Padilla, R., 2014. Selective arsenic removal from enargite by alkaline digestion and water leaching. Hydrometallurgy 150, 20–26. https://doi.org/10.1016/j.hydromet.2014.09.004

Ruiz, M.C., Montes, K.S., Padilla, R., 2015. Galvanic effect of pyrite on chalcopyrite leaching in sulfate-chloride media. Miner. Process. Extr. Metall. Rev. 36, 65–70. https://doi.org/10.1080/08827508.2013.868349

Senanayake, G., 2009. A review of chloride assisted copper sulfide leaching by oxygenated sulfuric acid and mechanistic considerations. Hydrometallurgy 98, 21–32.

https://doi.org/10.1016/j.hydromet.2009.02.010

Senanayake, G., 2007. Chloride assisted leaching of chalcocite by oxygenated sulphuric acid via Cu(II)-OH-Cl. Miner. Eng. 20, 1075–1088. https://doi.org/10.1016/j.mineng.2007.04.002

Shiers, D.W., Collinson, D.M., Kelly, N.J., Watling, H.R., 2016. Copper extraction from chalcopyrite: Comparison of three non-sulfate oxidants, hypochlorous acid, sodium chlorate and potassium nitrate, with ferric sulfate. Miner. Eng. 85, 55–65. https://doi.org/10.1016/j.mineng.2015.10.019

Sokić, M.D., Marković, B., Živković, D., 2009. Kinetics of chalcopyrite leaching by sodium nitrate in sulphuric acid. Hydrometallurgy 95, 273–279. https://doi.org/10.1016/j.hydromet.2008.06.012

Sokić, M.D., Marković, B.R., Pezo, L.L., Stanković, S.B., Patarić, A.S., Janjušević, Z. V., Lončar, B.L., 2019. Copper leaching from chalcopyrite concentrate by sodium nitrate in sulphuric acid solution – chemometric approach. Bulg. Chem. Commun. 51, 457–463. https://doi.org/10.34049/bcc.51.3.5119

Taguchi, G., 1993. Robust technology development. Mech. Eng. 115, 60–62. https://doi.org/10.1115/1.801578_ch10

Taguchi, G., 1987. System of experimental design; engineering methods to optimize quality and minimize costs.

Tanda, B.C., Eksteen, J.J., Oraby, E.A., 2018. Kinetics of chalcocite leaching in oxygenated alkaline glycine solutions. Hydrometallurgy 178, 264–273. https://doi.org/10.1016/j.hydromet.2018.05.005

Tanne, C.K., Schippers, A., 2019. Electrochemical investigation of chalcopyrite (bio)leaching residues. Hydrometallurgy 187, 8–17. https://doi.org/10.1016/j.hydromet.2019.04.022

Torres, C.M., Ghorbani, Y., Hernández, P.C., Justel, F.J., Aravena, M.I., Herreros, O.O., 2019. Cupric and chloride ions: Leaching of chalcopyrite concentrate with low chloride concentration media. Minerals 9. https://doi.org/10.3390/min9100639

Torres, C.M., Taboada, M.E., Graber, T.A., Herreros, O.O., Ghorbani, Y., Watling, H.R., 2015. The effect of seawater based media on copper dissolution from low-grade copper ore. Miner. Eng. 71, 139–145. https://doi.org/10.1016/j.mineng.2014.11.008

Velásquez-Yévenes, L., Miki, H., Nicol, M., 2010a. The dissolution of chalcopyrite in chloride solutions: Part 2: Effect of various parameters on the rate. Hydrometallurgy 103, 80–85. https://doi.org/10.1016/j.hydromet.2010.03.004

Velásquez-Yévenes, L., Nicol, M., Miki, H., 2010b. The dissolution of chalcopyrite in chloride solutions: Part 1. the effect of solution potential. Hydrometallurgy 103, 108–113. https://doi.org/10.1016/j.hydromet.2010.03.001

Velásquez-Yévenes, L., Quezada-Reyes, V., 2018. Influence of seawater and discard brine on

the dissolution of copper ore and copper concentrate. Hydrometallurgy 180, 88–95. https://doi.org/10.1016/j.hydromet.2018.07.009

Velásquez Yévenes, L., 2009. The kinetics of the dissolution of chalcopyrite in chloride media. Murdoch University.

Veloso, T.C., Peixoto, J.J.M.M., Pereira, M.S., Leao, V.A., 2016. Kinetics of chalcopyrite leaching in either ferric sulphate or cupric sulphate media in the presence of NaCl. Int. J. Miner. Process. 148, 147–154. https://doi.org/10.1016/j.minpro.2016.01.014

Viñals, J., Roca, A., Hernández, M.C., Benavente, O., 2003. Topochemical transformation of enargite into copper oxide by hypochlorite leaching. Hydrometallurgy 68, 183–193. https://doi.org/10.1016/S0304-386X(02)00200-1

Vračar, R., Parezanović, I.S., Cerović, K.P., 2000. Leaching of copper(I) sulfide in calcium chloride solution. Hydrometallurgy 58, 261–267. https://doi.org/10.1016/S0304-386X(00)00137-7

Vyazovkin, S., 2016. A time to search: Finding the meaning of variable activation energy. Phys. Chem. Chem. Phys. 18, 18643–18656. https://doi.org/10.1039/c6cp02491b

Wang, J., Gan, X., Zhao, H., Hu, M., Li, K., Qin, W., Qiu, G., 2016. Dissolution and passivation mechanisms of chalcopyrite during bioleaching: DFT calculation, XPS and electrochemistry analysis. Miner. Eng. 98, 264–278. https://doi.org/10.1016/j.mineng.2016.09.008

Wang, S., 2005. Copper leaching from chalcopyrite concentrates. Jom 57, 48–51. https://doi.org/10.1007/s11837-005-0252-5

Warren, G.W., Wadsworth, M.E., El-Raghy, S.M., 1992. Passive and transpassive anodic behavior of chalcopyrite in acid solutions. J. Electron. Mater. 21, 571–579. https://doi.org/10.1007/BF02669170

Watling, H.R., 2013. Chalcopyrite hydrometallurgy at atmospheric pressure: 1. Review of acidic sulfate, sulfate-chloride and sulfate-nitrate process options. Hydrometallurgy 140, 163–180. https://doi.org/10.1016/j.hydromet.2013.09.013

Watling, H.R., Shiers, D.W., Li, J., Chapman, N.M., Douglas, G.B., 2014. Effect of water quality on the leaching of a low-grade copper sulfide ore. Miner. Eng. 58, 39–51. https://doi.org/10.1016/j.mineng.2014.01.005

Wilson, J.P., Fisher, W.W., 1981. Cupric Chloride Leaching of Chalcopyrite. J. Met. 33, 52–57.

Wu, B., Yang, X.L., Cai, L.L., Yao, G.C., Wen, J.K., Wang, D.Z., 2013. The influence of pyrite on galvanic assisted leaching of chalcocite concentrates. Adv. Mater. Res. 825, 459–463. https://doi.org/10.4028/www.scientific.net/AMR.825.459

Xingyu, L., Biao, W., Bowei, C., Jiankang, W., Renman, R., Guocheng, Y., Dianzuo, W., 2010. Bioleaching of chalcocite started at different pH: Response of the microbial community to environmental stress and leaching kinetics. Hydrometallurgy 103, 1–6.

https://doi.org/10.1016/j.hydromet.2010.02.002

Zeng, W., Qiu, G., Chen, M., 2013. Investigation of Cu-S intermediate species during electrochemical dissolution and bioleaching of chalcopyrite concentrate. Hydrometallurgy 134–135, 158–165. https://doi.org/10.1016/j.hydromet.2013.02.009

Zhang, R., Sun, C., Kou, J., Zhao, H., Wei, D., Xing, Y., 2019. Enhancing the leaching of chalcopyrite using Acidithiobacillus ferrooxidans under the induction of surfactant triton X-100. Minerals 9. https://doi.org/10.3390/min9010011

Zhang, W., Oganov, A.R., Goncharov, A.F., Zhu, Q., Boulfelfel, S.E., Lyakhov, A.O., Stavrou, E., Somayazulu, M., Prakapenka, V.B., Konoϕková, Z., 2013. Unexpected stable stoichiometries of sodium chlorides. Science (80-.). 342, 1502–1505. https://doi.org/10.1126/science.1244989

Zhao, H., Zhang, Yisheng, Zhang, X., Qian, L., Sun, M., Yang, Y., Zhang, Yansheng, Wang, J., Kim, H., Qiu, G., 2019. The dissolution and passivation mechanism of chalcopyrite in bioleaching: An overview. Miner. Eng. 136, 140–154. https://doi.org/10.1016/j.mineng.2019.03.014

Zhao, J., Brugger, J., Chen, G., Ngothai, Y., Pring, A., 2014. Experimental study of the formation of chalcopyrite and bornite via the sulfidation of hematite: Mineral replacements with a large volume increase. Am. Mineral. 99, 343–354. https://doi.org/10.1515/am.2014.4628

Zhong, S., Li, Y., 2019. An improved understanding of chalcopyrite leaching kinetics and mechanisms in the presence of NaCl. J. Mater. Res. Technol. 8, 3487–3494. https://doi.org/10.1016/j.jmrt.2019.06.020

7 Appendix

Appendix 1. Chalcopyrite initial simple

Appendix 2. Mine ore initial sample

Appendix 3. Chalcocite initial simple

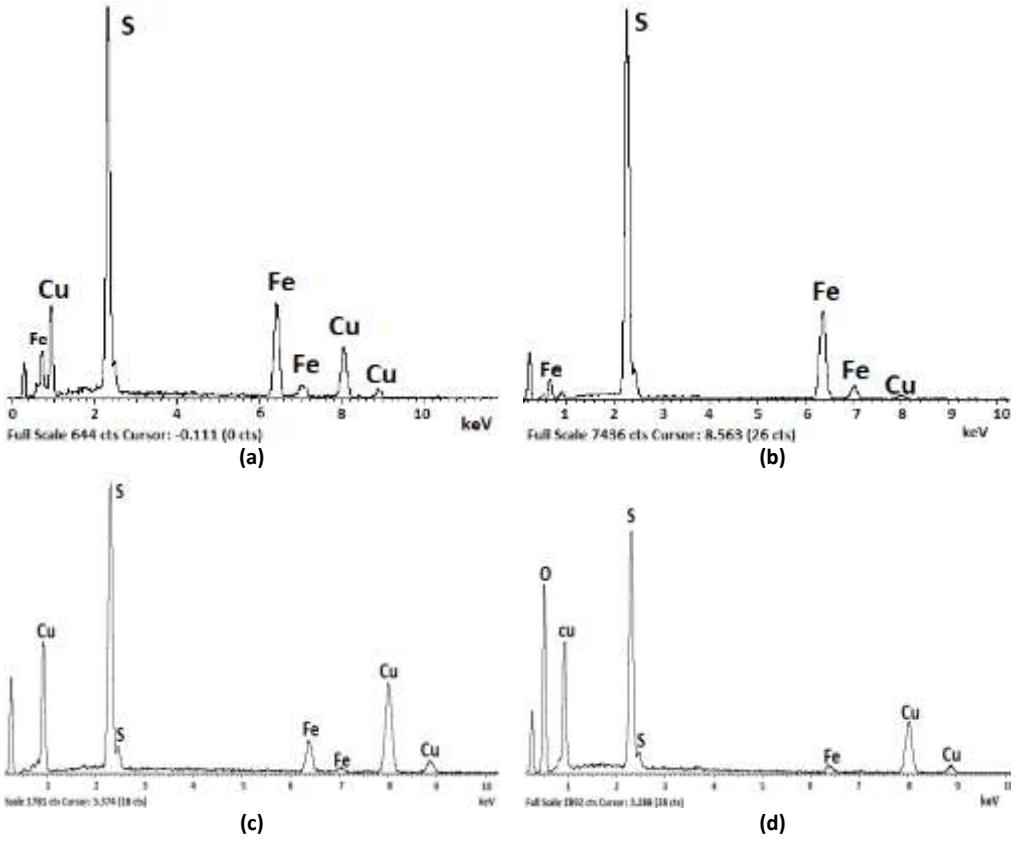

Appendix 4. EDS analysis associated with chalcopyrite initial sample: chalcopyrite (a) pyrite (b) covellite (c) and chalcanthite (d)

Leaching of chalcopyrite sample

Appendix 5. Copper and iron dissolution from chalcopyrite at 25 ° C with and without pretreatment

	Without pretreatment		With pretreatment	
Time (h)	% Cu extraction	% Fe extraction	% Cu extraction	% Fe extraction
0	0.00	0.00	0.00	0.00
0.5	13.4	9.73	14.6	7.43
1	14.5	10.8	20.2	15.5
2	16.9	14.0	22.6	15.1
4	17.5	17.5	25.4	14.5
8	18.2	20.3	25.6	19.4
12	19.5	21.3	25.8	23.0
24	28.5	29.5	27.5	28.5
36	30.6	33.8	28.4	28.6
48	30.1	33.2	29.0	32.7

Appendix 6. Copper and iron dissolution from chalcopyrite at 50 ° C with and without pretreatment

	Without pretreatment		With pretreatment	
Time (h)	% Cu extraction	% Fe extraction	% Cu extraction	% Fe extraction
0	0.00	0.00	0.00	0.00
0.5	14.9	16.3	22.2	16.3
1	14.9	15.9	23.3	12.5
2	15.0	15.4	24.4	23.1
4	19.2	21.2	26.4	27.8
8	23.5	26.3	28.8	31.3
12	30.3	34.5	34.4	35.3
24	51.5	52.8	56.0	51.1
36	71.1	75.9	74.6	81.1
48	71.0	76.0	76.8	83.0

Appendix 7. Copper and iron dissolution from chalcopyrite at 70 °C with and without pretreatment

	Without pretreatment		With pretreatment	
Time (h)	% Cu extraction	% Fe extraction	% Cu extraction	% Fe extraction
0	0.00	0.00	0.00	0.00
0.5	14.3	15.7	26.7	23.0
1	16.5	18.0	27.5	26.7
2	16.2	20.1	32.0	33.3
4	21.6	23.8	39.5	41.7
8	31.6	34.5	44.2	47.4
12	42.5	41.5	51.0	51.0
24	65.0	71.0	74.8	76.9
36	80.9	90.2	91.3	75.0
48	87.3	90.1	92.4	74.3

Appendix 8. Copper and iron dissolution from chalcopyrite at 90 °C with and without pretreatment

	Without pretreatment		With pretreatment	
Time (h)	% Cu extraction	% Fe extraction	% Cu extraction	% Fe extraction
0	0.00	0.00	0.00	0.00
0.5	23.3	26.9	33.5	36.7
1	29.2	27.2	35.6	39.6
2	33.2	28.9	43.5	48.4
4	38.7	38.9	47.3	60.1
8	47.7	48.0	56.5	61.7
12	58.0	55.1	66.1	63.8
24	79.8	62.1	83.9	64.5
36	86.9	78.1	91.8	75.0
48	89.6	75.7	93.6	72.5

Leaching of mine ore

Appendix 9. Copper and iron dissolution from mine ore at 25 °C with and without pretreatment

	Without pretreatment		With pretreatment	
Time (h)	% Cu extraction	% Fe extraction	% Cu extraction	% Fe extraction
0	0.00	0.00	0.00	0.00
0.5	12.5	2.38	20.7	3.37
1	14.3	3.18	22.9	4.76
2	14.7	3.18	23.9	5.55
4	15.2	3.77	24.9	6.15
8	15.6	3.97	25.3	6.55
12	15.7	4.37	25.0	6.94
24	15.9	4.76	25.3	7.34
36	16.2	5.75	25.6	7.74
48	16.7	6.35	25.9	8.33

Appendix 10. Copper and iron dissolution from mine ore at 50 °C with and without pretreatment

	Without pretreatment		With pretreatment	
Time (h)	% Cu extraction	% Fe extraction	% Cu extraction	% Fe extraction
0	0.00	0.00	0.00	0.00
0.5	18.2	14.5	23.8	6.1
1	21.7	14.7	27.9	6.3
2	27.0	14.8	33.8	10.5
4	29.2	17.5	37.1	16.4
8	35.5	17.7	41.5	19.8
12	38.1	18.1	44.0	24.6
24	39.4	19.6	46.5	24.8
36	43.1	20.1	47.7	25.4
48	44.3	21.6	48.9	26.0

Appendix 11. Copper and iron dissolution from mine ore at 70 °C with and without pretreatment

	Without pretreatment		With pretreatment	
Time (h)	% Cu extraction	% Fe extraction	% Cu extraction	% Fe extraction
0	0.00	0.00	0.00	0.00
0.5	29.4	17.5	33.2	18.3
1	35.5	18.4	40.9	22.6
2	41.7	19.4	47.3	24.0
4	46.8	20.3	54.7	25.8
8	50.5	22.8	57.7	26.6
12	53.5	24.4	60.6	27.4
24	58.3	29.3	65.5	28.6
36	61.8	34.2	68.5	37.1
48	64.3	36.7	70.2	42.0

Appendix 12. Copper and iron dissolution from mine ore at 90 °C with and without pretreatment

	Without pretreatment		With pretreatment	
Time (h)	% Cu extraction	% Fe extraction	% Cu extraction	% Fe extraction
0	0.00	0.00	0.00	0.00
0.5	41.7	23.6	38.0	25.2
1	44.3	25.2	56.9	27.4
2	56.3	26.8	69.0	31.9
4	69.6	29.9	77.8	34.3
8	77.8	31.3	82.3	37.7
12	80.4	33.7	86.7	40.1
24	84.2	36.5	89.8	44.2
36	86.7	39.7	91.7	46.0
48	88.6	40.7	93.1	47.8

Leaching of chalcocite

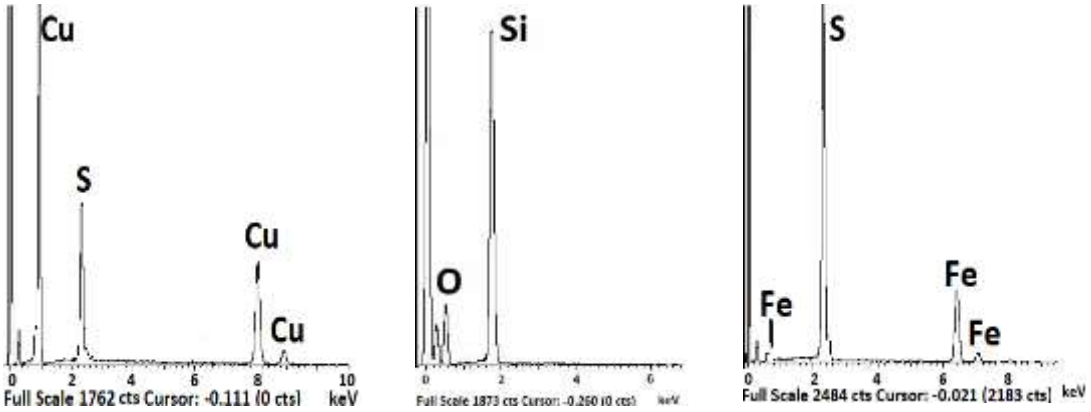

(a) **(b)** **(c)**

Appendix 13. EDS analysis associated with chalcocite initial sample (a) chalcocite (b) quartz and (c) pyrite

Appendix 14. Copper dissolution from chalcocite at 25 °C with and without pretreatment

Time (h)	With pretreatment % Cu extraction	Without pretreatment % Cu extraction
0.00	0.00	0.00
0.17	16.1	10.9
0.50	22.9	17.3
1.00	28.0	23.7
1.50	34.5	30.5
3.00	44.3	41.7
5.00	48.5	46.8
8.00	50.3	48.4
12.0	51.9	49.5

Appendix 15. Copper dissolution from chalcocite at 50 °C with and without pretreatment

Time (h)	With pretreatment % Cu extraction	Without pretreatment % Cu extraction
0.00	0.00	0.00
0.17	26.1	16.8
0.50	30.0	20.1
1.00	36.5	27.9
1.50	42.8	38.9
3.00	51.6	47.4
5.00	60.9	55.8
8.00	67.2	62.4
12.0	71.6	67.0

Appendix 16. Copper dissolution from chalcocite at 25 °C with oxygen and with nitrogen

Time (h)	Without pretreatment and O_2 injection % Cu extraction	Without pretreatment and N_2 injection % Cu extraction
0.00	0.00	0.00
0.17	26.4	5.31
0.50	36.0	5.90
1.00	46.9	6.50
1.50	52.4	8.45
3.00	57.3	14.1
5.00	61.1	15.6
8.00	65.6	18.3
12.0	68.6	21.2

The information provided in this chapter collects as the last update on November 14, 2020 according to Scopus Citescore

Publications

Journal: Journal of Materials Research and Technology-JMR&T
Quartile: Q1
Impact factor 2019: 5.289
Category: Metallurgy & Metallurgical Engineering (5/79)
Times cited: 1

Quezada, Víctor., Roca, A., Benavente, O., Cruells, M., Keith, B., & Melo, E. (2020). Effect of pretreatment prior to leaching on a chalcopyrite mineral in acid media using NaCl and KNO_3. Journal of Materials Research and Technology, 9(5), 10316–10324. https://doi.org/10.1016/j.jmrt.2020.07.055

Available online at www.sciencedirect.com
jmr&t
Journal of Materials Research and Technology
https://www.journals.elsevier.com/journal-of-materials-research-and-technology
ELSEVIER

Original Article

Effect of pretreatment prior to leaching on a chalcopyrite mineral in acid media using NaCl and KNO_3

Víctor Quezada[a,b,*], *Antoni Roca*[a], *Oscar Benavente*[b], *Montserrat Cruells*[a], *Brian Keith*[c], *Evelyn Melo*[b]

[a] Departamento de Ciencia de los Materiales y Química Física, Universitat de Barcelona, Barcelona, Spain
[b] Departamento de Ingeniería Metalúrgica y Minas, Universidad Católica del Norte, Antofagasta, Chile
[c] Departamento de Ingeniería de Sistemas y Computación, Universidad Católica del Norte, Antofagasta, Chile

ARTICLE INFO

Article history:
Received 8 May 2020
Accepted 16 July 2020

Keywords:
Pretreatment
Curing time
Chalcopyrite
Chloride
Nitrate

ABSTRACT

Chalcopyrite is the most abundant copper ore mined in Chile. Hydrometallurgical plants are currently changing to concentration by flotation-matte smelting deposits when oxide minerals run out and chalcopyrite appears in deposits. The change from hydrometallurgical processing to flotation is mainly dependent on whether comminution costs can be absorbed given the copper grade. It is important to develop alternative technologies to work profitably with low-grade copper sulphide ores. One alternative that has been recently studied is the pretreatment of low copper grade sulphide minerals, especially chalcopyrite, to improve leaching efficiency. The curing time, as pretreatment, improves dissolution kinetics and shortens leaching time. This study used a pure sample of chalcopyrite mineral with 28.5% copper. Chalcanthite (copper sulphate) represented 9% of total copper in the sample. The effect of curing time as a function of copper extraction prior to leaching was evaluated using different concentrations of sodium chloride (NaCl), potassium nitrate (KNO_3) and sulphuric acid (H_2SO_4). A 23% copper dissolution was obtained prior to leaching using 25 kg/t NaCl, 15 kg/t H_2SO_4 and 15 days of curing time. The ANOVA analysis reported that curing time was the most important variable (56.4 and 54.7% of contribution) in tests with NaCl and KNO_3. According to the results, KNO_3 does not have a significant effect on copper extraction prior to leaching.

Journal: Metals
Quartile: Q1
Impact factor 2019: 2.259
Category: Metallurgy & Metallurgical Engineering (18/79)
Times cited: 4

Beiza, L., **Quezada, V.,** Melo, E., & Valenzuela, G. (2019). Electrochemical Behaviour of Chalcopyrite in Chloride Solutions. *Metals*, *9*(1), 1–12. https://doi.org/10.3390/met9010067

metals

MDPI

Article

Electrochemical Behaviour of Chalcopyrite in Chloride Solutions

Luis Beiza [1,2], Víctor Quezada [1,3,*], Evelyn Melo [1] and Gonzalo Valenzuela [1]

1 Laboratorio de Investigación de Minerales Sulfurados, Departamento de Ingeniería Metalúrgica y Minas, Universidad Católica del Norte, Avenida Angamos 0610, 1270709 Antofagasta, Chile; lubeiza@ucn.cl (L.B.); emelo@ucn.cl (E.M.); g.valezma@gmail.com (G.V.)
2 Hydrometallurgy Research Group, Department of Chemical Engineering, University of Cape Town, South Lane, Rondebosch 7701, South Africa
3 CPCM Research Group, Department of Materials Science and Physical Chemistry, University of Barcelona, Martí i Franquès 1, 08028 Barcelona, Spain
* Correspondence: vquezada@ucn.cl; Tel.: +56-552651024

Received: 8 November 2018; Accepted: 6 January 2019; Published: 11 January 2019

check for updates

Abstract: Due to the depletion of oxidized copper ores, it necessitates the need to focus on metallurgical studies regarding sulphide copper ores, such as chalcopyrite. In this research, the electrochemical behaviour of chalcopyrite has been analysed under different conditions in order to identify the parameters necessary to increase the leaching rates. This was carried out through cyclic voltammetry tests at 1 mV/s using a pure chalcopyrite macro-electrode to evaluate the effect of scan rate, temperature, and the addition of chloride, cupric, and ferrous ions. Lastly, the feasibility of using seawater for chalcopyrite dissolution was investigated. An increase in the sweep rate and temperature proved to be beneficial in obtaining highest current densities at 10 mV/s and 50 °C. Further, an increase of chloride ions enhanced the current density values. The maximum current density obtained was 0.05 A/m^2 at concentrations of 150 g/L of chloride. An increase in the concentration of cupric ions favoured the oxidation reaction of Fe (II) to Fe (III). Finally, the concentration of chloride ions present in seawater has been identified as favourable for chalcopyrite leaching.

Journal: IOP Conference Series: Materials Science and Engineering
Quartile: Q3 (Scopus)
Impact factor 2019: 0.198
Category: Engineering
Times cited: 3

Quezada, V, Velásquez, L., Roca, A., Benavente, O., Melo, E., & Keith, B. (2018). Effect of curing time on the dissolution of a secondary copper sulphide ore using alternative water resources. IOP Conference Series: Materials Science and Engineering, 427(1). https://doi.org/10.1088/1757-899X/427/1/012030

Effect of curing time on the dissolution of a secondary copper sulphide ore using alternative water resources

V Quezada[1, 2], L Velásquez3, A Roca[1], O Benavente[2], E Melo[2] and B Keith[4]

[1] Departamento de Ciencia de los Materiales y Química Física, Universidad de Barcelona, Barcelona, España.

[2] Departamento de Ingeniería Metalúrgica y Minas, Universidad Católica del Norte, Antofagasta, Chile.

[3] Departamento de Ingeniería en Minas, Universidad de Santiago, Santiago, Chile.

[4] Departamento de Ingeniería de Sistemas y Computación, Universidad Católica del Norte, Antofagasta, Chile.

vquezare7@alumnes.ub.edu

Abstract. In the north of Chile, due to water shortages, the depletion of oxide ores and the abundance of chalcopyrite ore, mining industry is searching for sustainable hydrometallurgy processes that can use alternative water resources. The leaching process must enhance the dissolution of copper sulphide ore that are refractory to conventional leaching. This paper reports a study on the effect of addition of chloride ion using seawater and discard brine in the agglomeration stage of a secondary copper sulphide ore. The effect of curing time on the same ore also is reported. The leaching tests have been carried out in column irrigated with raffinate under ambient conditions. A size distribution with a P80 of 17 mm is used. A maximum of 72% of copper extraction is obtained using discard brine and 68% using seawater. The use of discard brine and seawater are favorable in all the tests performed. Through an Analysis of Variance (ANOVA), it is determined that the curing time has the highest contribution (92.37%) on the percentage of copper extraction.

Conference Proceedings

Quezada, Victor**;** Roca, Antoni; Benavente, Oscar; Cruells, M. (2020). Effect of pretreatment on the leaching of chalcopyrite concentrate. In Hydroprocess 2020. Santiago, Chile. ISBN 978-956-397-03 4-0

Hydroprocess 2020 | 12th International Conference on Process Hydrometallurgy

Effect of pretreatment on the leaching of chalcopyrite concentrate

Víctor Quezada[1, 2*], Antoni Roca[1], Oscar Benavente[2] and Montserrat Cruells[1]

1. *Departamento de Ciencia de los Materiales y Química Física, Universitat de Barcelona, Spain*
2. *Departamento de Ingeniería Metalúrgica y Minas, Universidad Católica del Norte, Chile*

ABSTRACT

In 2019, 27.3% of Chilean copper output was produced by hydrometallurgical processes. According to the Chilean Copper Commission (Cochilco), only 12% of output will be produced by this method by 2029 owing to a change in the mineralogy of deposits from oxides to sulfides, with chalcopyrite being the main feed in hydrometallurgical plants. Chalcopyrite is a highly refractory mineral under conventional leaching conditions. Therefore, mining companies are moving from hydrometallurgy to concentration by flotation, provided the process is profitable given the high costs associated mainly with grinding. This change in operation will result in 50% available capacity in existing hydrometallurgical plants by 2029, which represents an opportunity to strengthen the processing of low-grade copper sulfide by hydrometallurgy. One of the variables that has recently been studied is the leaching pretreatment of copper sulfide ores. Several studies have demonstrated that agglomeration and extended curing periods increase the solubility of minerals and thus improve the kinetics of copper extraction during leaching.

This document presents the main theoretical concepts associated with pretreatment, and investigates how extended curing periods benefit copper extraction from copper sulfide ores. As well, the effect of curing on the efficiency of leaching by agitation and leaching in columns is explained. Leaching agitation tests with chalcopyrite mineral (74% purity according to QEMSCAN) showed that the copper extraction increased by 6% with pretreatment. Depending on the pretreatment conditions, the leaching time can be reduced by 25 to 50%. Finally, leached residues were characterized by various techniques, and elemental sulfur, jarosite and copper polysulfides (CuS_2) were found.

Quezada, Victor; Roca, Antoni; Benavente, Oscar; Cruells, M. (2019). Effect of curing time on copper leaching from chalcopyrite. In COM Hosting Copper 2019 (p. 11). Vancouver, Canada. ISBN 978-1-926872-44-5

EFFECT OF CURING TIME ON COPPER LEACHING FROM CHALCOPYRITE

*V. A. Quezada, A. Roca and M. Cruells
Universidad de Barcelona
Departamento de Ciencia de los Materiales y Química Física
Martí i Franquès 1, Barcelona, Cataluña, España 08028
*(*Corresponding author: vquezada@ucn.cl)*

V. A. Quezada and O.A. Benavente
Universidad Católica del Norte
Departamento de Ingeniería Metalúrgica y Minas
Avenida Angamos 0610, Antofagasta, Antofagasta, Chile 1270709

ABSTRACT

The leaching pretreatment of copper ores is widely used in the Chilean mining industry. Agglomeration and acid curing have been identified as the most useful pretreatments. Of these, acid curing was recognized as beneficial in the dissolution of copper minerals, even in sulphides such as chalcopyrite. Extensive acid curing times have an impact on copper extraction, generate a homogeneous acid distribution in the mineral bed and benefit the inhibition of aluminum-silicate minerals (acid consumers). This document describes some of the theoretical background and results regarding the effect of acid curing in a chalcopyrite sample with 74% purity according to Qemscan analysis and a 28.5% of total copper. Leaching tests are carried out at 25, 50 and 70°C, evaluating the effect of a pretreatment on the chalcopyrite dissolution. The original sample and products generated were characterized by X-ray diffraction analysis and Scanning Electron Microscopy (SEM). The performed experiments indicate a direct relation between the effect of curing time and temperature in copper extraction. 92% of copper can be extracted in a leaching at 70°C and with 15 days of curing. Elemental sulfur, jarosite and copper polysulfide (CuS_2) have been detected in leaching products.

Conference presentations

Quezada, Victor; Roca, Antoni; Benavente, Oscar; Cruells, M. (2020). Effect of pretreatment on the leaching of chalcopyrite concentrate. In Hydroprocess 2020. Santiago, Chile.

Quezada, Victor; Roca, Antoni; Benavente, Oscar; Cruells, M. (2019). The use of NaCl and H_2SO_4 in the pretreatment to chalcopyrite leaching in chloride media. In Minerals Research Showcase 2019. Cape Town, South Africa.

Quezada, Victor; Roca, Antoni; Benavente, Oscar; Cruells, M. (2019). Effect of curing time on copper leaching from chalcopyrite. In COM Hosting Copper 2019. Vancouver, Canada.

Quezada, Victor; Velásquez, Lilian; Roca, Antoni; Benavente, Oscar; Melo, Evelyn & Keith, Brian. (2018). Effect of curing time on the dissolution of a secondary copper sulphide ore using alternative water resources. In Mineral Engineering Conference (MEC). Zawiercie, Poland.

Awards

Young Scientist Award. Best Oral Presentation. In Mineral Engineering Conference (MEC) 2018. Zawiercie, Poland.

Iberoamerican Young Professors and Researchers Scholarship granted by Banco Santander. Antofagasta, Chile. Scholarship used at Universitat de Barcelona.

Awarding of financial support by the Faculty of Chemistry in the 2nd call for support for research 2018, Universitat de Barcelona. Financial support used to present in MEC 2018.

Awarding of financial support by the Faculty of Chemistry in the 2nd call for support for research 2019, Universitat de Barcelona. Financial support used to present in COM Hosting Copper 2019.

Awarding of financial support by in the 1st call for support presentations at Conferences by The Office of the Vice Chancellor for Research and Technological Development, Universidad Católica del Norte. Financial support used to present in COM Hosting Copper 2019.

Internship

Internship at University of Cape Town, South Africa. November 2019 to February 2020. Tutor: Professor Dr. Jochen Petersen.

Other contributions

Conference presented at the Universitat de Barcelona, entitled “Chile país minero. Contexto actual y futuro”. Presentation date: November 26, 2018.

Seminar for the subject "Obtención y procesado de materiales" for the "Ingeniería de Materiales" career, Universitat de Barcelona. The seminar was titled “Uso de agua de mar en la minería”. Presentation date: November 21, 2018.

Documents pending to publish

Publication pending submission, under review by the authors

Title: Effect of pretreatment prior to leaching on a chalcocite mineral

Journal: Hydrometallurgy

Quartile: Q1

Category: Metallurgy & Metallurgical Engineering (13/79)

Impact factor 2019: 3.338

Effect of pretreatment prior to leaching on a chalcocite mineral

ABSTRACT

Agglomeration and acid curing have been identified as the most useful pretreatments before heap leaching. Of these, acid curing was recognized as beneficial in the dissolution of copper minerals, even in sulphides. In addition to improving copper extraction, the curing time (or repose time) generates a homogeneous distribution in the mineral bed (heap leaching) and benefit the inhibition of aluminum-silicate (acid consumers). This investigation describes the results regarding the pretreatment evaluating the effect of curing time, NaCl and H_2SO_4 concentration in a chalcocite sample with a purity of 93.7%, according to Qemscan analysis and a 75.0% of total copper. Leaching tests are carried out at 25 and 50 °C, evaluating the effect of a pretreatment on the chalcocite dissolution. The original sample, pretreatment products and leaching residues were characterized by X-ray diffraction analysis (XRD) and Scanning Electron Microscopy (SEM). As products formed in the pretreatment, using 30 kg/t H_2SO_4, 40 kg/t NaCl and 7 days of curing, the presence of $CuSO_4$, $Cu(OH)Cl$, Na_2SO_4 and $Cu_{1.75}S$ have been confirmed. The leaching experiments performed indicate a direct relation between the effect of curing time and temperature in copper extraction. A copper dissolution of 71.5% is achieved, rising 4.6% compared to the test without pretreatment at 50 °C. Elemental sulphur has been confirmed in leaching residues in tests using oxygen injection and 50 °C with pretreatment.

1. INTRODUCTION

Hydrometallurgical treatment of copper sulphides minerals has been studied almost 40 years ago (Bogdanović et al., 2020; Córdoba et al., 2009; Dutrizac, 1978; Haver F.P and Wong M.M, 1971; Herreros et al., 1999; Muñoz-Ribadeneira and Gomberg, 1971; Velásquez-Yévenes et al., 2010). Today, research focuses more on how to improve the kinetics dissolution of primary sulphides, mainly chalcopyrite (Beiza et al., 2019). Regarding secondary copper sulphides, chalcocite and covellite, there have been cases of implementation at industrial scale, like Cuprochlor Process (Herreros and Viñals, 2007). In the case of chalcocite, is the most abundant copper sulphide mineral after chalcopyrite. Through hydrometallurgical treatments it is known as the copper sulphide ore that is easier to dissolve (Miki et al., 2011). This property becomes very attractive mainly for those deposits with low copper grade and consider hydrometallurgical processes as an alternative. Similarly, chalcocite and covellite are two of the common copper-bearing minerals also formed as intermediate products during the leaching of chalcopyrite (Senanayake, 2009). Thus, it is known that chalcocite dissolution is carried out in two stages (Tanda et al., 2018).

Oxidative dissolution of chalcocite by Fe^{3+},O_2 or Cu^{2+}, either in a sulphate or chloride system, occurs in two different stages with the production of secondary covellite as an intermediate (Cheng and Lawson, 1991a; Fisher et al., 1992; Senanayake, 2009). The first stage of chalcocite leaching is very

In drafting process

Title: Effect of pretreatment prior to leaching on a chalcopyrite mineral

Journal: Journal of Materials Research and Technology-JMR&T

Quartile: Q1

Category: Metallurgy & Metallurgical Engineering (5/79)

Impact factor 2019: 5.289

Title: Effect of pretreatment prior to leaching on a copper sulphides ore

Journal: Metals

Quartile: Q1

Category: Metallurgy & Metallurgical Engineering (18/79)

Impact factor 2019: 2.259